Sleep Synchronisation, Sleep Onset Staging and Arousal Detection: A Polysomnogram Signal Analysis of Sleep Insomnia and Schizophrenia

A thesis submitted in fullfilment of the requirements for the degree of Doctor of Philosophy

Ramiro Chaparro-Vargas

School of Engineering
College of Science, Engineering and Health
RMIT University

January 2016

Declaration

I certify that except where due acknowledgement has been made, the work is that of the author alone; the work has not been submitted previously, in whole or in part, to qualify for any other academic award; the content of the thesis is the result of work which has been carried out since the official commencement date of the approved research program; any editorial work, paid or unpaid, carried out by a third party is acknowledged; and, ethics procedures and guidelines have been followed.

Ramiro A. Chaparro Vargas
November 30th, 2016

Abstract

College of Science, Engineering and Health
School of Engineering

Submitted for the degree of Doctor of Philosophy

by Ramiro Chaparro-Vargas

The present thesis discusses advanced polysomnogram signal processing approaches to perform computer-assisted sleep analysis and disorders characterisation and differentiation. Sleep electrophysiology and biomedical signal processing are branded by time-consuming assessments, inter-subjects' and inter-raters' variability. Those challenges compromise the analysis, characterisation and differentiation in terms of time analysis, tolerance to subjects' out-of-norm patterns and raters' biased sleep stages scoring. The proposed models explored computer-aided neuronal-cardiac synchronisation, sleep onset staging and arousal detection; looking forward to improve regular and abnormal sleep characterisation. Foremost, the differentiation of control, insomnia and schizophrenia groups and individuals was pursued throughout computational models and actual clinical datasets.

Four core studies elaborated the literature background, methods, models, experimental datasets, data analysis and insights to attain sleep, groups and individuals characterisation. These interrelated studies built up an initial preprocessing model, going through sleep onset, insomnia characterization to achieve subjects and groups differentiation. The first core study focused on the computer-assisted preprocessing of polysomnogram signals. Preprocessing addressed the removal of embedded cardiac-type pulses and muscular artefacts, accompanied by the suppression or attenuation of the additive white noise from cortical and ocular signals. The proposed model successfully performed artefact removal upon 80% of the 1200 analysed electroencephalographic (EEG) and electrooculographic (EOG) epochs and 100% concerning background noise suppression. The second core study concerned the synchronisation between the central and autonomic nervous system to characterise control, insomnia and schizophrenia cohorts. The calculation of computer-assisted correlation, coherence and coupling metrics measured the neuronal-cardiac functional interdependence by means of EEG and electrocardiographic (ECG) signals. Those approaches represented linear, nonlinear and statistical methods. The spectral synchrogram derived from Wavelet-based coherence outperformed the characterisation of control and schizophrenia groups by tracking the interdependence of EEG alpha band (α) to Heart Rate Variability Low Frequency (HRV-LF) as driving feature. The third core study centred in sleep onset staging for a computer-aided estimation of the sleep onset stages, and the computer-aided differentiation of control and insomnia individuals. Firstly, the approach introduced adaptive processing and machine learning tools for the automated sleep staging. Secondly, the approach suggested novel characterisation metrics for the differentiation of control, insomnia and schizophrenia cohorts dealing with out-of-norm patterns and raters' biased sleep stages scoring. The introduced biosignal modelling generalised polysomnogram

signals made of thousands of time points with only 10 reconstructive coefficients. The performance metrics of control and insomnia subjects' logistic classifier highly rated: sensitivity (87%), specificity (75%) and accuracy (81%). The fourth core study appointed the computer-aided arousal marking, performing fuzzy logic-based detection. The model identified spontaneous arousals, EEG with chin tension and limb movement-related arousals. The model demonstrated an average Arousal Index (ArI) in regular sleepers around 20, which agreed with expert scored assessments.

Overall, this original research work provides novel contributions in biomedical signal processing and a supporting role in the sleep electrophysiology towards a more comprehensive knowledge of insomnia and schizophrenia disorders.

Acknowledgements

I would like to acknowledge and thank to:

- A mis padres por ser los patrocinadores exclusivos de mi proyecto de vida
- A Jullie por ser una amiga incondicional, en el sentido más explícito del término
- A Migue por ser ese gran amigo nuevo
- To Dean for being a dedicated and supportive supervisor
- To Colciencias-Colfuturo for being the financial and logistic support of my doctoral studies
- To the Qatar National Research Fund (QNRF) for the financial support to my doctoral project

Contents

Abbreviations

AASM	**A**merican **A**cademy **S**leep **M**edicine
AIC	**A**kaike **I**nformation **C**riterion
ANN	**A**rtificial **N**eural **N**etwork
ANS	**A**utonomic **N**ervous **S**ystem
ArI	**Ar**ousal **I**ndex
ASDA	**A**merican **S**leep **D**isorders **A**ssociation
BIC	**B**ayesian **I**nformation **C**riterion
BSS	**B**lind **S**ource **S**eparation
BM	**B**ody **M**ovements
CAP	**C**yclic **A**lternating **P**attern
CCF	**C**ross **C**orrelation **F**unction
CNS	**C**entral **N**ervous **S**ystem
DSM	**D**iagnostic and **S**tatistical **M**anual
EEG	**E**lectro**E**ncephalo**G**ram
ECG	**E**lectro**C**ardio**G**ram
EMG	**E**lectro**M**yo**G**ram
EOG	**E**lectro**O**culo**G**ram
ERP	**E**vent **R**elated **P**otential
EVD	**E**igen**V**alue **D**ecomposition
FIS	**F**uzzy **I**nference **S**ystem
GST	**G**raph **S**pectral **T**heory
HF	**H**igh **F**requency
HRV	**H**eart **R**ate **V**ariability
ICA	**I**ndependent **C**omponent **A**nalysis

ISV	**I**nter **S**ubject **V**ariability
KC	**K**-**C**omplex
LOO	**L**eave **O**ne **O**ut
LF	**L**ow-**F**requency
M	**M**ean
MSE	**M**ean **S**quare **E**rror
N1	**n**on-REM**1**
N2	**n**on-REM**2**
N3	**n**on-REM**3**
OSA	**O**bstructed **S**leep **A**pnoea
PAT	**P**eripheral **A**rterial **T**one
PLV	**P**hase **L**ocking **V**alue
PSG	**P**oly**S**omno**G**ram
qEEG	**q**uantitative **E**lectro**E**ncephalo**G**ram
REM	**R**apid **E**ye **M**ovement
R&K	**R**echtschaffen & **K**ales
SD	**S**tandard **D**eviation
SOS	**S**econd **O**rder **S**tatistics
SS	**S**leep **S**pindle
SVD	**S**ingular **V**alue **D**ecomposition
SW	**S**awtooth **W**aves
VSW	**V**ertex **S**hape **W**aves
W	**W**ake
TVARMA	**T**ime **V**arying **A**uto**R**egressive **M**oving **A**verage
RMS	**R**oot **M**ean **S**quare
RRI	**R**-to-**R** **I**nterval
SIR	**S**ignal-to-**I**nterference **R**atio
SNR	**S**ignal-to-**N**oise **R**atio
TFA	**T**ime **F**requency **A**nalysis
WCOH	**W**avelet **C**oherence
WPT	**W**avelet **P**acket **T**ransform

Symbols

Symbol	Name	Unit
h	hour	n.a.
k	time index	n.a.
m	oscillator 1 cycles	n.a.
n	oscillator 2 cycles	n.a.
p	Autoregressive model order	n.a.
q	Moving Average model order	n.a.
s	second	n.a.
α	EEG alpha band	Hz
β	EEG beta band	Hz
δ	EEG delta band	Hz
θ	EEG theta band	Hz
γ	EEG gamma band	Hz
λ	G network eigenvalues	n.a.
μ	H network eigenvalues	n.a.
κ	Cohen's index	n.a.
η	System noise	mV
ν	Observation noise	mV
ς	EEG sigma band	Hz
ς_η^2	System noise dispersion	n.a.
σ_ν^2	Observation noise variance	n.a.
τ	Time lag	n.a.

ζ	Phase Locking Value	n.a.
$\mathbf{x}$	System coefficients vector	mV
$\mathbf{y}$	Observation vector	mV
A	Biosignal amplitude	mV
$\mathbf{A}$	Autoregressive matrix	n.a.
A	Adjacency matrix	V^2/Hz
$\mathbf{B}$	Moving Average matrix	n.a.
$\mathbf{C}$	Incidence matrix	n.a.
$\mathbf{D}$	Degree matrix	n.a.
$\mathbf{I}$	Identity matrix	n.a.
$\mathbf{L}$	Laplacian matrix	n.a.
$\mathbf{P}$	Relative band power	n.a.
$\mathbf{Q}$	Eigenvector matrix	n.a.
$\mathbf{U}$	Eigenvector matrix (SVD)	n.a.
$\mathbf{V}$	Eigenvector matrix (SVD)	n.a.
$\mathbf{S}$	Power spectrum	J Hz^{-1}
Λ	Eigenvalues matrix	n.a.
Σ	Singular values matrix	n.a.
$\mathscr{C}$	Cauchy distribution	n.a.
$\mathscr{N}$	Normal distribution	n.a.

Dedicado a mis padres

Preface

This thesis gathers the 5 years efforts to shed some sparks of light to sleep electrophysiology and advanced biomedical signal processing. Those efforts are comprehensively and extensively socialised with the scientific community through a series of peer-reviewed publications. All the people involved in the realisation of such papers, articles and book chapters deserve an acknowlegdement for its intellectual, material and moral support. Here, I would like to briefly share the milestones throughout such intellectual contributions, which served as the main input to the thesis presented in the upcoming chapters.

The first publication in Appendix A made a review of the existing literature about characterisation and classification of sleep, depression and schizophrenia disorders. In 2013, the conference paper in Appendix B introduced the initial approach and obtained results in respect to the preprocessing study. Such a start-up approach built up the definitive model presented in the journal paper in Appendix C, accompanied by conclusive findings and statements. In relation to the synchronisation study, two conference papers in Appendices D-E proposed the linear and non-linear methods for the estimation of functional interdependences upon regular subjects. The topic was substantially complemented with the publication in Medical & Biological Sciences & Computing Journal—Appendix F—, where the methods were extended to insomnia and schizophrenia groups with statistical validation. In respect to the sleep onset staging, conference papers in Appendices G-H proposed the approaches for the biosignal modelling, processing and classification upon regular sleep onset periods. The conference paper in Appendix I reported the pilot results for the quantification of regular and insomnia sleep onset patterns without previous computer-aided processing of features or stages classification. The integrated computational system was presented in the IEEE Transactions on Biomedical Engineering paper in Appendix J including novelties upon biosignal modelling and characterisation of insomnia sleep onset patterns. Finally, Chapter 8 and Appendix K refers to the study and conference paper addressing arousal detection. Both sections recalled the methods for biosignal modelling, feature extraction and posit a new classification approach to detect and differentiate standard types of arousals.

Chapter 1

Introduction

The academic community and general public with an interest in this higher research project will find the recurrent overlapping of two major disciplines: sleep electrophysiology and signal processing. Such a multidisciplinarity defined the essence of the research work conducted at each undertaken milestone, seeking a comprehensive understanding of sleep patterns and related disorders. Advancing upon the ever-growing prowess of the digital era, a novel approach is posited based on biomedical signal processing to overcome some of the emerging hurdles within clinical and scientific sleep community.

The leverage of sleep to regulate the physiopsychological processes has been an intricate matter that concerned control and disordered groups. Behavioural studies of large populations under regular and irregular sleep patterns have established a direct link between daily and overnight activity. Sleep is governed by a perplexing number of events and phenomena, whose slightly alterations could set in motion subtle disturbances to severe disorders. Since early sixties with Rechtschaffen and Kales (1968) standard, the medical community has established college bodies, expert committees, task forces and akin organisations to formalise sleep physiology in terms of staging, terminology, etiology, pathophysiologies and protocols. Hitherto, the published standards and manuals have constituted the primary source to grasp sleep structure, diagnose disorders and overall set up collaborative partnerships, like Iber et al. (2007). The outcomes of these joint efforts have advantaged the building of through standardisation endeavours.

However, a review of the state-of-the-art pointed out ongoing challenges or improvements associated to the sleep analysis and characterisation of insomnia and schizophrenia disorders. Through this research, such a collection of potential improvements were distilled into three main challenges: (i) time-consuming assessments, (ii) inter-rater variability and (iii) inter-subject variability. These challenges embody the major hurdles to the efficacy of the exercising procedures amongst specialists.

(i) Time-consuming assessments: The number of recording sensors, sampling rates, duration of recording sessions and daily-to-weekly recurrence of those sessions gathers up a vast amount of raw data. Turning the expert-based analysis in a time-consuming task.

(ii) Inter-rater variability: The dissimilar criteria of sleep scorers hinder the objective interpretation of sleep data. This situation leads to either an overestimation or underestimation of regular and irregular sleep patterns.

(iii) Inter-subject variability: The existence of subject-specific traits is an expected outcome of sleep analysis. Although, the oversight of misclassifications jeopardises the accuracy of the analyses.

The present work aims to overcome those main challenges by means of innovative approaches supported on biomedical signal processing and sleep electrophysiology. To accomplish this, four core studies were conducted: preprocessing, synchronisation, sleep onset staging and arousal detection. Each comprised its own literature review, mathematical modeling, clinical datasets, methods, experimental design, results and critical discussion. The compendium of such items conveyed to the ultimate motivation of the current work, i.e. provide an original contribution upon sleep electrophysiology by characterising insomnia and schizophrenia disorders using computer-aided analysis. This thesis takes the reader to the insights of each core study as a self-standing but interrelated checkpoint of the overall research journey.

The first study was oriented to the preprocessing, a computer-assisted pre-analysis and preparation of the most relevant signals collected from different body surface regions—i.e. brain, heart, muscles and eyes—time-aligned in the polysomnogram (PSG). The preprocessing addressed the preliminary analysis upon the PSG attempting to remove artefacts and exogenous sources of noise. Thereupon, the information obtained from the preprocessed biosignals shall lead to more reliable outcomes in upcoming processing and classification routines.

Attending to the enhancement of the preprocessing, the second study focused on the synchronisation or functional interdependence problem between central nervous system (CNS) and autonomic nervous system (ANS), represented by neuronal and cardiac dynamics with EEG and ECG, respectively. This work sought the characterisation of control, insomnia and schizophrenia patient groups. The characterisation was undertaken using computer-assisted synchronisation gauges called synchrograms, which rely on the linear, non-linear and statistical processing of brain-heart frequency bands. The EEG/ECG joint interaction can be measured by levels of correlation, coherence and coupling measures, indicating concomitant contributions between CNS and ANS during regular and disordered sleep. The emergence of statistically significant patterns led to differentiate particular electrophysiological traits in control, insomnia and schizophrenia.

The third study approached a second sleep analysis method, focusing on sleep onset periods to comply two main objectives: 1) a computer-aided estimation of the sleep onset stages and 2) the differentiation of regular and insomnia populations by computational techniques compliant with medical procedures, enacting a supportive role. For the former objective, the approach overcame the time-consuming assessment of PSG datasets by the introduction of adaptive processing and machine learning tools for the classification task. In addition, the approach suggested a series of novel characterisation metrics for the differentiation of regular and disordered sleeping patterns dealing with

subject-specific traits and deferring scoring criteria, namely known as inter-subjects' and inter-raters' variability, correspondingly.

The fourth study concerned the arousal detection. Arousals are denominated as sleep microcomponents, which have been deprived from substantial research so far. Though, Jurysta et al. (2009) showed that arousals are namely associated to the onset of abnormalities in the execution of daily activities till the comorbid occurrence of psychiatric disorders like insomnia or depression. The study revisited the adaptive processing and machine learning principles to support the detection of elusive arousal events, whilst the main challenges were systematically addressed.

Chapter 2 contains the literature review of the relevant works on sleep studies, insomnia and schizophrenia etiology and advancements in computer-assisted analysis. Chapter 3 states the outstanding main challenges, derived research questions, appointed hypotheses and rationale behind them. Chapter 4 gathers the information about the clinical data and implemented methods for the proof or refusal of the hypotheses related to the main challenges and research questions. This thesis' core builds upon Chapters 5-8 discussing the methods, models, principal findings and noteworthy considerations derived from each study. The four core studies were aligned with the state-of-the-art challenges, research questions and formulated hypotheses. The Discussion and Conclusions—Chapters 9 and 10—outline the major considerations and closing statements by answering the formulated research questions supported on the evidence obtained from the conducted studies. Lastly, the present document is supported by a collection of peer-reviewed publications in Appendices A-K, which are the extended version related to the preprocessing, synchronisation, sleep onset staging and arousal detection studies. The journal manuscripts, conference papers and book chapter followed a chronological timeline and sole-thread storyline from the deployment of biosignal processing tools towards the outcomes of main challenges.

Chapter 2

Literature Review

Sleep represents the cornerstone of consciousness that sets the difference between the regular and abnormal physiological processes. In Liang et al. (2012) work, sustainable sleep patterns guarantee physical and psychological recovery to cope with demanding motor and imaginary tasks on a daily basis. Behavioural and electrophysiological undertakings have been used to assess the interdependence of sleep with mind-and-body well-being. Its interdependence with the adequate functioning of the rational, subconscious and biological systems in humans has been proved through behavioural and electrophysiological undertakings. Even so, for Cirelli and Tononi (2008) it is still elusive the articulation of its crystal-clear purpose with evidence. Sleep is an intricate matter consisting of converging processes of different nature. The interpretation of its electrophysiological activity offers a valuable framework to decipher its structure and bodily relationships. Then, the departure point of this review is about the techniques and tools employed in the sleep analysis.

The PSG stands out as a unique tool for electrophysiological monitoring of sleep dynamics with spatial and temporal resolution, given the fixed location of the electrodes and time-oriented capture of their recordings. As per Fraiwan et al. (2012), PSG channels collect biological signals from different sources; such as neuronal, ocular, muscular, cardiac, respiratory, abdominal, etc. In fact, PSG is a merger of traditional monitoring techniques, namely: electroencephalogram (EEG), electrocardiogram (ECG), electromyogram (EMG) and electrooculogram (EOG). Additional biosensors capture supplementary activity like abdominal efforts, respiratory stress, video-based movement, actigraphy and snoring sounds. According to Fei-Long and Zhi-Zeng (2012), PSG has become the standard assisting tool for the screening of sleep stages, microcomponents (e.g. arousals) and related disorders.

In 1968, Rechtschaffen and Kales (1968) (R&K) manual presented the primal standard for the formal characterisation of sleep using EEG, EOG and other signals. For several decades, R&K manual became the gold standard to describe the sleep physiology analysing the electrical activity of neuronal, cardiorespiratory, vascular and muscular systems. The appearance of distinctive dynamics and abrupt changes in these recorded signals during sleep, coincided with the reduction of responses to external

stimuli, implying an immersion into deeper states of consciousness and unconsciousness. The mapping of both phenomena to benchmark the sleep physiology produced 6 sleep stages: wake (W), stage 1 (S1), stage 2 (S2), stage 3 (S3), stage 4 (S4) and rapid eye movement (REM). The manual introduced a reference framework for the terminology, practices and scoring of sleep stages. The identification of irregular patterns facilitated the classification of sleep disorders by symptoms, etiologies and pathophysiologies. The American Sleep Disorders Association (ASDA) and peer organisations as Buysse (1979, 1990) published guidelines for the appropriate distinction and treatment of the associated disorders. In 1975, the formation of the American Academy of Sleep Medicine (AASM) continued the revision of the specialised content associated to sleep by the periodic publication of state-of-the-art manuals.

Later in 2007, the updated terminology, scoring rules and recording guidelines led to a more consistent definition of sleep macrostructure entirely supported on PSG signals as in Iber et al. (2007). The screening of distinctive dynamics, changing patterns, reponses to external stimuli and diferent states of consciousness were enhanced by additional signals. The new information about the sleep electrophysiology improved the staging criteria and produced 5 sleep stages: wake (W), nonREM1 (N1), nonREM2 (N2), nonREM3 (N3) and REM. R&K's S4 stage was merged to form AASM's N3 stage. Following Marzano et al. (2013) nomenclature, each sleep stage is characterised by a single or combined EEG frequency bands, divided in delta δ (0.5-4 Hz), theta θ (4-7 Hz), alpha α (7-12 Hz), sigma ς (12-16 Hz), beta β (16-18 Hz) and gamma γ (18-32 Hz); EOG slow eye movements (SEM); and EEG transients like vertex shape waves (VSW), K-complexes (KC), sleep spindles (SS), sawtooth waves (SW), EMG body movements (BM) and chin tension. Figure 2.1 gives a good idea about the progressive changes in the EEG signals and transients associated with the process of falling asleep as referred in Ogilvie (2001).

Clinical sleep specialists are trained for the adequate recognition of those traits inspecting each 30-second EEG epoch at a time for a whole night of sleep. The stage scoring is ultimately determined using the supplementary activity delivered by the additional PSG channels, especially EOG and EMG. Turning the epoch analysis into an iterative process, sleep specialists reconstruct an overnight sleep pattern based on the stage scoring of consecutive 30-second epochs. This outcome is known as a hypnogram. The related hurdles presented in the Introduction denote the main challenges for the proper analysis of regular sleep and characterisation of related disorders: (i) a complete subject's recording requires the analysis of multiple channels of several hours for several nights, which further implies considerable periods of assessment by the specialists. Moreover, (ii) the existence of subject-specific traits hinders the application of adequate models to fit the whole population, such a drawback is referred as inter-subjects' variability. To complete the bundle, (iii) the backgrounds and criteria of scorers commonly defer in the identification of events, leading to inter-raters' variability.

The upcoming sections dissect the literature background in the identification of the main challenges, proposed approaches and remnant downsides to overcome.

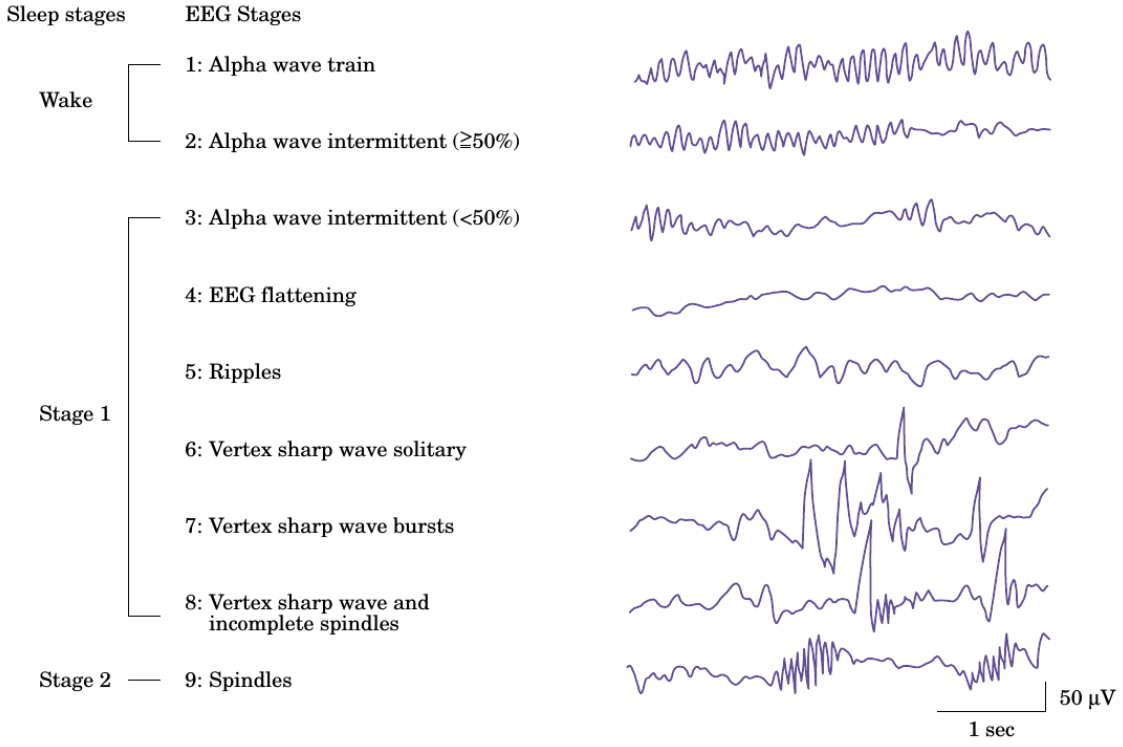

FIGURE 2.1: EEG signals and transients associated with the process of falling asleep (Ogilvie, 2001).

2.1 Sleep Analysis: Standardisation Era

The convergence of standardised manuals and sophisticated computational approaches has set forth a comprehensive solution to overcome these issues. Emerging concepts like biomedical signal processing by Mesin et al. (2011), Pereda et al. (2005) or quantitative EEG (qEEG) by Thakor and Tong (2004) have continuously suggested methods to bring timely fair analysis, detrend inter-subject variability and align inter-raters criteria. To Merica and Fortune (2004) and Ogilvie (2001) computer-assisted methods not only can contribute to a more accurate and efficient characterisation of sleep structure, but also a more robust identification and classification of disorders, particularly insomnia and schizophrenia.

The European SIESTA project described in Klosh et al. (2001) pioneered the analysis of inter-subject and inter-rater variability amongst experienced scorers from eight European sleep laboratories, including 196 recordings from 98 patients affected by depression, general anxiety disorder, insomnia, Parkinson's disease, period limb movements and sleep apnoea. The study conducted by Danker-Hopfe et al. (2004) using SIESTA data revealed some conclusions from the quantitative and qualitative point of view. For sleep staging, applying R&K rules, the overall rate of agreement amongst scorers was 0.6816, which in terms of Cohen's κ index [1] indicated a substantial agreement. In the

[1] It is one of the most popular statistics to measure the inter-rater agreement based on a numerical and categorical rating. The scores range from $0-0.2$ light, $0.21-0.4$ fair, $0.41-0.6$ moderate, $0.61-0.8$ substantial and $0.81-1$ as perfect agreement.

case of related disorders, the index values ranged between 0.6138 for Parkinson's disease and 0.8176 for generalised anxiety disorder with insomnia, as per Danker-Hopfe et al. (2004). Although, the study pointed out that R&K manual was developed for healthy individuals rather than disordered ones. Whereas, the EEG could exhibit irregular patterns that the existing rules failed to characterise. Moreover, the scoring of N1 obtained the lowest rate of agreement 0.3490, a stage commonly associated to sleep onset, also known as hypnagogic state. The transition from W-to-N1 and N2-to-N3 stages recurrently required a subjective estimation, due to inter-subject variability with respect to the α band decrease.

In the same direction, a review of sleep EEG patterns according to R&K rules in Rodenbeck et al. (2006) introduced some recommendations for their application in sleep scoring by clinicians and computer-aided systems. A multidisciplinary task force provided a consorted interpretation of relevant EEG patterns for sleep scoring, i.e. α, δ, θ waves, SS, KC,VSW and SW. The differing definitions were discussed and reformulated resulting in specifications and amendments of the scoring rules introduced by Rodenbeck et al. (2006). Each pattern was independently analysed to indicate onset and offset cues in terms of amplitude, frequency, duration, scalp derivations, morphology and surrounding events. The compilation of amended rules sought more reliable expert scoring and standardised algorithms supported on computational platforms. This initiative found a response in the AASM standard, which extended the repertoire of rules, cortical derivations and relevant channels, moving from EEG to PSG analysis. Once more, the inter-rater variability was under the scope of Danker-Hopfe and colleagues to measure the level of agreement as per AASM rules in Danker-Hopfe et al. (2009). The overall sleep staging agreement amongst scorers achieved Cohen's κ 0.76 and higher rates for all stages compared to R&K manual, except for N2. The team concluded that the improvements might be attributed to the integration of occipital, central and frontal derivations, as well as, the refined criteria to score frequency bands and transients. On the other hand, Danker-Hopfe et al. (2009) claimed that the N2 misinterpretation was explained by the omission of arousal events with concurrent submental activity as a critical indication for N2 termination.

A later study by Novelli et al. (2009) aimed to describe in detail the differences between R&K and AASM scoring criteria in a group of healthy children. The PSG recordings from 45 children (18 females and 27 males) aged between 3-16 years old were scored by three experienced scorers using both manuals. The applied statistical analysis reassured significant differences in the recognition of N1, N2 and REM stages. Foremost, low agreement was found in the number of N1 and N2 stages shifts per hour, minutes and percentage between the compared standards. The results advised some caution in the adoption of a new standard amongst children, specially in the percentage of N1 and number of shifts, which is more strictly measured in terms of arousals occurrence during sleep onset. For that reason, Iber et al. (2007) AASM manual includes a separate section of guidelines for sleep scoring in children.

Recently, Rosenberg and Van Hout (2013) conducted a comprehensive inter-scorer reliability study using 1800 epochs and more than 2500 experienced scorers in order to examine areas of disagreement for future revisions of AASM manual. Sleep stage agreement averaged 82.6%, where the highest match was reached by REM stage 90.5%,

followed by N2 85.2% and W 84.1%. N3 and N1 attained the lowest rates 67.4% and 63%, correspondingly. In addition, scorers had recurrent problems to identify the sleep onset transitions; i.e. last epoch of W stage, first epoch of N2 after N1 stage and first REM after N2 stage. This study reflected the persistent disagreements in N1 and N2 scoring, previously mentioned by examinations of the same type. Therefore, the study suggested a series of modifications to be included in later revisions of the manual: 1) scoring centres might wish to set a relatively lower average agreement (e.g. 75%) that reflects basic stage scoring competence; 2) changing the definition of stage N1 to require either decrease of α rhythm or the onset of low amplitude mixed frequency EEG; 3) providing more objective criteria for key waveforms like α rhythms, KC and SS; 4) changing the onset of REM stage to the first epoch of definite REM stage; and 5) using alternative methods for analysis of SW activity, such as frequency analysis.

2.2 Sleep Analysis: Digital Era

Automated or computer-assisted systems for sleep analysis have been extensively proposed to match the aforementioned guidelines and incoming recommendations of standardisation bodies. The (i) time-consuming assessments, (ii) inter-subjects' variability, (iii) inter-raters' variability and more recently the inter-rater-machine's variability, persist as the main challenges to be overcome using the computational power of digital era. However, it is important to review some of the most outstanding approaches that aimed to converge standard-based sleep analysis with computational processing. Most of the original contributions of this work were built upon the advancements of those approaches that in a bolder or subtler manner improved at least one of the identified main challenges.

The initial efforts have been oriented to migrate the sleep analysis, preprocessing and staging from entirely expert-based to computer-based analysis. The reduction of assessment times is the first tangible advantage, as well as, a more efficient management of inter-subjects' variability by the anticipation of outlying subjects' traits. Similarly, the inter-raters' variability tends to decrease due to resilience to ambiguity or disagreement of computational systems. However, comparisons between expert and automated systems, i.e. inter-rater-machine's variability is a work in progress. Yet, some studies have referred to the state-of-the-art with interesting findings.

2.2.1 Computer-Assisted Scoring Overview

Caffarel et al. (2006) compared the sleep staging of an automated neural network (ANN) and a human scorer using the R&K manual to characterise 114 patients presumably affected by obstructed sleep apnoea (OSA) syndrome. The coarsed classification of wake, light and deep sleep between manual and automatic scoring obtained an overall inter-rater Cohen's κ index of 0.305, i.e. a fair agreement. The inter-rater variability slightly improved to distinct wake from sleep stages (0.449). The clinical practice concluded that ANN-based analysis was not accurate enough to sleep staging based on the R&K

standard. Whereas, the automated system performed a second-by-second scoring rather than epoch-by-epoch as per the manual. The alternative Automatic Sleep EEG Analysis (ASEEGA) approach based on a single EEG channel to perform R&K automatic sleep scoring was compared against the manual scoring of two experts upon 15 healthy volunteers. Performing an epoch-by-epoch classification between 2 states (wake and sleep), 3 states (wake, REM and NREM), 4 states (wake, REM, N1/2 and N3) and 5 states (wake, REM, N1, N2 and N3); the overall Cohen's κ indexes were: 0.82, 0.81, 0.75 and 0.72, respectively, i.e. substantial agreement for all scenarios. Berthomier *et al.* claimed that the appealing results came from the implementation of an initial preprocessing stage, followed by a spectral-temporal feature extraction and adaptive fuzzy logic for stages classification. However, Berthomier et al. (2007) suggested larger cohorts to assess the impact of inter-subject variability and the inclusion of disordered subjects under up-to-date scoring standards.

Moving forward to AASM rules, Anderer et al. (2010) conveyed a validation study between a computer-assisted sleep classification system versus 2 sleep scorers. The approach Somnolyzer 24×7 was modified to comply with the AASM rules upon 72 PSG recordings from the SIESTA project. The cross-validation between manual and automatic scoring consisted of two Somnolyzer-assisted staging, two manual staging and two Somnolyzer versus two manual staging. The overall Cohen's κ index reached by the two computer-aided analyses was 0.99, the two manual scorings was 0.76 and the automatic against manual was 0.755, i.e. substantial agreement. The most pronounced disagreement occurred with the N1 stage with $0.55-0.6$ as maximum rates for all cases. This study highlighted the reduction of inter-rater variability by the application of the automatic approach, although expert corrections were required to obtain comparable results, thus a semi-automated scoring was the actual achievement.

A most recent multicentre validation study by Hedner et al. (2011) recruited 38 healthy subjects and 189 patients with Obstructive Sleep Apnoea (OSA) to simultaneously undergo an overnight PSG and Peripheral Arterial Tone (PAT) recording. The PAT system automatically scored light/deep and REM sleep based on features related to arterial tone amplitudes and interpulse periods using a proprietary finger probe to measure the blood flow variability. In turn, sleep onset stages N1 and N2 from PSG recordings were manually scored by sleep technicians. For the detection of light/deep and REM sleep, the overall inter-scorers' agreement was 0.88. Nonetheless, Cohen's κ indexes for the distinctive sleep stages were: sleep from wake 0.48, REM from nonREM sleep $0.55/0.59$ and deep from light sleep 0.46. In conclusion, the automatic PAT analysis performed a moderate agreement to manual scoring techniques either in control or OSA-affected subjects. The study argued that the overall inter-scorers' agreement might be insufficient to fulfil the accuracy required for a clinical use of PAT systems.

This thesis considered the previous findings and reviewed additional computer-based approaches about biosignals preprocessing and sleep staging. Here, it is recalled relevant insights from the aforementioned research works. Such a literature review assisted the hypotheses conception, methods implementation and comparative parameters of the proposed models, described as a whole in Chapters 3-8.

In the preprocessing field, Chang et al. (2000) suggested a blind signal separation (BSS) algorithm assuming coloured sensor noises, i.e. frequency range-specific noise, and nonstationary signals. PSG signals complied with those constraints making the signal extraction approach particularly suitable for EEG signals denoising. Although, the system used simulated data rather than clinical datasets, restraining the evaluation of practical applications. Delorme and Makeig (2004) achieved a big leap of development with EEGLAB toolbox by including artefact rejection, filtering, epoch selection, among other capabilities. The toolbox is a compelling benchmark, however, the processing load of most supported algorithms is a drawback for the reduction of computation periods. Precisely, Ting et al. (2006) introduced a BSS algorithm based on Second Order Statistics (SOS) for the analysis of brain responses as a result of specific sensory, cognitive or motor stimuli, defined as Event-Related Potentials (ERP). The lower complexity order of SOS proved its efficacy in terms of mean square error (MSE) reaching -20dB with 1000-sample signals, then its application seemed to be appropriate within the context of PSG preprocessing. Devuyst et al. (2008) tested the modified approach to remove ECG artefacts from simulated and real EEG signals. They obtained an overall removal of artefacts, namely correction rate of 0.91, disregarding other PSG signals of relevance for sleep analysis like EOG. More recently, the system proposed by Romo-Vázquez et al. (2012) merged in a single system artefact removal and denoising capabilities using BSS-SOS. Their correction rate was 0.96.

In this thesis, the proposed model embraced the outstanding contributions of the described approaches to extend them to a wider PSG preprocessing centred in sleep analysis, which will be discussed in Chapter 5.

2.2.2 Computer-Assisted Sleep Staging Overview

In regard to automatic sleep staging, Djuric et al. (2002) discussed the principles for the analysis of highly nonlinear and non-Gaussian signals, e.g. EEG signals. The solution consisted of time-varying non-Gaussian autoregressive processes to model simulated data with outperforming results in terms of MSE around 0.0005 μV^2. However, its application with real datasets remained elusive. The works of Liu and West (2001) and Arulampalam et al. (2002) supplemented the autoregressive process approaches with the iterative parameter estimation using particle filtering. This technique enabled the modelling of chaotic signals, e.g. EEG signals, through statistical approximations rather than conventional approaches based on oversimplified conditions of linearity and Gaussianity. Respectively, the publications Arulampalam et al. (2002), Liu and West (2001) are formatted as a book and a journal tutorial discussing the general conceptual framework instead of case-specific scenarios. In response, Prado proposed an algorithm integrating autoregressive models and particle filtering with different model orders, number of particles and realisations to compute the statistical approximations to the signals' processes Prado (2013). Prado developed a heuristic and comparative work upon simulated and real datasets to find the most performant parameters in the modelling of chaotic signals. For the present thesis, autoregressive processes with particle filtering were adopted for the modelling and processing of PSG signals looking forward to score sleep stages automatically. The method developed by Álvarez-Estévez

et al. (2013) for automatic analysis of sleep macrostructure in continuum suggested fuzzy inference system (FIS) to perform the classification of stages. A cross-validation between expert and system generated hypnograms attested an appealing performance using sensitivity 0.3, specificity 0.9, accuracy 0.64 and area under the curve 0.88. Foremost, the advantage of FIS underlies in the human-like classification rulesets to conceal standard scoring rules with the uncertain transition of sleep stages.

The computer-assisted sleep staging approach introduced in this project, exploited the FIS capabilities to achieve automated sleep stages classification by Dubois and Prade (1980), Kaufmann and Gupta (1985). Whilst, the inter-subject's and inter-rater's variability were considered. Whereas, FIS are supported on human-like decision making, outlying subject-specific traits or scorer-biased criteria can be integrated into a single but exception-tolerant classification ruleset. All related material about this awaits on Chapter 7-8.

Computer-assisted analysis has not been only applied to preprocessing or automatic sleep staging. It has also taken part in the characterisation of other complex behavioural, psychological, psychiatric pathophysiologies. The two following sections make a review of the definition, diagnosis and computer-aided characterisation of insomnia and schizophrenia disorders.

2.2.3 Computer-assisted Disorders Characterisation Overview

For Mayers and Baldwin (2006) sleep and psychiatric disorders have demonstrated an association with quantifiable physiological symptoms, such as dysregulation in the autonomic and neuroendocrine changes controlled by the hypothalamus. For example, depression is distinguished by the absence of sleep stage 4, difficulty to stay asleep, increased heart rate, hyperactivity of the sympathetic nervous system, hypothalamic pituitary overactive state, self-regulated body temperature variations, amongst others. Gillin et al. (1979) pioneered the classification of control, insomnia and depression patients based on EEG signals. The study proposed 8 variables for the distinction of depression patients: total sleep time, total recording time, sleep efficiency, sleep latency, early morning awake time, awake time, REM time and REM percentage. In the same direction, Nissen et al. (2001) posited spectral analysis to classify depression and insomnia patients by examining the changes in EEG δ ratio during NREM sleep. Staner et al. (2003) and colleagues supported the association of hyperarousal with sleep disturbance and abnormal levels of arousals in depressive insomnia patients. The study extracted EEG frequency bands during the sleep onset and first NREM from control, primary insomnia and depressive insomnia groups. The findings revealed that hyperarousals characterised the primary insomnia with stronger EEG activity during sleep onset, whilst depressive insomnia patients reported fewer SWS. In the next section, a more elaborated definition and description of hyperarousals is introduced in the dedicated context for insomnia characterisation.

As per Iverson et al. (2005), depression patients have shown a shortened REM latency and distinctive heart rate patterns than the normal signature of control subjects. Therefore, there has been a scaled interest for Heart Rate Variability (HRV) analysis during

sleep. The HRV patterns through the wake to sleep onset transition in generalised anxiety and depression patients are statistically different to melancholic depressed patients. The related study by Iverson et al. (2005) suggested heart rate as a marker for supporting diagnosis of mental illnesses. Jurysta et al. (2010) attempted to establish the relationship between cardiac activity and EEG δ power in major depression disorder. Albeit, non-significant link was found between control and patients cohorts; neither parasympathetic nor sympathetic parameters differed in both groups. Conversely, Udupa et al. (2007) identified an increased sympathetic and decreased parasympathetic activity in major depression patients in comparison to control subjects. The study reported the alteration between cardiac function and EEG δ band in the primary insomnia and depression patients, the understanding of that interaction has not fully described, yet.

The results from the aforementioned studies suggested that symptoms of heightened physiological arousal (hyperarousal) are common characteristics to differentiate control, insomnia and depression individuals. Hitherto, the advancements in computer-assisted classification of sleep and psychiatric disorders like insomnia, sleep apnoea, depression, bipolar disorder and schizophrenia have focused on EEG and ECG measures. Despite of spectral and wavelet analysis of EEG frequency bands have achieved a differentiation of control and disordered groups, the linear approach of those methods has not sufficed the extraction of meaningful information and abnormalities detection. In consequence, nonlinear methods have been introduced. Leistedt et al. (2007) employed Detrended Fluctuation Analysis (DFA) to analyse EEG time series in control and depression patients. Depression patients showed a weaker autocorrelation of DFA measures during SWS, which may indicate a breakdown of physiological complexity for depression specific conditions. However, a proper methodology and benchmarking for supervised predictions is still elusive to be widely adopted by the clinical community according to Boostani et al. (2009).

2.3 Sleep, Insomnia and related Disorders

The criteria found in the Diagnostic and Statistical Manual (DSM-IV-TR) of the American Psychiatric Association established that sleep disturbances resulting in impairments of daytime functioning or clinically significant distress are classified as insomnia APA (2000). Although, it is noteworthy to distinguish between primary and secondary insomnia. In regard to the former, the diagnostic criteria state as major traits: inhibition to fall asleep, maintain sleep, or both. Also, the disturbance should not concur with another mental disorder, e.g. major depression, anxiety, delirium or others. The DSM-IV-TR guidelines support the diagnoses of the International Classifications of Sleep Disorders, which defines primary insomnia essentially as the same as psychophysiological insomnia. This college body points out the most common causes: high concentration of overnight arousals and behavioural factors like stressful lifestyle.

For the secondary insomnia, the landscape is a bit more complicated. Since, its diagnostic criteria often report patient's inhibition of sleep accompanied by psychiatric disorders or aside pathologies. However, it is difficult to specify whether the insomnia

disorder is caused by the prescribed medication, the psychiatric pathology, psychological distress or a combination of the previous. A revision of the patient's medical history could assist to disclose correlations between side effects of medication, clinical distress and sleep patterns. Even though, APA (2000) states that sleep disturbance and insomnia are common symptoms of most psychiatric disorders.

It is not possible to characterise insomnia markers relaying on PSG recordings, exclusively. Furthermore, intended objective criteria of irregular sleep hardly match the patient's experience of insomnia due to the ever present inter-subjects' variability. Such a constraint hinders the application of objective criteria upon PSG signals. For that reason, the AASM scoring manual does not recommend the unilateral usage of PSG to evaluate chronic insomnia. Nonetheless, PSG analysis on patients employs metrics as prolonged latency to sleep onset, frequency of arousals, and reduced amounts of total sleep to set the lead towards abnormal sleep patterns. Hereupon, surveys, subjective tests (e.g. Epworth Sleepiness Scale) and interviews in APA (2000) play a supplementary role for a more comprehensive diagnosis. The challenge can be stated as a paradox. It is difficult to determine whether the abnormal PSG activity is caused by the sleep disturbances or vice versa. For instance, insomnia patients commonly report anxiety, distress or phobia of being unable to fall asleep, which have further consequences in an impaired daytime performance. In the study conducted by Morin et al. (2006) other patients pressure themselves with certain expectations about their sleep quality, then major disturbances happen when such expectations drift. This fixation is a product of a passive and persistent overreflection about negative emotions. Such a condition is known as rumination, which in turn, inflicts a psychophysiological distress that might derive in depression as sustained in Treynor et al. (2003). PSG analysis exhibits significantly reduced sleep duration and efficiency, increased arousal index, less REM sleep in insomnia patients compared to control subjects. In Staner (2010) work the initial findings revealed an increased EEG β activity during W, S1 and REM in insomnia with a reduction in EEG δ and θ bands in both REM and NREM. Conversely, it is not clear whether insomnia has a causal effect in the increased autonomic activity or such an activity triggers the insomnia symptoms. Jurysta et al. (2009) suggested a relation between autonomic activity and EEG δ sleep with the onset of chronic insomnia. Thalamic, thalamocortical and cortical neurons coproduce SWS during normal sleep; its interaction with the cardiac cycle is tracked down to the thalamus cells. There existed an attenuated linear correlation between cardiac vagal activity and EEG δ power in insomnia patients. On the contrary, it was found a strong cardiac parasympathetic activity preceded by EEG δ power appearance in control group.

Epidemiological research has indicated a high comorbidity of insomnia with depression, where common causal relationships might drive both disorders, as per Freeman et al. (2009). The analysis of PSG sleeping patterns at particular stages has supported the identification of symptoms and further classification. Staner (2010) showed that the induction of severe sleep restriction in healthy population led to EEG abnormalities and hormonal disturbances similar to depression cases. More precisely, increasing sleep latency and wake percentage, accompanied by low density of Slow Waves (SW) during REM sleep, have been acknowledged as usual cues of major depression. Primary insomnia and depressed patients shared strong β and γ activity during nonREM stages, whilst

only depressed individuals preserved high SW activity during REM sleep. That increasing EEG activity has been denoted as a wake promoting mechanism, i.e. hyperarousal, which has been observed in insomnia and depression patients. Arousals have gained attention as cues of sleep disruption linked to some sleep disorders. Long arousals (> 30 s) may have a noticeable impact in sustained sleep, whilst shorter ones (*ca.* 9 s) are likely a lack of self-awareness by subjects. However, PSG throughout EEG and ECG channels does assist in the objective marking of those events examining the appearance and duration of EEG frequency shifts. A study conducted by Nofzinger Nofzinger et al. (2004) linked an increased EEG β power during NREM sleep and high glucose metabolism with the occurrence of arousals in the prefrontal cortex and the right lateral inferior occipital cortex. The relationship of arousals with psychological, behavioural, physiological parameters of that nature requires further research.

Spiegelhalder et al. (2012) proposed a hyperarousal model of primary insomnia to measure its effects in nonrestorative sleep. The study examined the spectral power values related to wake-promoting and sleep-protective mechanisms of 29 healthy sleepers against 25 primary insomnia patients. The appearance of EEG β ($\kappa = 0.74$) and ς ($\kappa = 0.89$) frequency bands at N2 sleep stage in insomnia indicated concurrent activation of cortical arousal and sleep spindles by the end of the sleep onset. That opposed neural activity patterns, which could contribute to the experience of nonrestorative sleep in disordered subjects. Even though, the hyperarousal phenomenon could be better interpreted by observing the association of CNS and the ANS, e.g. HRV.

A retrospective study on PSG data Maes et al. (2013) analysed the spectral power of EEG and HRV power bands of 11 healthy controls and 17 primary insomnia patients. The results confirmed the importance of N2 sleep stage to delimit sleep onset completion towards deep sleep settlement. During the sleep onset period, the insomnia patients exhibited elevated EEG β activity immediately accompanied by KC and SS. Likewise, a strong association was found between high EEG α band with KC and low dominance of the parasympathetic ANS, i.e. weak HRV high frequency (0.15-0.4 Hz) power. Thus, the study implied that an increased arousal density was related to the delayed happening of the first KC amongst patients, that means, short-term waking disruptions inhibited the onset of deeper sleep promoters from the CNS and ANS. The initiation of sleep is not the only facet of insomnia, but also sleep maintenance has been a recurrent issue of clinical consultation. The computer-assisted processing has also contributed to its characterisation by the analysis of finer EEG frequency bands, such as β_1 (16-18 Hz), β_2 (18-30 Hz) and β_3 (30-40 Hz). Such a segmentation facilitated the extraction of meaningful features by digging into much specific regions of the spectrum. Besides, the remanence of the events in the lower bands could carry stronger effects in the neighbouring bands of β rather than the distant ones.

Cervena et al. (2013) study compared the power spectra features of 10 sleep onset insomnia, 10 sleep maintenance insomnia subjects and 10 healthy individuals. Their conclusions suggested that there are significant differences between sleep onset and sleep maintenance of insomnia in the EEG β_2 band, previous to sleep onset period. The primary insomnia concentrated elevated power values in EEG β_1 band, rather than EEG β_2 as it was shown by sleep maintenance patients. Furthermore, differences in the EEG

δ band activity between the two insomnia groups posited alternative mechanisms to hyperarousal in the wake-promoting sleep-protective dilemma.

A review prepared by Feige et al. (2013) explored in detail the hyperarousal concept from an ANS and CNS level, adding up subjective and existing computer-based methods. The analysed studies of Bastien et al. (2014) included self-questionnaires about sleep quality, Cyclic Alternating Pattern (CAP)[2], spectral analysis and assessment of ERP[3] during sleep. From ERP perspective, primary insomnia patients showed a more sensitive response to auditory stimuli during sleep onset periods, as well as a pronounced EEG negative stimulus-evoked potential occurring between 80-120 ms after the stimulus, known as N100. Also, ERP studies postulated REM as the sleep stage with greater relevance to reflect the perception of sleep quality, its latency's variance led to under or overestimations using self-evaluations, as Bastien et al. (2014) claimed. Some of the most interesting conclusions linked the increasing frequency of arousals during REM and NREM sleep in insomnia groups. Using PSG analysis and self-questionnaires, high EEG β powers, arousal density, CAP rates, sleep latency misperception were commonly implicated with NREM sleep instability, i.e. opposed wake-promoting and sleep-protective mechanisms.

Moving towards a more comprehensive diagnosis of insomnia, Morin et al. (2006) conducted a telephone survey across Québec territory (Canada) with 2001 participants to estimate the prevalence of insomnia symptoms and syndromes in the general population. The study concluded that 29.9% of the population confirmed the presence of insomnia symptoms, albeit only 9.5% met medical criteria for insomnia syndrome. Following a more rigorous model of clinical diagnosis and treatment, Petrovsky et al. (2014) proposed a proof-of-concept model based on sleep deprivation to assess behavioural (e.g. chronic fatigue) to psychiatric impairments (e.g. psychosis). Their findings pointed out that sleep deprivation accompanied by quantifiable biomarkers could model psychiatric disorders by mimicking their pathological origin. Such quantifiable biomarkers have become the main target of the most recent computer-assisted approaches.

The two-fold analysis of sleep macro and microstructure represented by sleep staging and arousal detection were explored in this thesis using novel techniques. For instance, graph spectral theory supported on the essays of Ipsen and Mikhailov (2002), Jakobson and Rivin (2002) and Stoica and Moses (2005) spanned the sleep analysis and biomarkers generation in the characterisation of hyperarousal and insomnia. Likewise, Álvarez-Estévez *et al.* proposed an automated processing and classification method for the detection of arousals. Its performance reported sensitivity 86% and specificity 76% rates. The approaches described in Chapters 7-8 addressed the same computational model aiming to deal with inter-subjects' and inter-raters' variability efficiently.

[2]CAP describes a periodic EEG activity between bursts of SS and KC events followed by more stable sleep.

[3]ERP waveforms exhibit positive and negative voltage deflections and a latency in milliseconds (e.g. P300) provoked by external visual, auditory or somatosensory stimuli.

2.4 Sleep, Schizophrenia and related Disorders

Schizophrenia is the second disorder studied during the course of the project and related works on sleep analysis with group differences. Zalesky et al. (2011a) understood schizophrenia as a severe psychiatric condition characterised by the abnormal integration of neural frequency bands and transients. Freeman et al. (2009) demonstrated comorbidity with anxiety, paranoia, depression and insomnia. The cognitive and behavioural impairments of schizophrenia revealed the brain's inability to integrate neural processes at different regions, which is know as functional dysconnectivity by Zalesky et al. (2011a).

An early study by Ferrarelli et al. (2007) examined schizophrenia markers upon PSG signals, focusing on the amplitude, duration and number of SS. These three parameters were compared amongst medicated schizophrenia patients, control and depressed patients during the initial NREM episodes. Therein was found an attenuated, shorter and reduced version of SS in schizophrenia cohort. Later on, Ferrarelli et al. (2010) investigated the abnormal SS activity in a larger schizophrenia cohort by the analysis of overnight recordings using NREM stages. The study recruited 49 schizophrenia, 20 medicated non-schizophrenia and 44 control patients. The experiment compared the average number of SWS and SS at different time slots (i.e. density), duration, amplitude and frequency. The results showed that schizophrenia patients had no changes in the SWS parameters, but did have a reduction in SS power (12-16 Hz) and in slow (12-14 Hz) and fast (14-16 Hz) SS amplitude, duration, number in the prefrontal, centro-parietal and temporal brain regions. And, no significant SS reduction was detected in the medicated non-schizophrenia patients. Based on this, the authors posited that schizophrenia clearly affects the neural thalamic reticular nucleus and thalamo-reticular network, responsible for the generation of SS.

The formal usage of computer-assited models to assist schizophrenia characterisation focused on the automated detection of EEG events and derived abnormal patterns. Timashev et al. (2012) introduced a computational method to analyse cross-correlations in EEG signals in order to diagnose schizophrenia. Based upon the synchronisation of frequency-phase estimates of 84 diagnosed children and adolescent subjects, EEG signals were clustered into 4 groups of risk level for susceptibility to schizophrenia. The cross-correlations of EEG γ and β frequency bands originated in the frontal regions of the scalp, could support the diagnosis of schizophrenia at early stages. The work also claimed the suitability of the approach in the diagnosis of neurodegenerative disorders (e.g. Parkinson's and Huntington's disease), measuring different cortical areas and including elder population.

Nikulin et al. (2012) conducted a study to quantify long-range (5-50 s) temporal correlations of multichannel EEG recordings at resting condition upon 18 schizophrenia patients and 28 healthy individuals. Despite of no difference in the amplitudes of the EEG α and β bands between healthy and patients, the temporal correlations demonstrated a serious decrease in both frequency ranges in patients. Most of the decrements were detected over the fronto-central areas, where β activity is usually generated. In

regard to the parieto-occipital regions, cross-frequency correlations were reported between α and β bands for schizophrenia group. These findings could imply that similar abnormalities affect the functional neural networks commanding α and β oscillations, and hence the decrease of temporal correlations due to excessive switching between neuronal states.

Such a hypothesis was recalled by Noh et al. (2013) in their study about the relation of coupled local and global feedback circuits in the cortical functional networks with the abnormal synchronisation in 15 schizophrenia patients. Noh et al. (2013) attributed the dysfunctional switching between neural states not only to the abundance of feedback connections, but also to the detailed coupling patterns. The feedback connections are a method based on noncausal impulse responses, i.e. the output of an input signal depending on past, present and future inputs. Then, the construction of functional feedback networks revealed that the coupled local and global feedback circuits were significantly reduced in schizophrenia subjects. Using Wilson-Cowen computational analysis, it was concluded that feedback circuits were intrinsically involved in the dynamical switching between EEG β and γ power bands. The former band showed an increasing circuits' synchronisation, whilst the latter had a reduction compared to the healthy group. Thereupon, it was claimed that schizophrenia patients might have an impaired coupling of inter and intraregional functional feedbacks and the derived circuits caused an abnormal synchronisation amongst neural oscillations.

Bob (2012) findings suggested that a candidate mechanism for the integration of conciousness neural processes was the EEG γ activity. It was shown that γ oscillations synchronise different neural networks with the sensory information to bind percepts, memories and conscience states. Physiological and anatomical evidences have posited the disturbances in the synchronisation of γ activity as a determinant of dysfunctional consciousness towards schizophrenia. Similar states of greatly reduced consciousness have been observed during deep sleep—N3 stage—and seizures, albeit they conserved intense levels of neuronal activity. For Chouinard et al. (2004), the sleep state has gained interest as an appropriate scenario to determine the dynamics of the neural networks related to schizophrenia. Hitherto, schizophrenia was approached through spatial neural synchronisation by the location of specific EEG oscillations at particular scalp locations. However, the examination of temporal dynamics framed only a representation of neural processes within short-term and long-term correlations. Optional spectrum, phase-dependent, nonlinear or hybrid approaches were disregarded.

The interpretation of schizophrenia traits has not only focused on the analysis of the interactions within the CNS, but also has counted on ANS expressions throughout heart rate variability (HRV). The HRV monitors the temporal variations of ECG R-to-R intervals and drives the predominance of sympathetic and parasympathetic subsystems. The study conducted by Bar et al. (2007) demonstrated that non-medicated schizophrenia patients exhibited decreased RMSSD (root mean square of successive R-to-R differences), pNN50 (percentage of adjacent R-to-R intervals that differ by more than 50 ms) and HF band power ($0.15 - 0.4$ Hz) compared to control subjects. These three HRV time-domain measurements are tightly correlated with a parasympathetic activity decrease in schizophrenia patients without effect of any medication in such dynamics. The connection of parasympathetic subsystem or vagal tone with schizophrenia was further

investigated by Henry *et al.*. The study included by Henry et al. (2010) hospitalised maniac bipolar, schizophrenia and control subjects using time-based, frequency-based and nonlinear methods to analyse HRV. Here, it was found that the parasympathetic activity was significantly reduced in bipolar and schizophrenia patients. A similar reduction was detected in control subjects, non-significant though. Also, the heart rate's complexity metrics significantly decreased in bipolar disorder patients appealing to linear and nonlinear approaches.

The Acharya et al. (2006) review made an illustrative discussion about the relationship of HRV with neighbouring body functions, pathologies and habits. On the same path, Jurysta et al. (2003) examined the interactions between HRV and EEG power spectra using PSG recordings of 8 healthy men. The study revealed that all EEG power bands were associated to the normalised HRV HF band. And more importantly, modifications on the cardiac vagal or parasympathetic activity were observed in parallel to changes in the EEG δ band. Such a finding took Dumont et al. (2004) to investigate whether the interdependency between HRV and EEG power spectra is linear or nonlinear. Their conclusions opened a new research trail based on nonlinear analysis, since they demonstrated the nonlinear interdependency of EEG δ, θ and α bands with HRV HF band. Thus, the synchronisation concept was introduced to estimate the linear and nonlinear interdependencies amongst power spectra. Later works expanded the synchronisation approach to amplitude estimations and statistical analysis; but phase synchronisation gained recognition due to its robustness tracking subtle transitions amongst EEG-HRV processes, as Bartsch et al. (2007), Palva et al. (2005) showed.

Considering a wider set of PSG sources, Schulz et al. (2012) worked on the relationship between schizophrenia and the cardiac ANS. The research demonstrated a dysfunctional cardiac activity in association with decreased parasympathetic and increased sympathetic activity in patients. The respiration was the third signal under examination due to its relationship with the brainstem and higher centres of the ANS, e.g. the hypothalamus. The experimental framework evaluated the cardiorespiratory regulation in schizophrenia patients, their first degree relatives and control groups. In order to characterise the autonomic regulation, the coupling metrics were computed; including linear, nonlinear, indices, respiratory variability, complexity and dynamics. The statistical findings evidenced a significant difference in schizophrenia patients compared to the two remaining cohorts in the respiratory variability and their dynamics. Specifically, increased complexity and reduced respiratory sinusarrhythmia—i.e. variation in the cardiac frequency occurring in a breathing cycle.— The reduction in the cardiorespiratory coupling maintained against the control and first degree relatives groups.

Synchronisation studies have gained popularity in the scientific community as an approach to integrate the diversity of physiological processes that participate in sleep dynamics and characterisation of comorbid disorders, like schizophrenia Mezeiova and Palus (2012). For instance, Uhlhaas and Singer (2010) investigated the cross-frequency synchronisation between EEG high and low frequencies considering long-range and local cortical areas. The research characterised schizophrenia through the abnormal synchronisation of EEG β and γ bands during cognitive, motor and at rest states. The dysfunctional synchronisation is claimed to be associated with the impairment or disconnectivity of cortical networks in medial frontal, parietal/occipital, and left temporal.

Generally, β and γ synchronisations were present in local cortical areas and the low frequency EEG δ and θ activity was restrained to and between more distant cortical areas. The authors acknowledged that it is uncertain to what extent the impairment in local cortical circuits promoted long-range synchronisation dysfunctions or conversely both were independent phenomena. Supporting studies by Cho et al. (2006), Uhlhaas (2006) characterised schizophrenia patients with a reduced activity of EEG θ band and phase synchronisation in the frontal cortical area during cognitive tasks.

The pharmacological component in the treatment of schizophrenia has also played an important role in the investigation of the abnormal EEG activity. Uhlhaas and Singer (2010) reported irregular amplitudes and phases of EEG γ bands in patients with schizophrenic symptoms and treated with medication. However, the evidence in favour of a causal relationship between EEG synchronisation dysfunctions and pharmacological treatments was not supported; due to the brief administration of the medication and the occurrence of similar EEG abnormalities in other psychiatric disorders, like autism and bipolar disorder. These results confirmed the need for more competent characterisation techniques of schizophrenia and related psychiatric disorders at different stages of conciousness.

Dimitriadis et al. (2009) developed a nonlinear approach to find functional clusters related to spontaneous brain activity during sleep. Their results suggested a differentiated functional dynamics for all stages, variable hemispheric asymmetry and the isolation of cortical regions during REM sleep. Even though, the synchronisation proof-of-concept has seemingly succeeded, its prowess within disorders' characterisation was still pending. Sakkalis et al. (2009) took an initial approach on this matter by conducting a study to estimate the synchronisation of cognitive function in children with mild epileptic seizures. They proposed that there is a significant difference in the nonlinear phase synchronisation between controls and epileptics in occipital and parietal lobes. In the same direction, Jurysta et al. (2010) investigated the major depressive disorder related to altered neuroplasticity and cardiovascular pathologies. By using spectral synchronisation, they showed that the disorder was related to an altered link between parasympathetic and EEG δ band leading to impairments in cardiovascular controls.

The present thesis is an innovative research work addressing the analysis of schizophrenia using synchronisation methods. The evidence drew forth by previous works and the given comorbidity of psychiatric pathologies with schizophrenia, motivated the characterisation decanted in Chapter 6.

Chapter 3

Aims and Hypotheses

The literature review supported the identification of the main challenges in regard to the computer-assisted sleep analysis and characterisation of insomnia and schizophrenia. Those gaps are summarised here.

(i) Time-consuming assessments: PSG recordings gather up biosignals at different body regions, such as brain, heart, chest, legs, eyes, etc. The number of electrodes, sensors, sampling rates, recording duration and frequency sessions put out a substantial amount of raw data. The expert-based analysis has a key role to find abnormalities cues within sleep patterns. This is an industrious and time-consuming task for specialists.

(ii) Inter-rater variability: The dissimilar background, experience and criteria of sleep scorers hinder the objective identification of sleep events upon the recorded data. This situation leads to either an overestimation or underestimation of regular and irregular sleep patterns. A variability amongst raters might produce deceiving assessments about the actual condition of the patient, compromising on-time diagnosis and treatment.

(iii) Inter-subject variability: The existence of subject-specific traits upon the recorded data is an expected outcome of sleep analysis. The oversight of non-compliant sleep patterns as per standard guidelines, become a challenge to the application of more accurate diagnosis procedures. Models that fit the average population are required to cope with minor and major variances amongst subjects' patterns.

The outlined main challenges framed the formulation of the project backbone based on the research questions and related testing hypotheses. The general research question (G1) embodies the uttermost objective of the research towards a better understanding of sleep electrophysiology and related disorders.

G1. How can sleep electrophysiology be analysed and characterised to differentiate between control, insomnia and schizophrenia groups or individuals?

However, more specific research questions were required to deconstruct the problem in a systematic way. The synchronisation core study in Chapter 6 was the first approach to characterise control and disordered groups, subject to the challenges of time-consuming assessment and inter-raters'/subjects' variability. The EEG and ECG signals might elucidate the nature of functional interactions; not only amongst healthy groups, but also regarding sleep disordered populations. For Zalesky et al. (2011b) cognitive and behavioural traits are the product of coordinated or dysfunctional neuronal processes, which can be tracked by cardiac dynamics as per Dumont et al. (2007) claimed. The interaction of cardiac control centres and the brainstem reflects oscillations derived from R-to-R intervals and neuronal discharges. The related research question (Q) and formulated testing hypotheses (H) are shown below.

Q1. How can neuronal and cardiac synchronisation from PSG analysis be estimated in order to detect regular sleep, insomnia and schizophrenia patterns?

H1.1. Control, insomnia and schizophrenia neuro-cardiac activity can be distinctively characterised by cross-frequency coherences across EEG-HRV bands and sleep stages.

H1.2. Control, insomnia and schizophrenia neuro-cardiac activity can be distinctively characterised by cross-frequency phase coupling across EEG-HRV bands and sleep stages.

The core study and hypotheses explore differences and commonalities amongst healthy, insomnia and schizophrenia sleep architecture and neuronal-cardiac interdependency. Two hypotheses intended to prove or disprove the cohorts differentiation through two documented major approaches in sleep analysis and biomedical signal processing. First, interdependence of brain and ANS subsystems comprises quantifiable levels of coherence and synchronisation across the sleep regulation process to distinct regular and abnormal patterns. This method refers to as a linear approach. And second, the computation of cross-frequency phase coupling (i.e. nonlinear approach) describes the interaction of neural and cardiac power bands. As the literature review pointed out, the nonlinear approaches have become a growing trend to characterise sleep dynamics, associated disorders and psychiatric pathologies. With the latter hypothesis, the prowess of nonlinear methods was evaluated in insomnia and schizophrenia groups simultaneously, whilst the first hypothesis benchmarked the findings with the traditional linear techniques.

Chapter 6 supported by the Methods and Discussion chapters, presents certain novelties about the biomedical signal processing and sleep characterisation revealed by the study.

The second question is related to the computer-assisted sleep onset staging and insomnia characterisation. Apart from the challenge *per se* of this two-fold study, the three main challenges affected once more the proposal of efficient models looking forward the patient's welfare. The two proposed hypotheses tested signal processing techniques rarely used in sleep analysis and disorders characterisation contexts, but proven by Ipsen and Mikhailov (2002) in physics and chaotic modelling. Whereas, fuzzy inference for

sleep onset staging and graph spectral theory for insomnia characterisation, fitted the ultimate goal and related constraints; it was worthwhile to address the hypotheses in that direction.

Q2. What processing and classification techniques can assist the characterisation of PSG activity into standard sleep onset stages for the analysis of regular sleep and insomnia disorder? What is an adequate validation method for the proposed techniques?

H2.1. Inter-subject and inter-rater variability in computer-assisted sleep staging can be appropriately mitigated by FIS.

H2.2. Control and insomnia sleep onset patterns can be sufficiently differentiated by graph spectral theory and statistical analysis.

PSG biosignals are analysed to score the sleep stages and identify disordered patterns. This task is time-consuming not only for the sleep experts, but also inconvenient for the patients. Therefore, the computer-assisted systems are a viable solution to reduce the time required in PSG analysis. Additionally, most existing computer-aided systems dismiss the nonlinear, nonstationary, non-Gaussian constraints on the PSG signals, as Gencaga et al. (2010) demonstrated. These constraints hinder the proper identification of key waveforms, transients and power bands. Even more, when inter-subjects' variability has a significant pull.

The characterisation of insomnia subjects through simple metrics is a challenge. Graph spectral theory explained by Stoica and Moses (2005) is a solution hypothesis, since it can model sleep stages transitions in terms of low-complex indexes. Thereupon, a distance measure is computed using those sleep transitions to quantify the degrees of similarity. A logistic regression is finally deployed to differentiate control from subjects with insomnia.

The Chapter 7 details the testing hypotheses' outcomes and Discussion Chapter 9 makes the final remarks about their confirmation or rejection.

The third and final research question about the computer-assisted arousal detection fabricated its hypothesis about the pertinence of fuzzy inference for this particular problem. Given the outperforming results of the previous study, it seemed reasonable to test a similar approach for the characterisation of sleep microevents or arousals.

Q3. What processing and classification techniques can assist the detection of arousal events in PSG activity amongst control and insomnia individuals? What is an adequate validation method for the proposed techniques?

H3. Inter-subject and inter-rater variability in computer-assisted arousal detection can be appropriately reduced by FIS.

The relationship of arousal occurrence with regular and abnormal sleeping patterns has yet to be defined, according to Jurysta et al. (2009). PSG recordings are commonly used to characterise the different kinds of arousals. For Danker-Hopfe et al. (2009) the computer-assisted detection deals with inter-subject and scorer-specific challenges, given the pesistent variability. The R&K, ASDA or AASM scoring manuals have differing criteria to pinpoint the onset and offset of arousals. Therefore, there is no consensus about these guidelines amongst specialists. Computer-assisted solutions have the potential of accurate arousal detection that can be tolerant to inter-rater and inter-subject variability.

The Chapter 8 frames all the relevant material about the validation of the testing hypothesis and further insights.

There is one more hypothesis to be introduced. Even though it is not a research headline, it does perform a fundamental role in the adequate preparation of data, methods, experimental set-ups and findings interpretation. It refers to the preprocessing core study and its corresponding hypothesis states as follows.

H4. The removal of embedded artefacts and high frequency noise upon PSG can be sufficiently decreased by BSS-SOS and WPT decompositions.

An appropriate PSG signals preprocessing is crucial to the success of subsequent processing and classification routines, in order to obtain reliable outcomes in sleep and disorders characterisation Penzel et al. (2007). The proposed model chases down the nonstationarity and nonlineatiry characteristics of namely EEG and EOG signals. The hypothesis evaluates whether computation time-efficient and low complex approach can surmount slow time-varying, pulse-type artefacts and EMG high-frequency noise. The eventual rejection of the null hypothesis posits a robust preprocessing framework to extract reliable information from sleep analysis and disorder characterisation in upcoming studies.

Chapter 4

Materials and Methods

The research presented in this thesis consists of 4 studies: preprocessing, synchronisation, sleep onset staging and arousal detection, which were the computational foundations to characterise the electrophysiology of sleep in terms of analysis and disorders identification—i.e. insomnia and schizophrenia—. This chapter summarises the relevant details of the existing testing and clinical data used for each study. Afterwards, the methods for the biomedical signal processing upon polysomnograms are described.

4.1 Materials

The preprocessing study used the existing data provided by Dr. Dean Cvetkovic as part of his biofeedback study conducted in 2006. The ethics consideration and procedures were approved by the local Ethics Committee of RMIT University. Table 4.1 depicts a summary of the recruited cohort and additional technical details of the recordings.

TABLE 4.1: Summary of data and short daytime polysomnogram (sdPSG) details for preprocessing study

Feature	Description
Subjects	10 male healthy ($M = 28.3, SD = 6.75$)
System	g.tec's MobiLAB System
sdPSG channels	EEG: O2-A1, C3-A2 REOG, LEOG ECG-lead II EMG: submental (chin)
sdPSG length	20 min
Epoch length	10 s
Sampling frequency	256 Hz
Provided by	Dr. Cvetkovic as part of his biofeedback study
Approval by	RMIT Ethics Committee

The synchronisation study focused on insomnia and schizophrenia characterisation relied on the existing PSG datasets provided by the Sleep Laboratory of the Central Institute of Mental Health in Mannheim (Germany). The ethics consideration and procedures were approved by the local Ethics Committee of the Medical Faculty Mannheim of the University of Heidelberg and RMIT Ethics Committee. Table 4.2 frames a summary of the recruited cohort and additional technical details of the recordings.

TABLE 4.2: Summary of clinical data and recording details for synchronisation study

Feature	Description
Subjects	10 healthy subjects (5 male, 5 female) 9 insomnia patients (4 male, 5 female) 10 schizophrenia patients (5 male, 5 female)
PSG channels	EEG: C4-A1, C3-A2, O2-A1, O1-A2, Cz-A1, F8-A1, F7-A2 EOG: F4-A1, F3-A2
PSG length	6-8 h
Epochs staging	R&K manual (W/S1/S2/S3/S4/REM)
Epoch length	30 s
Sampling frequency	250 Hz
Provided by	Sleep Laboratory of the Central Institute Mental Health Mannheim
Approval by	Ethics Committee of the Medical Faculty Mannheim RMIT Ethics Committee

Schizophrenia patients were diagnosed as per the DSM-IV-TR and recruited during in-house treatment in the Central Institute of Mental Health. The study's subjects and patients needed to fulfil the following inclusion criteria: age between 18 and 60 years, ability to provide informed consent, stabilised disease course and stable (at least two weeks) psychopharmacological treatment in the form of monotherapy with a second generation antipsychotic, as well as absence of psychiatric comorbidity. Antipsychotic medication consisted of risperidone, aripiprazole, amisulpride, quetiapine, olanzapine and clozapine. Insomnia patients were matched from a patient sample undergoing diagnostic procedures in the sleep laboratory. Their diagnoses were based on anamnese, i.e. clinical interviews, and PSG findings according to the International Classification of Sleep Disorders, 2nd edition (ICSD-2).

The studies conducted for the sleep onset staging for insomnia characterisation and arousal detection used the existing PSG recordings provided by the Interdisciplinary Centre for Sleep Medicine, Charité Universitätsmedizin in Berlin (Germany). The ethics consideration and procedures were approved by the local Ethics Committee of the Charité Universitätsmedizin Berlin and RMIT Ethics Committee. All subjects and patients gave their written consent. Table 4.3 shows a summary of the recruited cohort and additional technical details of the recordings.

Insomnia diagnosis was done according to the ICD-10 Classification of Mental and Behavioural Disorders of the World Health Organization Organization (1993). Their diagnoses were based on anamnese, i.e. clinical interviews, followed by the overnight PSG

TABLE 4.3: Summary of clinical data and recording details for sleep onset staging and arousal studies

Feature	Description
Subjects	20 male healthy subjects 20 male insomnia patients
PSG channels	EEG: C4-A1 EOG: right, left EMG: chin, left tibialis
PSG length	6-8 h
Epoch staging	AASM manual (W/N1/N2/N3/REM)
Epoch length	30 s
Sampling frequency	200 Hz
Provided by	Interdisciplinary Centre for Sleep Medicine Charité Universitätsmedizin
Approval by	Ethics Committee of the Charité Universitätsmedizin Berlin RMIT Ethics Committee

recordings to rule out comorbid sleep or psychiatric disorders. A group of sleep specialists (three technicians and one head physician) performed the sleep stages scoring, according to the guidelines of the AASM manual. Each 30-second epoch was evaluated and mapped to a particular stage: wake (W), nonREM1 (N1), nonREM2 (N2), nonREM3 (N3) and Rapid Eye Movement (REM).

For all the PSG recording, the EEG montage was compliant to the 10-20 international system in Figure 4.1.

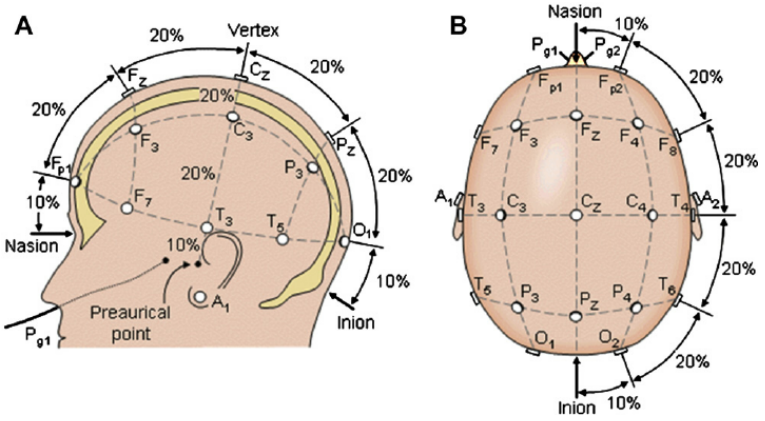

FIGURE 4.1: 10-20 international system EEG montage (Iber et al., 2007).

4.2 Methods

4.2.1 Biosignals Modelling

The main goal of this initial step is to generate a general representation of the PSG biosignals using a collection of coefficients that contribute to the extraction of high quality features in upcoming analysis. Also, the synthesis of biosignals consisting of thousands of time points into a few number of coefficients improved the computational efforts related to the processing load and memory storage. The studies on preprocessing, synchronisation, sleep onset staging and arousal detection deal with a collection of PSG signals, such as EEG, EOG, ECG and EMG. The proposed computer-assisted approach by Galka et al. (2011) used the state-space Time Varying Autoregressive Moving Average (TVARMA) realisations with order p, q to model each of them. Thus, system and observation model equations Eq. 4.1-4.2 governed the representation of PSG epochs, denoted as follows:

$$\mathbf{x}[k] = \mathbf{x}[k-1] + \eta[k] \tag{4.1}$$

$$\mathbf{y}[k] = \mathbf{A}\mathbf{x}[k] + \mathbf{x}^{\mathrm{H}}[k]\mathbf{B}\nu[k] \tag{4.2}$$

where $\mathbf{x}[k]$ is the estimated vector of system coefficients understood as the synthesis vector of the PSG epoch. The system noise vector $\eta[k]$ is divided in two terms $[\eta_{\mathbf{p}}[k]\ \eta_{\mathbf{q}}[k]]$ to distinguish AR(p) and MA(q) noise processes, where $\eta_{\mathbf{p}}$ is Cauchy-Lorentz[1] distributed with zero translation and $\varsigma^2_{\eta_{\mathbf{p}}}$ dispersion, $\eta_{\mathbf{p}} \sim \mathscr{C}(0, \varsigma^2_{\eta_{\mathbf{p}}}\mathbf{I})$. In turn, $\eta_{\mathbf{q}}$ is Gaussian distributed with zero mean and $\sigma^2_{\eta_{\mathbf{q}}}$ variance, $\eta_{\mathbf{q}} \sim \mathscr{N}(0, \sigma^2_{\eta_{\mathbf{q}}}\mathbf{I})$. The vector $\mathbf{y}[k]$ represents the estimated epoch, accompanied by $\mathbf{A}$ and $\mathbf{B}$ matrices in (4.3)-(4.4) to perform the weighted linear combinations. The vector $\nu[k]$ is the Gaussian distributed observation noise with zero mean and σ^2_{ν} variance, $\nu \sim \mathscr{N}(0, \sigma^2_{\nu}\mathbf{I})$.

$$\mathbf{A} = [\mathbf{y}[k-1], \cdots, \mathbf{y}[k-p] | 0, \cdots, 0] \tag{4.3}$$

$$\mathbf{B} = \begin{bmatrix} \mathbf{0}_{p\times p} & \mathbf{0} \\ \mathbf{0} & \mathbf{I}_{(q+1)\times(q+1)} \end{bmatrix} \tag{4.4}$$

As it is described in the sections 4.2.2 and 4.2.3, the preprocessing and synchronisation studies focused on Eq. 4.2, whereas the related analysis was performed upon the original PSG epochs or observations, rather than estimations.

The sleep onset staging and arousal detection studies included a previous estimation step using Eq. 4.1 to recursively model the PSG epochs. In this way, it was guaranteed the extraction of features with relevant information.

[1] Cauchy-Lorentz distribution belongs to the family of probability density functions with two-sided heavy tails, i.e. the typical Gaussian monotonically decaying values at the distant points from the distribution's mean are replaced by subtle bell-shaped curves.

4.2.2 Preprocessing Model

The first study introduced a model to remove embedded artefacts and attenuate additive white noise upon PSG epochs. The preprocessing model characterised the epochs using Eq. 4.2 to complete the biosignals' analysis throughout the 4 sequential modules, depicted in Figure 4.2.

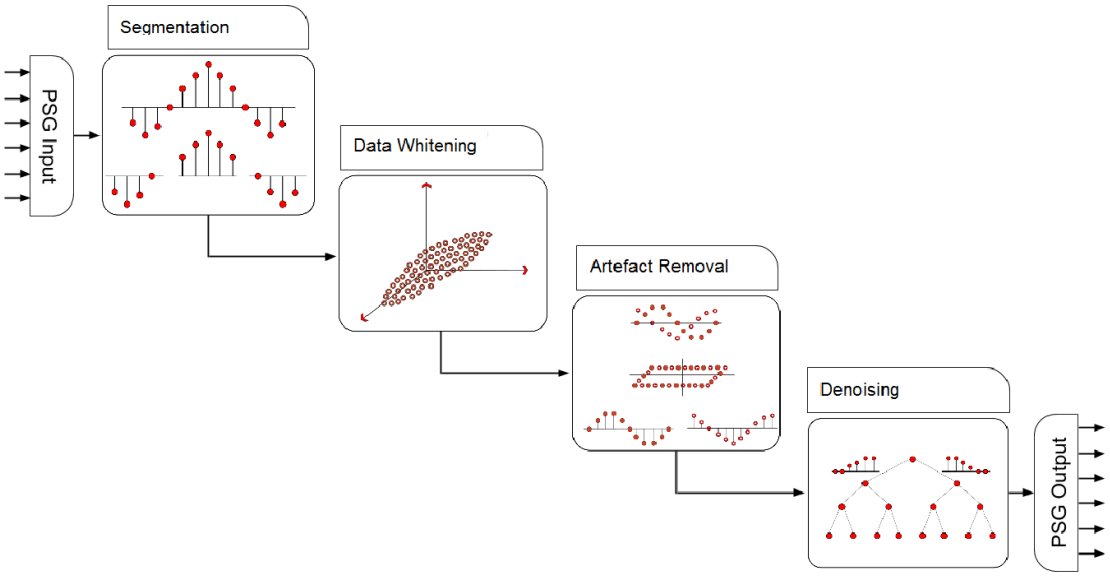

FIGURE 4.2: sdPSG preprocessing system. The system integrates an initial data segmentation module in charge of 10 seconds epochs generation, followed by a data whitening module to perform baseline correction. Thirdly, artefact removal module based on BSS-SOS methods handles the separation of pulse-type artefacts, and lastly denoising module attenuates additive noise and high frequency activity.

The first module fragmented the raw short daytime polysomnogram (sdPSG) signals into fixed-size epoch lengths. Secondly, the data whitening module strived to epoch stationarity, i.e. unchanging signals' expectations and variances at shifted time instants. Besides, Principal Component Analysis (PCA) strived towards the orthogonality amongst biosignals. The PCA-based whitening improved the spatial resolution and baseline correction. At the same time, the PSG signal power was maximised and eventual data redundancy withdrawn, as Delorme and Makeig (2004) showed. In the course of PSG recording, biosignals are prone to exhibit minor DC-signal offsets over time. Then, a baseline correction was performed by PCA transformation for even reference estimations.

The third module managed the artefacts removal separating EEG/EOG signals from the ECG/EMG embedded artefacts based on ICA with BSS-SOS methods for low-complexity and efficiency in assessment time. Muscular activity is normally fast time-varying with linear embedding upon the principal components, i.e. EEG and EOG. The heart rate signals are pulse-type distinguished by a periodic linear combination with the neighbouring channels. Therefore, ICA based on expectations and standard deviations was proposed by Cichocki and Amari (2005) as the most appropriate approach. Nonetheless, statistical constraints over the model needed to be assumed. For

instance, Delorme and Makeig (2004) showed that linear mixing of unobserved source signals and negligible differential time delays, as long as, estimated PSG signals are statistically independent.

Lastly, the denoising module suppressed the additive Gaussian noise, background noise and high frequency EMG activity using WPT decomposition to cancel out high-regime spectrum coefficients. EEG/EOG information is usually found below *ca.* 64 Hz (β band), the module was designed to remove the spectral content above that EEG band. The denoising process performed a tree-shaped decomposition based on WPT explained in Mallat (1999), which uses a low-pass and high-pass filtering, simultaneously. Haidekker (2011) forged a wavelet coefficient shrinkage to cancel out undesired frequency components of the original PSG signal. Thus, the WPT-based denoising approach by Thakor and Tong (2004) coped with the nonstationarity, pseudostochasticity and additive noise.

The overall preprocessing model set the ground for the efficacy of the ensuing core studies. The upcoming sections describe the associated models in detail.

4.2.3 Synchronisation Model

The second study about synchronisation pursued the differentiation amongst control, insomnia and schizophrenia subjects by deploying linear and nonlinear methods. Initially, the preparation of PSG channels had a neural parcellation, which aggregated EEG signals from neighbouring derivations into a single signal based on their correlation or divergence measures. This interareal aggregation sought a reduction of PSG channels dimension and efficiency in computation load, whereas a whole set of EEG scalp derivations could lead to an excessive processing time. From the resulting aggregated EEG signals, δ-θ-α-ς-β and γ frequency bands were extracted. The same decomposition routine obtained the Heart Rate Variability (HRV) frequency bands: LF (0.04-0.15 Hz) and HF (0.15-0.4 Hz) performing a R-to-R interval (RRI) computation upon the ECG channel.

The synchronisation model employed three different approaches to extract the features to estimate the functional interdependence between neuronal and cardiac oscillations. The first and second approaches were the cross-correlation function (CCF) and wavelet coherence (WCOH), both performed a linear analysis. The CCF $\mathbf{R}_{\mathbf{xy}}(\tau)$ in Eq. 4.5 calculated the linear correlation as a function of time lags τ to measure the mutual relationship between the EEG $\mathbf{x}[k]$ and HRV $\mathbf{y}[k]$ bands with N samples.

$$\begin{aligned}\mathbf{R}_{\mathbf{xy}}(\tau) &= E\{\mathbf{x}[k+\tau]\mathbf{y}^{\mathrm{H}}[k]\} \\ &= \frac{1}{N-|\tau|}\sum_{k=1}^{N-\tau}\mathbf{x}[k+\tau]\mathbf{y}^{\mathrm{H}}[k]\end{aligned} \tag{4.5}$$

The WCOH method in Eq. 4.6 computed the auto $\mathbf{S_{xx|yy}}(\omega_0)$ and cross $\mathbf{S_{xy|yx}}(\omega_0)$ power spectrum between EEG and HRV bands to produce a 0-to-1 value, where 0 meant no coherence and 1 complete coherence.

$$\begin{aligned} {\kappa_{\mathbf{xy}}}^2(\omega_0) &= \frac{|\mathbf{S_{xy}}(\omega_0)|^2}{|\mathbf{S_{xx}}(\omega_0)||\mathbf{S_{yy}}(\omega_0)|} \\ &= \frac{|\mathbf{S}\left({\mathbf{W_{xx}}}^{\mathrm{H}}(s,\tau)\mathbf{W_{yy}}(s,\tau)\right)|^2}{|\mathbf{S}\left(\mathbf{W_{xx}}(s,\tau)\right)||\mathbf{S}\left(\mathbf{W_{yy}}(s,\tau)\right)|} \end{aligned} \tag{4.6}$$

$\mathbf{W}(s,\tau)$ expressed the continuous wavelet transform at scale s and translation index τ.

The third and final approach came from the nonlinear dynamics, which was oriented to the analysis of instantaneous phases as product of successive convolutions with complex-valued Morlet wavelets. The phase locking value (PLV) $\zeta_{n,m}$ in Eq. 4.7 determined in a 0 (absent) to 1 (strong) scale the $n:m$ phase synchronisation of n cycles from one EEG band and m cycles of one HRV band. The vector $\hat{\varphi}_{n,m}[k]$ grouped the instantaneous phases to allocate them into a $[0, 2\pi m]$ interval.

$$\begin{aligned} \zeta_{n,m} &= \left|E\{\mathbf{e}^{\imath\hat{\varphi}_{n,m}[k]}\}\right| \\ &= \sqrt{\left(E\{\cos\hat{\varphi}_{n,m}[k]\}\right)^2 + \left(E\{\sin\hat{\varphi}_{n,m}[k]\}\right)^2} \end{aligned} \tag{4.7}$$

Figure 4.3 shows a diagram of the PLV method, including the aforementioned steps in a graphical way.

4.2.4 Sleep Onset Staging Model

The main goal of the staging model was the generation of computer-assisted hypnograms looking forward to characterise insomnia disorder supported on the pattern recognition during sleep onset periods. The sleep onset staging model comprised an initial biosignal processing, followed by the automated hypnogram generation, and the inference of transitions networks with the assessment of similarity distances. Figure 4.4 summarises the complete computational model.

The starting biosignal modelling was done with Time Varying Autoregressive Moving Average TVARMA (p,q) processes to model sudden and slow-paced changes within biosignals. Such an approach used Cauchy-Lorentz-distributed state-space realisations as in Eq. 4.1-4.2 to overcome the nonlinearity, nonstationarity and nonGaussianity constraints of PSG signals. The Cauchy-Lorentz distribution had a heavy-tailed deviations to give probabilistic relevance to abrupt fluctuations and a fastened dispersion in the central region to record smoother dynamics. Given that nonlinear and nonGaussian models have no closed-form solutions, we implemented a recursive Monte Carlo filter—a.k.a

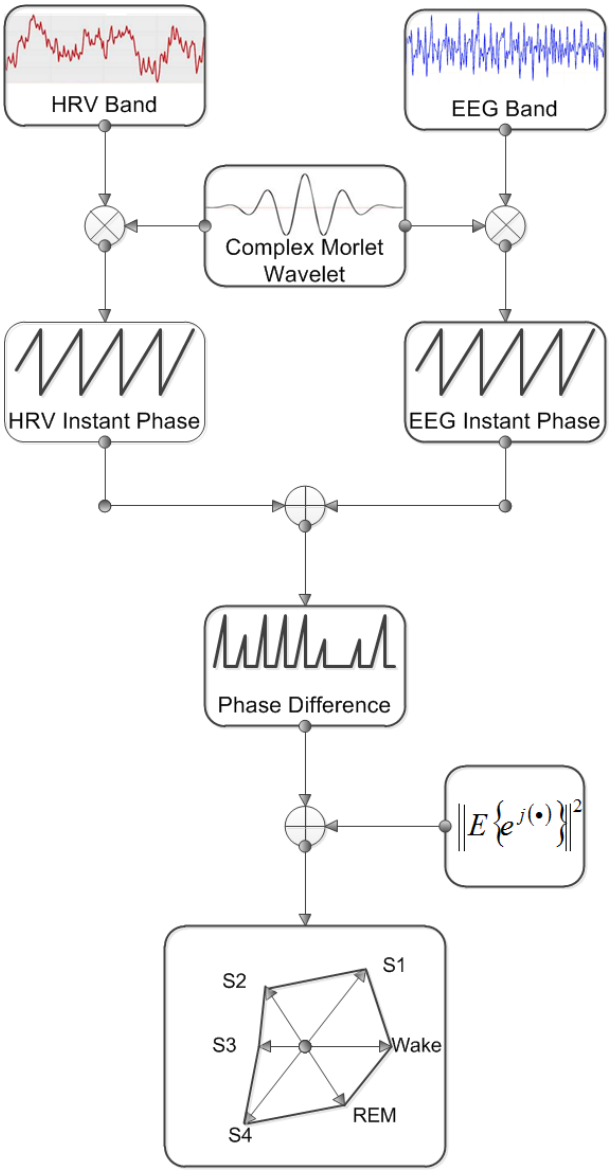

FIGURE 4.3: Flow diagram of Phase Locking Value (PLV) method. EEG and HRV decomposed bands are independently convolved with the complex-valued Morlet wavelet. The operation generates a time series of instant phases for EEG and HRV side, which are time instant-wise subtracted to find a vector of phase values, located within $[0, 2\pi]$ interval. Then, the magnitude and average of phase difference vector are computed to produce the PLV value at each sleep stage.

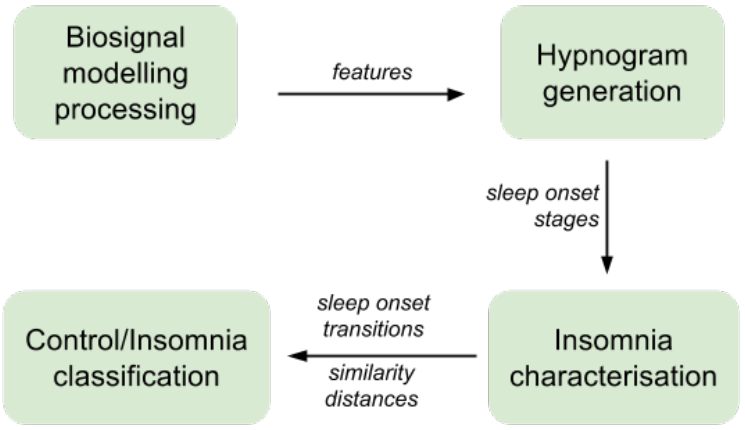

FIGURE 4.4: Block diagram of our modular computational approach for insomnia characterisation. The system uses biosignal processing based on TVARMA$(8,2)$ models and particle filtering to extract the biosignal features, which are fed into a fuzzy inference system to automatically generate a hypnogram of the subject's sleep onset period. From the hypnogram, a sleep stages transition network is derived to compute unidimensional metrics or similarity distances using graph spectral theory. Finally, a logistic regression classifies the subjects into control or insomnia groups.

particle filter—to compute the system's coefficients. The particle filter built up the time-changing dynamics of biosignals with probabilistic distributions approximated by a series of samples or particles. Akaike (AIC) and Bayesian Information Criterion (BIC) defined the optimal model orders $p = 8$ and $q = 2$ to balance over and underestimations.

In regard to the biosignals processing, the features were extracted convolving the non-Gaussian TVARMA(8,2) coefficients with a bank of complex Morlet wavelets. From the EEG derivation, δ (0.5-4 Hz), θ (4-7 Hz), α_1 (7-9.5 Hz), α_2 (9.5-12 Hz), ς_1 (12-14 Hz), ς_2 (14-16 Hz), β_1 (16-18 Hz), β_2 (18-30 Hz) and β_3 (30-40 Hz) instantaneous power bands $\mathbf{P}[k]$ were extracted; accompanied by transients counters of VSW, KC, SS. From the EOG channels, rapid and slow eye movements came from the differential amplitude levels of left and right derivations. The amplitude of EMG channels contributed with the features associated to the chin tension and limb movements. Table 4.4 lists the aforementioned features.

To produce the hypnogram of the sleep onset periods, a classifier was used to assemble W, N1 and N2 stages on a time sequential basis based on the extracted features. An initial classification approach consisted of an ensemble classifier, which engaged hundreds to thousands of weak sub-classifiers to fulfil a more comprehensive differentiation task. The ensemble classifier in Figure 4.5 gathered 300 tree-type sub-classifiers to map incoming EEG, EOG and EMG features to three possible output sets: W, N1 and N2. The classifier validation undertook a Leave-One-Out (LOO) strategy, where a single subject dataset had a training purpose at a time and the remaining recordings served as testing datasets.

Considering the uncertain and overlapping characteristics of sleep staging, the ensemble classifier evolved in the Mamdani FIS in Figure 4.6. The fuzzy logic-based classifier mapped an input space of the EEG/EOG/EMG features to an output space of W, N1 and

TABLE 4.4: Features for sleep onset estimation

#	Feature	Channel	Event/Freq. Band (Hz)
1	$P_{\delta}[k]$	EEG C4-A1	$0.5-2$
2	$P_{\theta}[k]$	EEG C4-A1	$4-7$
3	$P_{\alpha_1}[k]$	EEG C4-A1	$7-9.5$
4	$P_{\alpha_2}[k]$	EEG C4-A1	$9.5-12$
5	$P_{\varsigma_1}[k]$	EEG C4-A1	$12-14$, SS
6	$P_{\varsigma_2}[k]$	EEG C4-A1	$14-16$, SS
7	$P_{\beta_1}[k]$	EEG C4-A1	$16-18$
8	$P_{\beta_2}[k]$	EEG C4-A1	$18-30$
9	$P_{\beta_3}[k]$	EEG C4-A1	$30-40$
10-11	A_{EEG}	EEG C4-A1	VSW, KC
12-13	A_{EOG}	LEOG/REOG	Slow/rapid eye movement
14	A_{EMG}	EMG chin	Chin tension
15	A_{EMG}	EMG tibialis	Limb movement

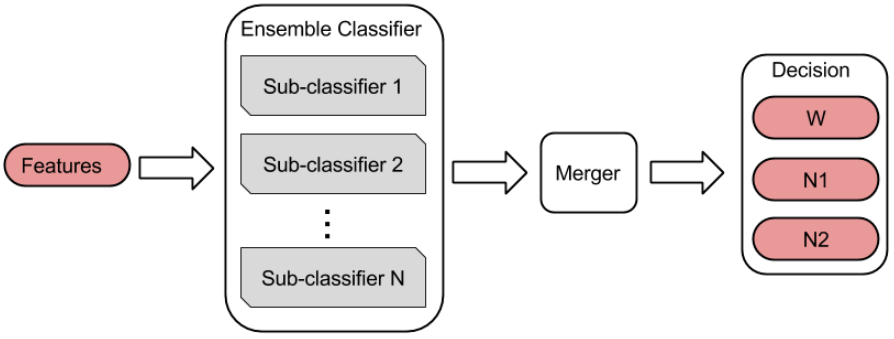

FIGURE 4.5: Diagram of ensemble classifier. The epoch's features act as inputs to 300 tree-type sub-classifiers, followed by a merger to produce an unambiguous decision either as W, N1 or N2 stage.

N2 sleep stages. The bridging between input and output spaces was defined by fuzzy rules or 'if-then' statements following the guidelines of AASM scoring manual and suggestions of experienced scorers. Either ensemble or fuzzy classifier complied with the automatic generation of a hypnogram describing one subject's sleep onset patterns.

Towards the insomnia characterisation, the expert-scored or automated generated hypnogram was transformed into a sleep transition network with 3 vertices—one per each sleep onset stage—and weighted directed edges denoting the inverse of the total number of transitions in both directions. Based upon the network representation, degree, adjacency and incidence matrices were inferred to perform a matrix factorisation in terms of eigenvectors, eigenvalues and singular values—i.e. graph spectrum—. Such a technique is commonly referred as Graph Spectral Theory (GST). Figure 4.7 depicts all the previous components.

The GST yielded a similarity measurement between two sleep transition networks (G,H) supported on the content of matrices and eigenvalues. The similarity distance $d_1(G,H)$ performed an eigenvalue decomposition (EVD) to the Laplacian matrix $\mathbf{L}_{G|H}$ to find

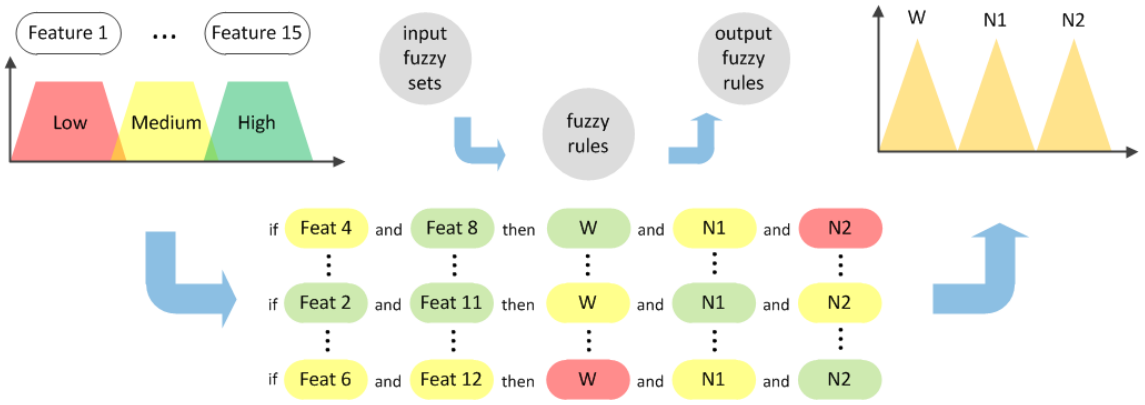

FIGURE 4.6: Diagram of fuzzy inference system consisting of input/output fuzzy sets and fuzzy rules. Each 30-second epoch is described by 15 features, whose values are mapped to 3 possible input fuzzy sets: low, medium and high; using trapezoidal functions of membership. The fuzzy rules follow a boolean logic of fuzzy variables with weighting selection. The output fuzzy sets determine the degree of membership of each 30-second epoch to a sleep onset stage.

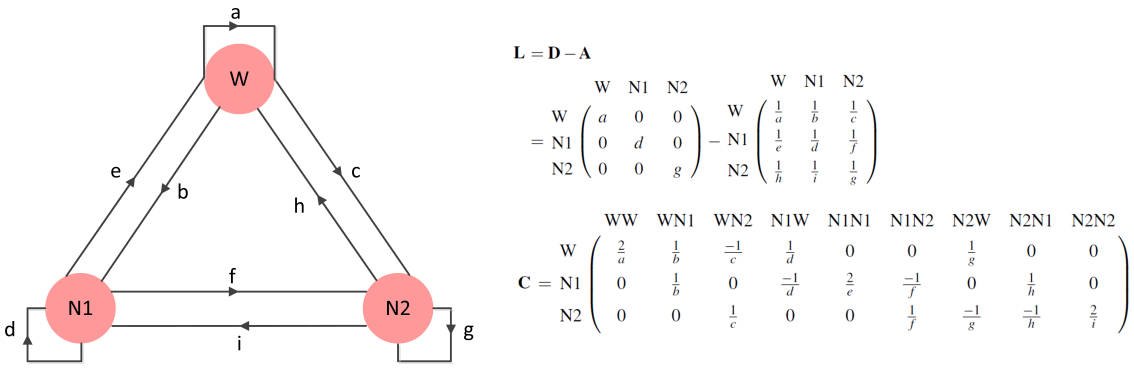

$$\mathbf{L} = \mathbf{D} - \mathbf{A}$$

$$\begin{array}{c} \\ \mathrm{W} \\ = \mathrm{N1} \\ \mathrm{N2} \end{array} \begin{array}{c} \begin{array}{ccc} \mathrm{W} & \mathrm{N1} & \mathrm{N2} \end{array} \\ \begin{pmatrix} a & 0 & 0 \\ 0 & d & 0 \\ 0 & 0 & g \end{pmatrix} \end{array} - \begin{array}{c} \begin{array}{ccc} \mathrm{W} & \mathrm{N1} & \mathrm{N2} \end{array} \\ \begin{array}{c} \mathrm{W} \\ \mathrm{N1} \\ \mathrm{N2} \end{array} \begin{pmatrix} \frac{1}{a} & \frac{1}{b} & \frac{1}{c} \\ \frac{1}{e} & \frac{1}{d} & \frac{1}{f} \\ \frac{1}{h} & \frac{1}{i} & \frac{1}{g} \end{pmatrix} \end{array}$$

$$\mathbf{C} = \begin{array}{c} \\ \mathrm{W} \\ \mathrm{N1} \\ \mathrm{N2} \end{array} \begin{array}{c} \begin{array}{ccccccccc} \mathrm{WW} & \mathrm{WN1} & \mathrm{WN2} & \mathrm{N1W} & \mathrm{N1N1} & \mathrm{N1N2} & \mathrm{N2W} & \mathrm{N2N1} & \mathrm{N2N2} \end{array} \\ \begin{pmatrix} \frac{2}{a} & \frac{1}{b} & \frac{-1}{c} & \frac{1}{d} & 0 & 0 & \frac{1}{g} & 0 & 0 \\ 0 & \frac{1}{b} & 0 & \frac{-1}{d} & \frac{2}{e} & \frac{-1}{f} & 0 & \frac{1}{h} & 0 \\ 0 & 0 & \frac{1}{c} & 0 & 0 & \frac{1}{f} & \frac{-1}{g} & \frac{-1}{h} & \frac{2}{i} \end{pmatrix} \end{array}$$

FIGURE 4.7: Sleep stages transition network and related matrices based upon a subject's hypnogram. A transition network consists of 3 vertices (i.e. one per sleep onset stages W/N1/N2) and 9 directed edges with a weight equal to the inverse of the total number of transitions between the corresponding vertices. Three matrices are derived from the transition network: degree **D**, adjacency **A** and incidence **C**. The adjacency **A** and incidence **C** matrices values correspond to the inverse of the total number of transitions from one stage to another. And the degree matrix **D** only includes the non-inverse of the total transitions from each node to itself, therefore it is diagonal. The Laplacian matrix **L** comes from the subtraction of the diagonal degree matrix **D** and the adjacency **A** matrix.

the eigenvalues λ_i and μ_i of G and H networks, correspondingly. The normalised subtraction in Eq. 4.8 produced a scalar non-negative value, fulfilling a distance measure condition.

$$\mathbf{L}_{G|H} = \mathbf{D}_{G|H} - \mathbf{A}_{G|H} \overset{\text{EVD}}{=} \mathbf{Q}_{G|H} \begin{pmatrix} \lambda_1 & 0 & 0 \\ 0 & \lambda_2 & 0 \\ 0 & 0 & \lambda_3 \end{pmatrix} \mathbf{Q}^{\mathrm{T}}_{G|H}$$

$$d_1(G,H) = \begin{cases} \sqrt{\dfrac{\sum_{i=0}^{N-1} (\lambda_i - \mu_i)^2}{\sum_{i=0}^{N-1} \lambda_i^2}} & \text{if} \quad \sum_{i=0}^{N-1} \lambda_i^2 \leq \sum_{i=0}^{N-1} \mu_i^2 \\ \sqrt{\dfrac{\sum_{i=0}^{N-1} (\lambda_i - \mu_i)^2}{\sum_{i=0}^{N-1} \mu_i^2}} & \text{if} \quad \sum_{i=0}^{N-1} \mu_i^2 \leq \sum_{i=0}^{N-1} \lambda_i^2 \end{cases} \tag{4.8}$$

The similarity distances $d_2(G,H)$ factorised the adjacency matrix $\mathbf{A}_{G|H}$ into an eigenvalues $\Lambda_{G,H}$ and two eigenvectors $\mathbf{Q}_{G,H}$ $\mathbf{Q}^{\mathrm{T}}_{G,H}$ matrices. They are operated to make the transformation Δ in Eq. 4.9 to extract a set of diagonal values. The root mean square (RMS) relation in Eq. 4.10 computed the final similarity distance.

$$\mathbf{A}_{G|H} \overset{\text{EVD}}{=} \mathbf{Q}_{G|H} \Lambda_{G|H} \mathbf{Q}^{\mathrm{T}}_{G|H}$$

$$\Delta = \mathbf{A}_G - \mathbf{Q}^{\mathrm{T}}_G \mathbf{Q}_H \mathbf{A}_H \mathbf{Q}^{\mathrm{T}}_H \mathbf{Q}_G = \begin{pmatrix} \delta_1 & 0 & 0 \\ 0 & \delta_2 & 0 \\ 0 & 0 & \delta_3 \end{pmatrix} \tag{4.9}$$

$$d_2(G,H) = \frac{1}{N} \sqrt{\sum_{i,j=1}^{N} \delta_{i,j}^2} \tag{4.10}$$

In the same way, similarity distance $d_3(G,H)$ decomposed the ill-ranked incidence matrix $\mathbf{C}_{G|H}$ with a singular value decomposition (SVD) in $\mathbf{U}_{G,H}$ $\Sigma_{G|H}$ $\mathbf{V}^{\mathrm{T}}_{G,H}$ matrices. $\hat{\Delta}$ in Eq. 4.11 transformed the derived matrices to obtain the similarity distance in Eq. 4.12.

$$\mathbf{C}_{G|H} \overset{\text{SVD}}{=} \mathbf{U}_{G|H}\Sigma_{G|H}\mathbf{V}_{G|H}^{\text{T}}$$
$$\hat{\Delta} = \mathbf{C}_G - \mathbf{U}_G^{\text{T}}\mathbf{U}_H\mathbf{C}_H\mathbf{V}_H^{\text{T}}\mathbf{V}_G = \begin{pmatrix} \hat{\delta}_1 & 0 & 0 \\ 0 & \hat{\delta}_2 & 0 \\ 0 & 0 & \hat{\delta}_3 \end{pmatrix} \tag{4.11}$$

$$d_3(G,H) = \frac{1}{N}\sqrt{\sum_{i,j=1}^{N} \hat{\delta}_{i,j}^2} \tag{4.12}$$

The last and fourth distance $d_4(G,H)$ evaluated a Cauchy-Lorentz probability density function (pdf) $\rho_{G,H}(\omega)$ in terms of eigenvalues ω to generate the similarity measure in Eq. 4.13.

$$\mathbf{L}_{G|H} = \mathbf{D}_{G|H} - \mathbf{A}_{G|H} \overset{\text{EVD}}{=} \mathbf{Q}_{G|H} \begin{pmatrix} \omega_1 & 0 & 0 \\ 0 & \omega_2 & 0 \\ 0 & 0 & \omega_3 \end{pmatrix} \mathbf{Q}_{G|H}^{\text{T}}$$
$$d_4(G,H) = \sqrt{\int_0^\infty [\rho_G(\omega) - \rho_H(\omega)]^2 \mathrm{d}\omega} \quad \text{s.t.} \tag{4.13}$$
$$\rho_{G|H}(\omega) = K\sum_{i=1}^{N-1} \frac{\gamma}{(\omega-\omega_i)+\gamma^2}$$

For the final differentiation of control and insomnia subjects a logistic regression classifier was engineered using the number of transitions made amongst W, N1 and N2 stages in the hypnogram. The logistic regression model is given by (4.14).

$$\begin{aligned} logit(\mathrm{E}\{\mathbf{y}^i|\mathbf{x}^i\}) = logit(p^i) &= ln\left(\frac{p^i}{1-p^i}\right) = \hat{\beta}\mathbf{x}^i \\ &= \hat{\beta}_0^i + \hat{\beta}_1^i \mathrm{WW}^i + \cdots + \hat{\beta}_9^i \mathrm{N2N2}^i \end{aligned} \tag{4.14}$$

where the Bernoulli distributed variable $\mathbf{y}^i$ is predicted by the product of the regression coefficients $\hat{\beta}$ and i^{th} subject's sleep onset stages transitions $\mathbf{x}^i = \{\mathrm{WW}^i, \mathrm{WN1}^i, \ldots, \mathrm{N2N2}^i\}$. The logistic model was then tested using a leave-one-out crossvalidation (LOOCV), i.e. the regression coefficients $\hat{\beta}$ are estimated using 31 subjects during the training phase, and the 32^{th} subject is used to the test the model. Finally, we computed the sensitivity, specificity and accuracy performance rates between the foreknown and predicted distributions of the cohorts, where 0 denotes control and 1 insomnia.

4.2.5 Arousal Detection Model

The study centred in arousals aimed the identification and distinction of EEG-originated (spontaneous) events, accompanied by chin tension and limb movement-related arousals. The preprocessing and processing routines explained in the previous sections also took part here, adding up a subfragmentation of each 30 s epoch in 3 s sub-windows, i.e. 10 sub-windows per epoch. As per Iber et al. (2007) AASM manual, a spontaneous arousal was defined as an abrupt shift of EEG frequency including θ, α and/or frequencies greater than 16 Hz (but no spindles) that lasts at least 3 s, with at least 10 s of stable sleep preceding the change. Accompanying increases in submental EMG lasting at least one second during REM sleep was marked as spontaneous arousal with chin tension. Limb movement arousal were related to the activity in the EMG tibialis.

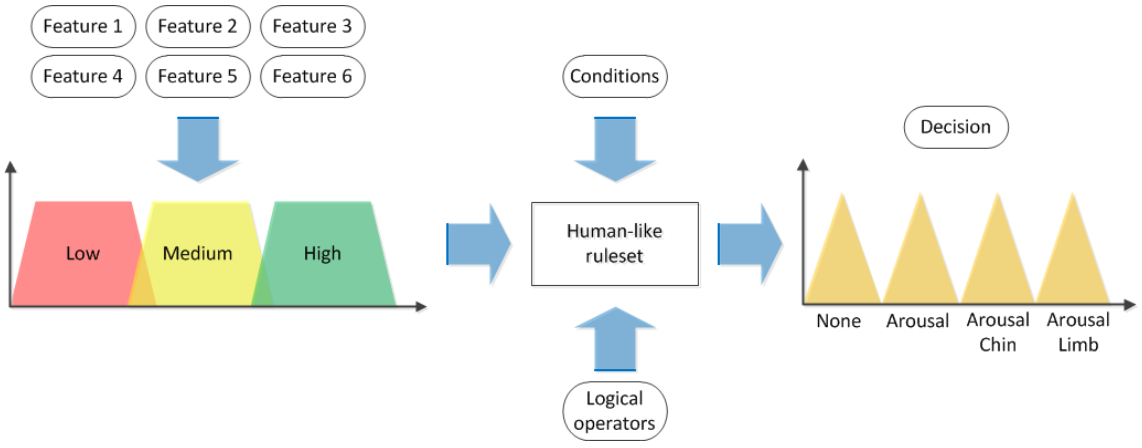

FIGURE 4.8: Fuzzy Inference System for the detection of spontaneous, spontaneous with chin tension and limb movement arousals.

In comparison to the fuzzy system used for automatic sleep onset staging, the major difference resided in the output fuzzy sets and fuzzy rules implemented for the Mamdani FIS shown in Figure 4.8. The arousal-oriented FIS mapped the input fuzzy set of powers $\mathbf{P}[k]$ and amplitudes $\mathrm{A}[k]$ in Table 4.5 to four output decisions: none, spontaneous, spontaneous with chin tension and limb. Here, the FIS evaluated 60 decision rules to strictly interpret the definitions of AASM scoring manual. The final output comprised a hypnogram with marked arousal events epoch-wise.

TABLE 4.5: Features for sleep arousal detection

#	Feature	Channel	Event/Freq. Band (Hz)
1	$\mathrm{P}_{\theta}[k]$	EEG C4-A1, O1-A2	$4-7$
2	$\mathrm{P}_{\alpha}[k]$	EEG C4-A1, O1-A2	$7-12$
3	$\mathrm{P}_{\varsigma}[k]$	EEG C4-A1, O1-A2	$12-16$
4	$\mathrm{P}_{\beta}[k]$	EEG C4-A1, O1-A2	$16-30$
5	$\mathrm{A}_{EMGc}[k]$	EMG chin	Chin tension
6	$\mathrm{A}_{EMGt}[k]$	EMG tibialis	Limb movement

Since, the preprocessing study is the common platform that sustains the remaining three core studies. The next chapter makes a formal description of the performance of the preprocessing model.

Chapter 5

Preprocessing Study

The first core study focused on the computer-assisted preprocessing of the relevant PSG signals for the upcoming studies. The preprocessing addressed the removal of embedded ECG and EMG artefacts from EEG and EOG signals, whereas the two latter are the main supporting sources for sleep scoring. In turn, the denoising module carried out the suppression or attenuation of the additive white noise from EEG and EOG signals. Thereafter, the preprocessed biosignals shall lead to more reliable information extraction from ensuing processing and classification proceedings. The driving hypothesis states that the removal of embedded artefacts and high frequency noise upon PSG can be sufficiently decreased by BSS-SOS and WPT decompositions. Having described the computational model in Section 4.2.2, the model's performance and related findings after deploying the preprocessing system to 1200 randomly selected 10 seconds epochs is described.

Using the 10 sdPSG datasets of Table 4.1 as experimental data, the performance metrics measured rates of success on artefact withdrawal and noise cancellation. The qualitative criterion was a visual inspection of distorted sdPSG epochs, i.e. data segments affected by noisy and embedded ECG/EMG artefacts. With respect to the quantitative criteria by Cichocki and Amari (2005), Signal-to-Interference Ratio (SIR) measured up the difference between the primary EEG/EOG signals $\hat{\mathbf{x}}'[k]$ and the estimated artefactual components $\hat{\mathbf{x}}[k]$. Signal-to-Noise Ratio (SNR) and Root Mean Square Error (RMSE) evaluated the denoising capability. Both computed the difference between the observed signals and the estimated ones $\hat{\mathbf{x}}[k]$. The latter metric square rooted the noise power, whilst the former used that power to normalise the power of the EEG/EOG signal. The quantitative gauges are mathematically described in Eq. 5.1-5.3.

$$\mathrm{SIR}_{\mathrm{dB}} = 10 \cdot \log_{10} \left(\frac{\mathrm{E}[\| \hat{\mathbf{x}}'[k] \|^2]}{\mathrm{E}[\| \hat{\mathbf{x}}[k] - \hat{\mathbf{x}}'[k] \|^2]} \right) \tag{5.1}$$

$$\mathrm{SNR}_{\mathrm{dB}} = 10 \cdot \log_{10} \left(\frac{\mathrm{E}[\| \hat{\mathbf{x}}[k] \|^2]}{\mathrm{E}[\| \mathbf{x}[k] - \hat{\mathbf{x}}[k] \|^2]} \right) \tag{5.2}$$

$$\mathrm{RMSE}_{\mathrm{dB}} = 20 \cdot \log_{10} \left(\sqrt{\mathrm{E}[\| \mathbf{x}[k] - \hat{\mathbf{x}}[k] \|^2]} \right) \tag{5.3}$$

Afterwards, statistical N-way ANOVA tests were conducted using the selected 1200 EEG/EOG 10 seconds epochs as per Cochran's principles for sample size determination, as per Bartlett et al. (2001). The margin error, alpha level and t-value were set to 0.03, 0.05 and 1.96, respectively. The 10 seconds epoch length balanced out between episodic stationarity and zero cross-correlation over the EEG/EOG signals.

5.1 Qualitative Evaluation

A visual inspection of EEG/EOG epochs was conducted to identify embedded artefacts and additive noise. The evaluation showed that 80% sdPSG epochs were successfully denoised and deartefacted, i.e. 960 out of 1200 EEG/EOG exhibited a complete removal of ECG/EMG-related activity and suppression of noise. The remaining 240 sdPSG epochs still presented periodic ECG peaks embedded into the EEG/EOG waveforms, which is a sign of ill-separated sources. However, the denoising module maintained a substantial attenuation of the low-amplitude and rippled noise, i.e. EMG background activity. The set of unsuccessful preprocessed epochs belonged to S08 and S10 volunteers. Presumably, the compliance of ICA-BSS-SOS statistical assumptions might had been violated during in data acquisition's time. The Figure 5.1a-h depict an exemplary EEG/EOG-epoch (S01, S07), subject to successful withdrawal of noisy and artefactual distortions. Conversely, Figure 5.1i-l illustrate an example of S10 with remnant presence of embedded artefacts.

5.2 Quantitative Evaluation

The SIR metric measured the one-to-all channel correlation using dB-scaled signal and interference powers arranged in bidimensional heat maps. The maps allocate the neuronal and ocular PSG channels in the y-axis and artefactual and noisy signals in the x-axis. Then, the cross-correlated values are plotted between the estimated primary EEG/EOG sources and the ECG/EMG disrupting signals. Figure 5.2a and Figure 5.2b show the heat maps of two robust methods from the EEGLAB software package by Delorme and Makeig (2004). Extended Infomax and JADE exhibit power values around -2 dB, which implies a limitation to deal with slow time-varying signals and transient

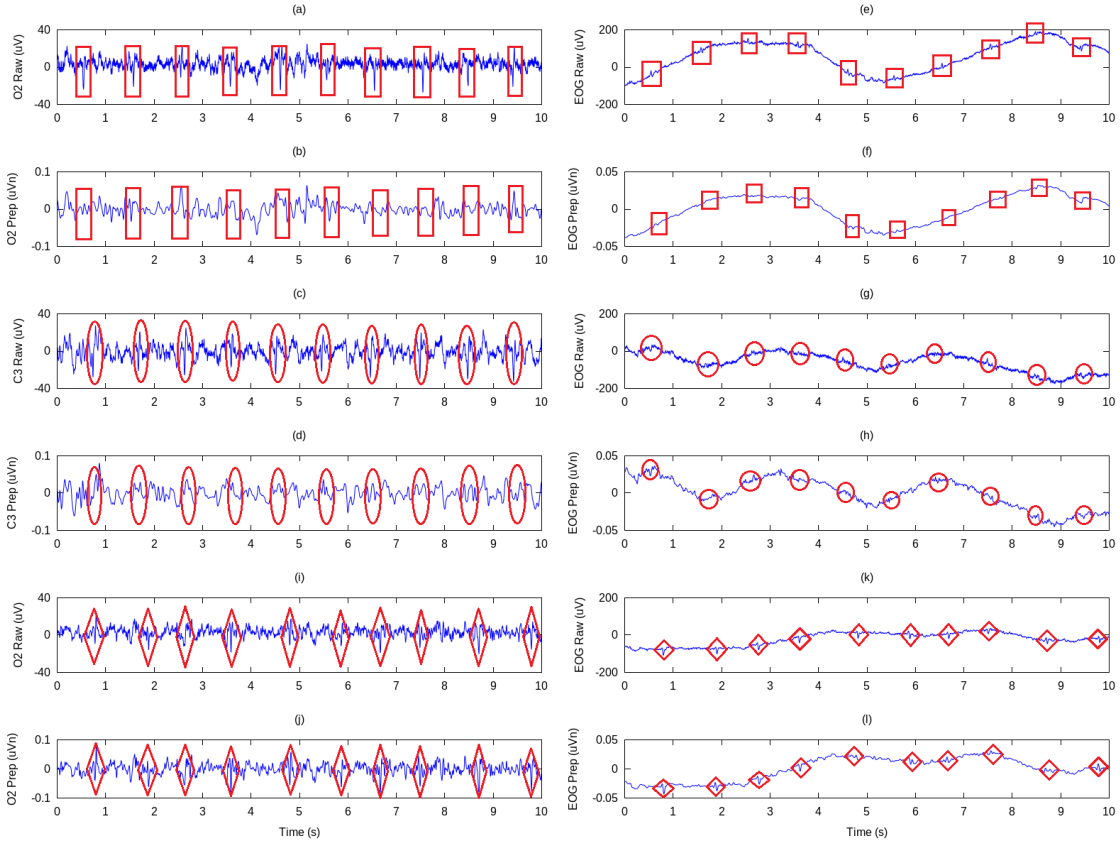

FIGURE 5.1: Examples of preprocessed EEG/EOG epochs from three different volunteers (S01, S07 and S10). (a)-(h) are successfully deartefacted and denoised EEG and EOG signals from O2, C3 and EOG electrodes. The □ marker highlights embedded and removed artefacts upon the EEG/EOG signal for subject S01. Also, the additive noise and high frequency EMG activity was withdrawn from the epochs. Correspondingly, ◯ marker supports the previous results for subject S08 in terms of pulse-type artefacts removal and attenuation of high frequency components. (i-l) display unsuccessful artefact extraction procedure upon EEG/EOG signals for subject S10. ◊ mark pinpoints the presence of artefacts upon the raw and preprocessed EEG/EOG signals. Although, the denoising process was carried out as expected by cancelling out high frequency EMG activity.

pulse-type artefacts. In comparison to the intensity map of the developed ICA-BSS-SOS method—i.e. SOBIRO algorithm—, the EEG activity power is uniformly concentrated around 0 dB. In turn, the EOG heat traces distinct between right and left sensor. Whilst the right ocular sensor has a stronger power under cardiac and muscular influence within 0.15-0.4 dB, left sensor reaches weaker powers. (approx. -0.3 dB). The proposed method outperformed due to a stream-wise estimation, opposed to iterative convergence carried out by the EEGLAB algorithms. Figure 5.2c depicts the heat map of the SOBIRO algorithm.

In order to prove an undisclosed advantage amongst the three mechanisms, a two-way ANOVA statistical test was conducted using the SIR values with Bonferroni correction

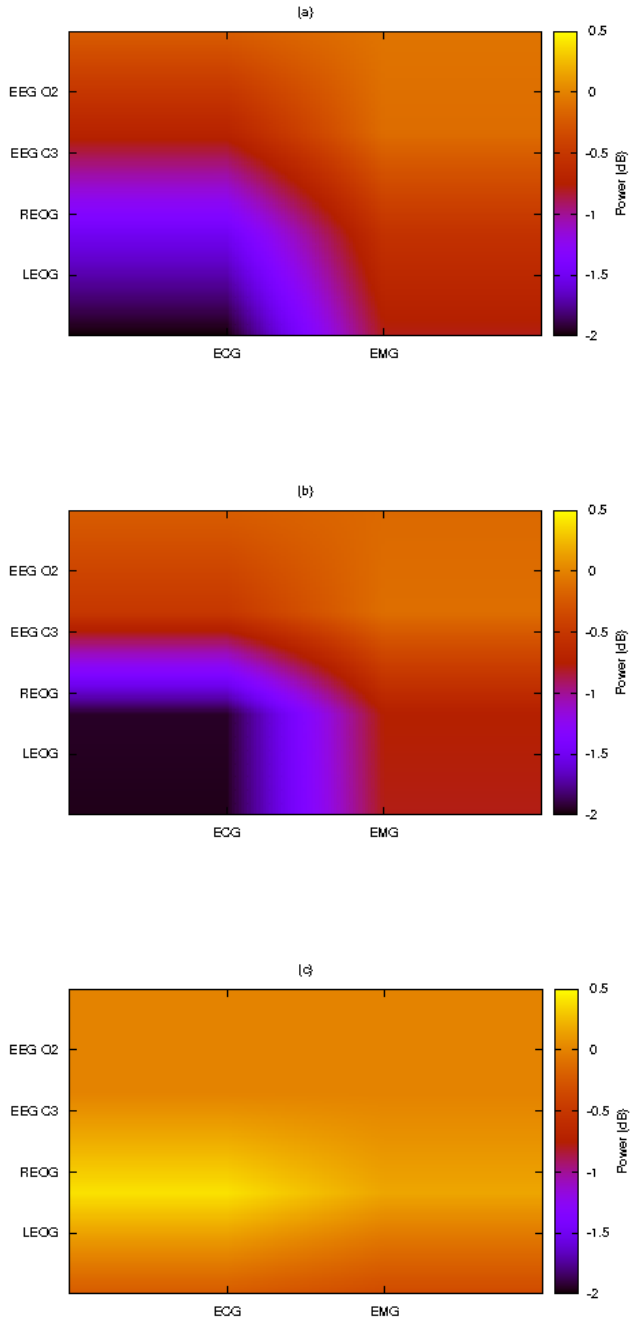

FIGURE 5.2: Heat maps of average SIR for (a) EEGLAB extended Infomax, (b) EEGLAB JADE and (c) SOBIRO algorithms. The heat map quantifies the SIR amongst EEG/EOG versus ECG/EMG channels, after ICA-BSS-SOS is applied.

($p < 0.005$). The column-space dimension aggregated the three algorithms and the row-space dimension compared the SIR values of EEG against EOG channels. The column-space evaluation cast enough evidence to reject the null hypothesis $p = 0.0033$; i.e. the SIR values significantly differ to suggest that SOBIRO outperformed its counterparts. Conversely, the row-space dimension test did not have significant difference ($p = 0.016$) amongst EEG O2, EEG C3, REOG and LEOG channels. In other words, SOBIRO, Infomax and JADE did not perform an outstanding correction of cardiac and muscular interferences upon neuronal and ocular channels. The results summarised in Table 5.1 confirm the findings presented by Ting et al. (2006) Romo-Vázquez et al. (2012), which deepened into SOBIRO properties for adaptive artefact extraction.

TABLE 5.1: Results of 2-way ANOVA statistical tests applied to SIR quantitative performance metric. The displayed values correspond to dimension (Dim), degrees of freedom (DoF), error, mean squares per source (MS), F-statistic and p-value.

		Dim	DoF	Error	MS	F	p-value
2-way	SIR	Column-space	2	14	1.59	8.87	**0.0033**
		Row-space	7	14	0.68	3.80	0.0160

The quantitative RMSE and SNR metrics audited the efficacy of the denoising module, comparing the usage of universal and hSURE thresholds for the WPT decompositions. Figure 5.3a-d portray the performance metrics based on an epoch-by-epoch computation. The universal threshold exhibits a strong 'peaky' and random activity from one epoch to another, i.e. high variability, which diminished the reliability to track EEG/EOG varying moments. The more epochs were processed, the larger deviations built up. On the other hand, hSURE spanned a smoother activity, then a more stable denoising process was ascertained.

Accordingly, a three-way ANOVA test with Bonferroni correction ($p < 0.003$) was also conducted over the average RMSE and SNR metrics. The test looked for meaningful differences with respect to EEG/EOG channels (y dimension), thresholding values (x dimension) and voluntary subjects (z dimension). In regard to RMSE metrics, no significant difference could be concluded between EEG O2 and EEG O3 channels $p = 0.4695$. It agreed with the statistical test upon SIR mean values, so the system performed evenly in the artefact removal and denoising for both neuronal channels. However, the thresholding scheme set out enough evidence $p = 0.0001$ to consider this parameter as a determinant in the denoising success. The same applied to SNR metric, only thresholding scheme deters the rejection of the null hypothesis $p = 0.0001$, which confirmed the preliminary claims derived from Figure 5.3. The universal threshold failed to characterise fast-varying moments of EEG channels and slow-varying of ocular ones. It produced unstable SNR and RMSE performance that demerited its application. Lastly, subject factor did not gave significant evidence in RMSE $p = 0.4919$ or SNR $p = 0.6241$ tests, i.e. the denoising performance had no substantial difference in regard to certain subjects. Although, studies in the future might include additional variables (e.g. gender or larger age interval) to better elaborate this statement. The statistical three-way ANOVA test is shown in Table 5.2.

Having analytically and statistically attested the most appropriate assembly for the preprocessing system, let's proceed with the core studies about sleep analysis and disorders

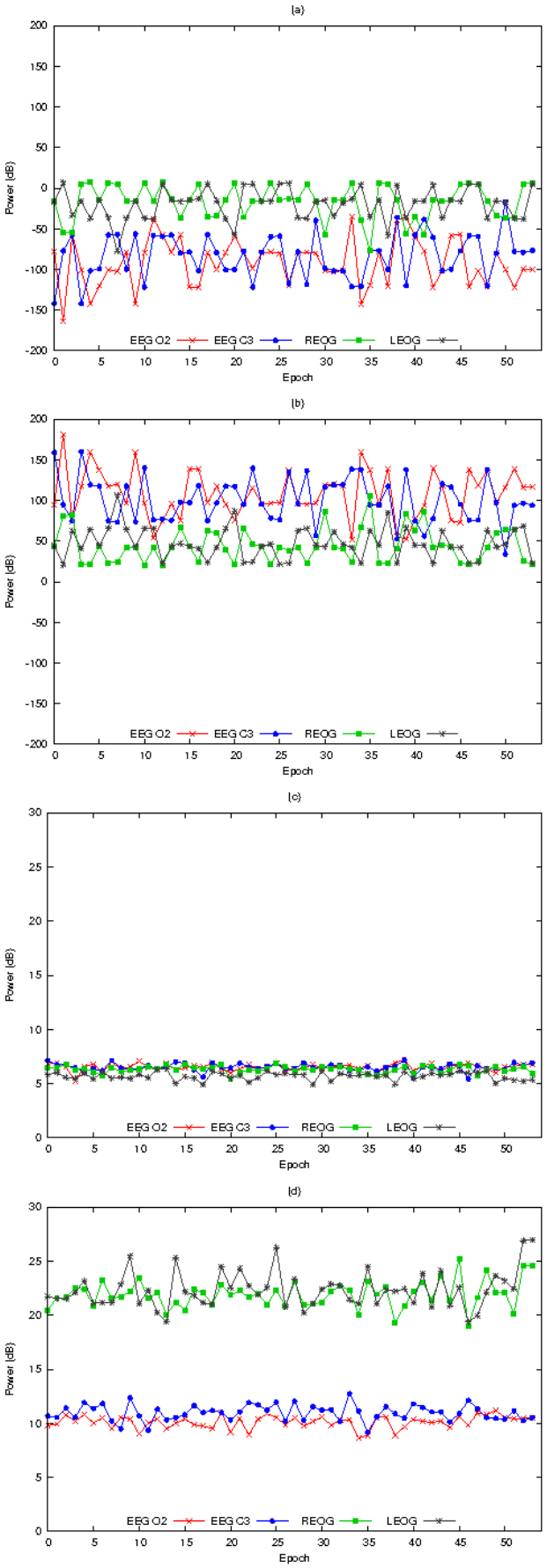

FIGURE 5.3: Average RMSE and SNR performance curves on EEG O2, EEG C3, REOG and LEOG channels along the 55 'shuffled' epochs. (a) presents dB-scaled RMSE for neuronal and ocular channels with universal threshold option. (b) sketches the SNR over both sort of channels employing universal threshold. (c) and (d) depict the quantitative measures making use of hSURE scheme.

TABLE 5.2: Results of 3-way ANOVA statistical tests applied to RMSE and SNR quantitative performance metrics. The displayed values correspond to dimension (Dim), degrees of freedom (DoF), error, mean squares per source (MS), F-statistic and p-value.

		Dim	DoF	Error	MS	F	p-value
3-way	RMSE	Y	1	28	157.9	0.54	0.4695
		X	1	28	84704.03	288.35	**0.0001**
		Z	9	28	282.09	0.96	0.4919
	SNR	Y	1	28	109.5	0.38	0.5402
		X	1	28	85235.6	299.33	**0.0001**
		Z	9	28	2035.8	0.79	0.6241

characterisation. From now on, the preparation of PSG datasets relied on a preprocessing routine undertook with the model described in the Chapter 4 and present chapter.

Chapter 6

Synchronisation Study

The second core study concerned the synchronisation between the CNS and ANS to characterise control, insomnia and schizophrenia cohorts. The calculation of computer-assisted correlation, coherence and coupling metrics measured the neuronal and cardiac functional interdependence. Such methods represented linear, nonlinear and statistical approaches, whose suitability for the cohorts differentiation was the substance in the hypotheses formulation: (i) Control, insomnia and schizophrenia neuro-cardiac activity can be distinctively characterised by cross-frequency coherences across EEG-HRV bands and sleep stages. (ii) Control, insomnia and schizophrenia neuro-cardiac activity can be distinctively characterised by cross-frequency phase coupling across EEG-HRV bands and sleep stages.

In regard to the EEG δ-θ-α-ς-β-γ frequency bands, the study considered the electrical activity originated in the central, occipital and frontal cortical regions. That interareal parcellation was divided in C_{4z3}, F_{87} and O_{21} sources following the 10-20 system for the standardised EEG location and acquisition protocol. The HRV frequency bands denoted as HF and LF, were the cardiac counterparts. The EEG-HRV cross-frequency metrics—linear and nonlinear—were computed for the clinical datasets summarised in Table 4.2.

6.1 Linear Approach: Pearson's Coefficient

The linear approach used the Pearson's coefficient, i.e. the CCF at zero-th time delay over the 6 decomposed EEG power bands, 2 HRV frequencies and 3 clinical cohorts. Figure 6.1 displays the corresponding histogram of means and standard deviations (whiskers). The first significant finding is related to control and patient groups, since the former kept a sustained coefficient around 0.6 for each power band and cortical region. In turn, insomnia and schizophrenia groups were located in the [0.6-0.8] interval. The cross-frequencies $\delta - \gamma \leftrightarrow$ HF maintained steady values across the cortical regions for control group. Unlike to EEG $\leftrightarrow$ LF, central and frontal regions weakened their coefficients in 0.1 points versus the occipital region. Insomnia group attained a

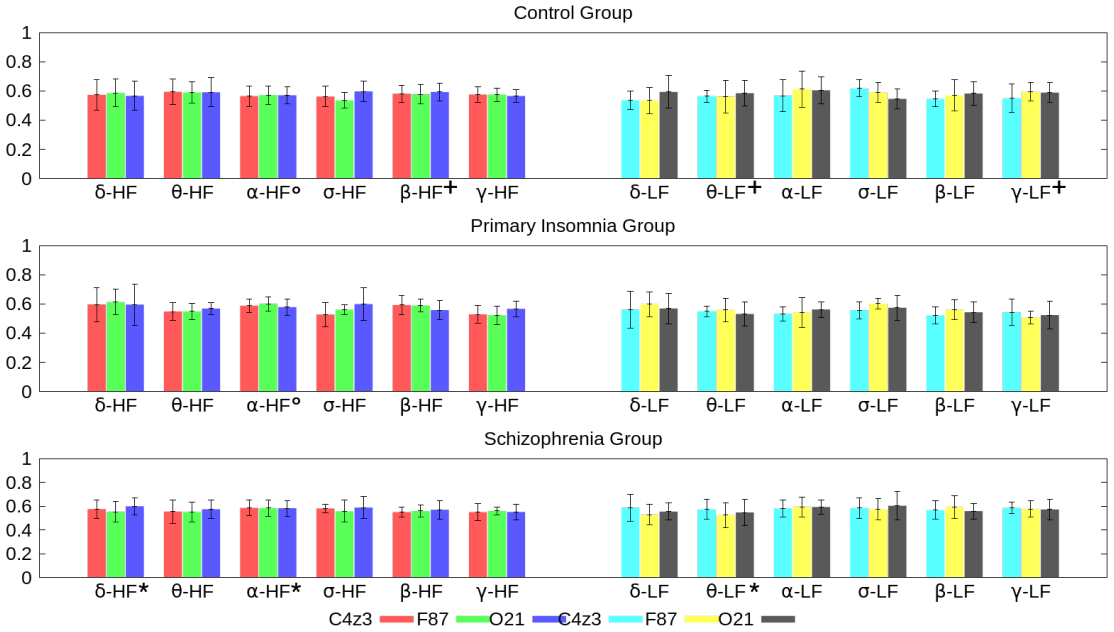

FIGURE 6.1: Histogram of Pearson's coefficient for EEG δ, θ, α, ς, β and γ versus HRV LF and HF bands for control, primary insomnia and schizophrenia cohorts. Each set of coloured bars represent the mean value of inter-hemispheric cortical regions: C_{4z3}, F_{87} and O_{21} with their standard deviations as whiskers. $*$ statistically significant ($p < 0.05$) to distinguish schizophrenia patients from healthy and insomnia subjects, † statistically significant ($p < 0.05$) to distinguish healthy subjects from insomnia and schizophrenia patients, $\circ$ statistically significant ($p < 0.05$) to distinguish healthy subjects from insomnia patients.

more uniform pattern between EEG $\leftrightarrow$ HF and EEG $\leftrightarrow$ LF cross-frequencies, whereas no radical variations occurred to bands or cortical regions. Schizophrenia group seemingly showed indistinct coefficients for EEG $\leftrightarrow$ HF across central, occipital and frontal regions. Although, $\delta - \theta \leftrightarrow$ LF interdependencies strengthened its correlation in 0.1 units for the central region. Apart from this, non-significant statistical dissimilarity laid between EEG $\leftrightarrow$ HF and EEG $\leftrightarrow$ LF power bands for the different clinical cohorts.

6.2 Linear Approach: Wavelet-based Coherence

The Wavelet-based Coherence performed a Time Frequency Analysis (TFA) of the EEG/HRV frequency bands for an entire sleep cycle from W-to-REM. The visualisation of coherence in time and frequency domains were mapped in the macroperiodogram or spectral synchrogram in Figure 6.2. It shows the coherences in a 0-to-1 scale between each EEG and HRV power bands at every sleep stage for control, insomnia and schizophrenia groups. With respect to the low-spectrum power bands, δ-$\theta \leftrightarrow$ LF coherences are particularly stronger $(0.5 - 0.7)$ in wake and REM than the remaining sleep stages. Insomnia patients reach mid coherences (~ 0.5) and higher values (~ 0.7) for schizophrenia cohort. Also, $\delta \leftrightarrow$ LF, HF coherences intensify to mid-high values during S4 and REM stages for insomnia and schizophrenia groups. Similar trend for the same

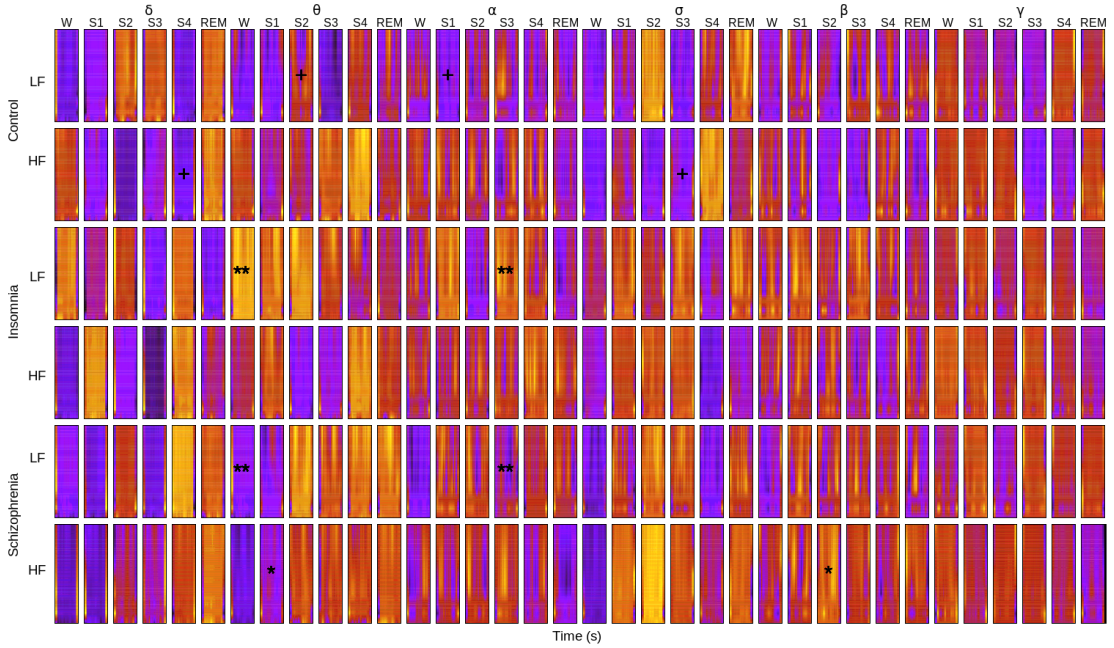

FIGURE 6.2: Macroperiodogram (a.k.a. spectral synchrogram) of Wavelet-based Coherence considering EEG δ, θ, α, ς, β and γ at C_{4z3} neural region versus HRV LF and HF bands for control, insomnia and schizophrenia cohorts across sleeps stages wake, S1, S2, S3, S4 and REM. On the x-axis, each periodogram's cell portrays averaged out 30-second epochs in respect to a particular sleep stage. Twelve pseudo-frequencies are ordered on the y-axis starting on $\sim$ 89.8 Hz till (top scale) 0.04 Hz (bottom scale). The colour scale assigns the black-violet spectrum to low coherence, whilst red-yellow represent the maxima values. $*$ statistically significant ($p < 0.05$) to distinguish schizophrenia patients from healthy and insomnia subjects, † statistically significant ($p < 0.05$) to distinguish healthy subjects from insomnia and schizophrenia patients, $**$ statistically significant ($p < 0.05$) to distinguish insomnia from schizophrenia patients.

groups occurred during light sleep stages (S1, S2), which reported coherences around 0.75.

Nonetheless, an outstanding finding is the $\theta \leftrightarrow$ HF coherence across the 6 sleep stages, when it referred to the control cohort. The ς power band had uniform coherence in every sleep stage depending on the group of interest; such as control, insomnia and schizophrenia coherence attained 0.5, 0.75 and 0.95, respectively. In regard to the high-regime EEG power bands, ς, β and γ exhibited no significant coherence regardless specific sleep stage, HRV band or clinical cohort. For the macroperiodograms of the remaining neural regions (not shown here), the coherences of EEG low-regime bands—i.e. δ, $\theta \leftrightarrow$ LF/HF—reside in $(0.6 - 0.75)$ interval, which coincide with the results of the central region. The α-γ power bands maintained low coherence levels. However, schizophrenia group revamped to mid-high coherences amongst α-$\varsigma \leftrightarrow$ HF and β-$\gamma \leftrightarrow$ HF in frontal and occipital regions during W, S1 and S2 stages.

6.3 Nonlinear Approach: Phase Synchronisation

The n:m phase synchronisation or Phase Locking Value (PLV) was the chosen nonlinear approach to differentiate control, insomnia and schizophrenia groups. Firstly, the outline of the oscillation ratios n:m was applied to the study of the synchronisation phenomenon between EEG and HRV bands. The used n and m integers, central frequencies f_c and n^2+m^2 variance relation for the cross-frequency analysis, are listed in Table 6.1. It is noteworthy, the large deviation of cross-frequencies caused by the 'spread-out' of central frequencies. This might lead to unstable or spurious synchronisations.

TABLE 6.1: n:m integers, central frequency and variance relation for phase synchronisation between EEG and HRV power bands

Bands	δ	θ	α	ς	β	γ
f_c (Hz)	2	6	10	14	24	48
LF 0.055	1:40	1:120	1:200	1:280	1:480	1:960
n^2+m^2	1601	14401	40001	78401	230401	921601
HF 0.125	1:16	1:48	1:80	1:96	1:192	1:384
n^2+m^2	257	2305	6401	9217	36865	147457

The polar diagrams or phase synchrograms in Figure 6.3-6.4 show a 0-to-1 synchronisation measure known as phase-locked coupling between EEG $\leftrightarrow$ HRV power bands at C_{4z3} neural region at every sleep stage. Schizophrenia group demonstrated a strong coupling $(0.6-0.8)$ between EEG high-regime bands β, $\gamma \leftrightarrow$ HF along the entire sleep cycle, except S4 stage. The same was observed in ς-$\gamma \leftrightarrow$ LF bands during light (S1,S2) to deep sleep (S3,S4) transition. In insomnia cohort, δ-θ-$\varsigma \leftrightarrow$ HF reached significant couplings around 0.8 in S1, S2 and REM sleep stages. Couplings in α-$\gamma \leftrightarrow$ LF cross-frequencies were larger than 0.8 during the initiation of light and deep sleep. Whilst the rest of power bands and stages decreased to mid-rank values, less than 0.6. Control group maintained a medium coupling (0.5) over the whole power bands and sleep stages, which agrees with the results of the linear approach Pearson's coefficient. The results for the neural regions (not shown here) introduced additional insights. The neural region F_{87} had couplings in the $[0.8-1.0]$ interval for α-$\varsigma \leftrightarrow$ LF cross-frequencies with insomnia subjects. A top-scale coupling was also produced by $\gamma \leftrightarrow$ LF bands during S1, S2 and REM sleep stages within schizophrenia group. Finally for O_{21} region, δ-$\theta \leftrightarrow$ LF and α-$\varsigma \leftrightarrow$ LF reported the strongest couplings $[0.6-0.7]$ during S3 and S4 stages for schizophrenia and insomnia groups, respectively.

6.4 Statistical Analyses: Omnibus and Post-hoc tests

An omnibus Kruskal-Wallis test[1] was conducted to evaluate signficant differences ($p < 0.05$) using the aforementioned linear and nonlinear approaches amongst control, insomnia and schizophrenia cohorts. Taking into account all possible interdependencies of EEG $\leftrightarrow$ HRV power bands, neural regions and sleep stages. The Pearson's coefficient approach obtained significant correlations when the α-β-$\gamma \leftrightarrow$ HF $-$ LF cross-frequencies at S3 and S4 sleep stages ($\chi^2 = 6.48, p = 0.039$ and $\chi^2 = 7.20, p = 0.027$). The related linear approach, wavelet-based coherence set forth even more significant differences for θ-$\alpha \leftrightarrow$ LF ($\chi^2 = 6.48, p = 0.039$) and θ-$\beta \leftrightarrow$ HF cross-frequencies during S1 and S2 sleep stages ($\chi^2 = 7.20, p = 0.027$). Besides, δ-$\varsigma \leftrightarrow$ HF statistically significant coherences stood out during S4 stage ($\chi^2 = 6.48, p = 0.039$). And, $\theta \leftrightarrow$ LF interaction during W stage came up ($\chi^2 = 7.20, p = 0.027$). The PLV synchronisation pointed out meaningful differences in $\gamma \leftrightarrow$ LF ($\chi^2 = 6.48, p = 0.039$) during S2 sleep stage ($\chi^2 = 6.48, p = 0.039$). Interestingly, a concentration of significant differences came up for $\varsigma \leftrightarrow$ LF coupling from S1 to S4 stages. Table 6.2 gathers up the statistically significant p-values amongst clinical groups, cross-frequencies and sleep stages. Likewise, Figures 6.1-6.4 distinctively mark the significant values per cohort, frequency pair and sleep stage.

The previous omnibus Kruskal-Wallis test permitted the existence of significant different amongst the groups. However, it was more insightful the identification of statistical differences amongst the specific groups. Thus, three simultaneous post-hoc Mann-Whitney U rank tests with heuristic correction were undertaken. The post-hoc evaluations compared all posible group pairs; such as healthy-to-insomnia, healthy-to-schizophrenia and insomnia-to-schizophrenia to determine which group comparison set the largest contribution to the rank differences. Pearson's coefficient approach with $\beta \leftrightarrow$ HF and α-$\gamma \leftrightarrow$ LFc crosscorrelations produced statistical significance to differentiate the control group from the disordered ones during deep sleep stages ($z = 1.30, ranksum = 15, p = 0.08$). Likewise, $\alpha \leftrightarrow$ HF cross-frequencies suggested a statistical distinction of control-vs-disordered and schizophrenia-vs-insomnia groups ($z = -0.87, ranksum = 6, p = 0.08$). In the case of wavelet-based coherence approach, post-hoc tests elicited significant differences for control-vs-disordered groups focusing on the δ-$\varsigma \leftrightarrow$ HF coherence at S3 and S4 stages ($z = -1.74, ranksum = 6, p = 0.08$). The θ-$\beta \leftrightarrow$ HF coherences ($z = 1.74, ranksum = 15, p = 0.08$) during S1 and S2 stages to characterise schizophrenia-vs-others groups. And, the θ-$\alpha \leftrightarrow$ LF cross-frequencies during W, S1, S2 and S3 stages could assist the differentiation of insomnia-vs-schizophrenia cohorts ($z = 1.74, ranksum = 15, p = 0.08$). The post-hoc tests using PLV approach suggested $\gamma \leftrightarrow$ LF activity during S2 stage to distinguish control-vs-disordered groups ($z = -1.74, ranksum = 6, p = 0.08$). In summary, neither W nor REM stages played an important role in the differentiation of the different clinical cohorts, whilst Pearson's coefficient and wavelet-based coherence elicited the broadest amount of statistical differences. Please refer to Table 6.2 for a whole picture of the conducted omnibus and post-hoc tests.

[1] An omnibus test was used to evaluate the overall hypothesis about significant differences amongst the three cohorts. However, it is not possible to determine which group drives the difference with an omnibus test, then post-hoc or contrast tests were required.

TABLE 6.2: Kruskal-Wallis and Mann-Whitney tests p-values applied to clinical groups based on power bands and sleep stages

Method	CCF	WCOH	PLV
$\delta \leftrightarrow$ HF	Wake$(6.48, 0.039)^{*}$	S4$(6.48, 0.039)^{\dagger}$	-
$\theta \leftrightarrow$ HF	-	S1$(7.20, 0.027)^{*}$	-
$\alpha \leftrightarrow$ HF	S3$(7.20, 0.027)^{\circ}$	-	-
	S4$(6.48, 0.039)^{*}$	-	-
$\varsigma \leftrightarrow$ HF	-	S3$(6.48, 0.039)^{\dagger}$	-
	-	S2$(6.48, 0.039)^{*}$	-
$\beta \leftrightarrow$ HF	S3$(7.20, 0.027)^{\dagger}$	-	-
$\gamma \leftrightarrow$ HF	-	-	-
$\delta \leftrightarrow$ LF	-	-	-
$\theta \leftrightarrow$ LF	S1$(6.48, 0.039)^{*}$	Wake$(7.20, 0.027)^{**}$	-
	S3$(7.20, 0.027)^{\dagger}$	S2$(6.48, 0.039)^{\dagger}$	-
$\alpha \leftrightarrow$ LF	-	S1$(6.48, 0.039)^{\dagger}$	-
	-	S3$(7.20, 0.027)^{**}$	-
$\varsigma \leftrightarrow$ LF	-	-	-
$\beta \leftrightarrow$ LF	-	-	-
$\gamma \leftrightarrow$ LF	S4$(7.20, 0.027)^{\dagger}$	-	S2$(6.48, 0.039)^{\dagger}$

$p < 0.05$ for Kruskal-Wallis test (χ^2, p)
$*$ post-hoc statistically significant to distinguish schizophrenia patients
† post-hoc statistically significant to distinguish control subjects
$\circ$ post-hoc statistically significant to distinguish control subjects from insomnia subjects
$**$ post-hoc statistically significant to distinguish insomnia from schizophrenia patients

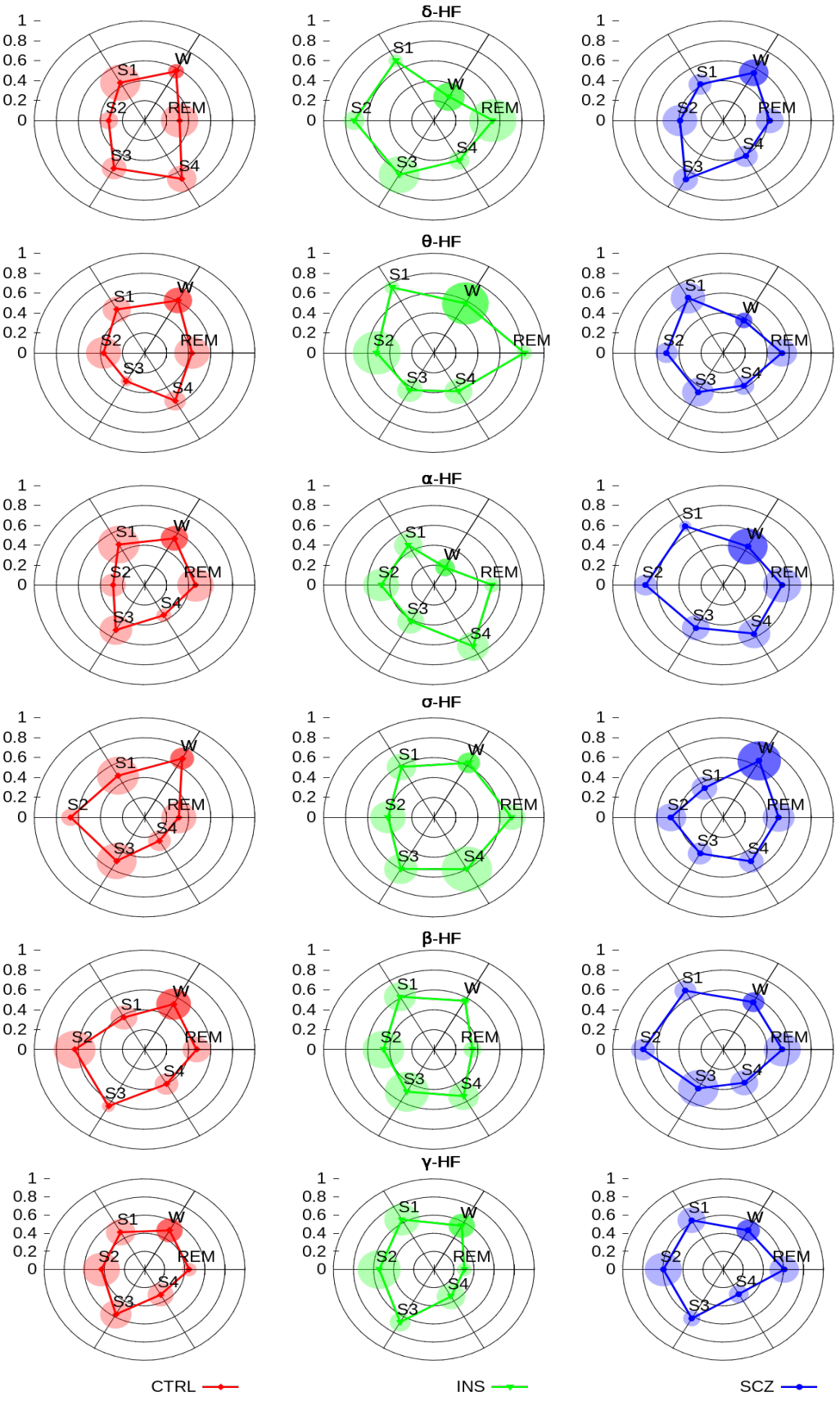

FIGURE 6.3: Polar diagram (a.k.a. phase synchrogram) of *n*:*m* Phase Synchronisation for control (CTL), insomnia (INS) and schizophrenia (SCZ) cohorts, identified by red, green and blue line, respectively. Phase Locking Value between C_{4z3}-δ, θ, α, ς, β and $\gamma \leftrightarrow$ HRV HF band. The coloured points represent the mean PLV at each sleep stage, accompanied by a centred circle expressing the standard deviation amongst the group subjects and patients.

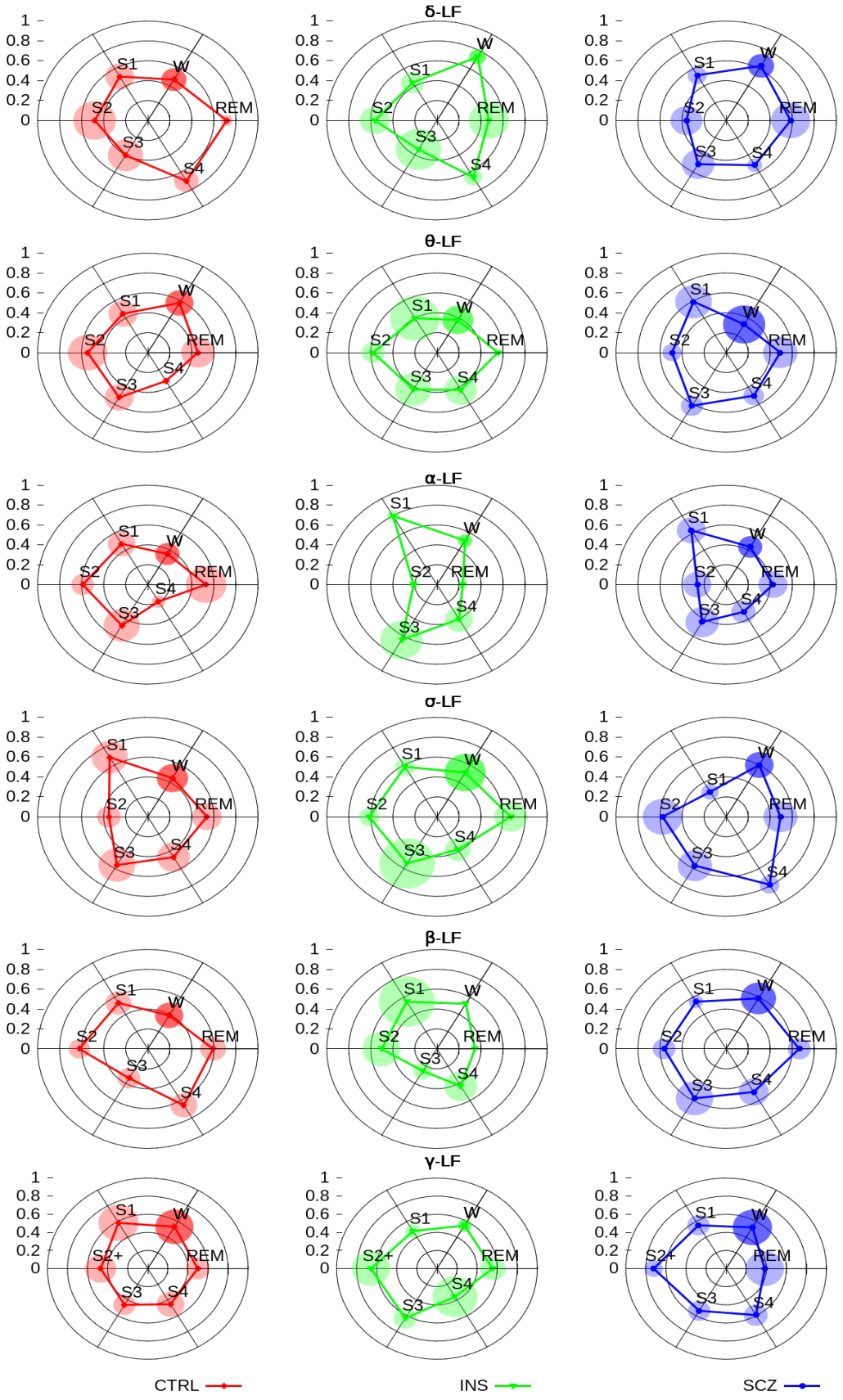

FIGURE 6.4: Polar diagram of *n*:*m* Phase Synchronisation for control (CTL), insomnia (INS) and schizophrenia (SCZ) cohorts, identified by red, green and blue line, respectively. Phase Locking Value between C_{4z3}-δ, θ, α, ς, β and $\gamma \leftrightarrow$ against HRV LF band. The coloured points represent the mean PLV at each sleep stage, accompanied by a centred circle expressing the standard deviation amongst the group subjects and patients. † statistically significant ($p < 0.05$) to distinguish healthy subjects from insomnia and schizophrenia patients.

Chapter 7

Sleep Onset Staging Study

The third core study centred in sleep onset staging pursuing two main objectives: (i) a computer-aided estimation of the sleep onset stages, and (ii) the computer-aided differentiation of the control and insomnia individuals reported in Table 4.3, enacting a supportive role compliant with standard medical procedures Iber et al. (2007). For the classification task, the approach introduced adaptive processing and machine learning tools. The approach also suggested some novel characterisation metrics for the differentiation of control and abnormal patterns to deal with inter-subjects' and inter-raters' variability. Correspondingly, the two hypotheses in this study stated: (i) Inter-subject and inter-rater variability in computer-assisted sleep staging can be appropriately mitigated by fuzzy logic inference. (ii) Control and insomnia sleep onset patterns can be sufficiently differentiated by graph spectral theory and statistical analysis.

7.1 PSG Biosignals Modelling

The particle filtering played a key role in the computation of the TVARMA $(8,2)$ coefficients of the PSG biosignals using the features in Table 4.4, 300 particles and 2000 iterations. Figure 7.1 illustrates a W epoch with its original waveform, particle filter-based estimation, and the periodogram as output of the complex Morlet wavelet decomposition. The heatmap of power bands made a time and frequency analysis of steady EEG bands with sudden transients, simultaneously. For example, the dominant α band with scattered δ and θ powers are hallmarks of W stages as per Iber et al. (2007) AASM manual.

In order to test the performance of the modelling approach in the main PSG sources, EOG and EMG were processed by the TVARMA$(8,2)$ processes with particle filtering. Figures 7.2 and 7.3 depict the biosignal's estimations for the EOG and EMG electrodes, tracking slow-paced and abrupt changes. Therein, ocular eye movements and spontaneous muscular bursts were adequately captured.

Table 7.1 summarises RMSE for the displayed exemplary epochs', which is a traditional analytical metric of performance in filtering. In previous works by Arulampalam et al.

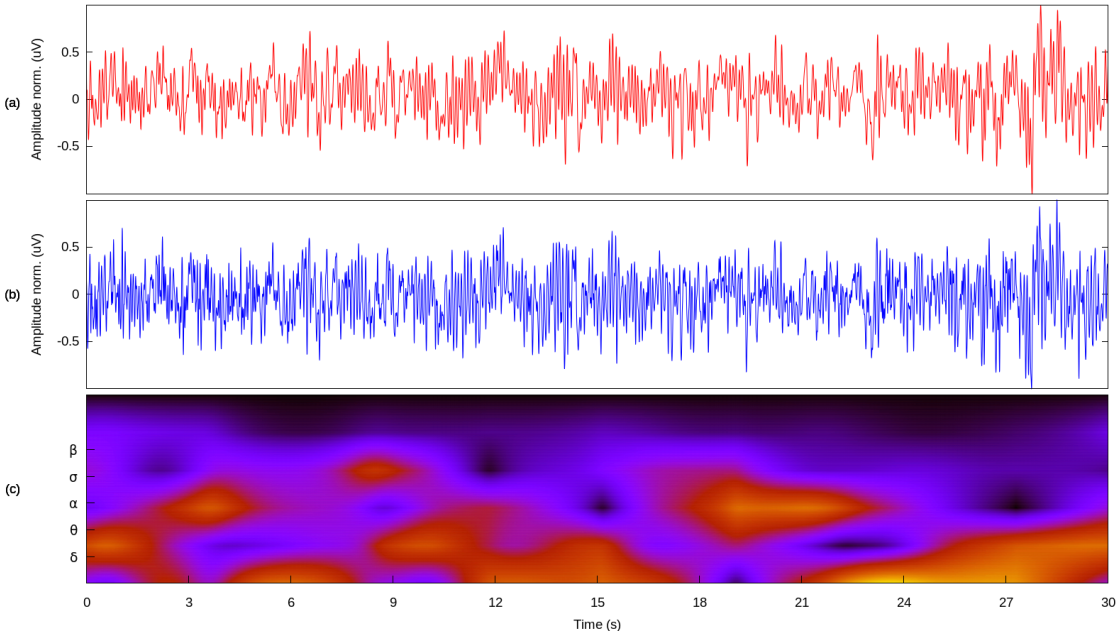

FIGURE 7.1: Example of a 30-second EEG Wake epoch. (a) Original EEG signal recorded by C3 electrode (normalised amplitude). (b) Estimated TVARMA(8,2) EEG C3 signal by particle filter approximation (normalised amplitude). (c) Periodogram of power spectral densities with 30-second time length on x-axis versus δ, θ, α, ς and β frequency bands on y-axis. The heat map sets black-blue range as low power moving to red-yellow to represent high power densities.

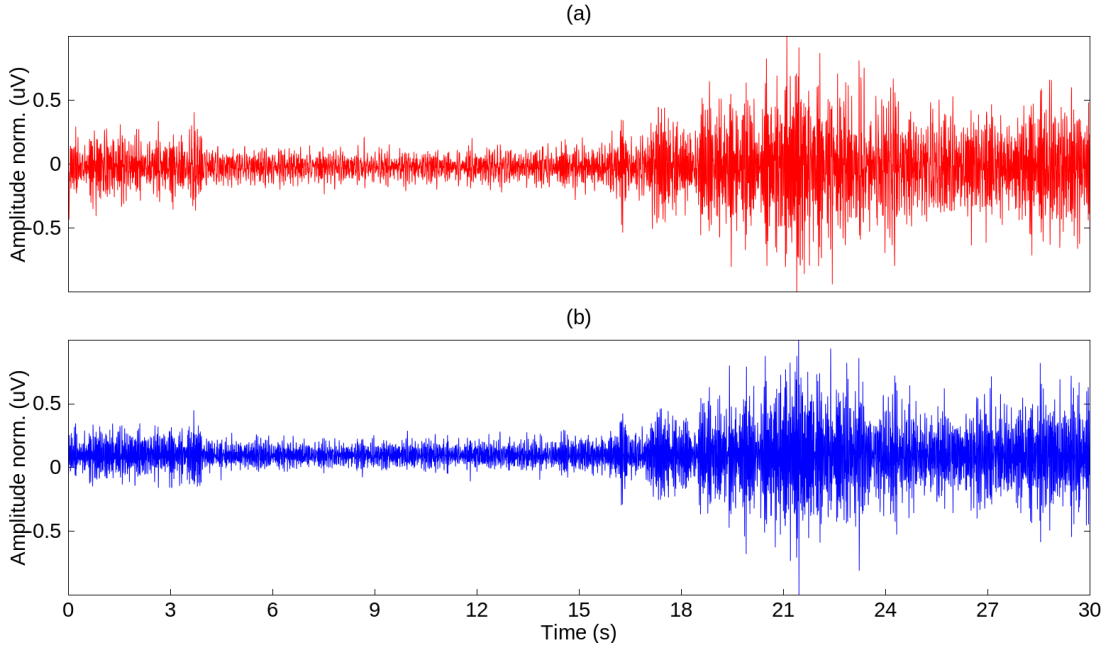

FIGURE 7.2: Example of a 30-second EMG N1 epoch. (a) Original EMG signal recorded by chin electrode (normalised amplitude). (b) Estimated TVARMA(8,2) EMG chin signal by particle filter approximation (normalised amplitude).

(2002) Djuric et al. (2002), RMSE values reported from 0.001 to 6 dB for simulated

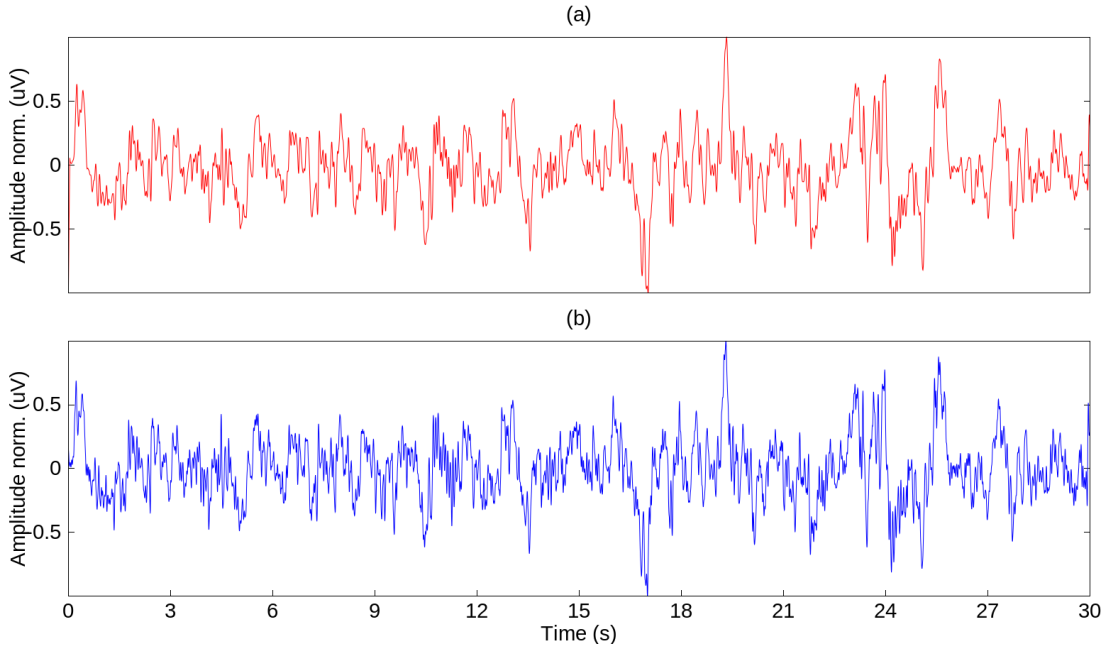

FIGURE 7.3: Example of a 30-second EOG N2 epoch. (a) Original EOG signal recorded on the left eye (normalised amplitude). (b) Estimated TVARMA(8,2) left EOG signal by particle filter approximation (normalised amplitude).

chaotic systems, up to the specific particles and runs. The proposed approach obtained similar or surpassing values shown in Table 7.1.

TABLE 7.1: RMSE performance for channels and stages

Channel	W	N1	N2
EEG C3	0.0837	0.0204	0.0294
Left EOG	0.0580	0.0163	0.0169
EMG chin	0.1277	0.0914	0.5346

7.2 Hypnogram Generation

The FIS classified the features extracted from the modelled biosignals into sleep epochs to generate an automated hypnogram. To achieve this, the fuzzy classifier mapped the features to input fuzzy sets following more than 60 fuzzy rules. Figure 7.4 illustrates the applied fuzzy operation behind the automated generation of hypnograms using subject H09 recording as an example. Figure 7.4a shows the first sleep onset cycle, the dotted lines mark initial and final epochs, where the classification took place. The solid lines marked the specific epochs subject of fuzzy inference in the example. To classify epoch #33 as a W epoch, the relative power in α_2 and β_1 bands circumvent 0.2, which fit into the middle input fuzzy set. As per the 'if-then' statements governing the FIS, such conditions were associated to the highest degree of membership of W stage. The same logic concerned the classification of epochs #38 and #42 as N1 and N2. In Figure 7.4b,

the FIS used the relative power of θ band and number of VSW events, whilst in Figure 7.4c, it processed the relative power in ς_2 band and number of KC. The FIS decision making computed the dominant θ activity and VSW transients during N1 episodes, and concurrent appearance of KC and SS—associated with the ς_2 band—at N2 stages.

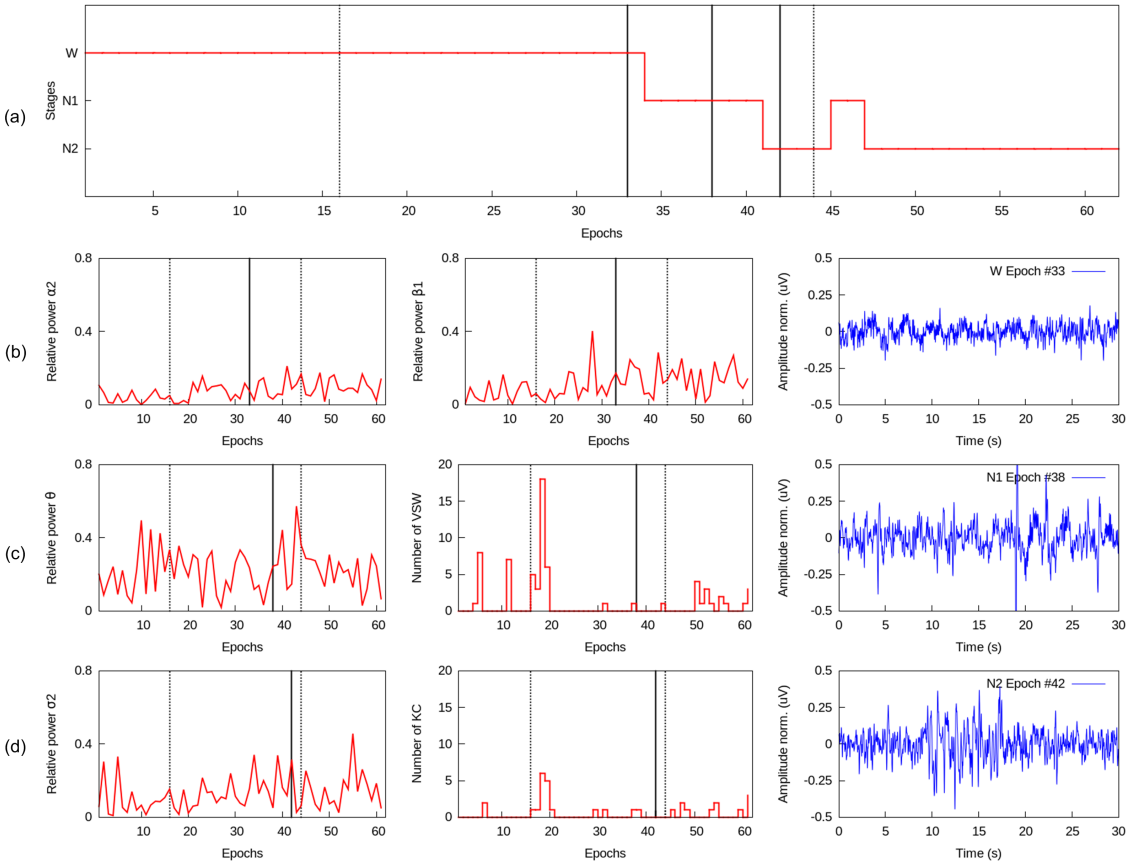

FIGURE 7.4: Fuzzy logic classification for the automatic generation of sleep onset hypnograms. A subset of features are displayed to explain the mechanics of the fuzzy inference system in the mapping of powers, amplitudes and events to sleep stages. (a) The hypnogram corresponds to the first sleep onset cycle of subject H09. The dotted lines delimit the initial and final epochs that went through the classification process. The solid lines locate the specific epochs that are classified as part of the sleep onset period in the example, i.e. epoch #33. (b) Relative power of EEG α_2 band and β_1 bands versus sleep onset epochs to detect epoch #33 as W. (c) Relative power of θ band and number of VSW versus sleep onset epochs to detect epoch #38 as N1. (d) relative power in ς_2 band and number of KC versus sleep onset epochs to detect epoch #42 as N2.

7.3 Insomnia Characterisation

The characterisation of insomnia patients comprised a two-fold process: (i) the translation of expert scored and automated hypnograms in similarity distances. (ii) the classification of subjects between control and insomnia based on the available hypnograms.

7.3.1 Transition Networks and Graph Spectral Theory

After following the methods in Chapter 4 for the computation of the similarity distances, their analysis used the standard deviation to compare the spread between control and insomnia sleep onset patterns constrained to the inter-subjects' variability. Figure 7.5 depicts the standard deviation of the d_1-d_4 similarity distances between each of the control subjects and all the other control and insomnia patients, computed using expert scored and automated hypnograms. The red squared pointers denote the standard deviation of the set of distances for each of the 16-subject control cohort, whilst the blue triangular pointers indicate the standard deviations referred to the 16-subject insomnia group. Figure 7.5 depicts how strongly inter-subjects' variability affected the similarity distances between sleep onset patterns of control and insomnia groups. A greater variation in the standard deviation between control and patients compared to the distances amongst control subjects, meant that the sleep onset transitions of insomnia group were better differentiated from those of the control group. The standard deviations coming from expert and automated hypnograms also showed inter-raters' variability leverage in the similarity distances of both groups. Subtle differences in stage transitions led to subtle different hypnograms, and thereby transition networks with different similarity distances were derived. For instance, expert scored d_1 had larger deviations (0.2) for half of the control subjects with the respect to the control group. Then, d_1 exhibited an alternated variability in the sleep onset patterns of control versus insomnia and control versus control. The automated version had the same alternated deviations, but controls showed larger deviations with respect to the control and insomnia groups. The d_1 standard deviation for subjects H01, H05-H09, H14, H16 remained smaller $(0.1-0.2)$ for control and more spread $(0.2-0.25)$ for insomnia. The distance d_2 with expert and automated scoring follows the expected tendency for most of the subjects, reaching a smaller deviation for the control cohort (0.1) than insomnia $(0.15-0.2)$. Conversely, d_3 obtained from the expert scoring exhibited a larger drift for half of the subjects with stretched values for control $(0.2-0.25)$ compared to insomnia $(0.1-0.12)$. The d_4 standard deviations obtained from expert and automated scoring not only showed larger origin-off deviations for all the subjects, but also the controls were uniformly spread out over a shorter range (0.3) as opposed to the insomnia group (0.4).

The inter-subjects' and inter-raters' variability challenged the generalisation of a model to characterise control and insomnia subjects. Therefore, a statistical analysis was required to unmask significant differences, smoothing the strength of the spreading factor introduced by each subject and rater scoring. We conducted an unpaired two-tailed t-test to evaluate the hypothesis that the similarity distances between control and insomnia cohorts were significantly different. The t-test compared each possible similarity distance between control and patients, assumed as independent random samples of normal distributions with equal means but unknown variances. Prior, a two-sample F-test evaluated the distribution normality and inequality of variances. After, the t-test computed the significance values using expert scored hypnograms and then re-ran the same protocol using automated hypnograms. The t-test compared the similarity distances in two groups: (i) each control subject and all other control subjects (HXX$\rightarrow$HXY) plus each insomnia patient and all other insomnia patients (IXX$\rightarrow$IXY), and (ii) each control subject and all the insomnia subjects (HXX$\rightarrow$IXX) plus each insomnia subject and

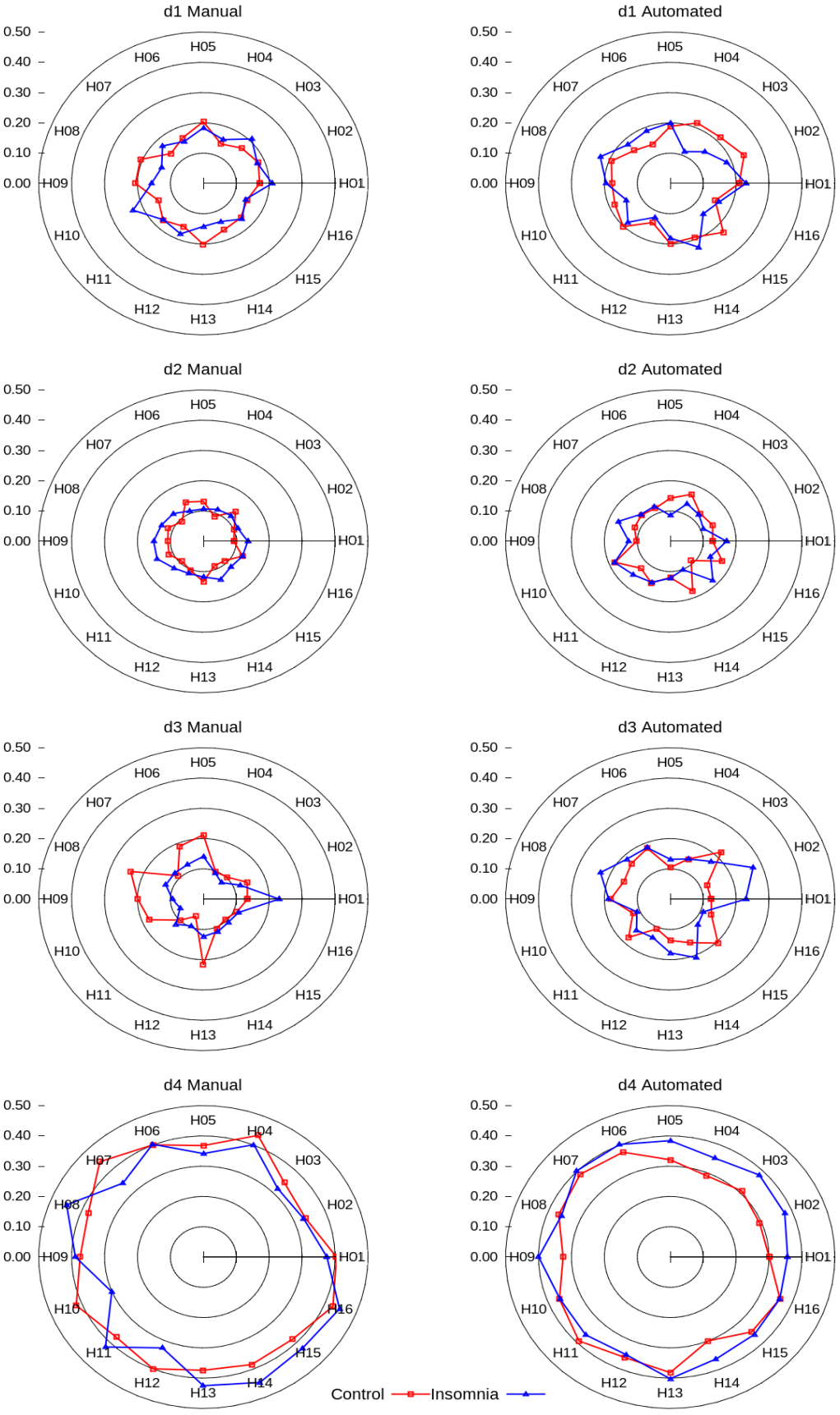

FIGURE 7.5: Standard deviations of similarity distances for each control vs. control and insomnia cohorts. Each similarity distance was compared based on whether it is derived from expert-scored or automatic hypnogram. The red squared pointers denote the standard deviation of the set of distances for the 16-subject control cohort with respect to each control subject. The blue triangular pointers indicate the standard deviations referred to the 16-patient insomnia group with respect to each control subject.

all control subjects (IXX→HXX). Thus, the obtained p-values with Bonferroni correction ($p < 0.0031$) came from paired comparisons of control-to-control versus control-to-insomnia and insomnia-to-insomnia versus insomnia-to-control groups. Table 7.2 depicts the t-values and p-values for each similarity distance and group comparison.

TABLE 7.2: Unpaired two-tailed t-test statistics of similarity distances

Distance	t-value,p-value (Expert)	t-value,p-value (Automatic)
d_1	$t = -2.28, p = 0.02$	$t = -4.01, p = \mathbf{0.0019}$
d_2	$t = 0.50, p = 0.61$	$t = -3.71, p = \mathbf{0.0019}$
d_3	$t = -5.07, p = \mathbf{0.0019}$	$t = -0.47, p = 0.63$
d_4	$t = -1.39, p = 0.16$	$t = -2.22, p = 0.02$

$p < 0.0031$

The similarity distance d_3 was significantly different between the peer control and disordered groups using both types of scored hypnograms. Distances d_1 and d_2 attained statistical significance for the control and insomnia groups using automated hypnograms. Based upon this, the statistical results encouraged the usage of a classifier based on the sleep stages transitions to distinct control and insomnia individuals.

7.3.2 Subjects Classification

Table 7.3 depicts the performance of the logistic classifier in terms of sensitivity, specificity, accuracy rates. Also, the confusion matrix shows the complete expert-based diagnosis (column-space) against the logistic regression classification (row-space) using either expert scored or automated generated hypnograms. The performance of the logistic regression was higher when tested with automated hypnograms as compared to expert scored hypnograms. Such that, one control and two patients more were correctly classified using the automated hypnograms.

TABLE 7.3: Confusion matrices and performance rates of logistic regression using expert vs. automatic hypnograms

		EXPERT			AUTOMATIC	
		Control	Insomnia		Control	Insomnia
EXPERT	Control	13	3	Control	14	2
	Insomnia	6	10	Insomnia	4	12
	Sens= 0.81 Spec= 0.62 Acc= 0.71			Sens= **0.87** Spec= **0.75** Acc= **0.81**		

Chapter 8

Arousal Detection Study

The fourth core study appointed the computer-aided arousal detection. Arousals or microarousals are transients commonly found during light, deep or rapid eye movement sleep (REM). Therefore, individuals are normally not aware of having experienced arousal episodes. Their scattered appearance over the entire sleep cycle elicits further concerns about the composition of sleep architecture; turning the attention to the identification and interpretation of those transients, namely known as arousals. The relation of those events with sleep abnormalities and associated physiopsychological disorders is an area of growing expansion, as Jurysta et al. (2009) sustained.

Hitherto, scoring manuals—e.g. R&K, ASDA or AASM—have had different criteria to identify the onset/offset of arousals using multiple channels; such as EEG, EMG-submental, EMG-tibialis, nasal pressure, airflow, thorax and abdomen effort. Therefore, there is still a missing consensus about assessment guidelines amongst specialists, as Danker-Hopfe et al. (2009) showed. Computer-assisted solutions have the potential to homogenise the criteria and being tolerant to inter-subjects' and inter-raters' variability, which are the top-misleading factors in the scoring tasks and two of our main challenges. Appealing to adaptive extraction and classification of features, the automatic detection could manage subject-dependent events, whilst the compliance with up-to-date scoring manuals is preserved. Then, the related hypothesis states that inter-subject and inter-rater variability in computer-assisted arousal detection can be appropriately reduced by fuzzy logic inference.

The proposed computational approach performed a fuzzy logic-based arousal detection to be tested with the 20 control subjects referred in Table 4.3. The methods were introduced in Chapter 4 to deal with the mentioned hurdles that compromise the proper characterisation of sleep components, sleep microfragmentation, hyperarousals or related disorders similar to Jurysta et al. (2009) work. The detection system was capable of identifying EEG-originated arousals—a.k.a spontaneous arousals—, EEG with chin tension and limb movement-related arousals. It is noteworthy to say that the system was originally limited to the detection of the PSG electrophysiological leads, disregarding behavioural or psychological markers. So, the benchmarking and performance evaluation was based on the definitions according to the AASM manual. Such a definition states: *a spontaneous arousal is as an abrupt shift of EEG frequency including* θ, α

and/or frequencies greater than 16 Hz (but no spindles) that lasts a least 3 s, with at least 10 s of stable sleep preceding the change[1]. Arousals shall be only marked whether occur during NREM and REM stages and transitions amongst them.

Moving forward to the results of the study, the arousal detection supported its processing and classification modules on the same computational approaches used for the sleep onset staging study in Chapter 7. This means, the biosignal modelling and feature extraction revisited non-Gaussian state-space TVARMA(8,2) processes with recursive particle filtering and complex Morlet wavelet decompositions. The classification routine employed a restructured Mamdani (FIS) with fuzzy input/output sets and rules oriented to arousal detection upon the control subjects. Figure 8.1 revised the classification process stepwise using exemplary EEG epochs #22 and #42. Figure 8.1a displays the first sleep cycle's hypnogram of subject H01, where the dotted lines marked the epochs where arousals were detected by the FIS, and solid lines pinpointed the exemplary epochs with spontaneous arousals. The 3 s subwindows within 30 s EEG epochs #22 and #42 are shown in Figure 8.1b. For the arousal detection in epoch #22, FIS evaluated the medium β power 0.4 in the fourth 3 s subwindow in company of a low-medium ς power 0.2 in the previous subwindows. In turn, epoch #42 held a medium-high α power 0.58 concurrent with low-medium θ power in the previous 3 sub-windows. Both EEG power band dynamics in Figure 8.1c qualified as spontaneous arousals, according to the AASM definition.

The performance analysis of the proposed approach was quantified in terms of two AASM-related metrics: number of arousals and arousal index (ArI). A constant in the obtained results was the inter-subject variability, where error deviations dramatically varied from one subject to another. Subjects H01, H11 and H15 achieved the lowest error rates in the ArI, i.e. ± 7.05, ± 3.69 and ± 1.15, respectively. However, subjects H01 and H12 reached error deviations around ± 30 addressed either by over- or underrating of number of arousals across NREM sleep stages. Most disagreement between expert and automated detection were related to the large amount of marked arousals for subject H07—i.e. 60 events within N1-N3—and no marked arousal for subject H12.

Taking into the acount the entire research roadmap of this thesis, the arousal findings could be perceived not as comprehensive as the 3 previous studies. The arousal detection study represented the last stage to visit in the sleep analysis and disorders characterisation walk-through. Thereof, the candidate attempted to set the foundations for an insightful elaboration of this topic in a future research taken by himself or interested community. However, the results deserved an analysis, therefore, an in-depth discussion about the previous findings are found in the Discussion Chapter 9.

[1] Iber et al. (2007) pg. 36 - V. Arousal Rule

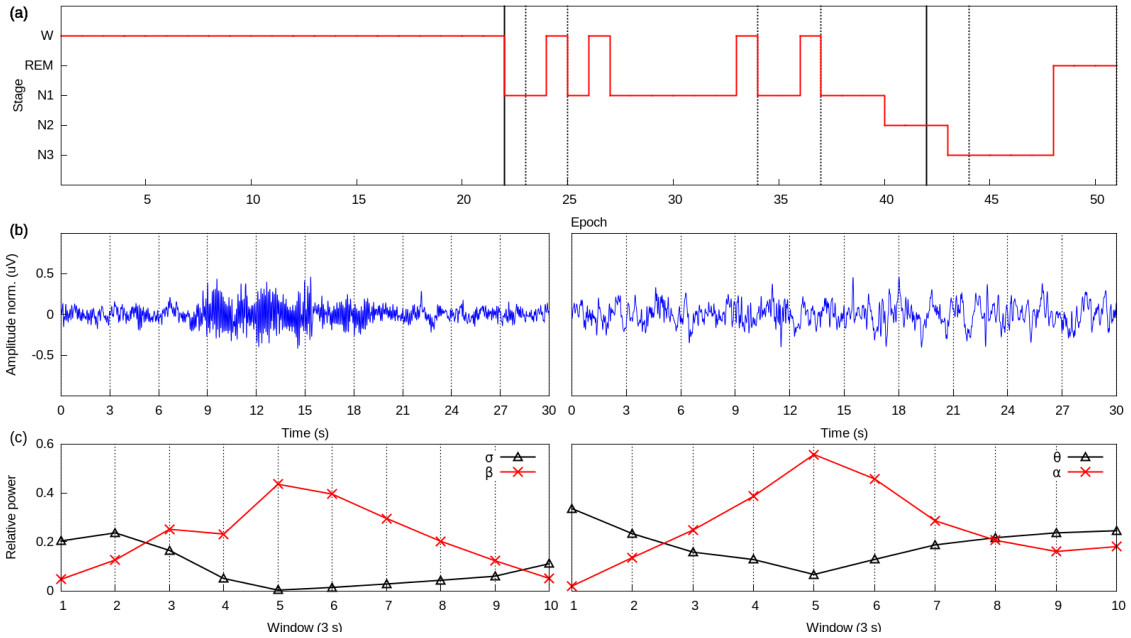

FIGURE 8.1: Arousal detection based on fuzzy inference system. (a) Hypnogram of the first sleep cycle recorded from subject H01. The dotted lines localise the epochs with detected arousals. The solid lines mark the epochs #22, #42 of the two spontaneous arousals detected by the fuzzy inference system. (b) 3 s windowing of epoch #22 with detected α frequency shift and epoch #42 driving β band fluctuations. The dotted lines delimit the 3 s windows used to evaluate the average relative power corresponding to θ, α, ς and β bands. (c) Relative power bands of EEG epochs #22 and #42 against 3 s windows.

TABLE 8.1: Arousals metrics for NREM and REM sleep

		H01	H02	H04	H05	H07	H08	H09
Expert	Ar NREM	18	1	0	1	60	0	1
	Ar REM	0	0	0	0	0	0	1
	Ar Index †	**42.35**	0.96	0	1.76	**48.15**	0	0.41
Auto	Ar NREM	14	17	9	8	15	34	20
	Ar REM	1	2	2	6	7	9	5
	Ar Index	**35.29**	18.38	20.95	24.71	**17.36**	16.48	10.38
	ArI error	**7.05**	-14.41	-20.95	-22.94	**30.78**	-16.48	-9.96
		H11	H12	H13	H15	H16	H17	H20
Expert	Ar NREM	12	0	1	11	1	42	1
	Ar REM	0	0	0	1	0	0	0
	Ar Index	**22.15**	**0**	1.22	**13.84**	0.91	35.24	0.65
Auto	Ar NREM	10	35	7	9	21	13	17
	Ar REM	0	7	0	2	4	2	5
	Ar Index	**18.46**	**30.92**	8.57	**12.69**	22.55	12.58	14.34
	ArI error	**3.69**	**−30.92**	-7.34	**1.15**	-21.65	22.65	-13.69

† $\frac{\#\ Arousals}{First\ Cycle\ Sleep\ Time} * 60$

Chapter 9

Discussion

The findings and related methods of the preprocessing, synchronisation, sleep onset staging and arousal detection studies confirmed some conclusions of previous research works. Also, novel and original contributions have come up to support the involvement of computer-assisted systems for sleep analysis and disorders characterisation. The present chapter not only discusses insights of the major findings and elaborates the rationale behind, but also dissects the flaws and inconsistencies that deserve a further discussion, following the timeline of the conducted studies and related publications.

9.1 Preprocessing Study

The ultimate outcome of the preprocessing study was a modular system to prepare PSG signals for ensuing and more sophisticated routines of processing and classification. Therefrom, the information obtained from the preprocessed biosignals can convey a more appealing feature extraction and thereby meaningful aftermaths. The study's key-points were presented in the Chapter 5. The hypothesis suggested that the removal of embedded artefacts and high frequency noise upon PSG can be sufficiently decreased by BSS-SOS and WPT decompositions, respectively. To prove this, the proposed biomedical signal preprocessing successfully attained artefact removal upon 80% of the 1200 analysed EEG/EOG epochs and 100% concerning background noise suppression.

The implementation of a BSS-SOS algorithm accomplished artefact removal based on epochs with fewer samples and higher flexibility about non-Gaussian constraints, compared to higher-order approaches by Delorme and Makeig (2004). The proposed algorithm iteratively computed time-delayed covariance matrices to counteract the effects of such constraints upon the original biosignals; whilst it reduced the white Gaussian noise until making it absent from the estimated signals, as Cichocki and Amari (2005), Galka et al. (2011) showed. However, embedding ECG artefacts persisted in 240 (20%) of the 1200 EEG/EOG epochs after the deartefact process. The complete set of preprocessed and still distorted epochs belonged to H08 and H10 subjects, exclusively. Upon those particular datasets, it could be assumed the violation of the condition of statistical

independence during biosignals' recording. Under this situation, the source separation capabilities of the proposed BSS-SOS were exceeded, compromising its efficacy in 20% of the 1200 total epochs.

In regard to the denoising module, the cornerstone of the preprocessing approach was the WPT decomposition and its inherent 'shrinkage' effect to 'cancel off' EMG high frequency noise and background tributaries of distortion. The design of the module comprised the selection of Daubechies wavelet family, due to its demonstrated locality property over time and spectrum domain, following Estrada et al. (2011), Fei-Long and Zhi-Zeng (2012) work. Henceforth, the chosen 4^{th} order model attempted the avoidance of spurious components—e.g. 'fake' artefacts—, where such events have been a well-known collateral effect of higher order wavelet convolutions, as Inuso et al. (2007) explained. In terms of SIR and SNR performance metrics, the proposed approach achieved equipotential results compared to previous works in a similar direction to Chang et al. (2000), Romo-Vázquez et al. (2012), Ting et al. (2006), but exceeded the SNR and RMSE criteria for noise suppression reported by Estrada et al. (2011).

In retrospection, the usage of a preprocessing analysis of this kind conveyed several advantages towards the refinement of original PSG recordings. However, a trade-off came up concerning the required computational resources and implicit latency in the preparation of biosignals to actual processing and classification steps, where actual relevant information should be extracted. Despite of the low-complex techniques adopted for PSG preprocessing, the margins of tolerance upon machine-resources utilisation and assessment periods play a critical role heading to a robust computer-assisted solution. Moreover, the deletion or alteration of meaningful information as an aside effect of the preprocessing procedure is a research issue that remains open and worth a proper study. At what extent are the preprocessing routines compromising the integrity of underlying information in biosignals?

9.2 Synchronisation Study

Advancing to the synchronisation study to characterise insomnia and schizophrenia patients as function of the neuro-cardiac functional interdependence and causal relationship, the initial system undertook a pair of linear approaches—i.e. Pearson's coefficient and Wavelet Coherence—evaluated with 10 control, 9 insomnia and 10 schizophrenia subjects. Afterwards, the synchronisation model incorporated a nonlinear version—i.e. $n : m$ phase synchronisation PLV—and statistical testing of characterisation. The final model differentiated control and disordered groups supported on the proposed linear, non-linear and statistical methods. The first hypothesis stated that control, insomnia and schizophrenia neuro-cardiac activity can be distinctively characterised by cross-frequency coherences across EEG-HRV bands and sleep stages. Closely, the second hypothesis proposed that control, insomnia and schizophrenia neuro-cardiac activity can be distinctively characterised by cross-frequency phase coupling across EEG-HRV bands and sleep stages.

To begin, Pearson's coefficient demonstrated an ambiguous performance in the differentiation of neuronal to sympathetic and parasympathetic synchronisations upon the clinical groups. There were no important differentiators between EEG-to-HRV frequency bands to characterise control from disordered cohorts. On the other hand, Wavelet Coherence found discerning cues of cross-frequency interdependencies, including sleep stages, power bands and clinical groups. The macroperiodograms or spectral synchrograms confirmed the accentuated LF activity during W and REM stages and HF during NREM episodes within control individuals by Jurysta et al. (2009, 2010). Additionally, it was revealed substantial variations of coherences in δ and θ power bands depending on the clinical group. Particularly, schizophrenia patients exhibited a more intense β, γ-to-LF, HF synchronisations than control and insomnia cohorts. Based upon this, it is suggested that functional interdependences between sympathetic and parasympathetic systems during the entire sleep cycle seemingly behaved in all clinical groups. EEG slow frequencies and transients—e.g. SW, VSW, KC and SS—and HRV power bands produced distinctive coherence values amongst control individuals and insomnia and schizophrenia patients. Although, the PLV approach agreed on the synchronisation of the sympathetic system during W and REM stages towards a phase coupling of the parasympathetic band—i.e. HF—along NREM stages in patient groups. However, it was found that $\alpha, \varsigma, \gamma$ bands showed an opposed tendency, since parasympathetic activity decreased its PLV strength during NREM stages. From the nonlinear point of view, α, ς and γ power bands could be a differentiator of insomnia and schizophrenia groups, correspondingly. These findings coincided with previous claims on this matter by Noh et al. (2013). On top of that, the results of Kruskal-Wallis omnibus test and Mann-Whitney U post-hoc tests attested Wavelet Coherence as the most performant approach to discriminate control and disordered individuals, subject to the functional interaction of $\delta, \theta, \varsigma, \beta$ power bands and the parasympathetic activities. The synchrogram generated by Wavelet Coherence characterised better than another, control and schizophrenia groups by tracking the interdependence of α-to-LF.

Insomnia and schizophrenia are complex pathologies manifested by physical, psychiatric and behavioural symptoms; therefore the proposed analysis and characterisation demands a wider multidisciplinary contribution to debate about the mentioned findings. The interaction between the CNS and the ANS involves an intricate number of physiological variables that cannot be completely covered for a single study and do require a collaborative examination. An initial strategy should recruit a larger number of control and disordered subjects and partner sleep research initiatives with assorted levels of expertise to assist with the validation of the designed methods. Furthermore, nonlinear dynamics applied to biological systems and sleep studies is a field with enormous potential, but still require confirmation of their techniques and related outcomes, specially when they comprise a supportive role in the diagnosis of pathologies. The synchronisation study on this particular matter advised to the readers some caution in the interpretation of the results obtained with approaches like PLV in the characterisation of insomnia and schizophrenia.

9.3 Sleep Onset Staging Study

The upcoming steps of the overall research project led to the sleep onset staging study in order to characterise insomnia based upon a complete computer-assisted analysis, including biosignal modelling, features processing, hypnogram generation and disorder identification.

The modelling of PSG signals and feature extraction described in Chapter 4 performed the automated staging by means of an ensemble classifier. But not until the application of the fuzzy classifier supported on the prowess of rule-based classification, the main challenges of sleep onset staging characterisation were satisfied; and finally sufficed with graph spectral theory playing the central role to differentiate control and insomnia cohorts. The first hypothesis driving the study implied that inter-subject and inter-rater variability in computer-assisted sleep staging can be appropriately mitigated by fuzzy logic inference. Following the second hypothesis to posit that control and insomnia sleep onset patterns can be sufficiently differentiated by graph spectral theory and statistical analysis.

With respect to biosignal modelling, the key contribution consisted on the deployment of non-Gaussian state-space TVARMA(8,2) processes with recursive particle filtering to gain time-varying analysis and resilience to nonlinear, nonstationary and non-Gaussian constraints. The omission of those conditions by traditional methods could jeopardise the accuracy of further processing and classification steps according to Kitagawa (2009). The computation of features related to the EEG/EOG/EMG signals convoluted with TVARMA(8,2) coefficients and complex Morlet wavelets facilitated the detection of abrupt and smooth signal dynamics. The ensemble classifier attained the identification of N2 stages, thanks to the detection of SS events and EOG/EMG low amplitudes. Sensitivity and specificity rates subperformed for N1 stage classification. The scoring of N1 has been traditionally one of the most challenging tasks in automated staging, due to the vast number of overlapping events—e.g. δ, θ, α activity, VSW, ripples, flattening and truncated spindles— Ogilvie (2001). Comparatively, the proposed biosignal modelling and ensemble classification approach performed as accurate as the system reported in Álvarez-Estévez et al. (2013), but it was still slightly behind of the rates in Koley and Dey (2012), Zhovna and Shallom (2008) works. The second approach based on Mamdani FIS aimed to overcome such downsides by exploiting the rule-based classification schemes. Fuzzy logic eased the automatic generation of hypnograms with a customisable level of flexibility, as sleep onset staging required. Input fuzzy sets of features, output fuzzy sets of stages and human-like fuzzy rules seamlessly adapted to AASM scoring guidelines, inter-subject and inter-rater variability. As per the performance results, expert scored and computer-assisted system held a fair agreement, but prone to improvement adjusting scoring rules and inter-raters criteria proposed by Danker-Hopfe et al. (2004, 2009). Both topics have been a controversial matter amongst sleep specialists due to the persistent disagreement in the scoring of specific phenomena towards a consolidated sleep staging. Most inter-raters disagreements have been associated to the completion point of sleep onset periods, since the recognition of the first KC and SS is recurrently undermined by multiple interpretations. Thereof, the lack of consensus is evident given the existence of mutually exclusive or ambiguous rules when mixed

frequencies and transients amplitude occur. A set of recommendations on this direction were suggested by the inter-scorer reliability program in Rosenberg and Van Hout (2013) study, which were included in the internal decision architecture of the proposed FIS. Thus, the outcome of the sleep onset staging study was a robust computer-assisted approach for hypnograms generation capable of optimising assessment times and counterweighing ambivalent guidelines.

Thereupon, the study focused on the characterisation of insomnia appealing to an alternative repertoire of analysis resources. In this case, graph spectral theory with its similarity distances in Eq. 4.8-4.13, was proposed. The distances d_1, d_2 and d_3 successfully accomplished the characterisation of controls and insomnia patterns using either expert scored or automated hypnograms. The previous similarity measures shared an eigenvalue-based computation, which impressed stability and robustness for the disorder characterisation. The distance d_4 was resilient to origin-out deviations. Also, control and insomnia deviations were consistently confined to uniform range of the phase synchrograms, respectively. No significant difference was revealed by the statistical test. It demonstrated the strong influence added by inter-subjects' and inter-raters' variability and proved the prowess of statistical analysis to smoothen the spreading factor through distributions with larger samples, i.e. time series of the compared distances.

The findings emphasised the importance of the eigenvalues to determine the degree of similarity of sleep onset patterns in terms of low-complex metrics, based on Jurman et al. (2011) work. The eigenvalues represented the hypnogogic fingerprints per subject, obtained by the processing of a single or multiple recording sessions. The chance of duplication became statistically small, whereas it would be hardly expected an exact stage sequence of two distinct hypnograms.

To the best of candidate's knowledge, the proposed biosignal modelling and sleep onset similarity estimation methods are an original contribution to the state-of-the-art in the sleep studies, since there is no previous record of approaches using state-space TVARMA $(8,2)$ processes with particle filtering applied to automated sleep staging. Foremost, such an approach substantially contributes to ameliorate the first main challenge, i.e. the reduction of time processing of PSG recordings. Hundreds of thousands of time points compose a single dataset, the proposed biosignal modelling generalises PSG time series with only ten coefficients and incoming observations. Throughout the study, we evaluated the modelling performance through qualitative and analytical metrics with appealing results comparing original against estimated biosignals to guarantee a meaningful feature extraction.

Undoubtedly, inter-subject and inter-rater variability and their impact in the obtained results are the major concerns for a reliable insomnia characterisation. Few subtle features in the sleep patterns of particular control and disordered subjects, might be in conflict with standardised scoring guidelines and classification ruleset for the automatic generation of hypnograms. Such an inter-subject variability or second main challenge is still on a work-front, looking forward to assess how well the proposed system is prepared to handle individuals with outlying sleep dynamics and how this affects the graph spectrum to maintain the metrics of similarity distances as an efficient insomnia differentiator. On

this matter, the proposed FIS included human-like rules that efficiently addressed inter-subject discrepancies in sleep staging. Most of these discrepancies were due to the ambiguous marking of VSW, KC or SS transients in transitional stages. N1 sleep stage disagreement has led to a disagreement between human versus human and human versus machine scorers, as Anderer et al. (2010), Caffarel et al. (2006), Rodenbeck et al. (2006) evidenced. Some studies by Danker-Hopfe et al. (2004, 2009), Rosenberg and Van Hout (2013) have proposed recommendations towards a more objective amplitude criteria or the identification of band attenuation or low amplitude mixed frequencies in epochs to detect N1 stage. The automated hypnogram generation module included these suggestions in its fuzzy ruleset.

A final novel contribution concerned the characterisation of insomnia patients using graph spectral theory applied to sleep onset periods rather than entire sleep cycles. The transformation of sleep onset patterns into stage-oriented networks and transitions matrices allowed the reinterpretation of sleep complexity into scalar metrics, i.e. similarity distances. The eigenvalues used to compute the scalar similarity distances from a set of hypnogogic fingerprints for each subject, which mapped the transition patterns amongst sleep stages with a minimal chance of duplicity. A logistic regression classifier examined the bottommost accuracy of the systems to discriminate between control and insomnia sleep onset patterns. The performance metrics highly rated: sensitivity (87%), specificity (75%) and accuracy (81%). In the reviewed literature, there is no record of a graph spectrum-based approach over minimal sleep datasets (onset stages) to characterise insomnia. More conventional computer-assisted approaches by Álvarez-Estévez et al. (2013) pivoted between high rates (specificity 90%) and average ones (sensitivity 30% and accuracy 64%) for sleep onset classification. Additional studies by Cervena et al. (2013), Prado (2013) focused on the proposal of alternative characterisation metrics (e.g. bands ratios or complexity) without a classification-type evaluation of performance.

Similarly, inter-rater variability or third main challenge draws forth an inconclusive issue related to the expert side. The disagreement rates attributed to differing scoring criteria biases the characterisation of insomnia and control sleep onset patterns, hence the consistency of hypnograms, transition networks and similarity distances might be compromised. The concern refers to what is the basic level of scoring competence to guarantee the efficacy of the described method. The sleep onset study offered partial answers on those matters based on its own findings and third-party works, however, a consorted roadmap is elusive, yet.

9.4 Arousal Detection Study

Taking into the account the prowess of biosignal modelling and fuzzy sleep staging approaches, the arousal study recalled these methods in the detection of such events as microcomponents of sleep electrophysiology. The modifications and innovation on the overall computer-assisted system were articulated in the Chapter 8.

The study's hypothesis assumed that inter-subject variability in computer-assisted arousal detection can be appropriately reduced by fuzzy logic inference. It introduced a computational approach to automatically detect spontaneous and limb movement-related arousals, as per the AASM criteria. Given that EEG band powers and amplitude fluctuations occurred within constrained time windows, the Mamdani FIS and its human-oriented ruleset decided based on features' tendencies rather than certain states. The fuzzy membership functions were in charge of a smoother transition of feature values from one input fuzzy set to another. The membership to more than one fuzzy set at a time increased the detection rates. Since, frequency shifts in less than 3 s sub-window had a larger chance of detection, thanks to the sensitivity of fuzzy rules to associate low-to-medium or low-to-high band powers.

The AASM manual introduced substantial amendments for the arousal marking compared to the previous R&K and ASDA standards: (i) definition of 3 s as minimum time windows for frequency shifts in EEG α and β bands; (ii) 10 s of stable sleep in foregoing EEG power bands, (iii) necessary and satisfactory scalp derivations, i.e. central and occipital; and 4) supporting channels like EMG, ECG and nasal pressure. All the previous were complied by the proposed approach by Rosenberg and Van Hout (2013), in order to lessen biased scoring as a response to inter-rater variability. The Chapter 8 described some commonalities and disagreements between expert scored and automated detection. Thereof, underscoring and overscoring of arousals cast the major discrepancies during NREM stages. For instance, the expert report accounted no arousals for H04, H08 and H12 subjects, whilst computer-assisted detection marked 17, 34 and 35 events for the same individuals. Recent works like Agarwal (2005), Álvarez-Estévez and Moret-Bonillo (2011) supported the evidence that occurrence of spontaneous arousals are an inherent component of regular sleep. On the other side, the elevated number of arousals in adjacent epochs for subjects H07 and H17 could indicate the violation of AASM detection rules, referred to minimum windows lengths and preceding stable sleep between arousal events.

The proposed approach gave special attention to these restrictions by the strict application of AASM guidelines. As a topic of recent popularity within sleep community, the presented computer-assisted system supposes a novel contribution, whereas to candidate's best knowledge, only one approach by Álvarez-Estévez and Moret-Bonillo (2011) based on ANN has been proposed with comparable results in terms of arousal index (ArI). Both works demonstrated an average ArI in regular sleepers around 20, which agreed with expert scored assessments. The other performance metrics examined accuracy, sensitivity and specificity rate. These classification metrics were not an active part in the present study. The arousal characterisation is a topic with an extensive coverage from clinical studies, however, computer-aided approaches are still missing to the extent of automated classifications like the ones presented here. Therefore, alternative models for benchmarking are not handful, but expected due to uprising popularity of the topic.

Once more, the inter-subject and inter-rater variability appear as relevant concerns for the analysis of sleep microstructure, i.e. arousal detection. The implicit classification component made it so. The considerations for the expert and computer-assisted sides moved over a more delicate line. The scoring and automatic detection of arousals is

defined by more subtle time windows, interacting EEG frequency bands and supporting PSG activities, e.g. muscular or cardiorespiratory. Hereupon, the proposed computer-aided analysis system posited its worth in the assessment of those detailed events. However, subjects with outlying arousal patterns are still awaiting to be accounted not only by automated platforms, but also expert scoring manuals.

The compilation of results and discussion set forth the most important claims of the research work, thus we can proceed to the resolution of the original research questions and hypotheses verdicts in the next conclusions and future work section.

Chapter 10

Conclusions and Future Work

The four main studies: preprocessing, synchronisation, sleep onset staging and arousal detection decomposed the computer-assisted sleep analysis and disorders characterisation in cascading research questions and related hypotheses. Those served as the driving statements to build up the collection of presented models, methods, experimental setups, analysis protocols and major contributions. This chapter is dedicated to the closing remarks for research questions and hypotheses following a bottom-up elaboration, starting with the specifics to the general one. Likewise, some improvements fronts are proposed as future work guidelines for those interested in the topics here discussed.

H4. The removal of embedded artefacts and high frequency noise upon PSG can be sufficiently decreased by BSS-SOS and WPT decompositions.

Ans. The hypothesis was proven based on the outcomes of qualitative and quantitative metrics. The removal of embedded artefacts was achieved through an ICA-SOBIRO algorithm, which separated the ECG pulse-type signal from the EEG and EOG sources in 80% (960) of the preprocessed epochs. The suppression of high frequency noise was successfully accomplished with WPT decompositions, zeroing-out the EMG and external noise spectral components in the whole 1200 preprocessed epochs.

Q1. How can neuronal and cardiac synchronisation from PSG analysis be estimated in order to detect regular sleep, insomnia and schizophrenia patterns?

Ans. The research work postulated Wavelet Coherence and PLV methods to quantify the synchronisation of EEG-to-HRV frequency bands, covering linear and non-linear approaches. The main goal of the characterisation of control, insomnia and schizophrenia groups was undertaken by the analysis of computer-assisted synchrograms based on cross-frequency spectral coherences and phase couplings. The statistically tested results posited δ-to-HF and ς-to-LF synchronisations to characterise insomnia from healthy and schizophrenia, as well as ς-β-γ-to-HF to distinct insomnia from schizophrenia during REM sleep.

Kruskal-Wallis omnibus statistical test and Mann-Whitney U post-hoc tests validated the correlation, coherence and coupling analytical findings, considering the

linear and nonlinear nature of the proposed techniques and non-Gaussian constraints of the features datasets.

H1.1. Control, insomnia and schizophrenia neuro-cardiac activity can be distinctively characterised by cross-frequency coherences across EEG-HRV bands and sleep stages.

Ans. The first hypothesis was confirmed in the light of the spectral synchrograms' results and omnibus-post-hoc statistical analyses. The Wavelet-based coherence elicited a specific set of EEG-to-HRV cross-frequencies to statistically characterised each clinical group, i.e. δ-to-HF, ς-to-LF and ς-β-γ-to-HF.

H1.2. Control, insomnia and schizophrenia neuro-cardiac activity can be distinctively characterised by cross-frequency phase coupling across EEG-HRV bands and sleep stages.

Ans. The second hypothesis cannot be entirely proved or disproved. Despite of the differentiation of control, insomnia and schizophrenia groups achieved by the PLV approach and further statistical evaluation of specific EEG-to-HRV couplings, the degree of reliability and stability of the nonlinear phase-oriented methods outside of simulated scenarios and within biological systems is still elusive.

Q2. What processing and classification techniques can assist the characterisation of polysomnogram activity into standard sleep onset stages for the analysis of regular sleep and insomnia disorder? What is an adequate validation method for the proposed techniques?

Ans. The sleep stages scoring shall translate the AASM guidelines related to EEG band powers and associated PSG channels amplitudes into machine learning approaches, gaining margins of tolerance to inter-subject and inter-rater variability therein. To achieve this, the research project postulated a modular computer-aided approach covering biosignal modelling, feature extraction and fuzzy logic-based classification; i.e. non-Gaussian state-space TVARMA(8,2) processes with particle filtering, complex Morlet wavelet-based transformations for processing and fuzzy inference classification. Based upon this, similarity distances characterised the sleep onset patterns of control and insomnia subjects, which enclosed in a scalar measure the overall sleep stages transitions. Thus, a logistic regression finally performed a computer-assisted differentiation of control and disordered groups.

The validation of the processing, classification and characterisation techniques relied on the unpaired two-tailed t-test applied to the derived similarity distances. Moreover, the approach took into the account sleep statistics from AASM manual to support the conclusions; such as latencies, sleep efficiency and stage percentages.

H2.1. Inter-subject and inter-rater variability in computer-assisted sleep staging can be appropriately mitigated by fuzzy logic inference.

Ans. The hypothesis was directed to the mitigation of two main challenges: inter-subjects' and inter-raters' variability. With respect to the former, the FIS's human-like rules commanded the adaptive classification of sleep onset stages with fuzzy margins of tolerance to describe subject-specific sleeping patterns. It permitted the generation of automated hypnograms, which in turn, were the main input for the differentiation of control and insomnia subjects. Thus, the hypothesis was proven for inter-subjects' variability challenge. On the other hand, the mitigation of inter-raters' variability could not be completely proven. Even though, the comparison of expert and automated scored sleep onset stages led to the characterisation of regular and abnormal sleeping patterns; it is still required a larger number of experts to confront the judgements of colleagues and the computer-assisted system. Further work is needed to attest the promising preliminary results obtained with fuzzy inference.

H2.2. Control and insomnia sleep onset patterns can be sufficiently differentiated by graph spectral theory and statistical analysis.

Ans. The hypothesis was confirmed. An initial unpaired two-tailed t-test attested the pertinence of similarity distances to map the complex transitions of sleep onset stages into scalar metrics. The subsequent analysis of the distances' standard deviations within control and insomnia cohorts set the ground to attempt the subject-oriented differentiation. Ultimately, the logistic regression classifier demonstrated sufficient performance rates—sensitivity (87%), specificity (75%) and accuracy (81%)—to distinct between regular and insomnia sleep onset patterns.

Q3. What processing and classification techniques can assist the detection of arousals events in polysomnogram activity amongst control and insomnia individuals? What is an adequate validation method for the proposed techniques?

Ans. The computer-assisted detection of arousal shall be compliant with the definition and guidelines as per AASM scoring manual. The machine learning approach represented by a fuzzy inference system managed the related scoring rules, whilst inter-subjects' and inter-raters' variability could be attended. The proposed approach consisted of a modular system including biosignal modelling, feature extraction and fuzzy logic-based classification. Like sleep onset staging study, the system adopted non-Gaussian state-space TVARMA(8,2) processes with particle filtering, complex Morlet wavelet-based transformations for processing and fuzzy inference classification. The system's output automatically detected spontaneous, chin and body movement related arousal events.

The suggested validation method followed the AASM manual parameters, i.e. arousal density and arousal index.

H3. Inter-subject and inter-rater variability in computer-assisted arousal detection can be appropriately reduced by fuzzy logic inference.

Ans. Similar to the hypothesis H2.1., the reduction of inter-subject and inter-rater variability using fuzzy inference had a certain and a partial proof, correspondingly. Once more, the FIS's human-like fuzzy rules achieved the detection of arousal events regardless of subject-specific PSG patterns. So, the application of fuzzy

inference did reduce the impact of such a variability in the identification the sleep microcomponents. The inter-raters' variability was not only constrained by the number of contesting scorers, but also by the reliance on legacy standards—e.g. ASDA—to mark arousals. Under those circumstances, it was cumbersome to fully ascertain the outperformance of expert or automated scoring.

G1. How can sleep electrophysiology be screened, analysed and characterised to differentiate between control, insomnia and schizophrenia groups or individuals?

Ans. The computer-assisted sleep analysis and characterisation of insomnia and schizophrenia disorders consisted of four interwoven systems oriented to preprocessing, synchronisation, sleep onset staging and arousal detection. The preprocessing focused on the removal of artefacts produced by neighbouring channels and the suppression of broadband noise. The synchronisation and sleep onset staging methods were directed to the quantification of healthy and disordered cohorts. The $n : m$ phase synchronisation—PLV—outperformed the coarse differentiation of healthy from disordered, whilst spectral coherence—WCOH—refined the distinction between insomnia and schizophrenia. The sleep onset staging introduced eigenvalues-fed similarity distances to discriminate healthy and insomnia sleeping patterns. Metaphorically, the eigenvalues are the fingerprints of individual sleep onset patterns, which guaranteed reliable rates of differentiation. And, a fuzzy inference for arousal detection strived to the identification of those sleep microevents, which are presumably related to more severe pathologies, as per up-to-date scientific evidence.

Multiple fronts of improvement could be mentioned from this research project that concern the sophistication of the proposed techniques and methods. Nonetheless, it was demonstrated the robustness of the approaches here explained, it is expected the refinement of the experimental protocols in future works. The recruitment of larger healthy and disordered subjects would promote the advancement of computer-assisted resources in the sleep clinical practice. Also, the alignment of a wider number of experienced scorers might contribute to better understand the diversity of scoring criteria in regular and abnormal sleep analysis. In the same way, the critical discussion of the most relevant claims and arguments expect to incentive the participation of medical and engineering peers in the search of further insights.

Appendix A

Peer-reviewed book chapter

Title: A review of methods to characterize and classify sleep, depression and schizophrenia disorders

Authors: Dean Cvetkovic and Haslaile Adbullah and Ramiro Chaparro-Vargas

Publication: Mobile Health (mHealth): The Technology Road Map

Year of Publication: 2015

4. A Review of Methods to Characterize and Classify Sleep, Depression and Schizophrenia Disorders

Dean Cvetkovic*, Haslaile Abdullah, and Ramiro Chaparro-Vargas

School of Electrical and Computer Engineering, RMIT University,
Melbourne, VIC 3001 Australia
dean.cvetkovic@rmit.edu.au

Keywords: depression, schizophrenia, sleep, insomnia, brain and heart interaction.

1 Introduction

Why investigate depression and schizophrenia during sleep? Because studying spontaneous neural activity during sleep minimises factors related to waking such as attention, cognitive behaviour and any presence of active symptoms. Sleep architecture also activates particular neural networks and interacts with cardiovascular activity, which can be compared between depressed and schizophrenic patients, healthy and sleep disorders.

The overview of this chapter consist of the following sections: insomnia and psychiatric disorders, electrophysiological interaction and characterisation of disorders, depression in schizophrenia, schizophrenia and sleep, schizophrenia and biomarkers, author's past and current research projects and future directions.

2 Insomnia and Psychiatric Disorders

Sleep and psychiatric disorder does not only reduce the quality of life but also increases the financial burden individually and the public health care system in whole [Ozminkowski et al, 2007, Walsh et al, 1999]. In the US, almost $30 billion -$35 billion has been spent for insomnia related disorder [Chilcott L.A. and Shapiro C.M, 1996] while the overall cost of sleep disorders in Australia in 2004 was $7494 million [Hillman et al, 2006]. The estimated prevalence rate of insomnia varies greatly worldwide. In the US, the prevalence rate was approximately 25% [Ancoli Israel et al, 1999], Canada was about 9.5% [Morin et al, 2006], Japan was at 21.4% [Liu et al, 2000], Australia approximately at 7% [Lack et al, 1988] and the Europ from 4% to 22% [Chevalier et al, 1999] where in France itself the estimated prevalence was reported at 9% [Leger et al, 2000].

Experimental results have consistently shown that insomnia is a risk factor for the development of anxiety and depressive disorders [Neckelmann et al., 2007,

* Corresponding author.

S. Adibi (ed.), *Mobile Health*,
Springer Series in Bio-/Neuroinformatics 5, DOI: 10.1007/978-3-319-12817-7_4

Dombrovski et al., 2008, Lustberg et al, 2000]. The 20 and 34-year longitudinal studies have reported insomnia to be associated with risk of depression [Buysse et al, 2008, Chang et al, 1997]. The same finding was reported in the 7-year study of adolescent insomnia that increased the risk of depression and suicide [Roane et al, 2008]. In fact, insomnia can act as an independent predictor or risk factor for developing depression [Rieman et al, 2003].

Diagnostic and Statistical Manual of the American Psychiatric Association criteria for insomnia state that the sleep disturbance(s) must result in impairments of daytime functioning (or mood) or cause clinically significant distress in order to be classified as insomnia. For primary insomnia, the main symptoms are difficulty falling asleep, maintaining sleep, or a combination of both these problems. One of the diagnostic criteria for primary insomnia is: *"The disturbance does not occur exclusively during the course of another mental disorder (e.g., major depressive disorder, generalised anxiety disorder, a delirium)"* [Kennedy & Solin, 2004]. How do we measure or quantify whether sleep disturbance does or does not occur exclusively during depressive or anxiety disorder? The DSM-IV-TR diagnosis of primary insomnia subsumes several insomnia diagnoses in the *International Classifications of Sleep Disorders.* Primary insomnia is essentially the same as psychophysiological insomnia. The term psychophysiological insomnia has been used to more accurately reflect the most common causes of insomnia, which typically include inappropriate arousal and conditioning or learned factors.

In relation to secondary insomnia, people with psychiatric conditions can report a wide range of sleep-related problems [Perlis et al., 2001]. However, it can be difficult to determine whether the sleep problems are due to medications (neuroleptics), the psychiatric disorder, or both these factors together. Careful review of the person's medical records and taking a thorough history may allow the causal roles of medications and disease factors in the sleep problem(s) to be determined. Sleep disruption and insomnia are common symptoms of most psychiatric disorders. Depression can be complicated by the problem of early morning awakening and difficulty returning to sleep [Livingston et al., 1993]. About 30% of people suffering from major depression report sleep problems (e.g., insomnia, hypersomnia or dream disorders). Studies have suggested that people with depression and insomnia are particularly at risk for suicide [Fawcett et al., 1990]. The National Survey of Mental Health and Wellbeing reported within 12 months period, one in ten (8.6%) people with mental disorders reported being suicidal [Australian Bureau of Statistics (ABS), 2009].

In contrast people experiencing a manic episode usually have insomnia and sleep very little, but usually do not complain of sleeplessness. The physical and psychological symptoms associated with premenstrual syndrome (PMS) can disrupt sleep. The severity and duration of sleep disruption depends on the severity of the symptoms and the number of days that they are experienced. During pregnancy sleep can often be disrupted and daytime sleep can be a problem for some women. Insomnia can be a common problem in new mothers and should also be regarded as an indicator of possible postnatal depression.

A condition, known as sleep state misperception, is characterised by complaints of insomnia, but there is usually a marked discrepancy between reported and

observed estimates of sleep duration [Edinger & Krystal, 2003]. When diagnosing primary insomnia, patient complaints of poor sleep are either related to medical problem or duration of sleep problems. If sleep is more than 7 hours per day, it may be diagnosed as sleep state misperception, or paradoxical insomnia, reported with no clear reference to corresponding PSG findings or its clinical significance. In other words, subjective estimation may be over or under estimated the amount of sleep by few hours as reported by objective normal PSG sleep duration. The psychological profile of insomniac patients, suggests that rumination may influence the sleep misperception.

There are *no clear* objective markers from PSG signals to characterize insomnia. PSG studies on insomnia patients generally show abnormalities, such as prolonged latency to sleep onset, frequent arousals, and reduced amounts of total sleep. However, objective measures of sleep do not always correlate well with the patient's experience of insomnia, which may be partially due to the fact that the function of sleep itself is still unknown, making it difficult to pinpoint which objective sleep abnormalities contribute to the clinical entity of insomnia. It is why subjective tests and interviews are necessary. American Academy of Sleep Medicine (AASM) state that PSG should not entirely be used to routinely evaluate of chronic insomnia for a number of good reasons because there is a great *discrepancy between the PSG measures and the subjective experience* of primary insomnia [Riemann, et al., 2010]. In the 2003 American Sleep Disorders Association (ASDA) Practice Parameter Report, it was stated that the use of *PSG as a diagnostic tool for insomnia is still somewhat controversial* and was not recommended for the routine evaluation of chronic insomnia or insomnia associated with psychiatric disorders,[Littner et al., 2003]. It is challenging to find the cause of insomnia, described by the ''chicken and egg'' dilemma, which makes it unclear whether the cortical state determines subcortical activity or vice versa (i.e., is it the daytime worrying that causes alterations in EEG or vice versa?). In patients with insomnia worrying may include phobia or fear of not being able to sleep and its consequences on daytime functioning. Other insomniac sufferers have certain expectations on their sleep requirements and worry when such requirements are not met [Morin et al., 2007]. This worrying is related to self-reflective, repetitive and passive focus on one's negative emotions, known as rumination. This rumination can, in turn, affect the psychophysiological state of insomniac sufferer, and lead to depression. There have been many experimental and correlational studies which have shown that rumination predicts depressive symptoms and onset of major depressive episodes [Treynor et al., 2003].

Although much of the research has been done to determine the cause of insomnia, its specific cause has not yet been demonstrated and remains elusive. In general, insomnia can be secondary to a psychiatric or sleep disorder and sometimes it can be a primary or independent. Primary insomnia is a term used to describe a subtype of insomnia that constitutes the disorder itself and is not a consequent to any other disorder. Secondary insomnia is known as comorbid insomnia, which is usually associated with new episodes of depression. Many articles have been published demonstrating insomnia as a risk factor for developing

psychiatric disorders particularly depression and anxiety disorder. A study by [Taylor et al., 2005] has claimed that people with insomnia were 9.82 and 17.35 times as likely to have depression and anxiety disorder, respectively. A directional risk study of insomnia with anxiety and depressive disorders by [Johnson et al., 2006] reported that a prior insomnia was associated with onset of depression, but less association is observed from depression to insomnia. This result is in agreement with a study conducted by [Gregory, et al., 2009] which confirmed that sleep problems at age 8 predicted depression at age 10. Whereas, the depression symptoms did not predict later sleep problems. Longitudinal study across 34 years follow up found that insomnia in young men is indicative of a greater risk for subsequent clinical depression and psychiatric distress [Chang et al., 1997]. In another study, the prevalence of major depressive episode among general hospital patients with insomnia was reported to 46.9% [Rocha, et al., 2005]. In contrast, there were several studies which claimed that insomnia causally related to depression. For example, a study by [Ohayon & Roth, 2003] showed that a previous history of a mental disorder was closely related to the severity and the chronicity of current insomnia. A recent study by [Jansson-Fröjmark & Lindblom, 2008] with a one year follow up revealed that anxiety, depression and insomnia are bi-directionally related over time. The advantage of this study was its ability to show directional relationship between insomnia and depression.

3 Electrophysiological Interaction and Characterisation of Disorders

It is understood that some mental disorders such as depression, are associated with measurable physiological changes. Symptoms of depression often reflect dysregulation in the autonomic and neuroendocrine systems, which are mostly controlled by the hypothalamus. Some of the examples of physiological changes are; sleep disturbance (characterised by the loss of stage 4 sleep and difficulty staying asleep), increased resting heart rate, hyperactivity of the sympathetic nervous system, hypothalamic pituitary overactive state, temperature changes and others [Mayers & Baldwin, 2006]. Recent research has demonstrated that overnight sleeping heart rate in patients with various psychiatric disorders are distinctly different than the ‘signature normal’ patterns in healthy (i.e. no psychiatric illness) patients [Stampfer, 1998]. The 'categorically' different patterns of heart rate during sleep in different psychiatric disorders may be reflected in other objective parameters. It is known that there is a shortened REM latency in depression, but there are likely other EEG changes. There has been a focus on the analysis on heart rate and heart rate variability (HRV) patterns during sleep. Medications are a major confounding factor on HRV. Therefore, any recruitment of patients will need to consider medication-free and other groups. Also, the mean trend heart rate patterns would allow one to distinguish between medication effects as opposed to therapeutic change. It has been shown that the heart rate patterns throughout the wake to sleep transition (related to insomnia) in

generalised anxiety and depressed patients are 'categorically' different to that found in 'melancholic' depressed patients and one would expect that this should also be reflected in EEG activity. Previous study results have revealed that the heart rate may be used as a marker to diagnose or predict whether a human is suffering from a mental illness [Iverson et al., 2005]. There has been some advancement in trying to classify various sleep and psychiatric disorders (i.e., insomnia, sleep apnoea, depression, bipolar disordered and schizophrenia) from electrophysiological EEG and ECG (objective) measures [Boostani et al., 2009]. However, the current body of knowledge lacks the proper methodology to objectively make an accurate diagnosis or prediction of any sleep or mental disorder.

It is unclear whether increased autonomic activity is causing insomnia or whether insomnia and its sleep loss triggers increased autonomic activity, prompting the investigation of ECG in the cause and effect of insomnia. In terms of EEG, PSG shows significantly reduced sleep duration and efficiency, increased arousal index, and slightly, but significantly, less REM sleep in insomniacs compared to the healthy controls. The findings revealed that the difference between healthy and insomniacs, is that EEG beta band was higher during W, S1 and REM in insomniacs, and there was a reduction in EEG delta and theta bands in both REM and NREM.

Arousal is gaining more interest to be used as a marker of sleep disruption which involved in some sleep disorders. A study in healthy men has applied a cortical arousal from EEG alpha activity to identify bouts of tachycardia-bradycardia [Togo et al., 2006]. Some arousals (shorter) may not be subjectively estimated, but may be measured objectively using EEG and ECG. Whereas, longer arousals may be better estimated subjectively. Arousals can be both objectively measured and subjectively reported. However, the problem lies with sleep fragmentation (brief arousals) where patients are not aware of their shorter period awakenings in their sleep and cannot report it subjectively. Patients are generally aware of their longer awakenings, characterised with longer periods of arousals. This heightened level of arousal commonly appeared in the people likely suffer from depression [Staner, L, 2010]. A study of EEG beta power spectral during NREM sleep and glucose metabolism has shown an increased values of these two measures which associated with arousal particularly in the prefrontal cortex and the right lateral inferior occipital cortex [Nofzinger et al., 2000]. Hyperarousals have been described as a potential key factor in the maintenance of insomnia. However, there is a need for further research to characterise the nature of this arousal and its relationship to psychological, behavioural and physiological parameters, especially the *EEG and ECG interaction.*

Jurysta et al. hypothesized that chronic insomnia will alter the relationship between autonomic cardiac activity and delta sleep EEG [Jurysta et al., 2009]. During normal sleep, thalamic, thalamocortical and cortical neurons interact and are associated with generation of Slow Wave Sleep (SWS) particularly of delta rhythms and arousals. The interaction with the cardiac cycle is observed within the cells of thalamus. In insomniacs, it was observed that the linear correlation is

decreased between cardiac vagal and delta EEG in comparison to the healthy controls. In the healthy controls, the High Frequency (HF) component of HRV which reflects the cardiac parasympathetic activity was preceded by delta EEG. However, in the primary insomnia patients the time delay between these two variables was less predictable. The interaction between cardiac activity and delta sleep power has also been studied in a major depressive disorder [Jurysta et al., 2010]. The link between cardiac and delta EEG activity was not significant between the healthy and depressed patients. Besides, none of the HRV parameters differed between both groups. In contrast, a study by Udupa et al. has shown increased sympathetic and decreased parasympathetic activity in the major depression patients compared to healthy controls [Udupa et al., 2007]. Despite the fact that this study has reported the alteration between cardiac function and delta EEG in the primary insomnia and depressed patients, the understanding about this interaction has not yet been fully established and will be studied in this project.

In the late 70s, Gillin and colleagues [Gillin, 1979] were the first to have successfully separated or classified healthy, insomnia and depressive patients using EEG signals. Patients with depression have a sleep abnormality patterns which could be used as an input variable in the classification. Gilin and colleagues have suggested eight objective variables namely as total sleep time, total recording period, sleep efficiency, sleep latency, early morning awake time, awake time, REM time and REM%. Similarly, a study by Steiger et al has also acknowledged sleep EEG as a potential biomarker in the classification of depression and other psychiatric disorders particularly desinhibition of REM sleep, changes of NREM sleep and sleep continuity disturbance [Steiger et al., 2010]. Nissen et al. introduced delta sleep ratio of spectral analysis to show changes in NREM in the deep sleep stage of sleep deprived patients. A higher value of delta sleep ratio was observed in the patient [Nissen et al., 2001]. Staner et al., suggested that hyperarousal could be related to sleep disturbance and abnormal levels of arousal in the depressive insomnia patients [Staner, et al., 2003]. All night sleep EEG frequency bands were extracted during the sleep onset and first NREM from the healthy, primary insomnia and depressive insomnia patients. The results have revealed the hyperarousal only characterized the primary insomnia with higher EEG activities during sleep onset, whereas the depressive insomnia showed a lower slow wave sleep (SWS). Bonnet et al. have demonstrated an increase metabolic rate in insomnia that was associated with difficulty sleeping [Bonnet et al., 1995]. Functional neuroimaging studies have reported a similar findings that insomnia patients have shown higher whole brain metabolism which failed to decline in activity from wake to sleep and resulted in greater NREM sleep [Nofzinger et al, 2004]. The findings from all these studies suggest that symptoms of heightened physiological arousal (hyperarousal) are common characteristics that could differentiate insomnia from depressed and healthy.

In recent year, various methods have been applied to extract different features in the sleep EEG to characterize different pathological conditions. Although linear methods like spectral analysis of EEG frequency bands and wavelet have

successfully classified healthy, depressed, and insomnia patients, these methods may not be sufficient enough to extract valuable information and detect abnormalities in the signals. Therefore, various methods based on non-linear analyses are necessary for the study of the complex systems. Non-linear EEG time series in the healthy and depressed patients have been studied by Leistedt et al. using detrended fluctuation analysis (DFA) [Leistedt et al., 2007]. Depressed patients have displayed less autocorrelation of DFA measures during SWS which reflect breakdown of fractal physiologic complexity during specific pathologic conditions. In this research project, linear and non-linear methods will be applied to extract the useful features from EEG and ECG that can be used as markers to separate healthy controls from depressed and insomnia patients.

4 Depression in Schizophrenia

Cotton et al. highlighted that there needs to be a better understanding of the nature and characterization of depression in the first episode schizophrenia, as depressive symptoms are often neglected in first episode schizophrenia patients [Cotton et al., 2012]. Evidence suggests that depressive symptoms initially appear during the first schizophrenic episode and continue the course of positive symptoms in schizophrenia.

5 Schizophrenia and Sleep

Previous studies have evaluated that that medicated schizophrenia patients had a reduced sleep spindles (amplitude, duration and number), compared to healthy and depressed patients during the initial NREM episode [Ferrarelli at al., 2007]. Ferrarelli and colleagues decided to investigate whether similar reduction in spindle activity was consistent in the larger schizophrenia group, throughout the whole night during all NREM stages and if this spindle impairment was related to any specific neuronal network. Ferrarelli and colleagues conducted an overnight PSG study on 49 schizophrenia, 20 medicated non-schizophrenia and 44 healthy patients [Ferrarelli at al., 2010]. The results consisted of comparing the slow wave sleep (SWS) and the mean number of sleep spindles per time (i.e. density), duration, amplitude and frequency. Findings revealed that schizophrenia patients had no changes in SWS but had a reduction in spindle power (12-16 Hz) and in slow (12-14 Hz) and fast (14-16 Hz) spindle amplitude, duration, number in the prefrontal, centro-parietal and temporal brain regions. The medications did not affect the spindle reduction during the night. Schizophrenia clearly affects the neural thalamic reticular nucleus and thalamo-reticular network, responsible for the generation of sleep spindles.

Whilst Ferrarelli and colleagues [Ferrarelli at al., 2010] found no changes in SWS, Goder and his colleagues [Goder et al., 2006] tested the hypothesis that delta power in sleep was associated with neuropsychological performance in 17

healthy patients but impaired in 16 medicated schizophrenic. The results from the neuropsychological tasks did not reveal any significant differences between patient groups. But the SWS was significantly reduced (in temporal and occipital region) in schizophrenia patients and delta was not significantly different during stage 2 and REM in comparison to healthy patients. These findings were interpreted as a dysfunction of thalamocortical and prefrontal networks in schizophrenia, linked to cognitive impairment in schizophrenia patients.

It was hypothesised that beta and gamma power bands were a suitable mechanism for describing the integration of spatially distributed brain activities [Noh et al., 2013]. Given that, both bands involved abnormalities in the oscillatory behaviour (i.e. synchronisation) related to cognitive impairments and other symptoms [Bob, 2012]. For instance, Uhlhaas reported phase synchronisation deficits in 'Gelstat' perception amongst schizophrenia patients in beta band, but not the same case in gamma band. Based upon this, it was claimed that deficits in self-monitoring and willed actions could be produced by a communication dysfunction between the frontal and temporal lobes within the corollary discharge system. Such cognitive and behavioural disturbances of schizophrenia are an expression of central nervous system's inability to adequately bind neural processes segregated across distributed areas, a condition termed as functional dysconnectivity. Hitherto, neuroimaging and electrophysiological studies cannot agree upon whether functional dysconnectivity comes from the aberrant axonal connectivity or abnormal neuronal function amongst cortical areas interwoven by a functional circuit [Zalesky et al., 2010]. Regarding additional power bands, Siekmeier documented the increment of delta and theta power band oscillatory activity in the temporal lobes. Even more, several studies argued a positive correlation between temporal lobe activity and positive schizophrenia symptoms [Bob, 2012]. The suggestion made by Rolls stated that the abnormal brain activity in schizophrenia can be modelled as a reduction in excitatory and inhibitory synaptic transmission, which can lead to rapid changes of neuronal states across spatially diverse neuronal populations. Thus, alpha oscillations in occipito-parietal and central regions manifested similar functional interaction in relation to inhibitory processes. Likewise, beta oscillations primarily managed the maintenance of the current sensorimotor cognitive state [Nikulin et al., 2012]. On the same way, [Timashev et al., 2012] research work showed that dampening in alpha activity accompanied by the amplification of low frequency in delta and theta power bands, were essential signs of schizophrenic condition.

Some additional facts and findings in regard to the studies aforementioned are deeper detailed in Table 1, including subjects, methodology, conditions and conclusions.

6 Schizophrenia and Biomarkers

Schulz and colleagues highlighted that previous research demonstrated a dysfunctional cardiac autonomic nervous system, associated with a decreased

parasympathetic (vagal) and increased sympathetic activity [Schulz et al., 2012]. However, Schulz identified that respiration, responsible for the complex interaction between the brainstem and 'higher centres', was not investigated together with the cardiac activity, as part of cardiorespiratory regulation in schizophrenic, their first degree relatives and healthy patient groups. Various parameters (linear, nonlinear, indices, etc) were computed for cardiorespiratory coupling, respiratory variability and dynamics in order to characterise autonomic regulation. The results revealed a significant difference in schizophrenia patients as compared to healthy and first-degree relatives, for the respiratory variability and their dynamics, with increased complexity and reduced respiratory sinusarrhythmia (i.e. reduced cardiorespiratory coupling in schizophrenia but not for their first degree relatives).

In terms of HRV time domain measurements obtained from previous studies, it was shown that non-medicated schizophrenia patients exhibited decreased RMSSD (root mean square of successive RR differences – each RR difference is squared, summed, averaged and result of square root derived), pNN50 (the percentage of adjacent RR intervals that differ by more than 50 ms) and HF power compared to healthy subjects [Bar et al., 2007]. The SDNN (standard deviation of normal to normal RR intervals) reflects sympathetic and parasympathetic activity. The RMSSD and pNN50 correlate with HF power in HRV, more related to parasympathetic activity. These study results indicated that schizophrenia was characterised by a decrease in parasympathetic activity. The medication was not cause of this effect in HRV activity. Henry et al. study investigated HRV in acutely hospitalised manic bipolar, schizophrenia and healthy patients [Henry et al., 2010]. The HRV was analysed in time and frequency domains as well as nonlinear analyses. The results revealed that in bipolar patients, parasympathetic activity (vagal tone) was significantly reduced, and in schizophrenia patients a similar but 'not significant' reduction in the same HRV activity was evident, as compare to healthy patients. The reduction in heart rate complexity was also evident in bipolar disorder patient group when analysed using linear and nonlinear methods.

Uhlhaas and Singer claimed that in schizophrenia patients, the synchronisation of EEG beta and gamma bands was abnormal due to dysfunctional oscillations that occur during cognition, behaviour and at rest [Uhlhaas and Singer, 2010]. This synchronization abnormality was due to the impairment involving disconnectivity of cortical networks particularly in medial frontal, parietal/occipital, and left temporal [Zalesky et al., 2011]. This EEG beta and gamma synchronisation was typically present in local cortical areas [Womelsdorf et al., 2007] and the lower EEG activity (i.e. delta, theta and beta bands) synchronization was observed over and between more distant cortical areas [von Stein et al., 2000]. It is currently unknown *"to what extent impairments in local circuits contribute to long-range synchronisation impairments or whether these are two independent phenomena"* [p. 102, Uhlhaas and Singer, 2010]. *Our research study is aligned in investigating the cross-frequency synchronization between EEG high and low frequencies, related to more distant (long-range) and*

local cortical synchronization, respectively. Other studies revealed that patients with schizophrenia were characterized by reduced EEG gamma and theta amplitudes in the frontal cortical area [Cho et al., 2006] mainly during cognitive tasks accompanied by reduced phase synchronization [Uhlhaas and Singer, 2010]; reduced synchronization in EEG beta and gamma bands during visuo-perceptual organization and auditory processing [Uhlhaas et al., 2006]; and reduction in coherence at EEH theta band. Some studies have investigated whether the pharmacological treatments (medication) have any influence on the particular abnormal EEG activity in patients with schizophrenia. For example, *is the abnormality in EEG beta and gamma bands due to schizophrenia disorder alone or does medication plays any part in its abnormality?* Uhlhaas and Singer recommend that more research is necessary to shed light on this, but at the moment, various studies have reported abnormalities in the amplitude and phase of EEG gamma bands in patients treated briefly with medication and who started exhibiting schizophrenic symptoms [Uhlhaas and Singer, 2010]. Thus, it is evident that even at the onset development of abnormalities in EEG activities, medication which was administered briefly, may not play any part in it. Evidence shows that several psychiatric disorders may exhibit similar abnormal EEG activities [Uhlhaas and Singer, 2010]. For example, adults with autism spectrum and schizophrenia disorders typically are characterized with changes in EEG gamma during perceptual organisation. Bipolar and schizophrenia disorders have similar impairments during auditory steady-state evoked potentials (SSEP). These findings suggest that there is a need for an improved characterization of psychiatric disorders during wake and sleep, and linked to sleep disorders as it has been discussed in this chapter.

Timashev et al. introduced a new quantitative measure of frequency-phase synchronization and spikiness factor which showed lower values and higher values respectively in the higher risk schizophrenia group as compared to the other groups [Timashev et al., 2013]. These may have corresponded to the disruption in the neural activity of cortex area in schizophrenia.

For cognitive tasks, the long-range brain regions are predominantly active, thus low EEG band oscillations can be observed. However, the relationship between cognition and EEG oscillations is still debatable topic. It is understood that the Anterior Cingulate Cortex (ACC) activity is reflected by frontal midline theta (fm-theta) frequency band (4-7 Hz) [Maron-Katz et al., 2013]. The ACC activity and fm-theta is associated with attention demanding, mental and cognitive tasks, also linked to meditation and stage 1 and REM sleep [Inanaga, 1999]. If these fm-theta oscillations can be altered, the cognition can be enhanced, and thus influence the schizophrenia and other psychiatric disorders. On the contrary, fm-theta can be induced by various mental tasks or stage 1 and REM sleep. One study found that the mean EEG theta band frequency measured over frontal midline (fm) in medicated and non-medicated schizophrenic patients was less than at parietal region when compared to healthy and neuroleptic medicated patients. Westphal and colleagues revealed that this slower fm-theta activity in schizophrenia patients was related to the ‘hypofrontality hypothesis’ [Westphal et al., 1990].

Dumont et al. stressed the focus given to the dynamic interaction between HRV and limited number of EEG power bands along previous studies [Dumont et. al., 2004]. His research strived to broaden the assessment of underlying relationships upon all available EEG power bands under general sleep conditions. From a general perspective, the introduction of linear and nonlinear approaches revealed the coupling between HRV normalised high frequency band (HF_{nu}) and each EEG power band across the different sleep stages. The strongest interaction or maximized coupling occurred between EEG delta and HRV HF_{nu} power bands. Having said that, this study exclusively considered healthy young adults without mental or sleep disorders, then the obtained findings were useful in the sense of sleep staging examination rather than comparative analysis amongst clinical conditions. Therefore, the authors extended their study to more defined conditions related to sympathetic and vagal cardiac activities, such as sleep apnea-hypopnea syndrome [Dumont et al. 2007]. By conducting inherited and novel linear/nonlinear investigations, the predominance of interaction between EEG delta and HRV HF_{nu} power bands was reaffirmed. Conclusively, it was argued that sleep apnoea condition did not influence significantly the functional interdependence between HF_{nu} component and all remaining sleep power bands. A complete description about the conduction of the studies is summarised in Table 1.

Critchley et al. study on healthy patients [Critchley, 2003] wanted to determine which brain areas were associated with the control of HRV during effortful cognitive and motor behaviours. The findings were that during effortful cognitive and motor behavior the dorsal ACC was influenced by associated autonomic states of cardiovascular responses (arousals). This study was performed using the event-related fMRI and simultaneous ECG with computed HRV parameters (heart rate, LF, HF). Non-linear methods have been applied to investigate the disturbance in cortical integration in schizophrenia, study based on the dynamical decoupling of brain regions in schizophrenia [Breakspear et al., 2003]. The results revealed that for schizophrenia patients dynamical interdependencies were present more often between multiple cortical sites and less often between only two sites, seen in healthy patients. The authors suggest that this relates to the “loss of balance” between independence and interdependence in large-scale cortical processes [Breakspear et al., 2003]. This larger-scale may not necessarily mean the long-range cortical synchronization related to lower EEG bands (delta, theta and alpha) and more distant cortical sites.

7 Author’s Past and Current Research Projects

There is growing evidence in an alteration between cardiac and neural functions in primary insomnia and psychiatric patients. This alteration is due to abnormal levels of heart rate, heart rate variability, sleep spindles, arousal and slow-wave sleep, but the understanding of this cardio-neural interaction has not yet been fully established. The synchronisation studies upon polysomnographic (PSG) recordings are primarily oriented to reveal functional interdependence and causal

relationships between neuronal regions of interest and heart rate variability (HRV) in healthy and disordered (obstructive sleep apnoea/hypopnoea, insomnia, depressed and schizophrenia) patients.

Our research project, initially undertaken over the last few years is currently progressing well and will continue into the future. The project is focusing on the development of automated tool and consists of several stages of development. For the first stage of the project, the co-author Abdullah has been investigating the interaction of electroencephalographic (EEG) and electrocardiographic (ECG) signals during sleep stages and utilize these signals to automatically classify healthy, sleep (i.e. insomnia, obstructive sleep apnoea/hypopnoea and schizophrenia) disorders. The objective of Abdullah's project was to investigate study how EEG and ECG interact (i.e. measure which activity drives each other) during sleep stages and whether this interaction differs between sleep and psychiatric disorder sleep architecture. The signal processing was conducted offline. The classification consisted of developing a computational model that was 'trained' to recognise each of the group disorders. One half of collected PSG data was used from this 'training' part of the study. The 'trained' model was then used to 'test' and classify the second half of subjects from all four groups. The final outcome from this study was to test the effectiveness of using a mathematical model to classify each of the disorders.

In the follow-up project currently conducted by another co-author Chaparro-Vargas, the objective is to utilse more advanced linear and non-linear signal processing methods in order to evaluate this EEG and ECG interaction and statistical classification in online (i.e. near real-time) mode. The online EEG and ECG interaction will be evaluated using novel synchrogram feature and online sleep staging (i.e. online hypnogram). The combined features, 'synchrohypnograms' will be the 'main engine' of the project in order to automatically classify the disorders. From this online 'synchrohypnograms', the neuronal and cardiac 'oscillators' and instantaneous coupling and decoupling phenomena in terms of amplitudes, cross frequencies and phase shifts across the different sleep stages, will be developed.

8 Future Directions

Although much of the research has been done to determine the cause of insomnia, its specific cause has not yet been demonstrated and remains elusive. It is unclear whether increased autonomic activity is causing insomnia or whether insomnia and its sleep loss triggers increased autonomic activity. This study might also help us better understand the connection of insomnia to psychiatric disorders (or vice versa). Our tool's systematic classification of patient PSG data could provide a clinician with invaluable information to treat depression and schizophrenia earlier before it worsens and becomes chronic and at the same time, treat insomnia.

Table 1 Literature review summary of subjective, objective PSG and EEG and ECG interaction and epidemiological studies on causes and effects of insomnia and psychiatric disorders. Literature review summary of epidemiological studies on causes and effects of insomnia and psychiatric disorders

Year	Disorder	Title	Author/Journal	Type of study, No. and type of participants	Methods	Findings
2013	Schizophrenia	Impaired coupling of local and global functional feedbacks underlies abnormal synchronization and negative symptoms of schizophrenia	Noh, K., et al. BMC Systems Biology	Patients: 12 M, 3 F (23.80 ± 4.6) Healthy: 11 M, 6 F (22.06 ± 2.11)	120 seconds MEG Diagnosis: DSM-IV, PANSS, DSM-IV (Non-patient version) MEG: 102 magnetometers Analysis: Time-Frequency and power analysis, Beta-gamma power switching, phase synchronization, feedback identification based on impulse reponses, Wilson-Cowan Model Statistics: Two-tailed t-test	Coupled local and global feedback (CLGF) circuits in the cortical functional network are related to abnormal synchronization and also correlated to the negative symptom of schizophrenia During rest an increase in beta band synchronization and a reduction in gamma band power compared to healthy controls
2012	Schizophrenia	Consciousness, schizophrenia and complexity	Bob, P. Cognitive Systems Research			Mental disintegration in schizophrenia could be described as a level of neural disintegration leading to more irregular neural states with higher complexity that negatively affect information integration and synchronization process in the brain
2012	Schizophrenia	Attention of long-range temporal correlations in the amplitude dynamics of alpha and beta neuronal oscillations in patients with schizophrenia	Nikulin, V., et al. Neuroimage	Patients: 16 M, 5 F (37.9 ± 5.1) Healthy: 21 M, 7 F (35.9 ± 7.1)	50 seconds EEG EEG: 21 electrodes Diagnosis: DSM-III, DSM-IV, SANS, SAPS Analysis: Instantaneous amplitude, detrended fluctuation analysis, cross-frequency correlation	Amplitude of neuronal oscillations in alpha and beta frequency ranges did not differ between patients and control subjects Long-range temporal correlations (LRTC) were strongly attenuated in patients with schizophrenia in both alpha and beta frequency ranges Cross-frequency correlation between LRTC belonging to alpha and beta oscillations was stronger for patients than

Table 1 (*Continued*)

						healthy controls
2012	Schizophrenia	Analysis of cross-correlations in electroencephalogram signals as an approach to proactive diagnosis of schizophrenia	Timashev, S. F., Physica A: Statistical Mechanics and its Applications	Subjects: 84 (12 ± 2)	60 seconds EEG EEG: 2 electrodes (F3, F4) Diagnosis: Diagnosed schizophrenia-spectrum symptoms Analysis: Flicker-noise spectroscopy, cross-correlation function, frequency-phase synchronization	Classification subjects into 4 categories corresponding to different risk levels of subjects' susceptibility to schizophrenia
2011	Schizophrenia	Disrupted Axonal Fiber Connectivity in Schizophrenia	Zalesky, A., et al. Biology Psychiatry	Patients: 47 M, 27 F (38 ± 11) Healthy: 15 M, 17 F (33 ± 13)	MRI: Preprocessing pipeline Diagnosis: Diagnostic interview for psychoses Analysis: Fibre tract network model, Network organization: nodal degree, efficiency, path length, clustering coefficient and small-worldness.	Impaired connectivity to involve a distributed network of nodes compromising medial frontal, parietal/occipital, and the left temporal lobe.
2010	Insomnia and depression	Comorbidity of insomnia and depression	Staner, L. Sleep Medicine Reviews	Review	-	Epidemiological studies show that insomnia could lead to depression.
2010		Altered interaction between cardiac vagal influence and delta sleep EEG suggests an altered neuroplasticity in patients suffering from major depressive disorder.	Jurysta, F., et al., Acta Psychiatrica Scandinavica	MDD: 10 M (38 ± 10) Healthy: 10 M (40 ± 9)	4 nights PSG MDD scored HDRS > 16 (Hamilton Depression rating Scale 24 items) EEG: Normalized delta power ECG: LF, HF, Total Power, LFnu, Hfnu, LF/HF Coherence analysis: Coherence function, gain function and phase shift Statistics: ANCOVA	Smoking and caffeine intake were related to the duration of the first three NREM-REM. MDD: Sleep latency increased, other sleep parameters not significant S1 and W duration were increased HRV: not significant Coherence: lower gain between HFnu and delta Modification in HF appear 8 and 10 min before modification of delta in MDD and healthy
2010	Sleep and depression	Wake and sleep EEG provide biomarkers in depression	Steiger, A. and Kimura, M. Journal of Psychiatric Research 4		Review article	REM sleep desinhibition, disturbed sleep continuity, lower SWS, shorter REM latency are potential biomarkers to characterize depression.
2009	Insomnia	The impact of chronic primary insomnia on the	Jurysta, F., et al.,	chronic primary insomnia : 14 M (42 ± 12)	3 nights PSG (used 2nd night) EEG: FFT on 5s data window, averaged every 20s	Insomnia: sleep efficiency was decreased, sleep latency longer

Table 1 (*Continued*)

		heart rate - EEG variability link	Clinical Neurophysiology	Healthy: 14 M (41 ± 10)-	Normalized delta power (0.5-3 Hz)=Sum delta power every 20s/mean power across full night ECG: RRI on 120s and shifting 20s ahead HRV: LFnu, HFnu, Total power HRV, LF/HF Coherence analysis: Coherence function, gain function, phase shift Statistics: ANOVA repeated measures within groups	NREM duration similar Larger mean duration REM HRV parameters not significant between groups in all sleep stages. Insomnia: decreased linear coupling between two markers. Similar gain and phase shift with the healthy. Decreased coherence represent desynchronization of both neural population.
2009	General sleep and depression	The direction of longitudinal associations between sleep problems and depression symptoms: a study of twins aged 8 and 10 years old	Gregory, A.M., et al., Sleep	Epidemiology-longitudinal 300 twin pairs aged 8-10 years old.	A cross-lagged model was used to examine the concurrent and longitudinal associations between sleep problems and depression.	Sleep problems at age 8 predicted depression at age 10 whereas depression symptoms did not predict later sleep problems.
2009	General mental	National Survey of Mental Health and Wellbeing of Australians: Summary of Results.	Australian Bureau of Statistics (ABS).	Report		20% of population had a mental disorders in any 12 months period
2008	Depression and insomnia	A bidirectional relationship between anxiety and depression, and insomnia? A prospective study in the general population	Jansson-Fröjmark, M. and Lindblom, K. Journal of Psychosomatic Research	Epidemiology-longitudinal 1498 Aged 20-60 years old	One year follow up study by posted questionnaires. Use Hospital Anxiety and Depression Scale (HADS). Sleep measures: Basic Nordic Sleep Questionnaires and Uppsala Sleep Inventory Define insomnia based on DSM and ICSD-reporting a sleep problem for 3 nights or more per week during the past 3 months Statistic: Correlation analysis for (depression-anxiety-insomnia relationship) Bidirectional analysis: Four stepwise logistics regression with odds ratio	Anxiety, depression and insomnia are bidirectional related over time. Insomnia at baseline had predictive power odds ratio=3.5 in relation to future depression.
2008	Depression and insomnia	Prevalence, course, and comorbidity of insomnia and depression in young adults	Buysse, D.J., et al., Sleep	Epidemiology-longitudinal 591 participants	20 years follow up.	Insomnia predicted future MDE and that MDE tended to predict future insomnia. Pure insomnia and insomnia comorbid with depression were strongly associated with each other longitudinally, whereas pure depression and insomnia comorbid with depression were less consistently related to each other longitudinally.
2008	Depression and insomnia	Adolescent insomnia as a risk factor for early adult	Roane, B.M. and Taylor, D.J.	Epidemiology-longitudinal 4494 adolescents, 12 to 18	6 to 7 years follow-up.	Insomnia symptoms during adolescence were a significant

Table 1 (*Continued*)

		depression and substance abuse	Sleep	years old at baseline, with 3582 young adults, 18 to 25 years.		risk factor for depression diagnosis
2008	Depression	Which symptoms predict recurrence of depression in women treated with maintenance interpersonal psychotherapy?	Dombrovski, A.Y., et al., Depress Anxiety	131 women aged 20-60.	Used Cox proportional hazards regression models	Persistent is associated with increased risk of recurrence of depression.
2007	Insomnia	The Direct and Indirect Costs of Untreated Insomnia in Adults in the United States	Ozminkowski, R.J., Wang, S. and Walsh, J.K. Sleep	Retrospective 138,820 younger adults and 75,558 elderly patients plus equal-sized, matched comparison groups	Used data from July 1, 1999 to June 30, 2003. Statistic: t-test, multiple regression (2-part regression process)	in average insomnia patients will spend $5790 within 6 months for treatment cost
2007	General sleep and sleep apnea-hypopnea	Scale-free dynamics of the synchronization between sleep EEG power bands and the high frequency component of heart rate variability in normal men and patients with sleep apnea-hypopnea syndrome	M. Dumont, F. Jurysta, J.-P. Lanquart, A. Noseda, P. van de Borne, and P. Linkowski Clinical Neurophysiology	Patients: 24 (44 ± 5) Healthy: 12 (43 ± 6)	2 overnight EEG recordings (20 second epochs) EEG: 3 electrodes (Fz-Ax, Cz-Ax, Oz-Ax) Analysis: Detrended Fluctuation Analysis	Sleep apnea-hypopnea syndrome does not affect the interdependence between the high frequency component of heart rate variability and all sleep power bands as measured by synchronization likelihood.
2007	Depression and cardio	Alteration of cardiac autonomic functions in patients with major depression: A study using heart rate variability measures	Udupa, K., et al., Journal of Affective Disorders	MDD: 26 M, 14 F (30.58 ± 7.4) Healthy: 26 M, 14 F (30.73 ± 7.1)	Subjective measures: DSM-IV TR HDRS > 16 Objectives: ECG: Lead II, 15 min basal recording , extract SDNN, RMSDD, LFnu, HFnu , LF/HF Deep breathing difference Valsava maneuver (intrathoracic pressure) Orthostatic test Statistic unpaired t-test and Pearson Correlation Coefficient	MDD: LF/HF sympathovagal balance was higher, LFnu showed increased sympathetic activity but not significant Significant negative correlation between age and parasympathetic
2007	Depression and sleep	Characterization of the sleep EEG in acutely depressed men using detrended fluctuation analysis.	Leistedt, S., et al., Clinical Neurophysiology	Healthy: 14 M (42.43 ± 5.67) Acute depressed: 10 M (41.7 ± 8.11)	Subjective measures: Pittsburgh Sleep Quality Index (PSQI). Hamilton Rating Scale for Depression (HAM-D) Meet DSM-IV-TR criteria. Objective measures: 3 nights PSG (only last 2 nights used) Extract DFA to each contiguous 20-s epoch during S2, SWS and REM. Statistics: Kruskal–Wallis test and the Spearman's rank correlation Coefficient sleep analysis, Student's	A strong linear correlation was observed between the DFA exponents and the HAM-D score during SWS. A decrease of long-range temporal correlations during stage 2 and SWS in depressive patients in comparison with the healthy controls.

Table 1 (*Continued*)

					t-test or Mann–Whitney	
2006	Insomnia	Epidemiology of insomnia: Prevalence, self-help treatments, consultations, and determinants of help-seeking behaviors	Morin, C.M., et al Sleep Medicine	Epidemiology 2001 Aged 18-91 years old	Telephone survey Used DSM-IV and ICD-10 to define insomnia Statistics: Between group comparison, Chi-squared Tests and logistic regression	9.5% of the population in Canada reported with insomnia which mainly caused by psychological distress (40%).
2006	Depression and insomnia	The association of insomnia with anxiety disorders and depression: Exploration of the direction of risk	Johnson, E.O., Roth, T. and Breslau, N. Journal of Psychiatric Research	Epidemiology 1014 participants age (13-15).	Use structured interviews of DSM-IV To examine directionality between insomnia, depression and anxiety Statistic: Cox Proportional hazards model. Factor: Sex, race/ethnicity, income, parent marital status, parent education	Prior insomnia was associated with onset of depression, prior anxiety may lead to insomnia but less association from depression to insomnia.
2006		The economic cost of sleep disorders.	Hillman, D.R., et al Sleep		Using data derived from national databases (including the Australian Institute of Health and Welfare and the Australian Bureau of Statistics).	The overall cost of sleep disorders in Australia in 2004 was $7494 million
2005	General sleep	Wake up Australia: The value of healthy sleep.	Report by Access Economics Pty Ltd for Sleep Health Australia,	Report		In Australia, it is estimated about 6% of the population are affected by sleep disorders
2005	Insomnia	Is insomnia a marker for psychiatric disorders in general hospitals?	Rocha, F.L., et al., Sleep Medicine	200 participants aged 18-65 years old	Used structured and codified questionnaires. Interviews by psychiatrist using DSM-IV Statistic: Multivariate logistics regression odds ratio	Insomnia is marker for major depressive episode in general hospital inpatients. The prevalence of MDE among patients with insomnia is 46.9%.
2005	Depression and insomnia	Epidemiology of insomnia, depression and anxiety	Taylor, D.J., et al., Sleep	722 participants aged 20-89 years old	Complete sleep diaries for two weeks. Factor: Sex, ethnicity	People with insomnia were 9.82 and 17.35 times as likely to have depression and anxiety. African American and women had higher depression level than Caucasian and men.
2004	General sleep	Interdependency between heart rate variability and sleep EEG: linear/nonlinear?	M. Dumont, F. Jurysta, J.-P. Lanquart, P.-F. Migeotte, P. van de Borne and P. Linkowski Clinical Neurophysiology	Healthy: 8 M (20.5)	2 overnight EEG recordings (20 second epochs) EEG: 3 electrodes (Fz-Ax, Cz-Ax, Oz-Ax) Analysis: Synchronization likelihood, surrogate data statistical analysis	The interaction between delta and HF_{nu}, requires a non-linear model while a more simplistic system (with less oscillators or synchronized oscillators), such as sigma and HF_{nu} interaction is described by a linear model. This study confirms that all sleep EEG power bands are coupled to HF_{nu} band of RRI in healthy young subjects. The interaction between delta, theta and alpha bands and HF_{nu}

Table 1 (*Continued*)

						is non-linear.
2003	Depression and insomnia	Primary insomnia: a risk factor to develop depression?	Riemann, D. and Voderholzer, U. Journal of Affective Disorders	Report from literature review of study conducted from 1966-2000	Investigate primary insomnia according to DSM-IV: insomnia complaints at least 1 month	Insomnia can act as independent predictor /risk factor for developing depression. Most study do not differentiate insomnia according to its subtype (eg. primary, secondary, chronic
2003	Depression and insomnia	Place of chronic insomnia in the course of depressive and anxiety disorders	Ohayon M.M. and Roth T. J Psychiatr Res.	14,915 subjects aged from 15 to 100 years old	Use Sleep EVAL system	previous history of a mental disorder is closely related to the severity and the chronicity of current insomnia
2001	Depression and sleep	Delta sleep ratio as a predictor of sleep deprivation response in major depression.	Nissen, C., et al., Journal of Psychiatric Research	Primary major depressive (SD responder): 5 M, 3 F (37.8 ± 11.5) Non responder: 5 M, 3 F (37.1 ± 13.8)	Subjective: HAMD scored > 18 SD responder: showed 50% improvement of 6 HAMD Non responder: showed <50% improvement of 6 HAMD 2 nights PSG: Sleep deprived study PSG sleep summary were calculated All night spectral analysis for frequency bands: delta, theta, alpha, sigma, beta1 and beta2. Delta sleep ratio is defined as a quotient of SWA in the first to the second NREM episode. All analysis done in log value (base e) Statistic: t-test and 2 factorial ANOVA	A high delta sleep ratio is a positive predictor for SD response.
2000	Insomnia	Prevalence of insomnia in a survey of 12 778 adults in France.	Leger, D., et al., Journal of Sleep Research	Epidemiology 12 778 subjects Aged 18-65+ years old	Questionnaires adapted from DSM-IV criteria for insomnia Factors: age, sex, profession and marital status Statistic: Student t-test, Chi-squared tests and odds ratio	9% of the population was reported with severe insomnia. Sleep complaints were higher in woman, increase significant with age, in retiree and white collar worker and in widows, divorcee
2000	General sleep	Sleep loss and daytime sleepiness in the general adult population of Japan.	Liu, X., et al Psychiatry Research	Epidemiology 3030 Aged 20+	Post questionnaire Statistic: Chi-squared test, Spearman rank correlation coefficients were computed to examine relationships between age and sleep duration, Statistic: Logistic regression analysis was applied to examine associations of sleep problems with age and gender	In Japan, the prevalence of insomnia was 21.4% and increase in elderly
2000	Depression and insomnia	Depression and insomnia: questions of cause and effect	Lustberg, Lisa Reynolds, Charles F.	Review		Chronic insomnia is a risk factor for depression and MDE. PSG revealed reduction of delta

Table 1 (*Continued*)

			Sleep Medicine Reviews			waves in NREM and decreased REM latency.
2000	Depression and sleep	Towards a neurobiology of dysfunctional arousal in depression: the relationship between beta EEG power and regional cerebral glucose metabolism during NREM sleep	Nofzinger, E.A., et al., Psychiatry Research: Neuroimaging,	Depressed: 4 M, 8 F (40.14 ± 10.5) Healthy: #1: 3 M, 6 F (32.02 ± 9.19) #2: 4 M, 8 F (40.11 ± 10.82)	Subjective measures: Depression: Meet diagnosis DSM-III-R (primary unipolar), HRSD min score 15 Healthy: Meet Research Diagnostic Criteria HRSD: score < 6 All must complete visual analog scale to describe sleep quality Objective measures: Depression: PSG sleep and NREM PET #1 PSG and NREM PET #2 PSG only PSG 3 night (used 2nd night as baseline sleep night) EEG: FFT of 4 s epochs to calculate beta power (20-32 Hz) PET: 2 nights Statistics: ANCOVA, t –test and Spearman's rho correlation to test sleep parameters	Depression: Described worse sleep quality on a baseline sleep night
1999	Insomnia	Characteristics of insomnia in the United States : Results of the 1991 National Sleep Foundation survey. I.	Ancoli Israel, et al American Academy of Sleep Medicine.	Epidemiology 1000		In US, the prevalence rate of occasional insomnia was 25% and 9% was reported for regular sleep disturbance
1999	Insomnia	Evaluation of severe insomnia in the general population: results of a European multinational survey.	Chevalier H, L.F. et al J Psychopharmacol,	Epidemiology	Face to face interview	prevalence of severe insomnia was ranged from 4% to 22% and was higher in female
1999	Insomnia	The direct economic costs of insomnia in the United States for 1995	Walsh J.K., Engelhardt C.L. Sleep	Report	Used data compiled by IMS America, Ltd and data of the 1994 National Ambulatory Medical Care Survey conducted by the National Center for Health Statistics and from the America Medical Association Center for Health Policy Research	In 1995, total direct costs in the United States for insomnia in were estimated to be $13.9 billion.
1997	Insomnia and depression	Insomnia in young men and subsequent depression. The Johns Hopkins Precursors Study	Chang, P.P., et al., American Journal of Epidemiology	1053 participants	34 years follow up. Use Cox proportional hazards analysis.	Insomnia in young men is indicative of a greater risk for subsequent clinical depression and psychiatric distress that persists for at least 30 years.
1996	Insomnia	The socioeconomic impact of insomnia. An overview.	Chilcott L.A. , Shapiro C.M. Pharmacoeconomics	overview		In 1994, the total direct, indirect and related costs of insomnia are conservatively estimated at $US30 to 35 billion annually in the US
1988	General sleep	A survey of sleeping difficulties in an Australian population	Lack, L., Miller, W. and Turner, D. Community Health Studies,	216 participants	Telephone survey in Adelaide	13-20% of population experienced various sleep disturbance with 6-7% have difficulty to initiate sleep

9 Conclusion

Most of this section of this chapter cover the comprehensive literature review on the studies published upto date based on the resting neuronal and cardiac signal interaction and synchronization during awake and sleep, in patients suffering from insomnia, depression and schizophrenia. The literature also characterises these disorders and sheds a spectrum of rays for authors and others to pursue their research towards one common cause, *and that is to assist in the diagnosis of sleep, depression and schizophrenia disorders.* The authors are currently conducting concurrent projects to better understand the connectivity between insomnia and schizophrenia by finding the reason why insomniac patients have an increase risk to develop depression that may become chronic or even lead to occurrence of first episodes of schizophrenia.

References

Neckelmann, D., Mykletun, A., Dahl, A.A.: Chronic insomnia as a risk factor for developing anxiety and depression. Sleep 30(7), 873–880 (2007)

Kennedy, G.A., Solin, P.: How to treat- insomnia- part I. Australian Doctor, 37–44 (2004)

Perlis, M.L., Sharpe, M., Smith, M.T., Greenblatt, D., Giles, D.: Behavioral Treatment of Insomnia: Treatment Outcome and the Relevance of Medical and Psychiatric Morbidity. J. Behav. Med. 24(3), 281–296 (2001)

Livingston, G., Blizard, B., Mann, A.: Does sleep disturbance predict depression in elderly people? A study in inner London. Br. J. Gen. Pract. 43(376), 445–448 (1993)

Fawcett, J., Scheftner, W.A., Fogg, L., Clark, D.C., Young, M.A., Hedeke, D., Gibbons, R.: Time-related predictors of suicide in major affective disorder. Am. J. Psychiatry 147, 1189–1194 (1990)

Riemann, D., Spiegelhalder, K., Feige, B., Voderholzer, U., Berger, M., Perlis, M., Nissen, C.: The hyperarousal model of insomnia: A review of the concept and its evidence. Sleep Medicine Reviews 14, 19–31 (2010)

Littner, M., Hirshkowitz, M., Kramer, M., Kapen, S., Anderson, W.M., Bailey, D., Berry, R.B., Davila, D., Johnson, S., Kushida, C., Loube, D.I., Wise, M., Woodson, B.T.: Practice Parameters for Using Polysomnography to Evaluate Insomnia: An Update. Sleep 26(6), 754–760 (2003)

Morin, C.M., Vallieres, A., Ivers, H.: Dysfunctional beliefs and attitudes about sleep (DBAS): validation of a belief version (DBAS-16). Sleep 30(11), 1547–1544 (2007)

Treynor, W., Gonzalez, R., Nolen-Hoeksema, S.: Rumination reconsidered: A psychometric analysis. Cognitive Therapy and Research 27(3), 247–259 (2003)

Edinger, J.D., Krystal, A.D.: Subtyping primary insomnia: is sleep state misperception a distinct clinical entity? Sleep Med. Rev. 7(3), 203–214 (2003)

Taylor, D.J., Lichstein, K.L., Durrence, H.H., Reidel, B.W., Bush, A.J.: Epidemiology of insomnia, depression, and anxiety. Sleep 28(11), 1457–1464 (2005)

Johnson, E.O., Roth, T., Breslau, N.: The association of insomnia with anxiety disorders and depression: Exploration of the direction of risk. Journal of Psychiatric Research 40(8), 700–708 (2006)

Gregory, A.M., Rijsdijk, F.V., Lau, J.Y.F., Dahl, R.E., Eley, T.C.: The Direction of Longitudinal Associations Between Sleep Problems and Depression Symptoms: A Study of Twins Aged 8 and 10 Years. Sleep 32(2), 189–199 (2009)

Chang, P.P., Ford, D.E., Mead, L.A., Cooper-Patrick, L., Klag, M.J.: Insomnia in young men and subsequent depression. The Johns Hopkins Precursors Study. Am. J. Epidemiol. 146(2), 105–114 (1997)

Rocha, F.L., Hara, C., Rodrigues, C.V., Costa, M.A., Castro e Costa, E., Fuzikawa, C., Santos, V.G.: Is insomnia a marker for psychiatric disorders in general hospitals? Sleep Medicine 6(6), 549–553 (2005)

Ohayon, M.M., Roth, T.: Place of chronic insomnia in the course of depressive and anxiety disorders. Journal of Psychiatric Research 37(1), 9–15 (2003)

Jansson-Fröjmark, M., Lindblom, K.: A bidirectional relationship between anxiety and depression, and insomnia? A prospective study in the general population. Journal of Psychosomatic Research 64(4), 443–449 (2008)

Mayers, A.G., Baldwin, D.S.: The relationship between sleep disturbance and depression. International Journal of Psychiatry in Clinical Practice 10(1), 2–16 (2006)

Stampfer, H.G.: The relationship between psychiatric illness and the circadian pattern of heart rate. Australian and New Zealand Journal of Psychiatry 32(2), 187–198 (1998)

Iverson, G.L., Gaetz, M.B., Rzempoluck, E.J., McLean, P., Linden, W., Remick, R.: A new potential marker for abnormal cardiac physiology in depression. Journal of Behavioral Medicine 28(6), 507–511 (2005)

Boostani, R., Sadatnezhad, K., Sabeti, M.: An efficient classifier to diagnose of schizophrenia based on the EEG signals. Expert Systems with Applications 36(3, Part 2), 6492–6499 (2009)

Togo, F., Cherniack, N.S., Natelson, B.H.: Electroencephalogram characteristics of autonomic arousals during sleep in healthy men. Clin. Neurophysiol. 117(12), 2597–2603 (2006)

Jurysta, F., Lanquart, J.-P., Sputaels, V., Dumont, M., Migeotte, P.-F., Leistedt, S., Linkowski, P., van de Borne, P.: The impact of chronic primary insomnia on the heart rate – EEG variability link. Clinical Neurophysiology 120, 1054–1060 (2009)

Jurysta, F., Kempenaers, C., Lancini, J., Lanquart, J.P., Van De Borne, P., Linkowski, P.: Altered interaction between cardiac vagal influence and delta sleep EEG suggests an altered neuroplasticity in patients suffering from major depressive disorder. Acta Psychiatrica Scandinavica 121, 236–239 (2010)

Udupa, K., Sathyaprabha, T.N., Thirthalli, J., Kishore, K.R., Lavekar, G.S., Raju, T.R., Gangadhar, B.N.: Alteration of cardiac autonomic functions in patients with major depression: a study using heart rate variability measures. J. Affect. Disord. 100(1-3), 137–141 (2007)

Gillin, J.C., Duncan, W., Pettigrew, K.D., Frankel, B.L., Snyder, F.: Sucessful separation of depressed, normal and insomniac subjects by EEG sleep data. Arch. Gen. Psychiatry 36(1), 85–90 (1979)

Steiger, A., Kimura, M.: Wake and sleep EEG provide biomarkers in depression. J. Psychiatr. Res. 44(4), 242–252 (2010)

Staner, L., Cornette, F., Maurice, D., Viardot, G., Le Bon, O., Haba, J., Staner, C., Luthringer, R., Muzet, A., Machner, J.-P.: Sleep microstructure around sleep onset differentiates major depressive insomnia from primary insomnia. J. Sleep Res. 12, 319–330 (2003)

Bonnet, M.H., Arand, D.L.: 24-Hour metabolic rate in insomniacs and matched normal sleepers. Sleep 18(7), 581–588 (1995)

Nofzinger, E.A., Buysse, D.J., Germain, A., Price, J.C., Miewald, J.M., Kupfer, D.J.: Functional neuroimaging evidence for hyperarousal in insomnia. Am. J. Psychiatry 161(11), 2126–2128 (2004)

Leistedt, S., Dumont, M., Lanquart, J.P., Jurysta, F., Linkowski, P.: Characterization of the sleep EEG in acutely depressed men using detrended fluctuation analysis. Clin. Neurophysiol. 118(4), 940–950 (2007)

Westphal, K.P., Grozinger, B., Diekmann, V., Scherb, W., Reeb, J., Leibing, U., Kornhuber, H.H.: Slower theta activity over the midfrontal cortex in schizophrenia patients. Acta Psychiatr. Scand. 81, 132–138 (1990)

Inanaga, K.: Frontal midline theta rhythm and mental activity. Psychiatry and Clinical Neurosciences 52(6), 555–566 (1999)

Critchley, H.D., Mathias, C.J., Josephs, O., O'Doherty, J., Zanini, S., Dewar, B.-K., Cipolotti, L., Shallice, T., Dolan, R.J.: Human cingulated cortex and autonomic control: converging neuroimaging and clinical evidence. Brain 126(10), 2139–2152 (2003), doi:10.1093/brain/awg216

Maron-Katz, A., Ben-Simon, E., Sharon, H., Gruberger, M., Cvetkovic, D.: A Neuroscientific Perspective on Meditation. In: Fábián, T.K. (ed.) Psychology of Meditations, Mind-Body Connections: Pathways of Psychosomatic Coupling under Meditation and Other Altered States of Consciousness, NOVA, Hungary, EU (2013) (in press)

Uhlhaas, P.J., Singer, W.: Abnormal Neural Oscillations and Synchrony in Schizophrenia. Nature Reviews, Neuroscience 11, 100–113 (2010)

von Stein, A., Chaing, C., Konig, P.: Top down processing mediated by interareal synchronization. Proc. Natl. Acad. Sci. 97, 14748–14753 (2000)

Womelsdorf, T., et al.: Modulation of neuronal interactions through neuronal synchronization. Science 316, 1609–1612 (2007)

Cho, R.Y., Konecky, R.O., Carter, C.S.: Impairments in frontal cortical gamma synchrony and cognitive control in schizophrenia. Proc. Natl. Acad. Sci. 103, 19878–19883 (2006)

Uhlhaas, P.A., et al.: Dysfunctional long-range coordination of neural activity during Gestalt perception in schizophrenia. J. Neurosci. 26, 8168–8175 (2006)

Cotton, S.M., Lambert, M., Schimmelmann, B.G., Mackinnon, A., Gleeson, J.F.M., Berk, M., Hides, L., Chanen, A., McGorry, P.D., Conus, P.: Depressive symptoms in first episode schizophrenia spectrum disorder. Schizophrenia Research 134, 20–26 (2012)

Breakspear, M., Terry, J.R., Friston, K.J., Harris, A.W.F., Williams, L.M., Brown, K., Brennan, J., Gordon, E.: A disturbance of non-linear interdependence in scalp EEG of subjects with first episode schizophrenia. NeuroImage 20, 466–478 (2003)

Schulz, S., Bar, K.J., Voss, A.: Respiratory variability and cardiorespiratory coupling analyses in patients suffering from schizophrenia and their healthy first-degree relatives. Biomed. Tech. 57(suppl.1), 104 (2012)

Bar, K.J., Boettger, M.K., Koschke, M., Schulz, S., Chokka, P., Yeragani, V.K., et al.: Non-linear complexity measures of heart rate variability in acute schizophrenia. Clinical Neurophysiology 118, 2009–2015 (2007)

Henry, B.L., Minassian, A., Paulus, M.P., Geyer, M.A., Perry, W.: Heart rate variability in bipolar mania and schizophrenia. Journal of Psychiatric Research 44(3), 168–176 (2010)

Ferrarelli, F., Peterson, M.J., Sarasso, S., Riedner, B.A., Murphy, M.J., Benca, R.M., Bria, P., Kalin, N.H., Tononi, G.: Thalamic dysfunction in schizophrenia suggested by whole-night deficits in slow and fast spindles. Am. J. Psychiatry 167, 1339–1348 (2010)

Ferrarelli, F., Huber, R., Peterson, M.J., Massimini, M., Murphy, M., Riedner, B.A., Watson, A., Bria, P., Tononi, G.: Reduced sleep spindle activity in schizophrenia patients. Am. J. Psychiatry 164, 483–492 (2007)

Goder, R., Aldenhoff, J.B., Boigs, M., Braun, S., Koch, J., Fritzer, G.: Delta power in sleep in relation to neuropsychological performance in healthy subjects and schizophrenia patients. Journal of Neuropsychiatry and Clinical Neurosciences 18, 529–535 (2006)

Zalesky, A., Fornito, A., Seal, M.L., Cocchi, L., Westin, C.-F., Bullmore, E.T., Egan, G.F., Pantelis, C.: Disrupted Axonal Fiber Connectivity in Schizophrenia. Biology Psychiatry 69, 80–89 (2011)

Bob, P.: Consciousness, schizophrenia and complexity. Cognitive Systems Research 13(1), 87–94 (2012)

Dumont, M., Jurysta, F., Lanquart, J.-P., Migeotte, P.-F., van de Borne, P., Linkowski, P.: Interdependency between heart rate variability and sleep EEG: linear/non-linear? Clinical Neurophysiology 115(9), 2031–2040 (2004)

Dumont, M., Jurysta, F., Lanquart, J.-P., Noseda, A., van de Borne, P., Linkowski, P.: Scale-free dynamics of the synchronization between sleep EEG power bands and the high frequency component of heart rate variability in normal men and patients with sleep apnea–hypopnea syndrome. Clinical Neurophysiology 118(12), 2752–2764 (2007)

Nikulin, V.V., Jönsson, E.G., Brismar, T.: Attenuation of long-range temporal correlations in the amplitude dynamics of alpha and beta neuronal oscillations in patients with schizophrenia. NeuroImage 61(1), 162–169 (2012)

Noh, K., Shin, K.S., Shin, D., Hwang, J.Y., Kim, J.S., Jang, J.H., Chung, C.K., Kwon, J.S., Cho, K.-H.: Impaired coupling of local and global functional feedbacks underlies abnormal synchronization and negative symptoms of schizophrenia. BMC Systems Biology 7(30), 1–13 (2013)

Timashev, S.F., Panischev, O.Y., Polyakov, Y.S., Demin, S.A., Kaplan, A.Y.: Analysis of cross-correlations in electroencephalogram signals as an approach to proactive diagnosis of schizophrenia. Physica A: Statistical Mechanics and its Applications 391(4), 1179–1194 (2012)

Questions

Q1. What is the causal relationship between insomnia and patho-physiological disorders (e.g. depression, schizophrenia, etc.)?

Q2. Which are the physiological cues characterising primary and chronic insomnia?

Q3. From a neuronal perspective, what is the relationship between schizophrenia disease and EEG spectral bands?

Q4. Explain the term functional dysconnectivity used in schizophrenia.

Q5. List the physiological changes that are associated with depression.

Q6. Differentiate the terms primary insomnia and secondary insomnia.

Appendix B

Peer-reviewed conference paper

Title: A Single-trial Toolbox for Advanced Sleep Polysomnographic Processing

Authors: Ramiro Chaparro-Vargas and Dean Cvetkovic

Publication: Proceedings of the 35th Annual International Conference of the IEEE Engineering in Medicine and Biology Society

Year of Publication: 2013

A Single-trial Toolbox for Advanced Sleep Polysomnographic Preprocessing

Ramiro Chaparro-Vargas[1], *Member* and Dean Cvetkovic[2], *Member*

***Abstract*— The application of polysomnographic (PSG) studies for monitoring sleep activity is a multi-parametric practice that involves a diverse group of biological signals. A suitable preprocessing of such signals assures a more profitable feature extraction and classification operations. Therefore, the proposed preprocessing toolbox performs segmentation, filtering, denoising, whitening and artefact removal tasks upon multi-channel PSG recordings. In order to assess toolbox's efficiency, clinical experiments are conducted, as well as, quantitative and qualitative metrics are discussed. Our findings reveal outperforming efficiency by artefacts and noise rejection after single-trial and multi-stage preprocessing.**

I. INTRODUCTION

The polysomnogram (PSG) is a monitoring technique for sleep structure assessment and detection of related anomalies or disorders. Due to the gathering of multi-parametric biological signals, such as neuronal, ocular, muscular, cardiac and respiratory; the encounter of accurate diagnosis can be promptly conveyed by specialists [4]. By convention, PSG recordings include a minimum of 3 electroencephalographic (EEG), 2 electrooculographic (EOG), 1 electromyographic (EMG), 1 electrocardiographic (ECG) and 1 respiratory channel. Though, the present work considers an arrangement of 6 channels as follows: EEG O2, EEG C3, Right EOG, Left EOG, ECG and EMG submental, whereas at least one biophysical source is required for toolbox deployment.

The development of computer-assisted or manual visualisation systems for sleep staging or disorders detection are commonly distinguished by feature extraction and classification stages [6]. Nevertheless, the presence of bodily endogenous and exogenous interferences, frequently denoted as noise and artefacts, tantalises the achievement of performant scores in autonomous recognition and diagnosis processes. For this reason, the introduction of a prior preprocessing stage is proposed to enhance the original signal properties by embedded artefacts correction and noise removal, whilst neither reduction nor expansion transformations are invoked [10]. In addition, the introduced toolbox intends to deal properly with the highly complex characteristics of EEG waveforms, since non-stationarity and non-linearity assets ground a major difference with its counterparts. Hereafter, the preprocessing settlement makes use of sophisticated techniques to ameliorate EEG attributes over platykurtic and slow time-varying EOG signals, peaky and periodic ECG leads, and leptokurtic and fast time-varying EMG datastream [5]. Once, the denoising and artefact rejection tasks are fully accomplished by the preprocessing toolbox, EEG/EOG channels are sufficiently spanned to provide valuable information about distinctive sleep construction [11]. This condition is expected to be applied in subsequent processing and clustering courses with more gainful aftermaths, in comparison to current approaches. In order to assess the toolbox's performance degree, a complete experimental framework was prepared, regarding a clinical cohort and measurable metrics from qualitative and quantitative perspectives [14]. Likewise, configuration guidelines are suggested to rendezvous outperforming preprocessing models, given the presented toolbox's modules.

The present paper is organised as follows: Section II makes a detailed description of the active modules within the preprocessing toolbox, including employed transformation and decomposition techniques. Section III summarises the experiment's conditions, test subjects, constraints and metrics; also the obtained results are discussed. Finally, Section IV argues additional insights and remarks about the generated results and overall preprocessing toolbox development.

II. METHODS

The proposed PSG preprocessing toolbox strives to fulfill two major concerns: modularity and time-efficiency. The former stresses the distinction of system functionalities on disjoint modules, such that, biosignal outputs correspond to a dynamic interaction rather than fixed-sequential rules. Thus, the attainment of partial outcomes (i.e. segmentation, noise removal, whitening or artefacts removal) turns into a feasible option by the overall system configuration under the operator's discretion. Furthermore, the preprocessing stage is intended to be a preparation phase with restrained complexity compared to subsequent signal proceedings. Therefore, computational efficiency and optimal resolution times are highly sought upon data representation, transformation and rendering.

Straightforward, a detailed description of the deployed modules is addressed. Also, some remarks about the core algorithms are introduced, in order to discuss the prowess and eventual downsides of toolbox's backbone.

A. Data segmentation module

Usually, polysomnographic recordings collect the biophysical activity related to an overnight period, that means 6-8 hours timeframe. From this point patient's dataset requires to

[1]R. Chaparro-Vargas is with School of Electrical and Computing Engineering, RMIT University, Melbourne VIC 3001, Australia s3361953@student.rmit.edu.au

[2]D. Cvetkovic is with School of Electrical and Computing Engineering, RMIT University, Melbourne VIC 3001, Australia dean.cvetkovic@rmit.edu.au

be segmented into fixed-size epochs, whereas the scoring system of sleep stages is based on successive EEG/EOG-epochs evaluation. On regard of this, the initial toolbox module aims to fragment each PSG channel into shorter chunks of samples, considering temporal alignment, sampling frequency and adjustable epoch length criteria. The module's output consists of a tridimensional array denoting data samples, time epochs and PSG channels. Such a disruption lightens the computational burden managed by the additional preprocessing modules, as well as, facilitates EEG/EOG sleep-data matching according to standard manuals [11].

B. Filtering module

Either rejection or enhancement of spectral components over PSG channels can be achieved by the filtering module application. Essentially, the module's logic performs a cancellation of interference frequencies from power lines (50 and 60 Hz), i.e. notch filter. Along with bandpass filtering to preserve the frequency ranges of particular significance for the detection of sleep abnormalities. In general, the module generates a quite similar data output, like that conveyed by the segmentation module, but undesired spectrum bands are effectively removed.

C. Whitening module

Basically, the module engages a Karhunen-Loève transformation (KLT)—a.k.a. Principal Component Analysis—characterised by the observation of correlated PSG channels and followed by a decomposition into uncorrelated components [10]. Accordingly, KLT arranges principal components in function of a maximised variance basis by selecting a subset of channels (e.g. EEG/EOG channels), which indexes the largest contributions from the original data block [8]. The KLT-based preprocessing reaches improved spatial resolution, baseline correction and decorrelated observations; whilst maximum power density and signals integrity are attained. The latter is strongly chased in the preservation of the original features of biological datasets. Additionally, baseline correction takes place to subtract minor deviations of time points from the reference level that might lead to misinterpretations in actual signals' amplitudes.

D. Artefacts removal module

Assuming an adequate whitening process, the correction of embedded artefacts is supported on the well-known Blind Source Separation (BSS) technique [12], and specifically by Independent Component Analysis (ICA) [1]. Recalling the biophysical nature of EEG/EOG observations, the presence of coloured noise and non-stationary sources is foreseen. Henceforth, ICA decomposition becomes a suitable approximation for a linear demixing of the channels, whilst differential time delays are neglected [4]. Besides, the implementation of second-order-statistics (SOS) methods stands out as a reasonable approach for the separation of multichannel PSG into statistically independent components [3] [5]. Taking advantage of the whitening and temporally decorrelation processes carried out by the previous module; AMUSE [13] and SOBIRO [14] algorithms are adopted as BSS-SOS-based representatives for EEG/EOG sources detachment from neighbouring ECG and EMG activity. Attending to the toolbox's low complexity principle, both algorithms guarantee closed form solution for the separation, disregarding iterative and time-extended computational effort [13].

E. Noise removal module

The denoising process can be tentatively applied to the raw epochs generated by the segmentation module or onto the outputs generated by the aforementioned units. Anyway, the module's elements converge in the attenuation of frequency components that reside either in the spectrum's bottommost till high-regime zones, as long as slow- or fast-varying signal properties are followed. The module's machinery is sustained by the Wavelet Packet Transform (WPT) [9] [7], which defines a group of filters to produce a collection of PSG frequency subbands at different resolution levels. The transformation forges a shrinkage process on each PSG epoch/channel, through the computation of approximation and detail coefficients. Given that spectral power of non-neuronal or non-ocular activity might likely drown EEG/EOG significant information, the WPT-based module outperforms as an alternative filtering choice [6].

III. EXPERIMENTAL FRAMEWORK

The PSG datasets used to conduct the experiments correspond to 10 male healthy subjects within (25-43) age interval, identified as S18, S19, S20, S21, S22, S23, S25, S27, S29 and S30. Each datastream contains 6 channels denoted as: EEG O2, EEG C3, right EOG, left EOG, ECG and EMG simultaneously recorded with 256 Hz as sampling rate and 20 minutes time duration. The electrode montage is 10-20 system-compliant.

The performance of PSG Preprocessing Toolbox is determined by one qualitative assessment and two quantitative metrics. A visual inspection of contaminated PSG-epochs constitutes the qualitative evaluation, i.e. noisy and artefact-affected epochs from 10 different patients are manually picked. Neither random nor statistical procedures are employed for the selection of testing epochs, since strongly distorted data samples are desired to challenge the actual toolbox's preprocessing capability. The two remaining metrics are Signal-to-Noise Ratio (SNR) [1] [3] and Root Mean Square Error (RMSE) [6]; both of them examine artefacts-free module's aftermaths and question denoising module's behaviour. Hereafter, a specific number of epochs per channel are drawn based on the sample size estimation method explained in [2]. So, SNR and RMSE metrics are computed with a confident PSG-epochs pool out of the entire dataset population.

A. Preprocessing model

The modularity in the toolbox design leads to a limited cluster of possible models, obtaining the full-equipped package for data transformation or at least a custom combination of it. For the experimental work, the toolbox modules are

aligned as Figure 1 depicts, subject to the following constraints.

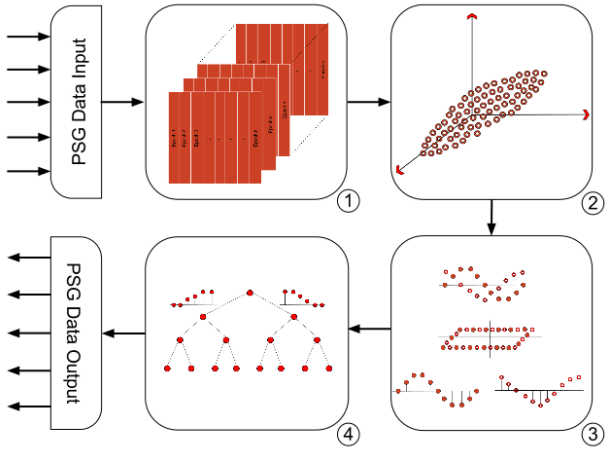

Fig. 1. Adopted model for PSG Preprocessing Toolbox.

The data segmentation module ① yields fixed-length and aligned 10-second epochs for all 6 channels. The chosen epoch length is short enough to allow the visual tagging of artefacts and noise-affected data fragments; and long enough to assure single-trial removal of embedded artefacts by the BSS-SOS-based algorithms [13]. The whitening module ② is not deeply intervened, since temporal decorrelation and baseline correction functions are addressed straightforward. However, the artefacts removal module ③ is set up to execute SOBIRO over AMUSE as blind separation method, whereas it has previously shown to be the most performant option for highly distorted EEG/EOG signals [14]. Additionally, the module is particularly conceived to get rid of ECG and EMG activity expressed as a pulse artefact over EEG and EOG channels. Similarly, the noise removal module ④ requires a more extensive tuning process, due to the constellation of drivers for WPT-based decomposition. Then, Table I summarises the adopted criteria. Finally, filtering module is overpassed from the final experimental model to avoid the appearance of spurious spectrum components in any of the PSG channels.

B. Results

From the 10 collected PSG recordings, 6 of them are profoundly contaminated by colour/white Gaussian noise and invasive artefacts, whilst 4 of them are only affected by high-frequency noise. After applying the assembled model

TABLE I
NOISE REMOVAL MODULE SETTINGS

Criterion	Argument
Levels	7
Wavelet family	db4
Thresholding	Soft
Threshold value	SURE

to noisy and artefact-related epochs from 10 different PSG-datasets, the following results were encountered: 6 datasets were successfully denoised and artefact-free processed, i.e. EEG/EOG channels were ostensibly disassociated from cardiac or muscular activity; 4 datasets were properly denoised, but not artefact-free processed. Nonetheless, the latter group of preprocessed recordings requires a distinction to explain its failure by removing the artefacts. A total of 2 datasets are originally artefact-free from the data acquisition stage, so only 2 recordings were slightly disjoint or failed to be released from ECG/EMG-artefacts. The Figure 2a portrays step-by-step a well-preprocessed EEG O2-epoch. Likewise, Figure 2b illustrates a denoised EEG O2-epoch with remnant presence of ECG artefacts.

With respect to the quantitative analysis, the results obtained by the testing cohort are shown in Table II. The RMSE metric exhibits a significant performance in EEG channels, as well as, EOG measurements. Hence, average 6 dB and 5 dB residual error are generally maintained by both group of channels, correspondingly . Such a condition allows to infer a substantial reduction of the error component upon biosignals by internal and external sources during data acquisition stage. Correspondingly, the lower part of Table II sets out the signal-to-noise ratios for both EEG and EOG signals. Thus, SNR driver outperforms with significant values for EEG channels, and even better quotients are obtained in EOG channels. Accordingly, the signal-to-noise ratios cover $9-13$ dB in O2 and C3 leads, whilst right and left EOG surpass with $17-29$ dB interval. Then, SOBIRO algorithm and WPT denoising perform a sophisticated data estimation to guarantee appealing ratios amongst EEG/EOG signals against distorted versions.

IV. DISCUSSION

Considering the obtained qualitative results, the proposed preprocessing toolbox demonstrates a formidable behaviour in noise removal task, since 10 out of 10 datasets were successfully decontaminated from coloured and high-frequency noise. In regard to artefacts rejection function, the toolbox displays a moderate efficiency with 6 satisfactory artefact-free recordings and only 2 failing datasets (the missing 2 datasets are originally artefacts dismissed). A plausible explanation for the separation failure might correspond to the violation of independence condition during acquisition stage. For an appropriate sources separation, each PSG channel must be strictly independent from the others, then a misplaced reference electrode or loose leads might point to this anomaly. Alternatively, the dimensional relation between number of channels and sources is a pulling assumption for BSS methods success. Therefore, a larger number of channels is always a highly pursued scenario. Taking into account the quantitative outcomes, SNR and RMSE metrics support the topmost toolbox's motivation by attaining remarkable figures in error components rejection and signal-to-noise ratio enhancement.

Summing up, qualitative and quantitative metrics prove the convenience of the presented preprocessing toolbox to

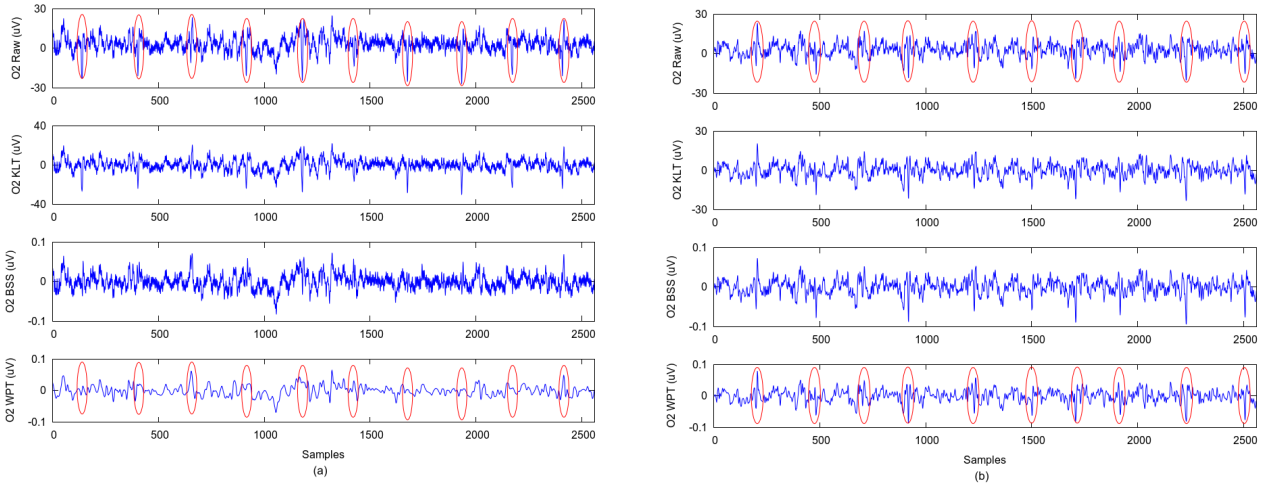

Fig. 2. (a) The enclosed transients represent the successfully removed ECG artefacts in EEG O2 for S18 and (b) unsatisfactory removal of artefacts in EEG O2 for S30.

TABLE II
RMSE AND SNR RESULTS UPON EEG/EOG CHANNELS

RMSE (dB)	S18	S19	S20	S21	S22	S23	S25	S27	S29	S30
EEG O2	7.5768	8.2038	7.6409	6.6084	6.0480	4.6745	7.2099	5.7904	5.3815	5.0329
EEG C3	7.1015	7.8408	7.4977	6.5809	5.8055	5.0593	7.0251	6.9191	5.8069	5.0527
REOG	7.1116	8.2896	5.2002	4.9131	6.2430	5.1415	5.5477	7.5475	5.3013	5.9435
LEOG	7.3253	8.6010	4.6650	4.9851	5.7716	4.9524	6.5611	4.0941	5.4662	4.2674
SNR (dB)	**S18**	**S19**	**S20**	**S21**	**S22**	**S23**	**S25**	**S27**	**S29**	**S30**
EEG O2	12.2688	7.9056	13.0977	8.3617	9.6807	11.8758	6.0281	10.6271	11.3378	8.9539
EEG C3	9.8238	8.4913	12.1245	9.3631	13.2425	13.7029	11.1958	9.0833	10.3479	9.0739
REOG	29.4871	14.2168	24.2674	20.9610	21.6794	16.8947	17.9017	23.4313	21.0104	25.6235
LEOG	27.8947	18.1229	24.7089	18.2550	20.6428	16.9675	19.9162	26.3425	20.6135	24.6627

engage elimination of embedded artefacts and substantial noise removal, respectively. Thereafter, feature extraction and classification proceedings can be more confidently conducted.

ACKNOWLEDGEMENT

The authors would like to thank all 10 human volunteers who in 2011 undertook a biofeedback study in PSG monitoring, at School of Electrical and Computer Engineering, RMIT University.

REFERENCES

[1] Cichocki A. and Amari S. *Adaptive Blind Signal and Image Processing*. Wiley, 2005.

[2] J.E. Bartlett, J.W. Kotrlik, and C.C. Higgins. Organizational research: Determining appropiate sample size in survey research. *Information Technology, Learning, and Performance Journal*, 19(1):43–50, 2001.

[3] C. Chang, Z. Ding, S. Fong Y., and F.H.Y. Chan. A matrix-pencil approach to blind separation of colored nonstationary signals. *Signal Processing, IEEE Transactions on*, 48(3):900–907, March 2000.

[4] A. Delorme and S. Makeig. EEGLAB: An open source toolbox for analysis of single-trial EEG dynamics including independent component analysis. *Journal of Neuroscience Methods*, 134(1):9–21, 2004.

[5] Stepahnie Devuyst, Thierry Dutoit, Patricia Stenuit, Myriam Kerkhofs, and Etienne Stanus. Cancelling ECG artifacts in EEG using a modified independent component analysis approach. *EURASIP Journal on Advances in Signal Processing*, 2008:1–13, 2008.

[6] E. Estrada, H. Nazeran, G. Sierra, F. Ebrahimi, and S.K. Setarehdan. Wavelet-based EEG denoising for automatic sleep stage classification. In *Electrical Communications and Computers (CONIELECOMP), 2011 21st International Conference on*, pages 295–298, 28 2011-March 2 2011.

[7] M.A. Haidekker. *Advanced Biomedical Image Analysis*. Wiley, 2011.

[8] D. Kang and L. Zhizeng. A method of denoising multi-channel EEG signals fast based on PCA and DEBSS algorithm. In *Computer Science and Electronics Engineering (ICCSEE), 2012 International Conference on*, volume 3, pages 322–326, March 2012.

[9] S. Mallat. *A Wavelet Tour of Signal Processing*. Elsevier Academic Press, 1999.

[10] L. Mesin, A. Holobar, and R. Merletti. *Advanced Methods of Biomedical Signal Processing*. IEEE Press, 2011.

[11] A. Rodenbeck, R. Binder, P. Geisler, H. Danker-Hopfe, R. Lund, F. Raschke, H.G. Wee, and H. Schulz. A review of sleep EEG patterns. Part I: A compilation of amended rules for their visual recognition according to Rechtschaffen and Kales. *Somnologie*, 10(4):159–175, 2006.

[12] A. Santillan-Guzman, U. Heute, A. Galka, and U. Stephani. Application of state-space modeling to instantaneous independent-component analysis. In *Biomedical Engineering and Informatics (BMEI), 2011 4th International Conference on*, volume 2, pages 640–643, Oct. 2011.

[13] K.H. Ting, P.C.W. Fung, C.Q. Chang, and F.H.Y. Chan. Automatic correction of artifact from single-trial event-related potentials by blind source separation using second order statistics only. *Medical Engineering & Physics*, 28(8):780–794, 2006.

[14] R. Romo Vázquez, H. Vélez-Pérez, R. Ranta, V. Louis Dorr, D. Maquin, and L. Maillard. Blind source separation, wavelet denoising and discriminant analysis for EEG artefacts and noise cancelling. *Biomedical Signal Processing and Control*, 7(4):389–400, 2012.

Appendix C

Peer-reviewed Journal Paper

Title: Advanced daytime polysomnographic preprocessing: A versatile approach for stream-wise estimation

Authors: Ramiro Chaparro-Vargas and Dean Cvetkovic

Publication: Digital Signal Processing: A Review Journal

Year of Publication: 2014

Digital Signal Processing 35 (2014) 95–104

Contents lists available at ScienceDirect

Digital Signal Processing

www.elsevier.com/locate/dsp

Advanced daytime polysomnographic preprocessing: A versatile approach for stream-wise estimation

Ramiro Chaparro-Vargas *, Dean Cvetkovic

School of Electrical and Computing Engineering, RMIT University, 124 La Trobe Street, Melbourne, VIC 3000, Australia

ARTICLE INFO

Article history:
Available online 16 September 2014

Keywords:
Artefacts rejection
EEG
Noise removal
Preprocessing
PSG sleep

ABSTRACT

The enhancement of monitoring biosignals plays a crucial role to thrive successfully computer-assisted diagnosis, ergo the deployment of outstanding approaches is an ongoing field of research demand. In the present article, a computational prototype for preprocessing short daytime polysomnographic (sdPSG) recordings based on advanced estimation techniques is introduced. The postulated model is capable of performing data segmentation, baseline correction, whitening, embedding artefacts removal and noise cancellation upon multivariate sdPSG data sets. The methodological framework includes Karhunen–Loève Transformation (KLT), Blind Source Separation with Second Order Statistics (BSS-SOS) and Wavelet Packet Transform (WPT) to attain low-order, time-to-diagnosis efficiency and modular autonomy. The data collected from 10 voluntary subjects were preprocessed by the model, in order to evaluate the withdrawal of noisy and artefactual activity from electroencephalographic (EEG) and electrooculographic (EOG) channels. The performance metrics are distinguished in qualitative (visual inspection) and quantitative manner, such as: Signal-to-Interference Ratio (SIR), Root Mean Square Error (RMSE) and Signal-to-Noise Ratio (SNR). The computational model demonstrated a complete artefact rejection in 80% of the preprocessed epochs, 4 to 8 dB for residual error and 12 to 30 dB in signal-to-noise gain after denoising trial. In comparison to previous approaches, N-way ANOVA tests were conducted to attest the prowess of the system in the improvement of electrophysiological signals to forthcoming processing and classification stages.

1. Introduction

In neuroscience, one of the most relevant fields of research concerns sleep as a pivotal state of consciousness. The regularisation of healthy sleeping patterns ensures physical and psychological recovery to cope with demanding tasks on a daily-based routine [1]. Although, sleep process is an intricate matter consisting of converging processes of different nature; the interpretation of their bioelectrical activity offers a valuable framework to decipher the structure and bodily relationships [2]. Thus, the polysomnogram (PSG) stands out as a technique for electrophysiological monitoring of sleep-related dynamics. Based on temporal and spatial capabilities, the PSG is a unique assisting tool for staging of sleep macrostructure and microstructure [3], as well as, diagnosis of sleep disorders [4]. Each PSG recording collects a set of biological signals from different sources; such as neuronal, ocular, muscular, cardiac, respiratory, body movement, etc. [5]. Those signals wait upon posterior application of feature extraction and classification mechanisms to deploy computer-aided systems to support clinical assessments.

Certainly, inspiring approaches have been formulated to improve the biosignals resolution, either to diminish artefactual effect or to shrink down noise disruption attending to the hectic variations. Hereafter, some meritorious models are elicited. The amalgamation of coloured noise and non-stationarity processes within the neuronal sources becomes distinguishable by signal extraction methods in [6]. However, the exclusive usage of simulated data in the evaluation of the algorithms restrains the possibility to assess the impact on actual clinical data. In correspondence, [7] suggests EEGLAB, a multi-purpose toolbox for processing electroencephalographic (EEG) recordings; including artefact rejection, filtering, epoch selection, etc. Although, the robustness of the estimation core is not debatable, the complexity of the related algorithms questions its efficiency with limited number of channels, samples or computational resources. On this direction, solutions founded on second-order-statistics (SOS) demonstrate sustainable error reduction over EEGLAB utilities. In one study [8], the artefact correction is applied to datasets with event-related potentials

* Corresponding author.
E-mail addresses: ramiro.chaparro-vargas@rmit.edu.au (R. Chaparro-Vargas), dean.cvetkovic@rmit.edu.au (D. Cvetkovic).

http://dx.doi.org/10.1016/j.dsp.2014.09.007
1051-2004/

(ERP). Therefore, the adaptation of the methods to polysomnographic data could convey new findings with dissimilar electrical responses. An alternative approach is proposed by [9] making use of wavelet-based decomposition to remove artefacts of semi-simulated data with 7.5 seconds of time duration. These two aspects motivate the enquire about the suitability of sleep-related data to be tested through such a multi-resolution analysis. Respectively, [10,11] describe comparable methodologies to weaken electrocardiographic (ECG) artefacts and additive noise from EEG channels. The manifested exclusion of electrooculographic (EOG) and electromyographic (EMG) activity as potential artefacts generators keeps an open discussion when multivariate PSG data is deconstructed. Recently in [12], a novel tandem arrangement to cope with preprocessing and classification tasks sets out remarkable conclusions in terms of consecutive separation-denoising function blocks. In this sense, the present work deploys a model to improve integration, time-to-diagnosis and algorithmic versatility; subject to hundreds of PSG epochs.

Here, we introduce a short daytime PSG (sdPSG) preprocessing model as part of an ongoing initiative to provide computer-assisted resources related to sleep studies. Therefore, its development bears a well-structured roadmap, starting on preprocessing middleware towards supporting systems in sleep staging and diagnosis of disorders. The system tracks and suppresses external and embedding interferences that tantalise the achievement of performant scores in self-guided recognition and diagnosis. The usage of a statistical-oriented middleware instead of event-specific allocation incorporates a software-based package with purpose-specific. Besides, pseudo-online preprocessing, here denoted as streaming operation mode, pursues the avoidance of iterative and time-extended computational effort by streaming the bodily activity, as soon as it is sensed and digitally converted. In order to remove additive Gaussian noise and artefact-embedded activity, whilst neither reduction nor expansion transformation on the original data is addressed [13]. Furthermore, the computational methods aim to deal adequately with the highly complex characteristics of EEG waveforms; since non-stationarity and non-linearity assets make a major difference in contrast to its counterparts. Hereafter, the preprocessing middleware makes use of sophisticated techniques to refine EEG features over 1) subgaussian and slow time-varying EOG signals; 2) supergaussian, spiky and periodic ECG leads; and 3) high frequency EMG distributions. Once, the denoising and artefact rejection tasks are fully accomplished, sdPSG channels are sufficiently spanned to provide valuable information about sleep composition or associated abnormalities [14]. This condition is meant to be applied in subsequent processing and classification routines, expecting gainful aftermaths in comparison to current approaches [15]. According to this, the present paper attempts to reveal the intrinsic constituents of the preprocessing model under low-order and time-to-diagnosis efficiency constraints, which convey to a plausible streaming orientation with operational outcomes. In order to attest the performance degree, a complete experimental framework was prepared, regarding a testing cohort and measurable metrics from qualitative and quantitative perspectives, such as signal ratio and residual error.

The paper is organised as follows: Section 2 makes a detailed description of the active modules within the preprocessing approach; including conditions of experiments, test subjects and employed transformation/decomposition techniques. Then, Section 3 portrays the final arrangement of modules and parameters for experimental proceedings. Section 4 discusses the product of performance metrics applied to actual clinical data. Afterwards, Section 5 realises a critical analysis about the obtained results, stressing strengths and downsides of the adopted methods. Finally, Section 6 argues additional insights and remarks about future challenges and opportunities of improvement.

2. Methods

In the present manuscript, we introduce a sdPSG preprocessing computational model conceived to fulfil operational and performing requirements over simultaneous electrophysiological recordings. The performing drivers are specifically oriented to surmount the most common tributaries of distortion upon biological signals, i.e. sdPSG self-embedded artefacts and additive noise.

According to this, the preprocessing system delegates to three independent modules the whitening of recorded channels, followed by artefact removal, and latest the noise mitigation. Furthermore, the operational conception engages time-to-diagnosis efficiency and modularity principles towards streaming preprocessing mode. The former exploits the native epoch-based analysis for sleep staging, whilst the non-stationarity constraint of biological signals is attended. Hence, the temporal gap between data acquisition and channels preprocessing is conveyed in a streaming basis for faster output retrieval. In turn, modularity stresses the differentiation of functionalities into autonomous modules, such that, outcomes respond to a customisable interaction amongst them, rather than ever-fixed sequential rules. Hereafter, a performant preprocessing system is attained, in order to support improved time-to-diagnosis frames and diversified paths of convergence. These conditions are highly sought upon multivariate sdPSG data representation, transformation and rendering; inasmuch as subsequent processing and classification stages are expected.

The forthcoming sections offer a more-detailed description about the constitutive modules of the system, as well as, determined metrics for the performance assessment with self-evaluation and comparative intentions.

2.1. Subjects

The short daytime polysomnographic recordings correspond to 10 male healthy subjects ($M = 28.3$, $SD = \pm 6.75$), identified as S01, S02, S03, S04, S05, S06, S07, S08, S09 and S10. Generally, sdPSG recordings include a minimum of 3 EEG, 2 EOG, 1 EMG, 1 ECG and 1 respiratory channel with pulse oximetry [16]. Although, this present paper is restricted to an arrangement of 6 channels full-complaint with international 10–20 electrode montage designated as: EEG-O2, EEG-C3, Right EOG (REOG), Left EOG (LEOG), ECG and EMG submental, since at least one representative biophysical source is required for the adequate model deployment. Correspondingly, each signal has 20 minutes duration with sampling frequency equivalent to 256 Hz. Besides, no filtering or previous preparation was applied. RMIT Ethics Committee approved the sdPSG recording for Dr. Cvetkovic's biofeedback study.

2.2. Notation

The polysomnographic recording is modelled as a multivariate system with the same number of inputs and outputs, since neither reduction nor expansion upon data length is pursued at the preprocessing stage. Then, a suitable representation of multidimensional sdPSG datasets resides in state-space realisations [17]. By the generalisation of the electrophysiological compound into the two model expressions, we obtain

$$\mathbf{x}[k] = \mathbf{x}[k-1]\mathbf{A}^{\mathrm{H}} + \eta[k]\mathbf{B}^{\mathrm{H}}; \quad \eta \sim \mathcal{N}(0, \Sigma_{\eta\eta}) \tag{1}$$

$$\mathbf{y}[k] = \mathbf{x}[k]\mathbf{C}^{\mathrm{H}} + \nu[k]; \quad \nu \sim \mathcal{N}(0, \Sigma_{\nu\nu}) \tag{2}$$

where Eq. (1) and Eq. (2) represent the system and observation model equations, respectively. Momentarily, the computational proceedings are exclusively focused on an observational characterisation of sdPSG data channels, therefore Eq. (1) is neglected from the modelling exercise [17]. In consequence, $\mathbf{y}[k]$ denotes

the vector of N observed sdPSG signals (channels); such that $\mathbf{x}[k]$ is the unobserved vector of M source signals, $\mathbf{C}^{\mathrm{H}} \in \mathbb{C}^{M\times N}$ is the hermitian observation matrix and $\nu[k]$ defines the N-dimensional observation vector of noise Gaussian distributed $\mathcal{N}(0, \Sigma_{\nu\nu})$ with zero-mean and $\Sigma_{\nu\nu}$ covariance matrix. Thus, the introduced preprocessing model exploits the estimation properties of this observation model (2), in order to generate a computer-assisted and streaming response for epoch-based data segmentation, whitening, detection/removal of embedding artefacts and additive noise cancellation; whilst the intrinsic features of the physiological signals are ostensibly preserved.

2.3. sdPSG recording segmentation

The assessment of PSG recordings in function of sleep staging and the identification of sleep disorders' conditions is formally standardised by medical and technical criteria (e.g. AASM Manual [18]). The specialised evaluation is based on the progressive scoring of 30-second epochs into one out of five stages: wake, NREM-I, NREM-2, NREM-3 and REM. Therefore, the first module of this system is in charge of segmentation tasks upon the raw sdPSG input channels, such that, datasets are fragmented into fixed-size epochs. The parameters related to epoch length and number of channels are completely customisable to impress a higher degree of flexibility in the structure of incoming sdPSG data files. Likewise, the configuration of epoch length eases the tractability of time-varying dynamics within EEG signals, as well as, the consumption of physical resources is lightened by the reduction of the dimensional space to be simultaneously computed. Once, the overall observation vector $\mathbf{y}[k]$ is uniformly broken up into fixed-size epochs, further estimation methods are applied to attenuate harmful effects from noisy and artefactual sources. For simplicity, the notation does not make distinction between epoch- and full dataset dimensions in the observation model, i.e. k index should be understood as an arbitrary time pointer.

2.4. Data whitening

Multivariate sdPSG data files might imply few number of channels. For sleep studies, EEG and EOG signals play a major role in categorisation and diagnosis endeavours. Hence, the present module is widely conceived to enhance epoch stationarity and zeroing out cross-correlation amongst neuronal and ocular channels. The whitening process is performed in correspondence to the weighted contribution of each input data to determine the amount of redundancy surrounding EEG and EOG channels. For this matter, the methodological approach calls for Karhunen–Loève Transformation (KLT) [19]. Basically, the identification of correlated biosignals in $\mathbf{y}[k]$ is followed by a decomposition into uncorrelated components, commonly called principal components. In such a way, KLT arranges principal components in function of a maximised variance basis by selecting a subset of channels with the largest contributions from the original observation vector [13].

The KLT-based preprocessing achieves improved spatial resolution and baseline correction; whilst maximum power density is attained and eventual data redundancy is withdrawn [7]. Usually, PSG data acquisition stage is likely to experience undergoing minor DC-signal shifts over time as a result of junction potentials amongst electrodes, misplaced ground references, humid contact surfaces (transpiration or moisture), muscular tension, inherent brain activity or environmental interferences. Thereupon, the plotting of observations will exhibit considerable differences with respect to zero-reference levels at the different input channels; besides the slightest DC-signal offset divergence promotes inaccurate aftermaths when future processing routines take place. Then, a baseline correction is required to assure equally referenced estimations that otherwise might lead to a non-confident computation of signal and noise estimators. From our model perspective, the construction of the covariance matrix $\mathbf{R}_{\mathbf{yy}} \in \mathbb{C}^{N\times N}$ involves the mean $m_{\mathbf{y}}$ subtraction from ith observation channel $\mathbf{y}_i[k]$ with $i = \{1, \ldots, N\}$, as follows

$$\begin{aligned}\mathbf{R}_{\mathbf{yy}} &= E\big\{\big(\mathbf{y}[k] - m_{\mathbf{y}}\big)^{\mathrm{H}}\big(\mathbf{y}[k] - m_{\mathbf{y}}\big)\big\}; \quad m_{\mathbf{y}} = E\big\{\mathbf{y}[k]\big\} \\ &= \frac{1}{N}\sum_{i=1}^{N}\big(\mathbf{y}[k]^{\mathrm{H}}\mathbf{y}[k]\big) - m_{\mathbf{y}}^{\mathrm{H}} m_{\mathbf{y}}; \quad m_{\mathbf{y}} = \frac{1}{N}\sum_{i=1}^{N}\mathbf{y}_i[k] \end{aligned} \tag{3}$$

The sorted realisation of decorrelated neuronal and ocular signals from the neighbouring biological processes, is obtained by an Eigenvalue Decomposition (EVD) of the observation covariance matrix $\mathbf{R}_{\mathbf{yy}}$. The amount of uncorrelated activity derived from the non-EEG/EOG principal components; in turn, helps out tagging the observed channels to be lately subtracted out. In fact, the upcoming module deepens on this matter, taking into consideration the KLT-reconstructed observation vector $\hat{\mathbf{y}}[k]$, which is described as:

$$\hat{\mathbf{y}}[k] = \big(\mathbf{y}[k] - \mu_y\big)\mathbf{Q}_{\mathbf{y}}^{\mathrm{H}}; \quad \mathbf{Q}_{\mathbf{y}}^{\mathrm{H}} \in \mathbb{C}^{N\times N} \tag{4}$$

where $\mathbf{Q}_{\mathbf{y}}^{\mathrm{H}}$ is the matrix gathering the eigenvectors corresponding to each observed channel $\hat{\mathbf{y}}_i[k]$.

2.5. Artefacts removal

The dominating tributaries of distortion on the EEG and EOG signals are represented by isolated or periodic pulses, such ones are interpreted as cardiac (RR interval peaks). In turn, muscular activity is characterised by fast time-varying to constant high frequency distributions with linear embedding upon the principal components. Taking into account that bodily electrical projections are seemingly overspread and non-orthogonal, it is required an estimation basis to cope with interweaving patterns. Henceforth, the review of Blind Source Separation (BSS) theory, specifically Independent Component Analysis (ICA), supposes a helpful approach [20]. Even though, model constraints are necessarily assumed in order to do an appropriate interpretation of the results. For instance, linear mixing of unobserved source signals $\mathbf{x}[k]$ and negligible differential time delays are considered [7], as long as, the estimation of statistically independent components is conveyed.

The aim of this module is the separation of independent sources in multivariate sdPSG recordings, subject to low-order operations and time-to-diagnosis efficiency. Therefore, the adoption of BSS variety, SOS, fosters an adequate benchmark for streaming computations whilst no more perplexing criterion than distribution variance of biosignals is assessed [8,6]. Thus, the applied BSS-SOS computational method, known as Second Order Blind Identification with Robust Orthogonalisation (SOBIRO) guarantees a closed-form solution or finite number of statistically separated sdPSG sources [12].

The estimated observation vector $\hat{\mathbf{y}}[k]$ is extended as referred in Eq. (2), but the observation matrix $\mathbf{C}^{\mathrm{H}}$ is from now on designated as mixing matrix. Then, our first objective is to find its corresponding inverse to infer the sdPSG sources vector $\hat{\mathbf{x}}[k]$ based on the assumptions described in Table 1 [17].

Firstly, the estimation of a set of L time-lagged covariance matrices leads to define an observation matrix $\mathbf{R}_{\hat{\mathbf{y}}\hat{\mathbf{y}}} \in \mathbb{C}^{N\times NL}$. By iterative singular value decomposition (SVD) and definition of vector of parameters $\alpha = \{\alpha_1, \ldots, \alpha_L\}$. But, we must guarantee the derivation of the positive definite covariance matrix $\bar{\mathbf{R}}_{\hat{\mathbf{y}}\hat{\mathbf{y}}}(\alpha) \in \mathbb{C}^{N\times N}$. To conclude the robust orthogonalisation, $\bar{\mathbf{R}}_{\hat{\mathbf{y}}\hat{\mathbf{y}}}(\alpha)$ is one more time decomposed via SVD to obtain the transformation matrix $\mathbf{W} \in \mathbb{C}^{M\times N}$, which is orthogonal and unbiased to observation noise $\nu[k]$.

Table 1
Assumptions to be considered for SOBIRO implementation.

Assumption	Description
$N = M$	Number of observation and source channels is the same
$Kurt(\mathbf{p}(\mathbf{x}_i[k])) \neq 0$	Probability distribution function (pdf) of $M-1$ independent sources are non-Gaussian
$\mathbf{p}(\mathbf{x}_i[k], \mathbf{x}_j[k]) = \mathbf{p}(\mathbf{x}_i[k]) \cdot \mathbf{p}(\mathbf{x}_j[k])$	Estimated sources are independent with $i \neq j$
$\mathbf{R}_{\mathbf{xx}} = \mathbf{I}_M$	Sources covariance matrix is an $(M \times M)$-dimensional identity matrix
$\mathbf{R}_{\nu\nu} = 0$	Noise components in the observation model are disregarded

And, such an operator strives a whitening procedure over sources vector $\bar{\mathbf{y}}[k] \in \mathbb{C}^M$ by ascertaining orthogonality to the global mixing matrix. Secondly, a Joint Approximate Diagonalisation (JAD) is applied to a new cluster of time-delayed covariance matrices, whose construction is made of the recently estimated sources vector $\bar{\mathbf{y}}[k]$. Finally, the estimation of the statistically independent components or sdPSG sources $\hat{\mathbf{x}}[k]$ is attained by Eq. (5) realisation:

$$\hat{\mathbf{x}}[k] = \hat{\mathbf{y}}[k]\mathbf{W}^{\mathrm{H}}\mathbf{Z} \tag{5}$$

whereas the SOBIRO non-hermitian mixing matrix is represented by $\mathbf{C} = \mathbf{W}^{+}\mathbf{Z}$.

2.6. Denoising process

The ultimate module of the preprocessing system consistently struggle to maintain the biophysical properties of sdPSG signals, so long as additive Gaussian noise $\nu[k]$ and high frequency EMG activity is substantially attenuated. Given that EEG/EOG relevant activity is usually allocated within frequency bands below ca. 64 Hz (β band), the module is tuned to remove the spectral content above the ultimate EEG band. Accordingly, the peril of information loss inside of the bands of interest is diminished. Foremost, the denoising instance is conceived to efficiently handle wideband processes that arbitrarily occur within sdPSG signals.

The implied machinery is supported by a tree-shaped decomposition based on Wavelet Packet Transform (WPT) [21], which performs a two-sided concatenated filtering, i.e. detail and approximations coefficients goes through decomposition. The Time Frequency Analysis (TFA) is strongly centred on the mother wavelet $\psi(t)$ to yield a scaled and translated wavelet subband trees $\psi_{s,\tau}(t)$; Eq. (6) depicts the equivalence between a canonical mother wavelet and the scaled/translated representation of the DWT:

$$\psi_{s,\tau}(t) = \frac{1}{\sqrt{s}}\psi\left(\frac{t-\tau}{s}\right) \overset{DWT}{\equiv} \psi_{j,k}(t) = \frac{1}{\sqrt{s^j}}\psi\left(\frac{t-k\tau s^j}{s^j}\right) \tag{6}$$

where $s = 2$ and $\tau = 1$ remain constant, whilst j and k denote the scale and translation parameters, respectively. By the deployment of a binary branched set of low pass and high pass filters, i.e. Quadrature Mirror Filter (QMF) pair, a packet of frequency subbands is derived at diversified resolution levels. Eq. (7) and Eq. (8) establish the relation for the estimated sources vector $\hat{\mathbf{x}}$ and the conjugate filtering arrangement:

$$\mathbf{w}_{LP}[k] = \sum_{r=-\infty}^{\infty} \hat{\mathbf{x}}[r]\mathbf{h}[2k-r] \tag{7}$$

$$\mathbf{w}_{HP}[k] = \sum_{r=-\infty}^{\infty} \hat{\mathbf{x}}[r]\mathbf{g}[2k-r] \tag{8}$$

such that, $\mathbf{g}[r]$ and $\mathbf{h}[r]$ are the pair of conjugate mirror filters.

Such a decomposition forges a wavelet coefficient shrinkage throughout computation/cancellation of approximation and detail coefficients [19]. The hierarchical decomposition computes dynamically the optimal and maximum number of levels; i.e. each sdPSG channel per epoch is disjoint from noisy components by the usage of a depth-variant tree. Thus, the WPT-based denoising approach remarks its importance amongst sdPSG signals affected by non-stationarity, pseudo-stochasticity and additive noise [22].

This model member is equipped with a reasonable group of decomposition wavelets, seeking resolution variety in regard of scaling and translation issues [19]. Then, the available wavelets are: Daubechies-2, Daubechies-4, Coiflet-2, Coiflet-4, Symlet-2 and Symlet-4. Similarly, a pair of tunable thresholding schemes and threshold metrics are built-in. So, the former refers to the soft or hard thresholding for zeroing-out detailed wavelet coefficients; the latter fixes the central boundary ζ to be applied, following the universal threshold in Eq. (9) or heuristic Stein's Unbiased Risk Estimation (hSURE) value in Eq. (10) as referred [11]:

$$\zeta = \sqrt{2 \cdot \log(N)} \tag{9}$$

$$\zeta = 0.3936 + 0.1829 \cdot \log_2(N) \tag{10}$$

where N refers to the number of signal samples.

2.7. Performance evaluation

Having formulated a description of the computational model constituents across the previous sections, the performance examination was addressed in a holistic manner considering qualitative and quantitative metrics, explained in the current section. Making use of the 10 available sdPSG recordings of recruited subjects, the evaluative determinants were aligned to measure the efficacy level on artefact withdrawal and noise cancellation tasks, which are the primary drivers in analytical comparison with respect to existing systems and the sdPSG preprocessing model by itself. The initial qualitative criterion is supported by a visual inspection of distorted sdPSG epochs, that means, data segments severely affected by noisy and cross-channel artefacts (i.e. ECG and EMG). Since, strongly invaded observations are sought to challenge the actual prowess of our preprocessing middleware, the cohort of candidate sdPSG epochs is manually selected. The exploration assesses subjectively the reduction or discarding of artefacts transients or noisy overlays on sdPSG channels; ergo, neither random nor statistical procedures are employed for the selection of epochs or outcomes. In regard to the quantitative metrics, Signal-to-Interference Ratio (SIR) [20] weighs in the statistical detachment between the primary EEG/EOG signals $\hat{\mathbf{x}}'[k]$ against the estimated artefactual components $\hat{\mathbf{x}}[k]$. Similarly, the denoising capability is attended by Signal-to-Noise Ratio (SNR) and Root Mean Square Error (RMSE) [21], which computes the normalised and transformed difference between observed signals and the estimated ones $\hat{\mathbf{x}}[k]$; both analytically signify the resulting relation between signal and noise components, as well as, the residual error distance of non-preprocessed biosignals versus denoised versions. The quantitative performance gauges are expressed in Eqs. (11)–(13).

$$\mathrm{SIR}_{\mathrm{dB}} = 10 \cdot \log_{10}\left(\frac{\mathrm{E}[\|\hat{\mathbf{x}}'[k]\|^2]}{\mathrm{E}[\|\hat{\mathbf{x}}[k] - \hat{\mathbf{x}}'[k]\|^2]}\right) \tag{11}$$

$$\mathrm{SNR}_{\mathrm{dB}} = 10 \cdot \log_{10}\left(\frac{\mathrm{E}[\|\hat{\mathbf{x}}[k]\|^2]}{\mathrm{E}[\|\mathbf{x}[k] - \hat{\mathbf{x}}[k]\|^2]}\right) \tag{12}$$

$$\mathrm{RMSE}_{\mathrm{dB}} = 20 \cdot \log_{10}\left(\sqrt{\mathrm{E}\left[\left\|\mathbf{x}[k] - \hat{\mathbf{x}}[k]\right\|^2\right]}\right) \tag{13}$$

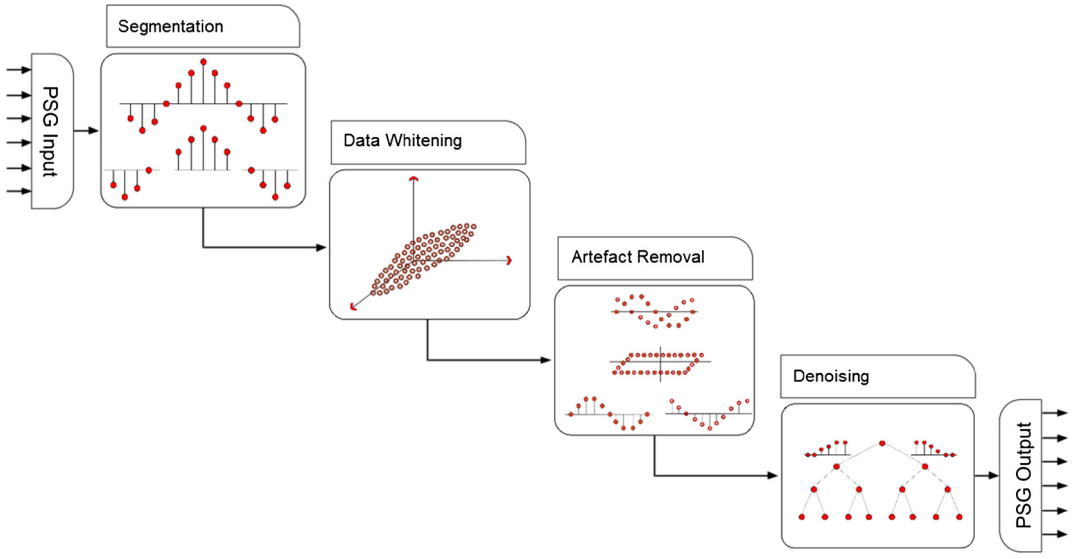

Fig. 1. sdPSG preprocessing system. The system integrates an initial data segmentation module in charge of 10-second epochs generation, followed by a data whitening module to perform baseline correction. Thirdly, artefact removal module based on BSS-SOS methods handles the separation of pulse-type artefacts, and lastly denoising module attenuates additive noise and high frequency activity.

Consequently, statistical N-way ANOVA tests were conducted with 10-second epochs, where the sample size estimation (i.e. total number of testing epochs) was based on the method explained in [23], which recalls the foundations of Cochran's sample size determination on continuous data, taking into account a total population of 1200 EEG/EOG epochs. Here, the determined margin error, alpha level and t-value were set to 0.03, 0.05 and 1.96, and plugged into Cochran's sample size expression. The agreed epoch length leverages a balance between episodic stationarity and zero cross-correlation, counterposing to standardised proceedings [18]. In order to maintain statistical validity, an amount of 110 and 550 epochs per channel were drawn on for SIR and SNR/RMSE calculations, correspondingly.

3. sdPSG preprocessing

Fastening the aforementioned modules, the deployed preprocessing system follows the model depicted in Fig. 1. Departing from the insertion of raw sdPSG signals till full-preprocessed data channels, passing through data segmentation, whitening, artefacts removal and denoising. This model resembles the arrangement in [12] that surmounts the advantages of performing source separation, followed by wavelet-based noise withdrawal.

Furthermore, the final configuration sets up the segmentation module to generate fixed-length and aligned 10-second epochs for the 6 sdPSG channels, which are long enough to assure removal of embedding artefacts by the BSS-SOS-based algorithms [8]. In turn, whitening module is not intervened, whereas temporal decorrelation and baseline correction functions are carried out straightforward. However, the artefacts removal module is prepared to perform SOBIRO-based blind separation with 100 time-lagged covariance matrices; given that, it has previously demonstrated to be the most performant option for highly distorted EEG signals. Lastly, the denoising module appeals to Daubechies-4 (db4) wavelet, soft thresholding and heuristic SURE threshold value to remain as default parameters [11].

4. Results

The introduced model coincides with a relevant goal on polysomnographic analysis, where significant outcomes elicits a successful separation of ECG/EMG-related activity from EEG/EOG signals, as it was initially presented in [24]. The current paper introduces an extended evaluation framework and statistical analysis based on ANOVA testing, which reaffirms the related findings. Nonetheless, the oversight of stipulated assumptions, like statistical independence, might compromise the appropriate performance of particular modules. For instance, violations about statistical independence, non-Gaussian observations or linear constraints could contribute to unexpected or misinterpreted findings. For that reason, let's proceed to take a closer view of the performance metrics, subject to the mentioned constrains.

Regarding the qualitative evaluation, a visual tagging of disturbed sdPSG epochs by cross-channel artefacts and additive noise, was conducted. The visual inspection draws forth that 80% sdPSG epochs were successfully denoised and deartefacted; i.e. 960 out of 1200 EEG/EOG epochs thrived on removing ECG/EMG-related activity and additive noise from the signal components. The remaining 240 sdPSG epochs exhibit regular ECG peaks embedded into the EEG and EOG waveforms, which is a clear sign of ill-performed source separation; although, the denoising module did perform a substantial suppression of noise and high frequency EMG activity in 100% of the sdPSG epochs according to the quantitative computations. Interestingly, those irregular sdPSG epochs are exclusively associated to two specific volunteers. In other words, the system was incapable of preprocessing the epochs from the polysomnographic recordings of subjects S08 and S10 volunteers, which questions the obedience to the BSS assumptions during data acquisition routine. Thus, Fig. 2a–h depict an exemplary EEG/EOG-epoch (S01, S07), whose noisy and artefactual disruptions were notoriously dismissed. At the same time, Fig. 2i–l illustrate a contrary sdPSG epoch (S10) with remnant presence of distortion agents.

The artefacts removal module makes use of SIR metric as its quantitative counterpart to establish a one-to-all channel correlation, where dB-scaled power of signal and interference sources are deployed into bidimensional heat maps. For example, Fig. 3c represents the intensity map of SOBIRO algorithm; the adopted BSS-SOS method by the preprocessing system to perform the sources separation. Here, each neuronal and ocular channel seizes a cross-correlated value between the estimated primary source $\hat{\mathbf{x}}'[k]$ and the disrupting signals (i.e. ECG and EMG leads). The power irradiated by EEG activity is uniformly located around 0 dB in respect to both interfering sources. In turn, EOG distribution makes a subtle distinction between right and left sensor; whilst the right

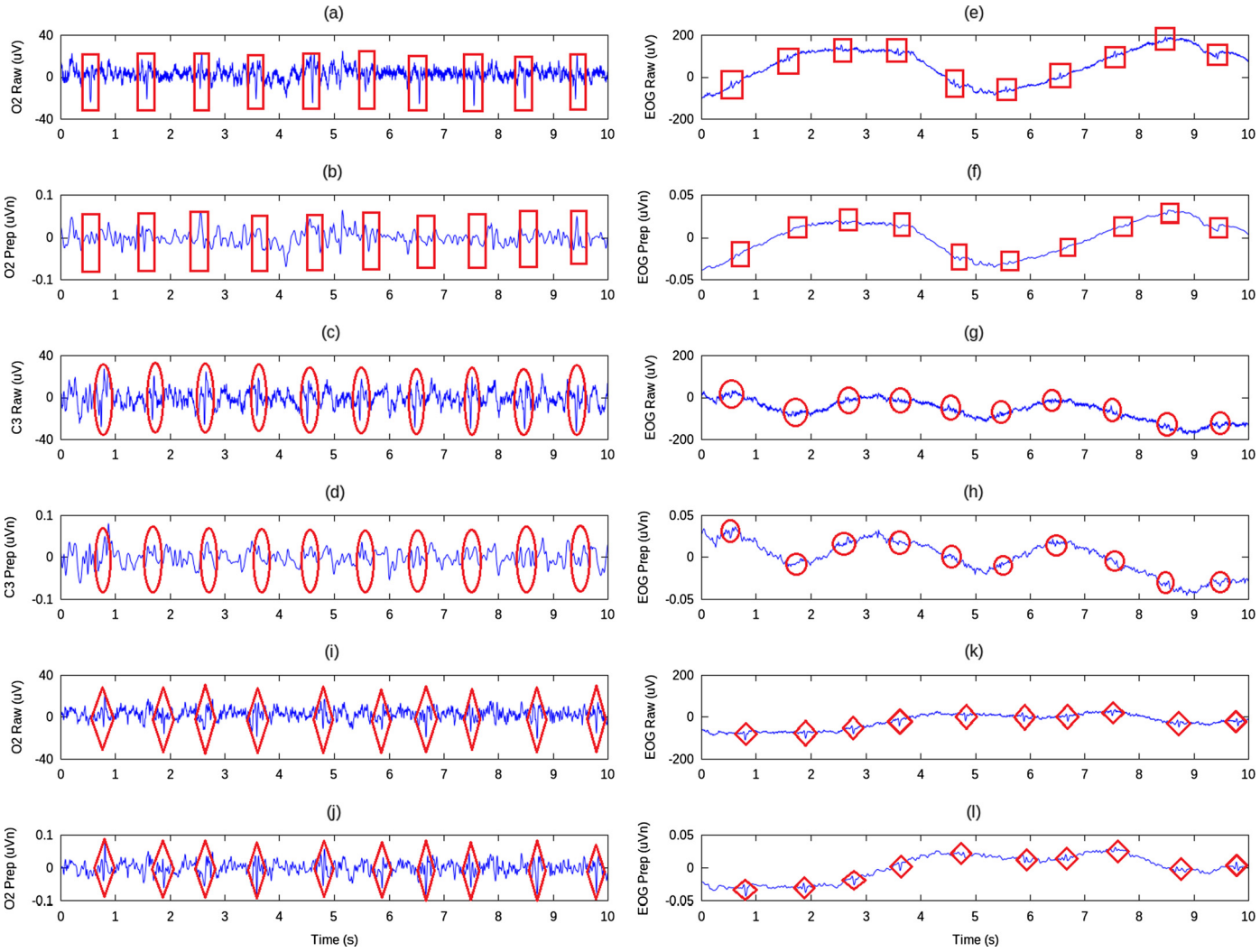

Fig. 2. Examples of preprocessed EEG and EOG epochs from three different test subjects (S01, S07 and S10). (a)–(h) depict successfully deartefacted and denoised, i.e. preprocessed EEG and EOG signals from O2, C3 and EOG electrodes. The □ marker highlights embedded and removed artefacts upon the EEG/EOG signal for subject S01. The additive noise and high frequency EMG activity was withdrawn from preprocessed epochs, as well. Correspondingly, ◯ marker supports the previous results for subject S08 in terms of pulse-type artefacts removal and attenuation of high frequency components. (i)–(l) display unsuccessful artefact extraction procedure upon EEG/EOG signals for subject S10. ◇ marker encloses the presence of artefacts upon the raw and preprocessed EEG/EOG signals. Although, the denoising process was carried out as expected by diminishing additive noise and high frequency EMG influence.

eye turns warmer under cardiac and muscular influence within 0.15–0.4 dB, left coequal reaches the most gelid stains amongst separation quotients (ca. −0.3 dB). Such a compelling pattern is the product of the aforementioned robust diagonalisation and the computation of multiple time-lagged covariance matrices. In order to reinforce this separation finding, the same experiment was reproduced employing extended Infomax and JADE algorithms from EEGLAB toolbox [7] to compare the respective efficacy. Then, Fig. 3a and Fig. 3b portray the coloured correlation amongst channels. Thereupon, competing methods exhibit negative power values from −2 to −1 dB for EEG/EOG signals versus artefactual sources, albeit it is more evident their limitation to deal with slow time-varying signals and transient pulse-type artefacts, such as EOG/ECG cross-correlation. Thus, SOBIRO ameliorates interference separation through stream-wise estimation, instead of iterative procedures to converge.

Even though, an analytical comparison is suitable to establish an undisclosed advantage amongst the three mechanisms. Thus, a two-way ANOVA test was conducted on both EEG and EOG channels to determine significant differences in the average SIR values with Bonferroni correction ($p < 0.005$), considering the three different algorithms (column-space dimension) and correction performance between EEG and EOG channels (row-space dimension). The former, SIR averages per algorithm, casts enough evidence to reject the null hypothesis $p = 0.0033$; i.e. the mean values significantly differ to proclaim SOBIRO as the most performant, whereas its separation ratio moves around 0 dB versus negative power ratios of Infomax and JADE. Contrarily, second dimension does not set forth fair indications to assume a significant divergence $p = 0.0160$ amongst EEG O2, EEG C3, REOG and LEOG channels. In a statistical sense, SOBIRO, Infomax and JADE do not make differentiation between neuronal and ocular channels to perform the correction of cardiac and muscular artefacts, indeed, a further description is conducted in this section later on. Owing to this, our findings confirm the results presented in [8,12], which stand out SOBIRO properties for adaptive artefact extraction.

Moving forward to the denoising module, the quantitative analysis of RMSE and SNR metrics audits the efficacy of noise cancellation, contrasting universal and hSURE threshold values. Hence, Table 2 gathers the average quantities of 550 epochs on EEG O2, EEG C3, REOG and LEOG channels, which were randomly selected from the voluntary cohort. Seemingly, the universal threshold outperforms in terms of residual error and signal strength by several factors, where RMSE values oscillate between −32 till −128 dB

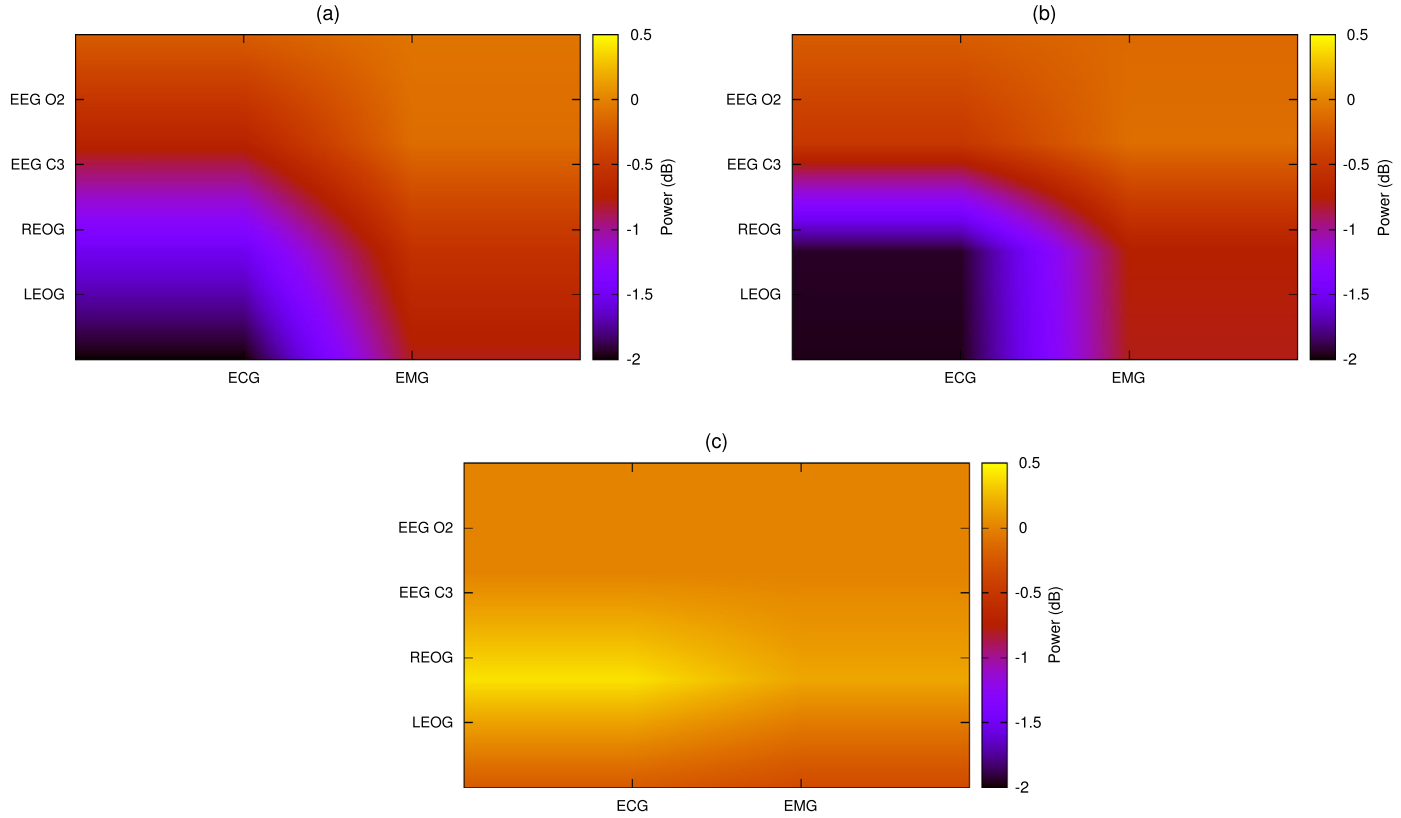

Fig. 3. Average heat maps of SIR for (a) EEGLAB extended Infomax, (b) EEGLAB JADE and (c) SOBIRO algorithms. The colour-scaled matrix quantifies the signal to interference relation amongst EEG/EOG versus ECG/EMG channels, after blind source separation is applied. (For interpretation of the references to colour in this figure, the reader is referred to the web version of this article.)

Table 2
Average RMSE and SNR values on EEG O2, EEG C3, REOG and LEOG channels. The results are extracted from the denoising module by performing the universal and heuristic SURE thresholding metrics in 10 subjects' sdPSG datasets.

	Subject		S01	S02	S03	S04	S05	S06	S07	S08	S09	S10
RMSE (dB)	EEG O2	Universal	−95.00	−80.80	−60.01	−69.60	−80.75	−83.75	−127.13	−96.33	−106.59	−112.66
		hSURE	7.77	8.32	7.93	6.78	6.19	4.93	7.19	5.88	5.34	4.99
	EEG C3	Universal	−100.53	−100.35	−78.66	−89.20	−54.19	−59.07	−32.16	−105.51	−83.28	−128.54
		hSURE	7.54	8.14	7.68	6.71	5.07	5.33	6.92	6.82	5.77	5.15
	REOG	Universal	0.17	1.32	−48.98	−37.17	−12.77	−6.86	−30.83	0.25	−11.22	−17.25
		hSURE	7.38	8.71	5.61	5.23	6.00	5.60	5.45	7.67	5.33	6.23
	LEOG	Universal	−4.17	5.55	−22.06	−15.62	−25.67	−38.59	−26.13	−34.13	−10.51	−23.46
		hSURE	7.49	8.92	5.16	4.82	5.88	4.43	6.62	3.95	5.47	4.05
SNR (dB)	EEG O2	Universal	115.17	97.57	81.78	85.26	96.81	100.58	142.18	113.57	123.99	126.87
		hSURE	12.15	8.55	13.27	8.37	9.50	11.79	5.99	10.86	11.54	9.16
	EEG C3	Universal	118.57	117.63	99.40	106.02	73.00	77.91	49.78	122.69	99.97	142.83
		hSURE	10.43	8.92	12.76	9.57	14.10	13.67	11.01	9.58	10.57	9.15
	REOG	Universal	37.82	21.73	78.21	64.14	40.82	29.37	54.51	31.03	38.28	48.27
		hSURE	30.02	15.75	23.38	20.68	23.08	16.20	18.04	24.21	20.70	27.14
	LEOG	Universal	40.53	22.07	50.93	39.79	54.02	60.94	52.96	64.69	38.17	52.30
		hSURE	27.44	17.79	23.15	19.04	22.85	17.41	20.55	26.90	21.45	27.03

for neuronal leads and −48 to 5.5 dB on ocular electrodes. Conversely, the error difference of hSURE scheme holds a less varying behaviour, no larger than 8 dB including predominantly positive values. Likewise, SNR measure reaffirms the previous tendency; universal threshold strives out of range powers above 100 dB, against hSURE intensities surrounding 12 and 30 dB upon neuronal and ocular channels, respectively.

In spite of the conjectures that Table 2 might initially suggest, the supremacy of universal threshold cannot be immediately assured. Indeed, Fig. 4a–d set out the performance trends based on an epoch-by-epoch computation. A closer observation of universal threshold indicates an excessive variability, characterised by a peaky and random activity from one epoch to another. Those conditions accompanied by the analytical values convey a non-confident traceability of EEG/EOG varying moments. Inasmuch as more appealing gauges are obtained, larger deviations are built up. On the contrary, hSURE spans a smoother activity, ergo a more stable denoising process can be inferred.

Accordingly, a three-way ANOVA test with Bonferroni correction ($p < 0.003$) was also conducted over average RMSE and SNR quantities to unveil meaningful divergence with respect to EEG/EOG channels (Y dimension), thresholding values (X dimension) and voluntary subjects (Z dimension). Regarding RMSE statistical results, non-important difference is concluded between EEG O2 and

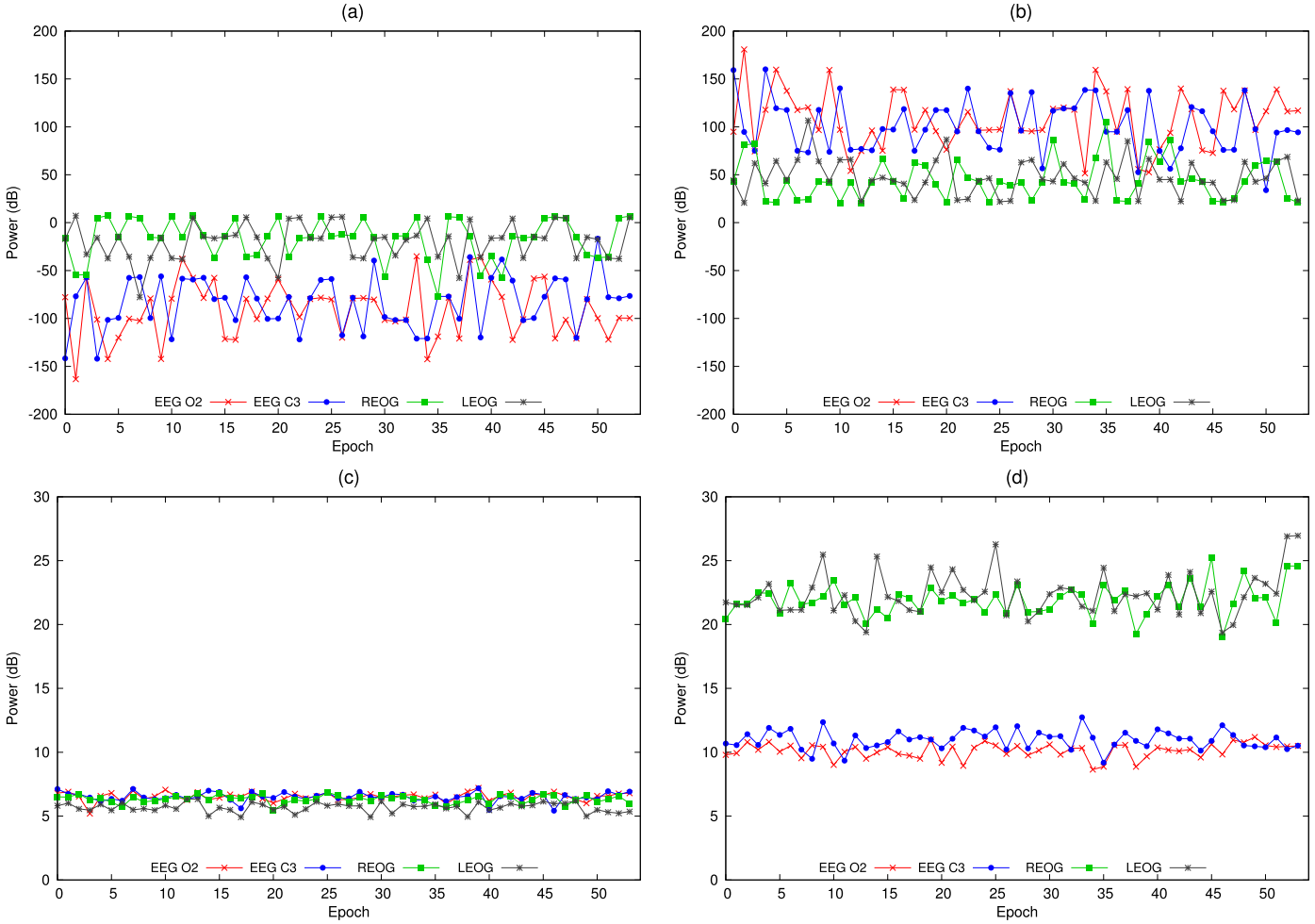

Fig. 4. Average RMSE and SNR performance curves on EEG O2, EEG C3, REOG and LEOG channels along the 55 drawn epochs. (a) Presents dB-scaled residual error for neuronal and ocular channels with universal threshold option. Correspondingly, (b) sketches the signal to noise relation over both sort of channels employing universal threshold. Ultimately, (c) and (d) depict the quantitative measures making use of hSURE scheme.

Table 3
Results of N-way ANOVA statistical tests applied to SIR, RMSE and SNR quantitative performance metrics. The displayed values correspond to dimension (Dim), degrees of freedom (DoF), error, mean squares per source (MS), *F*-statistic and *p*-value.

		Dim	DoF	Error	MS	*F*	*p*-value
2-way	SIR	Column-space	2	14	1.59	8.87	0.0033
		Row-space	7	14	0.68	3.80	0.0160
3-way	RMSE	*Y*	1	28	157.9	0.54	0.4695
		X	1	28	84704.03	288.35	0.0001
		Z	9	28	282.09	0.96	0.4919
	SNR	*Y*	1	28	109.5	0.38	0.5402
		X	1	28	85235.6	299.33	0.0001
		Z	9	28	2035.8	0.79	0.6241

EEG O3 channels $p = 0.4695$. In congruence with the statistical test applied to SIR mean values, the system engages an equipollent job in artefact removal and denoising for both neuronal leads; though, thresholding choice fosters ample evidence to nominate this parameter as an unquestionable decisive factor $p = 0.0001$ in noise suppression. Same case is applied to SNR ANOVA test, only thresholding decision deters the rejection of the null hypothesis $p = 0.0001$, which perfectly matches the inferences derived from Fig. 4. Indeed, universal threshold certainly fails tracing fast-varying moments of neuronal signals, as well as, slow-varying inflections of ocular peers; yielding asymptotic SNR and RMSE values that disqualify its application. Lastly, subject factor does not cast significant difference in RMSE $p = 0.4919$ or SNR $p = 0.6241$ test; although, future studies will require additional variables (e.g. gender or larger age interval) to reaffirm or deny this statement. Also, the complete values related to the statistical tests are shown in Table 3.

5. Discussion

Overall, sdPSG preprocessing model demonstrates to be a reliant preliminary approach in the preparation of electrophysiological signals for subsequent and more specialised processing routines of complete PSG. The deployment of a stream-wise algorithm for statistical source detachment proves its efficiency from an operational perspective by removing explicit and even subtle ECG-related artefacts of 960 EEG/EOG epochs. In fact, the selection of SOBIRO algorithm stems from its reliability to accomplish estima-

tion processes based on relatively fewer samples [8] and laxity on the non-Gaussianity condition for the observations [6]. The iterative computation of hundreds of time-delayed covariance matrices makes feasible the tangential deflection of such constraints; but foremost it monotonically blurs the effect of white Gaussian noise until this process is absent from the model [20,17]. The antagonist Infomax and JADE algorithms exploit High Order Statistics (HOS) and gradient descent optimisation over an iterative basis, which remarks their resilience to either subgaussian or supergaussian artefacts depending mostly on vast computational resources [7].

Notwithstanding, a group of 240 epochs still exposes embedding ECG artefacts after the preprocessing routine. Taking into account that the whole set belongs to a particular pair of subjects, it is reasonable to assume the violation of statistical independence condition during signals acquisition procedure, due to ill-ground references or lossy fixation of electrodes. In this case, the conditions of the recorded input data exceed the capabilities of BSS-SOS-based methods to procure separation.

On the same direction, the preprocessing model surmounts contamination of additive Gaussian noise, relied on WPT decompositions. Moreover, 1200 out of 1200 sdPSG epochs is a categorical testimony of the prolific command on this matter. In this matter, the selective cancellation of noisy wavelet coefficients is an intuitive explanation for this shrinkage effect. Undoubtedly, denoising methods based on wavelet packages involve a massive collection of parameters to be adequately tuned, in order to achieve outstanding signal reconstructions. Initially, the wavelet family plays a crucial role in the characterisation of biological signals by the estimation of approximation and detail coefficients. The authors in [4,11] demonstrate the prowess of Daubechies family in temporal and spectral domain thanks to its locality property. Also, the chosen fourth order is a deliberated attempt to avoid the generation of spurious components (e.g. fake artefacts), which is a recurrent side effect of high order wavelet convolutions [9]. Similarly, soft thresholding is amply preferred over the hard option, due to the growing possibility of artefacts appearance on the reconstructed signal, as a consequence of discontinuities in filtered subbands [11,19].

Comparatively, the proposed preprocessing system attains akin results with previous works [6,8,12], considering SIR and SNR gauges, and, it surpasses the discussed SNR and RMSE criteria in [11]. However, preliminary assumptions and general conditions shall be kept in mind before the predominance of the system is dictated above the others.

6. Conclusions

The introduced system posits a novel approach for preprocessing of sdPSG recordings making use of renowned techniques originated in diverse application fields. Also, their relevance to biosignal processing has been widely spread out in numerous publications. Nonetheless, the adaptation of computational methods to particular conditions of biophysical phenomena is an ongoing topic of discussion. Precisely, the proposed model is an original approach to take advantage of individual tools of estimation into a holistic alignment; subject to specific non-linear, non-stationary and ill-power constrains of electrophysiological components. Instead of boarding the implicit hurdles from isolated fronts, our solution scouts a cohesive solution, enriched by elements like low-order, time-to-diagnosis efficiency and modular autonomy. The overall performance is supported on the capabilities to withdraw sdPSG embedding artefacts and attenuation of additive noise. In order to assign analytical values to this purpose, SIR metric was introduced to contrast the separation efficacy of SOBIRO against Infomax and JADE algorithms. The obtained power values by SOBIRO above 0 dB opposed to ca. −2 dB intensity achieved by EEGLAB's algorithms assert its convenience as separation method. Besides of this, the conducted two-way ANOVA test stresses such a statement in a statistical way. Similarly, the mitigation of additive noise was measured by RMSE and SNR metrics to consolidate the tendency of regimes with higher signal strength than noise power and 0 to 8 dB of residual error between original and preprocessed EEG/EOG signals. As well, a three-way ANOVA test was called upon to postulate hSURE criterion as the adequate thresholding scheme for denoising proceedings based on WPT decomposition.

The forthcoming research suggests a self-improving dynamic of preprocessing mechanisms; so long as, the described findings promote the advancement in the processing and classification stages. The adequate preparation of sdPSG signals enhances the acquirement of more reliable results during feature extraction and classification tracks. It is advised to conduct further experiments to assess the performance of the proposed model against the existing alternatives; in regard of computational resources, additional mother wavelets, as well as, emergent optimisation criteria in signal decomposition. Ultimately, the estimation of signals integrity after preprocessing trials is a worthwhile field of study, since the conservation degree of the native attributes is a pending issue to be duly explored.

Acknowledgments

The authors would like to thank all 10 human volunteers who in 2011 undertook the biofeedback study, approved by RMIT Human Research Ethics Committee. R. Chaparro-Vargas acknowledges the financial support of COLCIENCIAS-COLFUTURO Conv#529 of the Colombian Government, as main sponsor for postgraduate studies.

References

[1] S.-F. Liang, C.-E. Kuo, Y.-H. Hu, Y.-H. Pan, Y.-H. Wang, Automatic stage scoring of single-channel sleep EEG by using multiscale entropy and autoregressive models, IEEE Trans. Instrum. Meas. 61 (6) (2012) 1649–1657.

[2] D. Cvetkovic, States of Consciousness: Experimental Insights into Meditation, Waking, Sleep and Dreams, Springer, Berlin, Heidelberg, 2011.

[3] A. Krakovská, K. Mezeiová, Automatic sleep scoring: a search for an optimal combination of measures, Artif. Intell. Med. 53 (1) (2011) 25–33.

[4] Y. Fei-Long, L. Zhi-Zeng, The EEG de-noising research based on Wavelet and Hilbert Transform method, in: 2012 International Conference on Computer Science and Electronics Engineering, ICCSEE, vol. 3, 2012, pp. 361–365.

[5] L. Fraiwan, K. Lweesy, N. Khasawneh, H. Wenz, H. Dickhaus, Automated sleep stage identification system based on time–frequency analysis of a single EEG channel and random forest classifier, Comput. Methods Programs Biomed. 108 (1) (2012) 10–19.

[6] C. Chang, Z. Ding, S.F. Yau, F. Chan, A matrix-pencil approach to blind separation of colored nonstationary signals, IEEE Trans. Signal Process. 48 (3) (2000) 900–907.

[7] A. Delorme, S. Makeig, EEGLAB: an open source toolbox for analysis of single-trial EEG dynamics including independent component analysis, J. Neurosci. Methods 134 (1) (2004) 9–21.

[8] K. Ting, P. Fung, C. Chang, F. Chan, Automatic correction of artifact from single-trial event-related potentials by blind source separation using second order statistics only, Med. Eng. Phys. 28 (8) (2006) 780–794.

[9] G. Inuso, F. La Foresta, N. Mammone, F. Morabito, Brain activity investigation by EEG processing: Wavelet Analysis, Kurtosis and Renyi's entropy for artifact detection, in: International Conference on Information Acquisition, ICIA '07, 2007, pp. 195–200.

[10] S. Devuyst, T. Dutoit, P. Stenuit, M. Kerkhofs, E. Stanus, Cancelling ECG artifacts in EEG using a modified independent component analysis approach, EURASIP J. Adv. Signal Process. 2008 (2008) 1–13.

[11] E. Estrada, H. Nazeran, G. Sierra, F. Ebrahimi, S. Setarehdan, Wavelet-based EEG denoising for automatic sleep stage classification, in: 21st International Conference on Electrical Communications and Computers, CONIELECOMP 2011, 2011, pp. 295–298.

[12] R.R. Vázquez, H. Vélez-Pérez, R. Ranta, V.L. Dorr, D. Maquin, L. Maillard, Blind source separation, wavelet denoising and discriminant analysis for EEG artefacts and noise cancelling, Biomed. Signal Process. Control 7 (4) (2012) 389–400.

[13] L. Mesin, A. Holobar, R. Merletti, Advanced Methods of Biomedical Signal Processing, IEEE Press, 2011.

[14] A. Rodenbeck, R. Binder, P. Geisler, H. Danker-Hopfe, R. Lund, F. Raschke, H.-G. Weeß, H. Schulz, A review of sleep EEG patterns. Part I: a compilation of amended rules for their visual recognition according to Rechtschaffen and Kales, Somnologie 10 (4) (2006) 159–175.
[15] T. Penzel, M. Hirshkowitz, J. Harsh, R.D. Chervin, Digital analysis and technical specifications, J. Clin. Sleep Med. 3 (2007) 109–120.
[16] S. Miyata, N. Akiko, N. Seiicho, H. Yagi, E. Yanagi, K. Honda, T. Sugiura, S. Nakai, T. Nakashima, Y. Koike, Daytime polysomnography for early diagnosis and treatment of patients with suspected sleep-disordered breathing, Sleep Breath. 11 (2007) 109–115.
[17] A. Galka, K.F.K. Wong, T. Ozaki, H. Muhle, U. Stephani, M. Siniatchkin, Decomposition of neurological multivariate time series by state space modelling, Bull. Math. Biol. 73 (2011) 285–324.
[18] C. Iber, S. Ancoli-Israel, A.L. Cheeson Jr., S.F. Quan, The AASM manual for the scoring of sleep and associated events, Tech. rep., American Academy of Sleep Medicine, 2007.
[19] M.A. Haidekker, Advanced Biomedical Image Analysis, Wiley, 2011.
[20] A. Cichocki, S. Amari, Adaptive Blind Signal and Image Processing, Wiley, 2005.
[21] S.p. Mallat, A Wavelet Tour of Signal Processing, Elsevier Academic Press, 1999.
[22] N.V. Thakor, S. Tong, Advances in quantitative electroencephalogram analysis method, Annu. Rev. Biomed. Eng. 6 (1) (2004) 453–495.
[23] J.E. Bartlett, J.W. Kotrlik, C.C. Higgins, Organizational research: determining appropiate sample size in survey research, Inf. Technol. Learn. Perform. J. 19 (1) (2001) 43–50.
[24] R. Chaparro-Vargas, D. Cvetkovic, A single-trial toolbox for advanced sleep polysomnographic preprocessing, in: 35th Annual International Conference of the IEEE Engineering in Medicine and Biology Society, EMBC, 2013, pp. 5829–5832, http://dx.doi.org/10.1109/EMBC.2013.6610877.

R. Chaparro-Vargas received the M.Sc. degree in Communications Engineering in 2010 from the Technical University of Munich, Munich, Germany. Currently, he is working towards the Ph.D. degree in the School of Electrical and Computing Engineering at RMIT University, Melbourne, Australia. His research interest resides in signal processing and computational modelling applied to biomedical applications, particularly in neurophysiology.

D. Cvetkovic received the M.Eng. and Ph.D. degree respectively in 2002 and 2005 from the RMIT University, Melbourne, Australia. At the present, he is a Senior Lecturer in Biomedical and Electronics Engineering at School of Electrical and Computer Engineering (RMIT University) and a member of Health Innovations Research Institute (HIRi). His research at RMIT University spans over the last 15 years in the engineering areas of biomedicine, electronics, mechatronics and design engineering education.

Appendix D

Peer-reviewed conference paper

Title: Interdependence of Electroenphalographic and Electrocardiographic Power Bands in Human Power Bands

Authors: Ramiro Chaparro-Vargas, Emad Malaekah, Claudia Schilling, Michael Schredl and Dean Cvetkovic

Publication: Proceedings of the 5th ISSNIP - IEEE Biosignals and Biorobotics Conference

Year of Publication: 2014

Interdependence of Electroencephalographic and Electrocardiographic Power Bands in Human Sleep

Ramiro Chaparro-Vargas[1], Emad Malaekah[2], Claudia Schilling[3], Michael Schredl[4], Dean Cvetkovic[5]

***Abstract*— The estimation of functional interdependencies within the autonomous nervous system (ANS) has gained increasing importance to quantify the relationship between neuronal and cardiac activity. The present paper introduces a biomedical signal processing approach based on computational resources to serve as a supportive tool in the characterisation of sleep. By making use of linear methods and statistical tests upon 10 electroencephalographic (EEG) and electrocardiographic (ECG) overnight sleep recordings; the computation of cross-correlation and wavelet coherence is focused on finding distinguishable features amongst the testing subjects. The results demonstrate that mid-range neuronal oscillations (e.g. θ, α and ς) interact with cardiac power bands at different levels, especially during unrelated REM sleep stages.**

I. INTRODUCTION

In the recent years, a topic of growing importance is the functional interdependence amongst power oscillations, generated by neuronal and cardiac activity [1]. The implicated mechanisms suggest an underlying interaction of cortical regions and heart regulated processes [2] [3]. The coordinated activity of neuronal assemblies into hypo- and hyperpolarisation states, accompanied by Heart Rate Variability (HRV) fluctuations, holds a tight association to sympathetic and vagal cardiac activities [4]. The deployment of biomedical signal processing techniques upon electroencephalographic (EEG) and electrocardiographic (ECG) channels attempts to elucidate the nature of functional interactions across sleep stages. Therefore, we suggest a computational approach supported by time and frequency-oriented methods to quantitatively estimate the functional interaction, that is assumed between EEG and HRV power bands.

Hitherto, the study of EEG-to-HRV interdependence has employed linear and non-linear approaches to enhance singularities during resting, task-specific or sleeping contexts [5]. The conduction of frequency and phase-based analyses has proved the existence of synchronised oscillations into high HRV and low EEG power bands; i.e. HRV-HF (0.15-0.4 Hz), δ (0.5-4 Hz), θ (4-8 Hz) and α (8-12 Hz), respectively [2] [4] [6]. Notwithstanding, such studies are focused on neuronal cross-spectrum or cardiorespiratory processes, restricted to short-length electrophysiological recordings (less than 1 hour). Additional research works foster scrutinising methodologies to characterise not only functional interaction, but also directional interdependence along recognised sleep stages [3] [7]. By introducing extended polysomnographic (PSG) recordings, the authors aimed to facilitate the observation of driving signals in function of sleep staging interdependences, exposing a linear versus non-linear comparative benchmarking. However, further findings are still pending to be discussed, considering emerging Time-Frequency Analysis (TFA) proceedings, larger population of subjects and physiological interpretation of observed patterns. In this paper, we introduce a computational approach to perform linear and statistical analyses upon long-term PSG recordings, including 15 EEG and 1 ECG channels. Based on extensively reported methods like Cross-correlation Function (CCF) and Wavelet Coherence; we aim to characterise the functional dynamics of 10 healthy subjects during overnight sleeping period. The findings indicated the presence of temporal and spectral dependencies of neuronal power bands and cardiac frequencies with spatial variations, subject to the episodic sleep stages. Apart from this, the sleep staging performed a major role in the differentiation of sympathetic and parasympathetic activity on each subject. In this sense, we encourage the adoption of biomedical signal processing as an assisting tool for the more precise interpretation of autonomous nervous system activity during prolonged resting times.

II. METHODS

The estimation of functional interdependence between EEG $\leftrightarrow$ HRV oscillation bands is divided in three main stages: pre-processing, processing and statistical analysis. The pre-processing framework offers a preliminary set-up for the raw EEG/ECG signals, including epoch-oriented segmentation, neural parcellation and band decomposition [8]. Then, the succeeding processing stage is performed recurring to TFA-based techniques to extract the data-describing features. The latter, statistical rank test seeks significant differences within the derived features and scored sleep stages, attending to the non-linear, non-stationary and non-Gaussian-distributed nature of original datasets. The entire computational analysis was developed with software package MATLAB© 7.13 (The MathWorks Inc., USA).

[1]R. Chaparro-Vargas is with School of Electrical and Computing Engineering, RMIT University, Melbourne VIC 3001, Australia ramiro.chaparro-vargas@rmit.edu.au

[2]E. Malaekah is with School of Electrical and Computing Engineering, RMIT University, Melbourne VIC 3001, Australia s3321008@student.rmit.edu.au

[3]C. Schilling is clinical research physician at the sleep laboratory of the Central Institute of Mental Health, Mannheim, Germany claudia.schilling@zi-mannheim.de

[4]M. Schredl is clinical research physician at the sleep laboratory of the Central Institute of Mental Health, Mannheim, Germany michael.schredl@zi-mannheim.de

[5]D. Cvetkovic is with School of Electrical and Computing Engineering, RMIT University, Melbourne VIC 3001, Australia dean.cvetkovic@rmit.edu.au

TABLE II
INTER-NEURAL PARCELS

Parcel	Electrodes	Abbreviation
1	C_3A_2, C_zA_1, C_4A_1	C_{4z3}
2	O_2A_1, O_1A_2	O_{21}
3	F_8A_1, F_7A_2	F_{87}
4	F_4A_1, F_3A_2	F_{43}
5	P_4P_3, P_4P_z, P_3P_z	P_{43}
6	T_3T_5, T_4T_6	T_{43}

A. Subjects and clinical data

We employed the clinical data recorded from 10 healthy (HEA) subjects. Each subject undertook an overnight PSG recording at the Sleep Laboratory of the Central Institute of Mental Health in Mannheim, Germany. The demographic and clinical parameters of recruited subjects are summarised in Table I.

Following the Rechtschaffen and Kales (R&K) scoring manual [9], EEG channels are segmented into 30-second epochs to score the overall sleep staging including Wake (W), Stage 1 (S1), Stage 2 (S2), Stage 3 (S3) and Stage 4 (S4) and Rapid Eye Movement (REM) sleep. Besides, the scoring monitored the number of 3-second segments with eye movements, body check, arousals and leg movements. The study was approved by the local ethic committee of the Medical Faculty Mannheim of the University of Heidelberg.

Straightforward, a detailed description about the introduced computational approach is done with respect to the three main stages.

B. Pre-processing

According to the guidelines of R&K scoring manual, the pre-processing routines execute a fragmentation of consecutive 30-second epochs on every PSG channel, aiming to preserve power and time alignment properties. So, subsequent pre-processing and processing routines are systematically applied to hundreds of generated epochs, serial-wise, until the end of the recording time.

Next, inter-neural parcellation manages to associate EEG signals into a single composite, relaying on correlation coefficients and distribution divergence measures amongst adjacent electrodes. For example, C_{4z3} merges three different sources, whereas it is foreseen that central electrodes located at the centre (Cz), right- (C4) and left hemisphere (C3) of the scalp plot statistically resemblant potentials subject to an inter-hemispheric context [7]. Such an aggregation of cortical regions obeys to two premises: dimensionality reduction and computational optimisation. Since, the excessive number of EEG channels leads to oversized processing burden, resources consumption and dilated computation times [10]. By averaging out the correlated EEG bipolar channels (monopolar electrodes are excluded for compatibility reasons), the parcellation routine clusters the inter-neural areas as Table II states [1] [11].

Finally, the band decomposition routine deconstructs the EEG parcels in six neuronal oscillatory bands, such as delta δ (0.5-4 Hz), theta θ (4-8 Hz), alpha α (8-12 Hz), sigma ς (12-16 Hz), beta β (16-32 Hz) and gamma γ (32-64 Hz). In the same way, HRV frequency bands LF (0.04-0.15 Hz) and HF (0.15-0.4 Hz) [12] [5] are calculated from the ECG channel by means of R-to-R interval (RRI) computation, peak detection algorithm, interpolated smoothing and upsampling processes, as the recommendations in [12] consign. From here, the usage of Wavelet Packet Transform (WPT) allows a time-frequency decomposition supported on the coefficients shrinkage principle. Due to its computational efficiency and inherited additional benefits, like noise filtering, energy conservation and selective removal of unwanted components [13]. The iterative operations sorting low-pass $\mathbf{h}^b[m]$, high-pass $\mathbf{g}^b[m]$ filter coefficients and aggregated signals at $j = \{1,\dots,Z\}$ levels with Daubechies-4 (db4) as mother wavelet with Z as maximum decomposition level, produced the EEG frequency bands, which are explained by the formulations in Eq. 1 and Eq. 2.

$$\mathbf{x}_{j+1}^{b,LP}[k] = \sum_{m=1}^{N} \mathbf{h}^b[m-2k]\mathbf{x}_j^{b,LP}[m] \quad ; \quad b = \{\delta,\dots,\gamma\} \tag{1}$$

$$\mathbf{x}_{j+1}^{b,HP}[k] = \sum_{m=1}^{N} \mathbf{g}^b[m-2k]\mathbf{x}_j^{b,HP}[m] \tag{2}$$

In correspondence, HRV frequency bands $\mathbf{y}^{\mathbf{HF}}[k], \mathbf{y}^{\mathbf{LF}}[k]$ are generated from a similar decomposition, summing up low-pass and high-pass filter coefficients, taking into account the narrow-band regime of cardiac spectrum. Then, Eq. 3 follows an equivalent derivation.

$$\begin{aligned} \mathbf{y}^{b'}[k] &= \mathbf{y}_{j+1}^{b'}[k] + \mathbf{y}_{l+1}^{b'}[k] && ; \quad b' = \{\mathbf{LF},\mathbf{HF}\} \\ &= \sum_{m=1}^{N} \mathbf{h}^{b'}[m-2k]\mathbf{x}_j^{b'}[m] + \cdots && ; \quad j = \{1,\dots,Z\} \\ &\quad \sum_{m=1}^{N} \mathbf{g}^{b'}[m-2k]\mathbf{x}_l^{b'}[m] && ; \quad l = \{1,\dots,Z'\} \end{aligned} \tag{3}$$

C. Processing

The processing stage pivots the features extraction in order to estimate the functional interdependence between neuronal and cardiac oscillatory power bands, represented by the previously decomposed frequency bands [3] [4]. For this reason, linear methods are developed and tested as part of the computational approach for biomedical signal analysis. So far, linear approaches have demonstrated their prowess in the computation of synchronised traces between biophysical oscillations, standing out common but well-referred techniques like cross-correlation function (CCF) and coherence [1], though we have adopted wavelet coherence variant, expressed by Eq. 5. In turn, CCF in Eq. 4 estimates the linear correlation in function of time lags, reflecting a weak or strong two-ways relationship between the signals, and whose maximised unit value is commonly assumed as the delay of the paired signals.

TABLE I

INFORMATION OF TESTING SUBJECTS AND TECHNICAL DETAILS OF PSG RECORDINGS

Variable	Healthy (HEA)										Mean ± SD*
Subject ID	HEA1	HEA2	HEA3	HEA4	HEA5	HEA6	HEA7	HEA8	HEA9	HEA10	
Gender	m*	m	m	m	m	f*	f	f	f	f	n.a.*
Age (years)	25	46	20	26	27	26	46	47	21	26	31.5 ±11.3
Total Recording (min)	483	498	477	447	482	482	476	489	484	526	490.9±23.6
W Latency (min)	210	113	26	77	68	41	14	53	89	90	77.2±55.6
S1 Latency (min)	48	48	47	40	90	52	16	29	195	45	66±50.8
S2 Latency (min)	132	228	221	44	207	288	218	231	163	223	211.8±41.4
S3 Latency (min)	29	0.5	100	118	14	20	131	50	115	39	51.25±46.8
S4 Latency (min)	1	0.5	1	1	1	1	1	1	1	2	1.05±0.36
REM Latency (min)	29	78	80	49	63	45	70	55	68	12.6	56.3±21.6
Sleep efficiency (%)	49.5	71.4	94.1	56.4	77.8	84.3	91.6	81.9	75.7	65.6	76.9±12.9
Bipolar channels†	$C_3A_2, C_4A_1, O_2A_1, O_1A_2, C_zA_1, F_8A_1, F_7A_2, F_4A_1, F_3A_2$										
Monopolar channels†	$P_4P_3, P_4P_z, P_3P_z, T_3T_5, T_4T_6, ECG$										

∗ SD = Standard deviation, m = male, f = female, n.a. = no applicable

† electrodes arrangement compliant with 10-20 international system

$$\begin{aligned}\mathbf{R}_{\mathbf{xy}}(\tau) &= E\{\mathbf{x}[k+\tau]\mathbf{y}^{\mathrm{H}}[k]\} \\ &= \frac{1}{N-|\tau|}\sum_{k=1}^{N-\tau}\mathbf{x}[k+\tau]\mathbf{y}^{\mathrm{H}}[k] \end{aligned} \tag{4}$$

Wavelet coherence computes the auto- $\mathbf{S}_{\mathbf{xx|yy}}(\omega_0)$ and cross- $\mathbf{S}_{\mathbf{xy}}(\omega_0)$ power spectrum to produce an unitary value, matching time translation and frequency scale domains. Therefore, periodograms and related techniques can be deployed to follow the interacting dynamics.

$$\begin{aligned}{\kappa_{\mathbf{xy}}}^2(\omega_0) &= \frac{|\mathbf{S}_{\mathbf{xy}}(\omega_0)|^2}{|\mathbf{S}_{\mathbf{xx}}(\omega_0)||\mathbf{S}_{\mathbf{yy}}(\omega_0)|} \\ &= \frac{|\mathbf{S}\left({\mathbf{W}_{\mathbf{xx}}}^{\mathrm{H}}(s,\tau)\mathbf{W}_{\mathbf{yy}}(s,\tau)\right)|^2}{|\mathbf{S}\left(\mathbf{W}_{\mathbf{xx}}(s,\tau)\right)||\mathbf{S}\left(\mathbf{W}_{\mathbf{yy}}(s,\tau)\right)|} \end{aligned} \tag{5}$$

where $\mathbf{W}(s,\tau)$ denotes the continuous wavelet transform at scale s and translation index τ.

Lastly, a normalisation fixture is applied to displace the generated features into $0-1$ interval, which homogenises the statistical analysis and interpretation of the further results.

D. Statistical analysis

Our computational approach applies multiple statistical tests to decide whether a Gaussian distribution is the fittest reference for the modelled data [14], as well as, (non-)parametric suitability and sample size determination [15]. An evaluation of Gaussianity conditions upon the scoped signals is required, in order to conduct a proper statistical analysis in the search of significant differences underlying the testing cohort [16] [17]. The Bartlett test assessed the graphical and analytical divergence of the mean and covariance of the modelled data versus the Gaussian distribution. The results of those tests showed a strong deviation of the samples from the Gaussian tendency curve, suggesting so the practice of Kruskal-Wallis test [18].

III. RESULTS

The stages of pre-processing, processing and statistical analysis considered the subjects with same the same type of bipolar montage (i.e. HEA1-HEA9) to yield the inter-hemispheric neural parcels. So, the selected neural areas are denoted as: C_{4z3}, F_{87}, O_{21}, such that, the biophysical activity located in the central, occipital and frontal cortical regions were cross-operated with the cardiac counterparts. In order to extract the CCF and wavelet coherence linear values from each clinical recording, we proceeded to compute the expectation and standard deviation amongst the 9 group members, because one subject did not fulfil the general recording conditions. Overall, that pair of basic statistics served as the main source for analytical and statistical findings.

Initially, the time-based linear analysis started by calculating the Pearson's coefficient or CCF value at zero-th time lag. Considering, 6 decomposed EEG power bands, 2 HRV frequency ranges and 9 healthy subjects, Fig. 1 illustrates a clustered histogram with the attained mean values and whiskers, denoting standard deviation. The first observation established a constant related to the whole set of correlation coefficients, since healthy patients kept a threshold never larger than 0.6 for each power band and neural parcel. In the case of EEG $\leftrightarrow$ HF cross-correlation, it was evident during low EEG bands, i.e. δ, θ and α, how the central, frontal and posterior positions maintained indistinct levels within the $0.55-0.6$ interval. Once, high EEG bands were inspected, the strength of central and frontal locations commenced to diminish. Similar behaviour can be inferred from EEG $\leftrightarrow$ LF power bands, although a weaker presence (0.55) of central activity became regular from low to high EEG oscillations. Apparently, non-significant difference existed amongst EEG $\leftrightarrow$ HF and EEG $\leftrightarrow$ LF power bands inside of the subjects group, albeit further statistical analyses were required to obtain a more precise testing of every possible pair of frequencies.

The second linear method, wavelet coherence counted

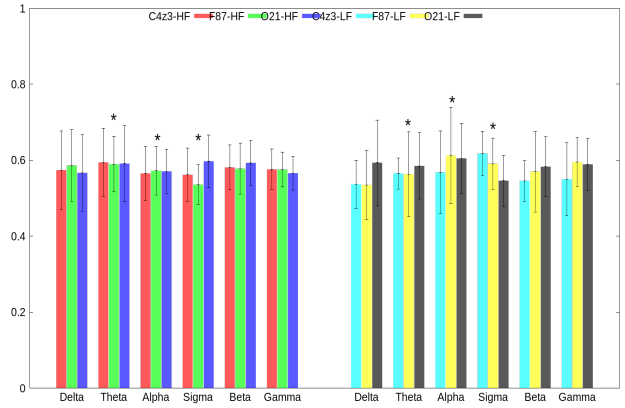

Fig. 1. Histogram of Pearson's coefficient or CCF at zero-th time lag including EEG δ, θ, α, ς, β and γ versus HRV LF and HF bands for testing cohort. Each set of coloured bars represent the mean value of inter-hemispheric neural parcels: C_{4z3}, F_{87} and O_{21} with their corresponding standard deviation as error bars. * statistically significant ($p < 0.05$) after Kruskal-Wallis rank test.

with the arrangement of one cycle of sleep into a multi-stage periodogram, which is accompanied by the described EEG/HRV power bands and averaged out subjects group. Out of the macro-periodogram in Fig. 2 some annotations are introduced in relation to the interdependencies within the designated EEG neural parcel C_{4z3}. The coherence between low EEG power bands, such as δ,$\theta \leftrightarrow$ LF, HF was accentually stronger $(0.4-0.5)$ during W and REM stages. As far as, we moved to θ, ς and β regions of the neuronal spectrum with HF, it was perceived the increasing intensity $(0.5-0.7)$ in deep sleep stages, S3 and S4. Unlike to EEG $\leftrightarrow$ LF relationship, whose cross-activity barely exceeded (0.4) coherence levels. But, one of the most relevant facts was the constant coherence between $\theta \leftrightarrow$ HF bands along the 6 sleep stages, which slowly faded out at the end of ς band region by casting a medium-value coherence (0.5). Going over high EEG power bands, i.e. β and γ, the lack of outstanding activity was evident, independent of sleep stages or HRV bands. Although, attenuated spots (*ca.* 0.15) stood out during deep sleep and REM stages. Regarding the remaining periodograms, which are not shown here; it was vindicated the noticeable activity $(0.6-0.75)$ of EEG low power bands $\delta/\theta \leftrightarrow$ LF/HF towards dissipated levels at α to γ frequencies.

At last, a Kruskal-Wallis omnibus test was conducted to elicit significant differences at the different sleep stages, attending to every interaction of EEG $\leftrightarrow$ HRV power bands, electrode parcels and sleep stages. Generally, CCF feature held some statistical evidence about functional interdependence between θ,α,$\varsigma \leftrightarrow$ HF at the end of light ($\chi^2 = 11.76, p = 0.038$) and deep sleep ($\chi^2 = 13.11, p = 0.022$), as well as, REM stage. The wavelet coherence (WCOH) method cast a slightly larger number of significant differences involving W, light (S2) and deep sleep (S3,S4) stages between θ,α,$\varsigma \leftrightarrow$ HF frequency pairs with ($\chi^2 = 11.76, p = 0.038$) and ($\chi^2 = 13.11, p = 0.022$) test values. In addition, statistical relevance was observed in θ,α,$\varsigma \leftrightarrow$ LF ($\chi^2 = 11.76, p =$ 0.038) and ($\chi^2 = 13.11, p = 0.022$) across W, S2, S3 and S4 stages, when CCF features concerned. Nonetheless, significant results become elusive between neuronal EEG bands and HRV-LF by the time of wavelet coherence evaluation. Thus, Table III sums up the statistical values amongst pair of frequencies, distinguishing sleep stages. Likewise, Figures 1-2 mark the statistically significant values according to these criteria.

IV. DISCUSSION AND CONCLUSIONS

The overall statistics of sleep parameters, referred in Table I, demonstrate the largest latencies in W, S1 and S2 stages, which were associated to sleep onset periods. Although, the mean values are evenly accompanied for large standard deviations, that is a strong lead of dissimilar sleeping patterns amongst the examined subjects. Therefore, a further interpretation of those initial conjectures needed to be treated by means of biomedical signal processing and computer-assisting tools.

The main purpose of the present paper involved a computational approach to detect functional interdependencies between neuronal activity, represented by EEG, and (para)sympathetic changes through HRV power bands. Albeit, the appearance of high and low correlated or coherent dynamics between frequency components at separated cortical regions, might lead to deceiving conclusions in a first term. For that reason, a statistical framework is set up to elicit probabilistic evidence rather than absolute certainty around cortical and cardiac dynamics [19]. Accordingly, we initially introduced the CCF method to distinct, at least in a analytical sense, the interaction of EEG oscillations with HF/LF power bands. The homogeneous behaviour of Pearson's coefficient by contrasting EEG $\leftrightarrow$ HF cast ambivalence about the dominance of neuronal oscillations across the scalp sources. However, EEG $\leftrightarrow$ LF, i.e. interacting cortical and sympathetic activity exhibited more pronounced alternations, as far as the locations varied. Foremost, it is important to note that the steady mid-value correlation $(0.5-0.6)$ for testing subjects, drove in consonance with previous findings focused on healthy population [7].

As a complement, wavelet coherence turned out to provide a more accurate tracking of interdependencies, integrating additional degrees of freedom, like sleep stages, power bands and electrode locations. Only if no forward or backward relationships were sought, the capability of phase difference computation of this method beheld; otherwise, other procedures for direction estimation should be convoked. Previous works had claimed the dominant activity of LF cardiac band during W/REM stages, as well as, HF along non-related REM periods [20]. Our findings extracted from periodograms not only confirmed that claim, but also set forth the increasing coherence values allocated in the low EEG frequency bands. As expected, W and REM stages were closely related to sympathetic coherence. In the same manner, a gradual relaxation was perceived during non-related REM stages, which is explained by a vagal cardiac system or HF power band surpassing. In consequence, a novel matter of this work

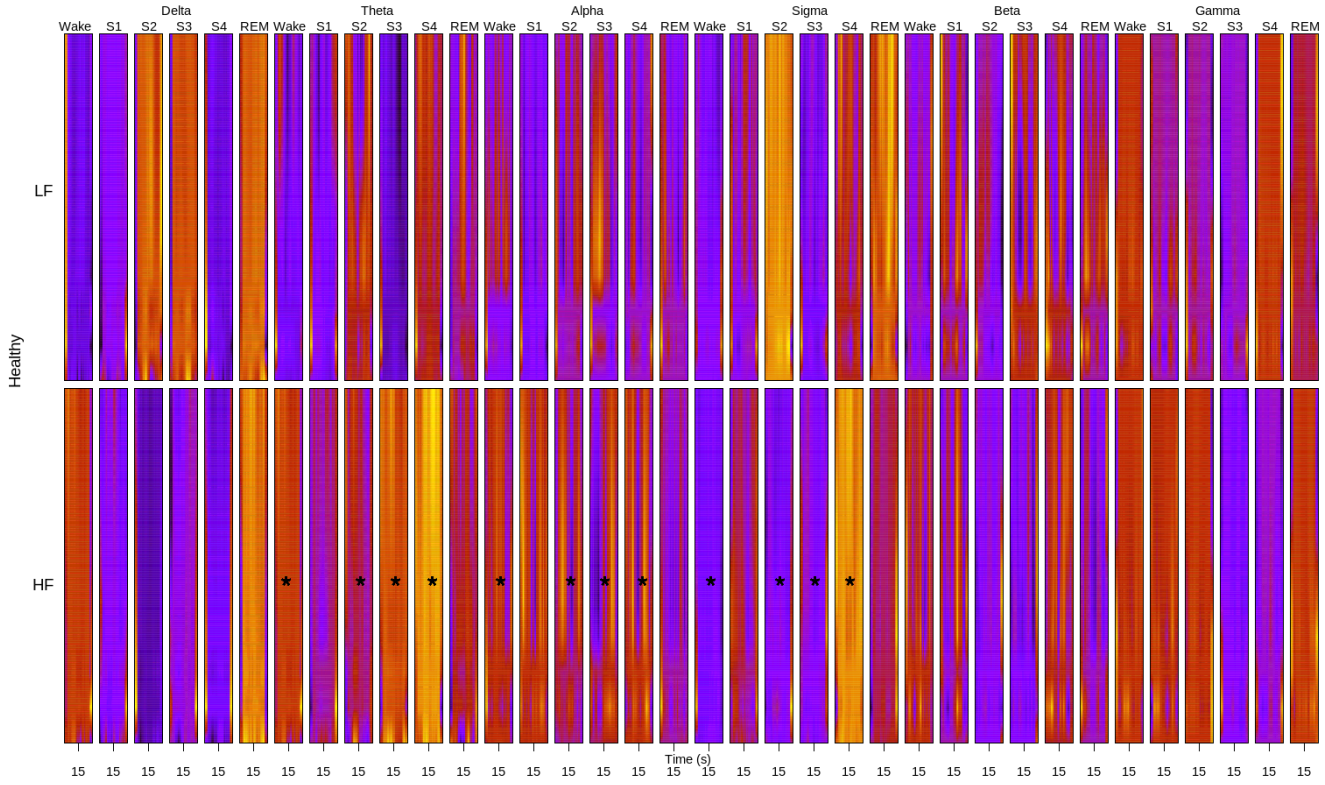

Fig. 2. Macro-periodogram of Wavelet Coherence considering EEG δ, θ, α, ς, β and γ at C_{4z3} parcel against HRV LF and HF bands for testing cohort across sleeps stages W, S1, S2, S3, S4 and REM. On the x-axis, each periodogram's cell portrays averaged out 30-seconds epochs corresponding to a particular sleep stage, and 12 pseudo-frequencies are ordered on the y-axis starting on *ca.* 89.8 Hz till (top scale) 0.04 Hz (bottom scale). The colour scale assigns the black-ultraviolet spectrum for low coherence values, whilst red-yellow intensities represent the surrounding unitary values, i.e. high coherence. * statistically significant ($p < 0.05$) after Kruskal-Wallis rank test.

TABLE III

KRUSKAL-WALLIS RANK TEST STATISTICAL VALUES APPLIED TO SUBJECTS GROUP BASED ON POWER BANDS AND SLEEP STAGES

Method	$\delta \leftrightarrow$ HF	$\theta \leftrightarrow$ HF	$\alpha \leftrightarrow$ HF	$\varsigma \leftrightarrow$ HF	$\beta \leftrightarrow$ HF	$\gamma \leftrightarrow$ HF
CCF	-	S2(11.76,0.038)	S2(13.11,0.022)	S2(11.76,0.038)	-	-
	-	S4(11.76,0.038)	S4(13.11,0.022)	S4(11.76,0.038)	-	-
	-	REM(11.76,0.038)	REM(13.11,0.022)	REM(11.76,0.038)	-	-
WCOH	-	S2(11.76,0.038)	S2(13.11,0.022)	S2(11.76,0.038)	-	-
	-	S3(11.76,0.038)	S3(13.11,0.022)	S3(11.76,0.038)	-	-
Method	$\delta \leftrightarrow$ LF	$\theta \leftrightarrow$ LF	$\alpha \leftrightarrow$ LF	$\varsigma \leftrightarrow$ LF	$\beta \leftrightarrow$ LF	$\gamma \leftrightarrow$ LF
CCF	-	W(11.76,0.038)	W(13.11,0.022)	W(11.76,0.038)	-	-
	-	S2(11.76,0.038)	S2(13.11,0.022)	S2(11.76,0.038)	-	-
	-	S3(11.76,0.038)	S3(13.11,0.022)	S3(11.76,0.038)	-	-
	-	S4(11.76,0.038)	S4(13.11,0.022)	S4(11.76,0.038)	-	-
WCOH	-	-	-	-	-	-

$p < 0.05$, such that Stage(χ^2, p)

counterweighted the strong presence of δ and θ power bands and the mild interaction forces at high spectrum regions, such as β and γ oscillations. Taking into consideration the argument that $\theta \leftrightarrow$ LF coherence reveals coupling dynamics between long-range brain regions, as well as, $\gamma \leftrightarrow$ HF defines more proximate interactions [21]. And, as far as the present findings dictated, we suggest that within healthy population the functional interdependences of sympathetic and parasympathetic is scarcely related to high neuronal oscillations. Furthermore, the existence of a larger variety of slow and fast time-varying neuronal events (e.g. K-complexes, sawtooth waves, sleep spindles, etc.) concentrated in low and mid spectrum regions, engages important changes in the regular and excitatory functions of the autonomous nervous system (ANS).

From the results of Kruskal-Wallis omnibus test, we could

statistically reaffirm some of the conclusions previously introduced. First, CCF method drew forth significant differences centred in θ, α, ς and parasympathetic or cardiac vagal activity during S2, S4 and REM sleep stages. Thereupon, a straightforward mapping of sleep stages and power oscillations can be done to explain those findings. Sleep stage S2 is characterised by the presence of sleep spindles in ς region and intermittent θ activity; S4 is fully-described by slow waves (SWS) with δ content, and REM sleep commonly reproduces α activity of W stage [9]. Similar results were obtained by crossing EEG oscillations and sympathetic-related frequency band LF, adding up S3 sleep stage to the testing group. Such a symmetry between HF and LF power bands inhibited the clear distinction of regular and excitatory activity of the ANS from CCF point of view. Opposite to this, wavelet coherence method aided to delimit the statistically relevant interactions at the same neuronal power bands, but only concurrent to vagal cardiac activity, during mostly non-related REM sleep stages (W,S2,S3,S4), in accordance with previous studies [22] [20]. We can hypothesise that TFA-based methods are more reliable to discriminate functional interdependencies within the ANS, subject to 10-individual healthy group. Foremost, the introduction of wavelet coherence revealed better than CCF the presumably strong interaction of θ,α,ς bands to differentiate sympathetic from parasympathetic activity.

Our findings suggest the existence of relevant differences between neuronal and cardiac power bands, in terms of cross-correlation and time-frequency coherence values across overnight sleep cycles. Moreover, the influence between mid-range EEG bands and vagal cardiac activity during light and deep sleep stages was spanned by the detection of functional interactions during W stage. Additional studies should be proposed to examine in more detail the impact of non-linear approaches, in order to disregard spurious interdependencies and improve TFA-based approaches.

ACKNOWLEDGEMENT

The authors would like to thank the Sleep Laboratory of the Central Institute of Mental Health for undertaking the recruitment and collection of polysomnographic recordings, which served as the main experimental source for the present research work. R. Chaparro-Vargas acknowledges the financial support of COLCIENCIAS-COLFUTURO of the Colombian Government, as main sponsor for his doctorate studies.

REFERENCES

[1] E. Pereda, R. Q. Quiroga, and J. Bhattacharya, "Nonlinear multivariate analysis of neurophysiological signals," *Progress in Neurobiology*, vol. 77, no. 12, pp. 1 – 37, 2005.

[2] J. Palva, S. Palva, and K. Kaila, "Phase synchrony among neuronal oscillations in the human cortex," *Journal of Neuroscience*, vol. 25, no. 15, pp. 3962–3972, April 2005.

[3] S. Dimitriadis, N. Laskaris, Y. Del Rio-Portilla, and G. Koudounis, "Characterizing dynamic functional connectivity across sleep stages from EEG," *Brain Topography*, vol. 22, no. 2, pp. 119–133, 2009, cited By (since 1996) 13.

[4] M. Dumont, F. Jurysta, J.-P. Lanquart, P.-F. Migeotte, P. van de Borne, and P. Linkowski, "Interdependency between heart rate variability and sleep EEG: linear/non-linear?" *Clinical Neurophysiology*, vol. 115, no. 9, pp. 2031 – 2040, 2004.

[5] U. R. Acharya, K. P. Joseph, N. Kannathal, C. M. Lim, and J. S. Suri, "Heart rate variability: A review." *Medical & Biological Engineering & Computing*, vol. 44, no. 12, pp. 1031 – 1051, 2006.

[6] R. Bartsch, J. W. Kantelhardt, T. Penzel, and S. Havlin, "Experimental evidence for phase synchronization transitions in the human cardiorespiratory system," *Phys. Rev. Lett.*, vol. 98, p. 054102, Feb 2007.

[7] K. Mezeiova and M. Palus, "Comparison of coherence and phase synchronization of the human sleep electroencephalogram," *Clinical Neurophysiology*, vol. 123, no. 9, pp. 1821 – 1830, 2012.

[8] S. Palva, S. Monto, and J. M. Palva, "Graph properties of synchronized cortical networks during visual working memory maintenance," *NeuroImage*, vol. 49, no. 4, pp. 3257 – 3268, 2010.

[9] A. Rodenbeck, R. Binder, P. Geisler, H. Danker-Hopfe, R. Lund, F. Raschke, H.-G. Wee, and H. Schulz, "A review of sleep EEG patterns. part I: A compilation of amended rules for their visual recognition according to rechtschaffen and kales," *Somnologie*, vol. 10, no. 4, pp. 159–175, 2006.

[10] S. Palva and J. M. Palva, "Discovering oscillatory interaction networks with M/EEG: challenges and breakthroughs," *Trends in Cognitive Sciences*, vol. 16, no. 4, pp. 219 – 230, 2012.

[11] F. Moroni, L. Nobili, F. D. Carli, M. Massimini, S. Francione, C. Marzano, P. Proserpio, C. Cipolli, L. D. Gennaro, and M. Ferrara, "Slow EEG rhythms and inter-hemispheric synchronization across sleep and wakefulness in the human hippocampus," *NeuroImage*, vol. 60, no. 1, pp. 497 – 504, 2012.

[12] T. F. of The European Society of Cardiology, T. N. A. S. of Pacing, and Electrophysiology, "Heart rate variability," *European Heart Journal*, vol. 17, pp. 354–381, 1996.

[13] S. Mallat, *A Wavelet Tour of Signal Processing*. Elsevier Academic Press, 1999.

[14] M. Marusteri and V. Bacarea, "Comparing groups for statistical differences: how to choose the right statistical test?" *Biochemia Medica*, vol. 20, no. 1, pp. 15–32, 2010.

[15] J. E. Bartlett, J. W. Kotrlik, and C. C. Higgins, "Organizational research: Determining appropiate sample size in survey research," *Information Technology, Learning, and Performance Journal*, vol. 19, no. 1, pp. 43–50, 2001.

[16] M. A. Haidekker, *Advanced Biomedical Image Analysis*, J. Wiley and I. Sons, Eds. Wiley, 2011.

[17] L. Mesin, A. Holobar, and R. Merletti, *Advanced Methods of Biomedical Signal Processing*, S. Cerutti and C. Marchesi, Eds. IEEE Press, 2011.

[18] D. Chicharro and R. G. Andrzejak, "Reliable detection of directional couplings using rank statistics," *Phys. Rev. E*, vol. 80, p. 026217, Aug 2009.

[19] C. Schaefer, M. G. Rosenblum, H.-H. Abel, and J. Kurths, "Synchronization in the human cardiorespiratory system," *Phys. Rev. E*, vol. 60, pp. 857–870, Jul 1999. [Online]. Available: http://link.aps.org/doi/10.1103/PhysRevE.60.857

[20] F. Jurysta, J.-P. Lanquart, V. Sputaels, M. Dumont, P.-F. Migeotte, S. Leistedt, P. Linkowski, and P. van de Borne, "The impact of chronic primary insomnia on the heart rate EEG variability link," *Clinical Neurophysiology*, vol. 120, no. 6, pp. 1054 – 1060, 2009.

[21] V. Sakkalis, C. Giurcaneanu, P. Xanthopoulos, M. Zervakis, V. Tsiaras, Y. Yang, E. Karakonstantaki, and S. Micheloyannis, "Assessment of linear and nonlinear synchronization measures for analyzing EEG in a mild epileptic paradigm," *Information Technology in Biomedicine, IEEE Transactions on*, vol. 13, no. 4, pp. 433 –441, july 2009.

[22] M. Dumont, F. Jurysta, J.-P. Lanquart, A. Noseda, P. van de Borne, and P. Linkowski, "Scale-free dynamics of the synchronization between sleep EEG power bands and the high frequency component of heart rate variability in normal men and patients with sleep apnea hypopnea syndrome," *Clinical Neurophysiology*, vol. 118, no. 12, pp. 2752 – 2764, 2007.

Appendix E

Peer-reviewed conference paper

Title: Linear and Non-linear Interdependence of EEG and HRV Frequency Bands in Human Sleep

Authors: Ramiro Chaparro-Vargas, P. Chamila Dissanayaka, Chanakya Reddy Patti, Claudia Schilling, Michael Schredl and Dean Cvetkovic

Publication: Proceedings of the 36th Annual International Conference of the IEEE Engineering in Medicine and Biology Society

Year of Publication: 2014

Linear and Non-linear Interdependence of EEG and HRV Frequency Bands in Human Sleep

Ramiro Chaparro-Vargas*[1] *Member*, P. Chamila Dissanayaka*[2], Chanakya Reddy Patti*[3], Claudia Schilling†[4], Michael Schredl†[5], Dean Cvetkovic*[6] *Member*

***Abstract*— The characterisation of functional interdependencies of the autonomic nervous system (ANS) stands an ever-growing interest to unveil electroencephalographic (EEG) and Heart Rate Variability (HRV) interactions. This paper presents a biosignal processing approach as a supportive computational resource in the estimation of sleep dynamics. The application of linear, non-linear methods and statistical tests upon 10 overnight polysomnographic (PSG) recordings, allowed the computation of wavelet coherence and phase locking values, in order to identify discerning features amongst the clinical healthy subjects. Our findings showed that neuronal oscillations θ, α and σ interact with cardiac power bands at mid-to-high rank of coherence and phase locking, particularly during NREM sleep stages.**

I. INTRODUCTION

The bioelectrical activity of the neuronal cortex, accompanied by Heart Rate Variability (HRV) fluctuations, are two major actuators in the regulation of the sympathetic and vagal cardiac dynamics of the Autonomic Nervous System (ANS) [1]. Henceforth, the development of biosignal processing techniques over electroencephalographic (EEG) and electrocardiographic (ECG) recordings points to elucidate the characteristics of interdependencies across sleep stages. We also suggest a computational approach supported by time-frequency and phase-oriented methods to quantify the functional interactions between EEG and HRV power bands.

Until now, the research works about EEG↔HRV interdependence have made use of linear and non-linear procedures to identify unique features during resting, task-oriented or sleeping conditions [2]. The application of analyses based on the extraction of instantaneous amplitudes, frequencies and phases has demonstrated the sporadic appearance of coupled oscillations between high-regime HRV and low-regime EEG power bands; such as HRV-HF (0.15-0.4 Hz), δ (0.5-4 Hz), θ (4-8 Hz) and α (8-12 Hz), respectively [3] [1] [4]. However, those investigations have been mainly undertaken for either EEG↔EEG or cardiorespiratory cross-evaluations, within electrophysiological recordings of limited duration (less than 1 hour). Subsequent studies have promoted more sophisticated methods to estimate apart from the functional interaction, also directional interdependence, taking into account sleep stages progression [5] [6]. In this paper, the aim is to introduce linear and non-linear directed interdependencies along sleeping periods, which were observed through more extensive polysomnographic (PSG) recordings. Additional findings are pending to be clarified, regarding fast time-varying events, recurrent patterns and the corresponding interpretation of their physiological relevance.

In this paper, we propose a computational approach to perform linear, non-linear and statistical analyses over long-term PSG recordings, considering 15 EEG and 1 ECG channels. Relaying on recognised methods, e.g. Wavelet Coherence and *n*:*m* phase synchronisation; we attempt to characterise the functional interdependences of 10 healthy subjects along an overnight sleeping period. Our results suggest the presence of spectral and phase-related dependencies of neuronal and cardiac power bands with spatial divergences and constrained to sleep stages. Also, the sleep staging plays a major role in the differentiation of sympathetic and parasympathetic activity on each subject. In this sense, we encourage the adoption of biosignal processing as an assisting tool for a more precise interpretation of ANS activity during sleeping periods.

II. METHODS

The characterisation of functional interdependence between EEG ↔ HRV power bands is composed by three main stages: pre-processing, processing and statistical analysis. The pre-processing stage strives a preliminary deployment for the raw EEG/ECG signals, including epoch segmentation, inter-neural clustering and power band decomposition [7]. Afterwards, the processing stage performs the extraction of features, appealing to Time-Frequency Analysis (TFA) and phase synchronisation techniques. The last but not least, a statistical rank test pursues significant differences within the yielded features and the previously scored sleep stages, attending to the non-linearity, non-stationarity and non-Gaussianity attributes of the original sets of data. The complete computational analysis was developed with the software package MATLAB© 7.13 (The MathWorks Inc., USA).

A. Subjects and clinical data

The PSG recordings were obtained from 10 healthy subjects. Each subject undertook an overnight PSG recording at the Sleep Laboratory of the Central Institute of Mental Health

* Affiliated to with School of Electrical and Computing Engineering, RMIT University, Melbourne VIC 3001, Australia

† Affiliated to clinical research physician at the sleep laboratory of the Central Institute of Mental Health, Mannheim, Germany

[1] E-mail: ramiro.chaparro-vargas@rmit.edu.au

[2] E-mail: s3304790@student.rmit.edu.au

[3] E-mail: s3315014@student.rmit.edu.au

[4] E-mail: claudia.schilling@zi-mannheim.de

[5] E-mail: michael.schredl@zi-mannheim.de

[6] E-mail: dean.cvetkovic@rmit.edu.au

in Mannheim, Germany. In accordance to the Rechtschaffen and Kales (R&K) scoring manual, EEG signals are partitioned into 30-second epochs to categorise the overall sleep staging with Wake (W), Stage 1 (S1), Stage 2 (S2), Stage 3 (S3) and Stage 4 (S4) and Rapid Eye Movement (REM) sleep categories. The study was approved by the local ethic committee of the Medical Faculty Mannheim of the University of Heidelberg, Germany.

B. Pre-processing

Initially, the pre-processing routine performs a partition of consecutive 30-second epochs per PSG channel, intending to conserve power and time alignment properties. Next, inter-neural clustering associates EEG signals into a single composite, based on correlation coefficients and distribution divergence measures amongst nearby electrodes. For instance, C_{4z3} merges three different sources, whereas central (Cz), right- (C4) and left hemisphere (C3) locations of the scalp, plot statistically resemblant potentials in an inter-hemispheric context [6]. By averaging out the correlated EEG monopolar channels (bipolar electrodes are excluded for compatibility reasons), the clustering routine groups the inter-neural areas [8] as Table I depicts.

At the end, the power bands decomposition routine deconstructs the inter-neural clusters into 6 oscillatory bands, such as delta δ (0.5-4 Hz), theta θ (4-8 Hz), alpha α (8-12 Hz), sigma σ (12-16 Hz), beta β (16-32 Hz) and gamma γ (32-64 Hz). Similarly, HRV frequency bands LF (0.04-0.15 Hz) and HF (0.15-0.4 Hz) [9] [2] are computed from the ECG signal by using R-to-R interval (RRI) computation, an algorithm for sequential peak detection, smoothing by interpolation and a final upsampling step, just as the guidelines in [9] consign. Here, the introduction of Wavelet Packet Transform (WPT) allows a time-frequency decomposition supported on the coefficients shrinkage principle to generate the aforementioned EEG and HRV frequency bands [10].

C. Processing

The processing stage deals with the features extraction task, in an attempt to characterise the functional interdependences between neuronal and cardiac power activity amongst the decomposed frequency bands [5] [1]. Previously, linear measures have demonstrated their suitability to estimate synchronisation tendencies, in this case, we employed coherence supported by the continuous wavelet transform (CWT) for its computation [8]. Wavelet coherence computes the auto- and cross-power spectrum $\mathbf{S}(\cdot)$ to produce an unitary value, matching time translation and frequency scale domains.

TABLE I
INTER-NEURAL CLUSTERS

Parcel	Electrodes	Abbreviation
1	C_3A_2, C_zA_1, C_4A_1	C_{4z3}
2	O_2A_1, O_1A_2	O_{21}
3	F_8A_1, F_7A_2	F_{87}
4	F_4A_1, F_3A_2	F_{43}
5	P_4P_3, P_4P_z, P_3P_z	P_{43}
6	T_3T_5, T_4T_6	T_{43}

$$\kappa_{\mathbf{xy}}{}^2(\omega_0) = \frac{|\mathbf{S}\left(\mathbf{W_{xx}}{}^{\mathrm{H}}(s,\tau)\mathbf{W_{yy}}(s,\tau)\right)|^2}{|\mathbf{S}\left(\mathbf{W_{xx}}(s,\tau)\right)||\mathbf{S}\left(\mathbf{W_{yy}}(s,\tau)\right)|} \tag{1}$$

where $\mathbf{W}(s,\tau)$ denotes the continuous wavelet transform at scale s and translation index τ.

For the present paper, we designate n:m phase synchronisation as the preferred approach for non-linear estimation. More precisely, the non-linear interdependence is quantified by the Phase Locking Value $\zeta_{n,m}$ [3], which casts a locking unitary value of n cycles from one oscillation to m cycles of the other. The n,m values are chosen based on the central frequencies relations for each pair of power bands. This method engages a couple of convolutions between the EEG or HRV filtered signal and the complex-valued Gabor wavelet [6]. Then, the differences of instantaneous phases $\hat{\varphi}_{n,m}[k]$ are computed at each time instant, which in turn, are mapped to a cyclic $[0, 2\pi m)$ interval. And, the strength of the interdependence is quantified by the magnitude of the phases differences expectation $E\{\cdot\}$; such a measure is known as PLV, as Eq. 2 denotes.

$$\zeta_{n,m} = \sqrt{(E\{\cos\hat{\varphi}_{n,m}[k]\})^2 + (E\{\sin\hat{\varphi}_{n,m}[k]\})^2} \tag{2}$$

To finalise, a normalisation routine is applied to fit the generated features into $0-1$ interval, to improve the results interpretation of further statistical analyses.

D. Statistical analysis

By dealing with biological signals, an evaluation of Gaussianity conditions is required, in order to conduct an appropriate statistical analysis beneath the clinical cohort. The Bartlett test assessed an analytical divergence of the mean and covariance of the modelled data versus the Gaussian distribution. Those preliminary inspections proved a strong deviation from the Gaussian tendency, suggesting the application of a series of Kruskal-Wallis rank tests [11]. Such an omnibus test lacks of the ability to differentiate the inter-neural cluster casting the significant difference, but its corresponding coupling/decoupling activity intends to elicit interactions with significant values $p < 0.05$ amongst bands and sleep stages.

III. RESULTS

The linear analysis represented by the wavelet coherence, arranged one sleep cycle into a multi-stage periodogram, which included EEG/HRV power bands and averaged out clinical group. Out of the macro-periodogram in Fig. 1, the coherence between low-regime EEG bands, such as $\delta,\theta \leftrightarrow$ LF, HF was turning stronger $(0.4-0.5)$ over W and REM stages. Inasmuch as, we moved to θ, σ and β oscillations in relation to HF, it was observed an increasing activity $(0.5-0.7)$ in deep sleep stages, S3 and S4. Opposite to this, EEG $\leftrightarrow$ LF relationship hardly exceeded $0.4-0.45$ coherence levels. One of the most interesting matters was the

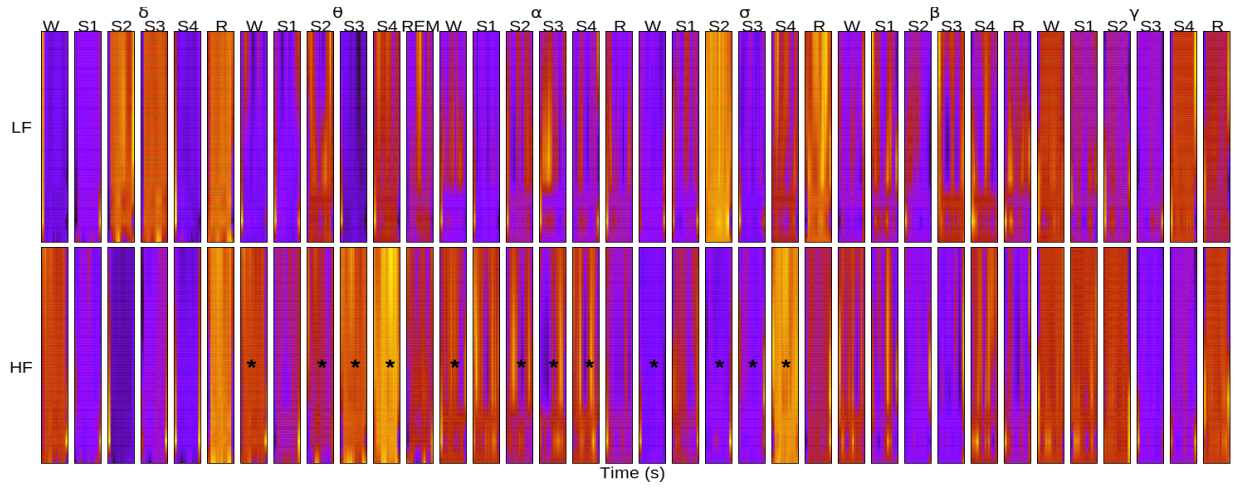

Fig. 1. Macro-periodogram of Wavelet Coherence considering EEG δ, θ, α, σ, β and γ at C_{4z3} parcel against HRV LF and HF bands for sleep stages W, S1, S2, S3, S4 and REM. On the x-axis, each periodogram's cell portrays averaged out 30-seconds epochs corresponding to a particular sleep stage over the 10 subjects, and 12 wavelet-scaled pseudo-frequencies are ordered on the y-axis starting on *ca.* 89.8 Hz till (top scale) 0.04 Hz (bottom scale). The colour scale assigns the black-violet spectrum for low coherence values, whilst red-yellow intensities represent the surrounding unitary values, i.e. high coherence. * statistically significant ($p < 0.05$) after Kruskal-Wallis rank test.

uniform coherence between $\theta \leftrightarrow$ HF bands along the 6 sleep stages, which slowly faded out to mid-level coherence (0.5) from σ band region. In respect to the remaining inter-neural clusters, which are not shown here; it was corroborated the bright activity $(0.6-0.75)$ of EEG low-regime bands $\delta/\theta \leftrightarrow$ LF/HF, moving towards dissipating levels at α to γ frequencies.

In correspondence to the non-linear analysis, *n*:*m* phase synchronisation realised polar diagrams to illustrate the cross-frequency locking values at each sleep stage. The functional interdependence in EEG $\leftrightarrow$ HF power bands maintained a regular mid-value $(0.3-0.4)$ for W, S1 and REM stages. Focusing on low-regime bands δ and θ, the S4 reached its highest value around 0.6. As far as we moved to α band, S3 took the lead, and finally S2 consolidated the strongest phase interaction within σ and β bands. Due to the lack of statistically significant results and space limitations, the polar diagrams for this case are not displayed. On the contrary, EEG $\leftrightarrow$ LF interactions in Fig. 2 showed that S4 and REM stages surpassed 0.6 locking level at both extremes of the neuronal spectrum, i.e. δ and β power bands. Similarly, S1 stage registered a noticeable deviation (0.7), when σ oscillation was concerned. For the remaining power bands and sleep stages, the synchronisation strength preserved homogeneous values around 0.4. None radical difference was found in the polar diagrams of the alternative inter-neural clusters.

Lastly, a series of omnibus Kruskal-Wallis rank tests were addressed in order to identify significant differences, attending to all interactions of EEG $\leftrightarrow$ HRV power bands, sleep stages and electrode clusters. Wavelet coherence (WCOH) method elicited a larger number of significant values including W, light (S2) and deep sleep (S3, S4) stages between θ, α, $\sigma \leftrightarrow$ HF frequency pairs with $(\chi^2 = 11.76, p = 0.038)$ and $(\chi^2 = 13.11, p = 0.022)$ test values. Nonetheless, no significant results turned to be sufficiently divergent between neuronal EEG bands and HRV-LF by the time of wavelet coherence evaluation. In contrast, PLV did reveal relevant differences between θ $(\chi^2 = 11.76, p = 0.038)$, α $(\chi^2 = 13.11, p = 0.022)$, σ $(\chi^2 = 11.76, p = 0.038)$ and HRV-LF cross-frequencies, located at S2 and REM stages. Figures 1 and 2 labelled the statistically significant values (using *) according to these criteria.

IV. DISCUSSION AND CONCLUSIONS

The predominant activity of LF cardiac band during W/REM stages, as well as, HF along NREM periods have been claimed by previous works [12]. Our findings not only reaffirmed that statement, but also evidenced the coherence related to the low-regime EEG frequency bands, i.e. W and REM stages kept a coherent interdependence with sympathetic system (HRV LF). Beside this, a progressive retreat of cross-frequency interaction was detected during NREM stages, which is explained by a vagal cardiac system emergence or HF power band ascendancy. A novel issue of this work suggested the strong interdependence of δ and θ oscillations, in contrast to the weak interactions of the high-regime power bands, such as β and γ. Consequently, we sustain that the functional interdependencies of sympathetic and parasympathetic are vaguely related to high neuronal oscillations within healthy population.

Wavelet coherence and PLV coincided on the interdependence of the sympathetic system (HRV LF) across W and REM stages. Furthermore, it was demonstrated from a non-linear approach, the intrinsic phase-coupled activity of parasympathetic system (HRV HF) during NREM episodes. Although, *n*:*m* phase synchronisation is strictly constrained to the choice of non-arbitrary pairs of central frequencies, whereas it can only exist a rational quotient in between. In this manner, we can assure that n, m integers are invariant

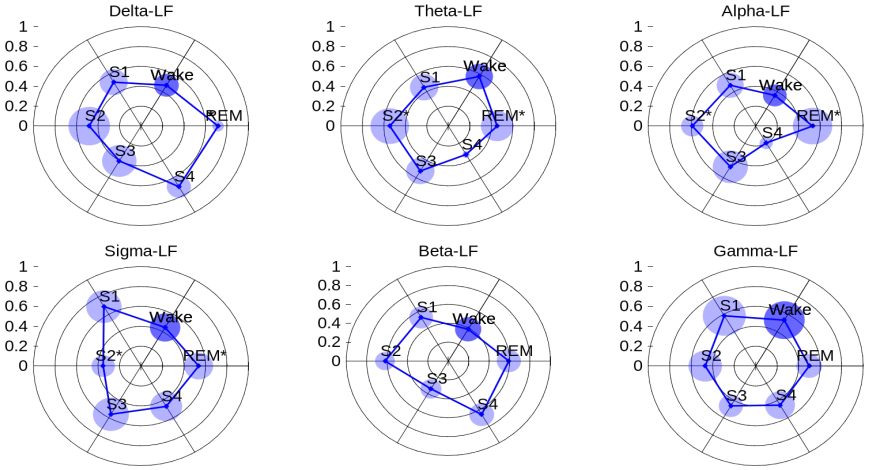

Fig. 2. Polar diagram of *n*:*m* Phase Synchronisation for clinical cohort. Phase Locking Value between C_{4z3}-δ, θ, α, σ, β and γ versus HRV LF band. The coloured point represent the absolute mean PLV between 0-to-1 scale at each sleep stage, accompanied by a centred circle expressing the standard deviation amongst the group members. * statistically significant ($p < 0.05$) after Kruskal-Wallis rank test.

to multiples of phase slips [13]. Even though this condition holds, larger n, m integer values could produce unstable and less robust synchronisations, e.g. spurious couplings, due to the implicit commutative variance.

From the results of Kruskal-Wallis rank tests, we could statistically confirm most of the conclusions here previously suggested. First, wavelet coherence method highlighted the statistically importance of interactions at θ, α and σ power bands, but only related to the vagal cardiac (parasympathetic) activity during NREM sleep stages (W, S2, S3, S4). However, PLV became a suitable complement to describe neuronal and sympathetic activity, which involved the same power bands, but limited to S2 and REM stages. Such findings concurred with previous studies [14] [12] with the novel corroboration of associated linear and non-linear approaches. Although, further data analyses should be conducted, in order to discard eventual overestimations misleading these findings. Until now, we can hypothesise that TFA-based methods are more reliable to discriminate functional interdependencies within parasympathetic system. Foremost, PLV estimated in a more accurate way the strong interaction of θ, α and σ bands to differentiate the sympathetic counterpart.

The obtained results indicate the existence of significant differences between EEG and HRV power bands, in terms of time-frequency coherence and phase synchronisation across overnight sleep cycles. Moreover, the influence between mid-range EEG bands and parasympathetic activity during light and deep sleep stages was enhanced by the tracking of functional interdependencies during W stage. It is advised, the conduction of additional studies to determine with more detail the impact of non-linear approaches, e.g. surrogate data analysis. In consonance, TFA-oriented approaches for the differentiation of sleep physiopathologies, should be more extensively explored.

REFERENCES

[1] M. Dumont, F. Jurysta, J.-P. Lanquart, P.-F. Migeotte, P. van de Borne, and P. Linkowski, "Interdependency between heart rate variability and sleep EEG: linear/non-linear?" *Clinical Neurophysiology*, vol. 115, no. 9, pp. 2031 – 2040, 2004.

[2] U. R. Acharya, K. P. Joseph, N. Kannathal, C. M. Lim, and J. S. Suri, "Heart rate variability: A review." *Medical & Biological Engineering & Computing*, vol. 44, no. 12, pp. 1031 – 1051, 2006.

[3] J. Palva, S. Palva, and K. Kaila, "Phase synchrony among neuronal oscillations in the human cortex," *Journal of Neuroscience*, vol. 25, no. 15, pp. 3962–3972, April 2005.

[4] R. Bartsch, J. W. Kantelhardt, T. Penzel, and S. Havlin, "Experimental evidence for phase synchronization transitions in the human cardiorespiratory system," *Phys. Rev. Lett.*, vol. 98, p. 054102, Feb 2007.

[5] S. Dimitriadis, N. Laskaris, Y. Del Rio-Portilla, and G. Koudounis, "Characterizing dynamic functional connectivity across sleep stages from EEG," *Brain Topography*, vol. 22, no. 2, pp. 119–133, 2009, cited By (since 1996) 13.

[6] K. Mezeiova and M. Palus, "Comparison of coherence and phase synchronization of the human sleep electroencephalogram," *Clinical Neurophysiology*, vol. 123, no. 9, pp. 1821 – 1830, 2012.

[7] S. Palva, S. Monto, and J. M. Palva, "Graph properties of synchronized cortical networks during visual working memory maintenance," *NeuroImage*, vol. 49, no. 4, pp. 3257 – 3268, 2010.

[8] E. Pereda, R. Q. Quiroga, and J. Bhattacharya, "Nonlinear multivariate analysis of neurophysiological signals," *Progress in Neurobiology*, vol. 77, no. 12, pp. 1 – 37, 2005.

[9] T. F. of The European Society of Cardiology, T. N. A. S. of Pacing, and Electrophysiology, "Heart rate variability," *European Heart Journal*, vol. 17, pp. 354–381, 1996.

[10] S. Mallat, *A Wavelet Tour of Signal Processing*. Elsevier Academic Press, 1999.

[11] D. Chicharro and R. G. Andrzejak, "Reliable detection of directional couplings using rank statistics," *Phys. Rev. E*, vol. 80, p. 026217, Aug 2009.

[12] F. Jurysta, J.-P. Lanquart, V. Sputaels, M. Dumont, P.-F. Migeotte, S. Leistedt, P. Linkowski, and P. van de Borne, "The impact of chronic primary insomnia on the heart rate EEG variability link," *Clinical Neurophysiology*, vol. 120, no. 6, pp. 1054 – 1060, 2009.

[13] M. Wacker and H. Witte, "On the stability of the n:m phase synchronization index," *Biomedical Engineering, IEEE Transactions on*, vol. 58, no. 2, pp. 332–338, 2011.

[14] M. Dumont, F. Jurysta, J.-P. Lanquart, A. Noseda, P. van de Borne, and P. Linkowski, "Scale-free dynamics of the synchronization between sleep EEG power bands and the high frequency component of heart rate variability in normal men and patients with sleep apnea hypopnea syndrome," *Clinical Neurophysiology*, vol. 118, no. 12, pp. 2752 – 2764, 2007.

Appendix F

Peer-reviewed Journal Paper

Title: Sleep Electroencephalography and Heart Rate Variability Interdependence amongst Healthy Subjects and Insomnia/Schizophrenia Patients

Authors: Ramiro Chaparro-Vargas, Claudia Schilling, Michael Schredl and Dean Cvetkovic

Publication: Medical & Biological Sciences & Computing Journal

Year of Publication: 2015

Med Biol Eng Comput
DOI 10.1007/s11517-015-1297-4

ORIGINAL ARTICLE

Sleep electroencephalography and heart rate variability interdependence amongst healthy subjects and insomnia/ schizophrenia patients

Ramiro Chaparro-Vargas[1] · Claudia Schilling[2] · Michael Schredl[2] · Dean Cvetkovic[1]

Received: 12 April 2014 / Accepted: 3 April 2015

Abstract The quantification of interdependencies within autonomic nervous system has gained increasing importance to characterise healthy and psychiatric disordered subjects. The present work introduces a biosignal processing approach, suggesting a computational resource to estimate coherent or synchronised interactions as an eventual supportive aid in the diagnosis of primary insomnia and schizophrenia pathologies. By deploying linear, nonlinear and statistical methods upon 25 electroencephalographic and electrocardiographic overnight sleep recordings, the assessment of cross-correlation, wavelet coherence and **n**:**m** phase synchronisation is focused on tracking discerning features amongst the clinical cohorts. Our results indicate that certain neuronal oscillations interact with cardiac power bands in distinctive ways responding to standardised sleep stages and patient groups, which promotes the hypothesis of subtle functional dynamics between neuronal assembles and (para)sympathetic activity subject to pathophysiological conditions.

Keywords EEG · HRV · Phase locking value · Phase synchronisation · Primary insomnia · Schizophrenia · Wavelet coherence

1 Introduction

In neuroscience, a matter of escalated interest is the leverage of functional interdependence within the autonomic nervous system (ANS), represented by neuronal and cardiac compounds [29]. There are underlying mechanisms that convey the dynamic interaction of the brain and the heart [7, 26], within spatially distributed regions. Starting at the cerebral domain, the medulla oblongata at the lower brainstem interconnects with disseminated regulation centres to encompass involuntary nervous functions, such as breathing, digestion, gastrointestinal movement, heart rate, amongst others [17]. Precisely, the firing synchronisation of brainstem and cortical neurons into oscillatory assemblies, accompanied by the fluctuations derived from the heart rate variability (HRV) bear a tight association to sympathetic and vagal cardiac activities [8]. The introduction of biosignal processing upon electroencephalographic (EEG) and electrocardiographic (ECG) channels attempts to elucidate the nature of functional interactions; not only amongst healthy groups, but also regarding sleep disordered populations. Cognitive and behavioural symptoms are the manifestation of fully coordinated or dysfunctional neuronal processes [39], which are reflected by cardiac conditions [9], as well. Henceforth, we suggest a computational approach supported by time-, frequency- and phase-oriented techniques to quantitatively characterise the functional interdependence existing between EEG and HRV power bands, in order to differentiate recruited clinical cohorts attending to the strength of their coherent or coupled dynamics [4, 16].

✉ Ramiro Chaparro-Vargas
s3361953@student.rmit.edu.au

Claudia Schilling
claudia.schilling@zi-mannheim.de

Michael Schredl
michael.schredl@zi-mannheim.de

Dean Cvetkovic
dean.cvetkovic@rmit.edu.au

[1] School of Electrical and Computing Engineering, RMIT University, Melbourne, VIC 3121, Australia

[2] Sleep laboratory of the Central Institute of Mental Health, Mannheim, Germany

Published online: 19 April 2015

In the recent years, the examination of EEG-to-EEG and EEG-to-HRV interdependency [1] has undertaken linear and nonlinear approaches [29] to elicit singularities during resting, task-induced, sleeping, controlled- or psychiatrically disordered contexts. The procurement of spectral analysis against phase-based proceedings has proved the existence of synchronised attractors [3, 8, 15, 26] into high-regime HRV and low-regime EEG power bands; i.e. HRV–HF (0.15–0.4 Hz), δ (0.5–4 Hz), θ (4–8 Hz) and α (8–12 Hz), correspondingly. Nevertheless, those studies are restrained to neuronal cross-spectrum or cardiorespiratory processes exclusively applied to short-term electrophysiological recordings within healthy population. Further research works foster more incisive methodologies to characterise apart from functional connectivity, also directional interdependence across standardised sleep stages [7, 21]. The incorporation of extended polysomnographic (PSG) recordings eased the observation of driving signals amongst far, near-distant and sleep staging couplings, vindicating linear versus nonlinear counterweight as comparative benchmarking. However, the exclusion of a pathophysiological context, i.e. psychiatrically affected subjects, circumscribes the results to a limited perspective, concerning the nervous and cardiac autonomic systems. Such limitations are diligently attended by ensuing investigations considering psychiatric-related syndromes; e.g. epilepsy [32], insomnia [22, 34] and schizophrenia [4, 24]. There is a evidence that persistent disturbances in the initiation and maintenance of sleep lead to emotional disruptions, psychosis and paranoia symptoms [10]. Furthermore, clinical trials [6, 30] have linked common signs of insomnia, e.g. increased sleep latency and decreased total sleep efficiency, with schizophrenia as comorbid conditions of this disorder. The recurrent findings reaffirm the changes in interdependent relationships due to functional abnormalities at particular cortical areas [32] and oscillatory frequency bands, specifically β (16–32 Hz) and γ (32–64 Hz) in respect to schizophrenic charts [25, 36]. Likewise, primary insomnia and insomnia [14, 33, 37] studies have drawn forth variations in linear, nonlinear and statistical interactions; albeit only a few studies have traced the influence of neuronal and cardiac cross-computations during sleeping periods [16]. Even though, it remains elusive, a performant differentiation of healthy and comorbid pathophysiologies, i.e. primary insomnia and schizophrenia, as the product of an analytical biosignal processing.

The mutual influence of cardiac control centre and the brainstem, both as part of the ANS, is reflected by power oscillations derived from R-to-R intervals and neuronal discharges. In this paper, we hypothesised that the interdependency of cerebral and ANS subsystems (i.e. sympathetic and parasympathetic) compromises quantifiable levels of coherence and synchronisation across the sleep regulation process. Apart from the hypothesis, our paper explores differences and commonalities amongst healthy, insomnia and schizophrenia sleep architecture and neuronal-cardiac interdependency.

Our objective addresses to propose a computational approach to perform linear, nonlinear and statistical analysis upon long-term polysomnograms (PSG), including up to 15 EEG and 1 ECG channels. Based on recognised techniques such as cross-correlation function (CCF), wavelet coherence and *n*:*m* phase synchronisation with phase locking value gauge; the characterisation of neuronal-cardiac activity for ten healthy subjects, eight primary insomnia and ten schizophrenia patients into statistically distinctive groups was the uttermost objective.

The overnight sleep PSG recordings offered a sufficient data length throughout sleep stages that are directly associated with the derived power bands, which in turn maintain a near pertinence with the studied diseases. The results suggested the existence of linear, as well as, nonlinear reciprocal dependencies of neuronal power bands and cardiac frequencies at different levels, depending on the clinical condition of the studied subjects. Besides this, the sleep staging plays a crucial role in the distinction of sympathetic and parasympathetic activities on each individual. On this way, we attempt to promote the integration of computational systems as supportive tools for the diagnosis of psychiatric disorders empowered by more efficient time to diagnosis windows and moderate misinterpreted assessments.

2 Methods

The search of synchronisation evidence between EEG $\leftrightarrow$ HRV oscillation bands consists of three core stages: pre-processing, processing and statistical analysis. The former provides a preparatory framework for the raw EEG/ECG signals, which includes epoch-oriented segmentation, neural parcellation and band decomposition [27]. Thereafter, the feature extraction is performed recurring to time- and frequency-based techniques, as well as, time–frequency (TFA) and nonlinear analysis. Lastly, a statistical rank test is conducted in order to explore significant differences within the derived features, considering the nonlinear, non-stationary and non-Gaussian-distributed character of data. The entire computational analysis was developed with software package MATLAB© 7.13 (The MathWorks Inc., USA).

2.1 Subjects and clinical data

In this paper, the employed clinical data summoned 28 subjects allocated into three different cohorts: 10 healthy

or control (CTL), 8 primary insomnia (INS) and 10 schizophrenia (SCZ). All participants spent two consecutive nights in the Sleep Laboratory of the Central Institute of Mental Health in Mannheim, Germany. The first night served as an adaptation night and was also used to rule out sleep apnoea or periodic leg movements by measuring nasal and oral airflow, chest and abdomen movements, blood oxygen saturation and anterior tibialis electromyogram in both legs. The second night was the baseline night providing sleep parameters of undisturbed sleep that were included into the present analysis. The profile of clinical subjects arranging demographic information and recording technical details is summarised in Table 1.

The study was approved by the local ethic committee of the Medical Faculty Mannheim of the University of Heidelberg (AZ 2010-208N-MA and 2007-250N-MA). All participants were informed about the aims and procedures of the study and gave their written consent prior to the investigation. Patients diagnosed with schizophrenia according to the Diagnostic and Statistical Manual (DSM) IV R were recruited during in-house treatment in the Central Institute of Mental Health; if they fulfilled the following inclusion criteria: age between 18 and 60 years, ability to provide informed consent, stabilised disease course and stable (for at least 2 weeks) psychopharmacological treatment in the form of monotherapy with a second generation antipsychotic, as well as absence of psychiatric comorbidity. Antipsychotic medication in the patient group consisted of risperidone, aripiprazole, amisulpride, quetiapine, olanzapine and clozapine. The insomnia patients were matched from a patient sample undergoing diagnostic procedures in the sleep laboratory. Their diagnoses were based on clinical anamnesis and polysomnographic findings according to the ICSD-2 (International Classification of Sleep Disorders, 2nd edition).

Polysomnography was performed from 11 p.m. to 6:30 a.m. with a Schwarzer Comlab 32 (Schwarzer GmbH, Munich) polysomnograph using a standard polysomnography montage according to the criteria of the American Academy of Sleep Medicine [13]. This included electroencephalography in seven derivations (F4/A1, C4/A1, O2/A1, Cz/A1, F3/A2, C3/A2 and O1/A2), left and right electrooculography (EOG), chin electromyography (EMG), surface EMG of both tibialis anterior muscles and recording of ECG and respiratory variables (oro-nasal airflow, thoracal and abdominal respiratory effort, and oxygen saturation). The EEG sampling rate was 250 samples per second. Sleep stage scoring, counting of arousals and periodic limb movements of sleep (PLMS) were performed visually, according to the standard procedures [13]. Each EEG channel was segmented into 30-s epochs to assess a chronological sleep staging including wakefulness, light (S1 and S2), deep (S3 and S4) and rapid eye movement (REM) sleep.

Next, a more detailed description about the proposed computational approach is introduced attending to the three core stages of analysis.

2.2 Pre-processing

In correspondence to the specialised scoring, the initial pre-processing routine attains a segmentation into consecutive 30-s epochs on each PSG channel, whilst properties of power and time alignment are preserved. The neural parcellation is referred as the next routine, which manages to aggregate EEG signals into a single source based on correlation coefficients or distribution divergence measures amongst adjacent electrodes, e.g. Kullback–Leibler divergence. For instance, C_{4z3} gathers three different sources, since it is foreseen that central electrodes located at the centre (Cz), right-(C4) and left hemisphere (C3) of the scalp report resemblant potentials in an interhemispheric neural context [21]. Such an interareal association obeys to dimensionality reduction and computational optimisation, given that the excessive number of EEG channels leads to asymptotic processing burden, resource consumption and dilated computation times [28]. Then, let define $\mathbf{x}^p[k] \in \mathbb{C}^{M\times N}$ as an M-dimensional vector gathering EEG signals with N samples indexed by k and p neural areas. By computing the expectation $E\{\cdot\}$ of two to three correlated EEG monopolar channels, parcellation routine assembles a single output $\mu_{\mathbf{x}^p}$ for each neural area p [23, 29]. Equations (1) and (2) formulate the corresponding expressions for the resulting expectation value and aggregated channels into p neural areas.

$$\begin{aligned} \mu_{\mathbf{x}^p} &= E\{\mathbf{x}^p[k]\} = \frac{1}{M}\sum_{i=1}^{M}\mathbf{x}_i^p[k] \\ p &= \{C_{4z3}, F_{87}, O_{21}, F_{43}\} \end{aligned} \tag{1}$$

where

$$\begin{aligned} \mathbf{x}^p[k]\big|_{p=C_{4z3}} &= \left[\mathbf{x}_{C4}[k]\,\mathbf{x}_{Cz}[k]\,\mathbf{x}_{C3}[k]\right] \\ \mathbf{x}^p[k]\big|_{p=F_{87}} &= \left[\mathbf{x}_{F8}[k]\,\mathbf{x}_{F7}[k]\right] \\ \mathbf{x}^p[k]\big|_{p=O_{21}} &= \left[\mathbf{x}_{O2}[k]\,\mathbf{x}_{O1}[k]\right] \\ \mathbf{x}^p[k]\big|_{p=F_{43}} &= \left[\mathbf{x}_{F4}[k]\,\mathbf{x}_{F3}[k]\right] \end{aligned} \tag{2}$$

The final pre-processing routine deconstructs the EEG aggregated sources $\mathbf{x}^p[k]$ in the well-known neuronal frequency bands: δ (0.5–4 Hz), θ (4–8 Hz), α (8–12 Hz), ς (12–16 Hz), β (16–32 Hz) and γ (32–64 Hz). Likewise, HRV frequency bands, i.e. LF (0.04–0.15 Hz) and HF (0.15–0.4 Hz) [1, 35] are extracted from the ECG channel by means of R-to-R interval (RRI) computation, following a peak detection algorithm, interpolated smoothing and upsampling process according to the recommendations in [35]. Hereafter,

Table 1 Information of clinical subjects and technical details of PSG recordings

Variable	Healthy (CTL)										Mean ± SD
Subject ID	CTL1	CTL2	CTL3	CTL4	CTL5	CTL6	CTL7	CTL8	CTL9	CTL10	
Gender	m	m	m	m	m	f	f	f	f	f	n.a.
Age (years)	25	46	20	26	27	26	46	47	21	26	31.5 ± 11.3
Sleep onset latency (min)	10.5	15	14	20.5	5	65.5	14	2	30	41.5	21.8 ± 19.25
REM latency (min)	76.5	70.5	111.5	180.5	115	129	77	25.5	138	111	103.45 ± 42.98
Percentage wake (%)	46.86	22.1	3.5	5.97	2.36	4.5	13.3	11.47	12.15	13.42	13.56 ± 13.14
Percentage S1 (%)	9.81	10.72	9.4	11.24	3.26	9.13	20.30	6.52	4.45	9.31	9.41 ± 4.65
Percentage S2 (%)	29.99	50	47.65	67.45	49.04	42.2	48.31	51.97	39.23	53.81	47.96 ± 9.82
Percentage S3/S4 (%)	6.73	0.11	21.86	4.8	29.58	31.22	3.38	11.36	27.68	10.16	14.69 ± 11.78
Percentage REM (%)	6.61	17.07	17.6	10.54	15.75	12.96	14.7	18.67	16.49	13.3	14.37 ± 3.66
Monopolar channels[a]	$C_3A_2, C_4A_1, O_2A_1, O_1A_2, C_zA_1, F_8A_1, F_7A_2, F_4A_1(EOG), F_3A_2(EOG)$										
Bipolar channels[a]	$P_4P_3, P_4P_z, P_3P_z(allchinEMG), T_3T_5, T_4T_6(tibialisEMG), ECG$										
Variable	Primary insomnia (INS)										Mean ± SD
Subject ID	INS1	INS2	INS3	INS4	INS5	INS6	INS7	INS8	INS9		
Gender	m	m	m	m	f	f	f	f	f		n.a.
Age (years)	45	20	35	26	40	44	30	18	24	–	31.3 ± 10.1
Sleep onset latency (min)	9	49.5	5	37	7.5	18	17.5	14	15.5	–	19.22 ± 14.67
REM latency (min)	72.5	208	79	265.5	72.5	84	78.5	118	107.5	–	120.61 ± 69.18
Percentage wake (%)	3.32	12.41	23.9	7.66	7.55	8.43	9.74	6.42	7.11	–	9.62 ± 5.89
Percentage S1 (%)	12.74	5.82	15.4	6.88	14.07	11.2	5.09	11.21	16.6	–	11 ± 4.21
Percentage S2 (%)	57.03	42.15	48.92	56.49	57.67	39.61	37.34	48.53	42.29	–	47.78 ± 7.90
Percentage S3/S4 (%)	16.61	31.65	9.4	16.75	4.46	32.45	36.8	26.01	16.8	–	21.21 ± 11.08
Percentage REM (%)	10.3	7.97	2.38	12.21	16.25	8.31	11.04	7.83	17.19	–	10.39 ± 4.54
Monopolar channels[a]	$C_3A_2, C_4A_1, O_2A_1, O_1A_2, C_zA_1, F_8A_1, F_7A_2, F_4A_1(EOG), F_3A_2(EOG)$										
Bipolar channels[a]	$P_4P_3, P_4P_z, P_3P_z(allchinEMG), T_3T_5, T_4T_6(tibialisEMG), ECG$										
Variable	Schizophrenia (SCZ)										Mean ± SD
Subject ID	SCZ1	SCZ2	SCZ3	SCZ4	SCZ5	SCZ6	SCZ7	SCZ8	SCZ9	SCZ10	
Gender	m	m	m	m	m	f	f	f	f	f	n.a.
Age (years)	26	47	22	31	28	28	46	26	19	44	31.7 ± 10.2
Sleep onset latency (min)	4	32	11.5	61.5	74	14	21.5	26	31.5	31.5	30.75 ± 21.84
REM latency (min)	84	97.5	30	142	342.5	101	99	104.5	253	117.5	137.1 ± 91.72
Percentage wake (%)	0.99	8.28	0.79	5.67	7.42	2.47	9.54	0.66	2.31	0.11	3.82 ± 3.56
Percentage S1 (%)	3.2	28.3	7.58	6.17	11.76	5.29	9.06	2.42	7.54	0.64	8.2 ± 7.79
Percentage S2 (%)	41.99	45.3	53.28	39.46	46.04	57.03	48.51	49.5	45.86	58.2	48.52 ± 6.13
Percentage S3/S4 (%)	30.94	0.22	27.60	23.8	13.04	11.02	23.24	23.98	31.63	21.44	20.69 ± 9.84
Percentage REM (%)	22.87	17.90	10.75	24.91	21.74	24.18	9.65	23.43	12.65	19.61	18.77 ± 5.78
Monopolar channels[a]	$C_3A_2, C_4A_1, O_2A_1, O_1A_2, C_zA_1, F_8A_1, F_7A_2, F_4A_1(EOG), F_3A_2(EOG)$										
Bipolar channels[a]	$P_4P_3, P_4P_z, P_3P_z(allchinEMG), T_3T_5, T_4T_6(tibialisEMG), ECG$										

SD standard deviation, *m* masculine, *f* feminine, *n.a.* no applicable

[a] Electrodes arrangement compliant with 10–20 international system

wavelet packet transform (WPT) engages a time–frequency decomposition supported on the principle of coefficients shrinkage, where additional benefits are inherited, such as noise filtering, energy conservation and selective removal of unwanted components [18]. The iterative convolutional operations between low-pass $\mathbf{h}^b[m]$, high-pass $\mathbf{g}^b[m]$ filter coefficients and aggregated signals at $j = \{1, \ldots, Z\}$ levels with Daubechies-4 (db4) as mother wavelet with Z as maximum decomposition level yield the differentiated EEG frequency bands b, as (3) and (4) explain.

$$\mathbf{x}_{j+1}^{b,LP}[k] = \sum_{m=1}^{N} \mathbf{h}^{b}[m-2k]\mathbf{x}_{j}^{b,LP}[m]; \quad b = \{\delta, \ldots, \gamma\} \tag{3}$$

$$\mathbf{x}_{j+1}^{b,HP}[k] = \sum_{m=1}^{N} \mathbf{g}^{b}[m-2k]\mathbf{x}_{j}^{b,HP}[m] \tag{4}$$

Respectively, HRV frequency bands $\mathbf{y}^{\mathbf{HF}}[k], \mathbf{y}^{\mathbf{LF}}[k]$ are originated from a comparable decomposition by summing up low-pass and high-pass filter coefficients, due to narrow-band regime of cardiac spectrum. Thus, (5) outlines the equivalent derivation.

$$\begin{aligned}\mathbf{y}^{b'}[k] &= \mathbf{y}_{j+1}^{b'}[k] + \mathbf{y}_{l+1}^{b'}[k];\ b' = \{\mathbf{LF}, \mathbf{HF}\} \\ &= \sum_{m=1}^{N} \mathbf{h}^{b'}[m-2k]\mathbf{x}_{j}^{b'}[m] + \cdots;\ j = \{1, \ldots, Z\} \\ &\quad \sum_{m=1}^{N} \mathbf{g}^{b'}[m-2k]\mathbf{x}_{l}^{b'}[m];\ l = \{1, \ldots, Z'\}\end{aligned} \tag{5}$$

2.3 Processing

The processing stage focuses on features extraction for the estimation of functional interdependence—a.k.a. synchronisation—between neuronal and cardiac oscillations, represented by the estimated frequency bands [7, 8]. For this purpose, linear and nonlinear methods are implemented as part of the computational approach for biosignals analysis. Hitherto, linear approaches have proved their reliability in the estimation of synchronisation cues between EEG $\leftrightarrow$ HRV oscillations, being the most common techniques cross-correlation function (CCF) in (6) and coherence [29], specifically, we adopted wavelet coherence in the form that (7) states. In turn, CCF measures the linear correlation in function of time lags that reflects a presumably mutual relationship between the signals, and whose maximised unit value is normally assumed as the delay of the paired sources. In that way, the expectation between the EEG oscillator represented by $\mathbf{x}[k+\tau]$ and the HRV power band $\mathbf{y}[k]$ produces a series of 0-to-1 time-lagged correlation values $\mathbf{R}_{\mathbf{xy}}(\tau)$.

$$\begin{aligned}\mathbf{R}_{\mathbf{xy}}(\tau) &= E\{\mathbf{x}[k+\tau]\mathbf{y}^{\mathrm{H}}[k]\} \\ &= \frac{1}{N-|\tau|}\sum_{k=1}^{N-\tau}\mathbf{x}[k+\tau]\mathbf{y}^{\mathrm{H}}[k]\end{aligned} \tag{6}$$

Wavelet coherence determines auto- $\mathbf{S}_{\mathbf{xx|yy}}(\omega_0)$ and cross- $\mathbf{S}_{\mathbf{xy}}(\omega_0)$ power spectrum between an EEG oscillator $\mathbf{x}$ and one HRV power band $\mathbf{y}$ to yield a 0-to-1 value $\kappa_{\mathbf{xy}}$, matching time-translated τ and frequency-scaled s domains; i.e. periodograms and related techniques of visualisation can be employed to track the interdependent dynamics.

$$\begin{aligned}{\kappa_{\mathbf{xy}}}^{2}(\omega_0) &= \frac{|\mathbf{S}_{\mathbf{xy}}(\omega_0)|^2}{|\mathbf{S}_{\mathbf{xx}}(\omega_0)||\mathbf{S}_{\mathbf{yy}}(\omega_0)|} \\ &= \frac{|\mathbf{S}\big(\mathbf{W}_{\mathbf{xx}}^{\mathrm{H}}(s,\tau)\mathbf{W}_{\mathbf{yy}}(s,\tau)\big)|^2}{|\mathbf{S}(\mathbf{W}_{\mathbf{xx}}(s,\tau))||\mathbf{S}\big(\mathbf{W}_{\mathbf{yy}}(s,\tau)\big)|}\end{aligned} \tag{7}$$

where $\mathbf{W}(s,\tau)$ denotes the continuous wavelet transform at scale s and translation index τ.

The ever-growing interest for nonlinear dynamics as complementary way to characterise cortical activity encourages the adaptation of phase-oriented methods within the general computational approach [12]. The implicit synchronisation study undertakes the estimation of instantaneous amplitudes, frequencies and oscillations phases [31] performing a pair of convolutions $\mathbf{F}_{\cdot\psi}(t)$ between EEG oscillation $\mathbf{x}^{b}[k]$ (8), HRV power band $\mathbf{y}^{b'}[k]$ (9) and the complex-valued Morlet wavelet $\psi(t_k)$ defined in (10) [21].

$$\begin{aligned}\mathbf{F}_{\mathbf{x}\boldsymbol{\psi}}(t) &= (\psi * \mathbf{x}^{b})[k] = \sum \psi[\tau]\mathbf{x}^{b}[k-\tau] \\ &= \mathbf{A}_{\mathbf{x}^{b}}[k]\mathbf{e}^{\iota\phi_{\mathbf{x}^{b}}[k]}\end{aligned} \tag{8}$$

$$\begin{aligned}\mathbf{F}_{\mathbf{y}\boldsymbol{\psi}}(t) &= (\psi * \mathbf{y}^{b\hat{a}\L^{TM}})[k] = \sum \psi[\tau]\mathbf{y}^{b\hat{a}\L^{TM}}[k-\tau] \\ &= \mathbf{A}_{\mathbf{y}^{b\hat{a}\L^{TM}}}[k]\mathbf{e}^{\iota\phi_{\mathbf{y}^{b\hat{a}\L^{TM}}}[k]}\end{aligned} \tag{9}$$

$$\psi(t_k) = \left(\mathbf{e}^{\iota\omega_0 t_k} - \mathbf{e}^{\frac{-\omega_0^2\sigma_{t_k}^2}{2}}\right)\mathbf{e}^{-\frac{t^2}{2\sigma_{t_k}^2}} \tag{10}$$

with ω_0 and σ_{t_k} representing the wavelet central frequency and bandwidth or decay rate, respectively.

In this paper, we make use of *n*:*m* phase synchronisation concept, and more specific its robust approach phase locking value $\zeta_{n,m}$ [26] to indicate the 0-to-1 locking value of n cycles from one oscillation to m cycles of the other (Fig. 1). This is achieved by the computation of the difference $\varphi_{n,m}[k]$ of instantaneous phases at sequential time instants (11) of one EEG oscillator $\phi_x[k]$ and one HRV power band $\phi_y[k]$, which is usually wrapped into a cyclic interval $[0, 2\pi m)$, as it is shown by (12).

$$\varphi_{n,m}[k] = n\phi_x[k] - m\phi_y[k] \tag{11}$$

$$\hat{\varphi}_{n,m}[k] = \varphi_{n,m}[k] \mathrm{mod} 2\pi m \tag{12}$$

The *n*:*m* phase synchronisation is strictly constrained to the selection of non-arbitrary frequency pairs, since it can only designate a rational quotient between them. Only in that sense, it is guaranteed that n, m integers are invariant towards multiples of phase slips [38]. Yet, if this condition holds, larger integer values could decree unstable and less robust pair of frequencies for synchronisation assessment, due to the implicit commutative variance, as Table 2 indicates. Even so, the chosen n, m values or f_c central frequencies look forward sufficient conditions, in terms of power

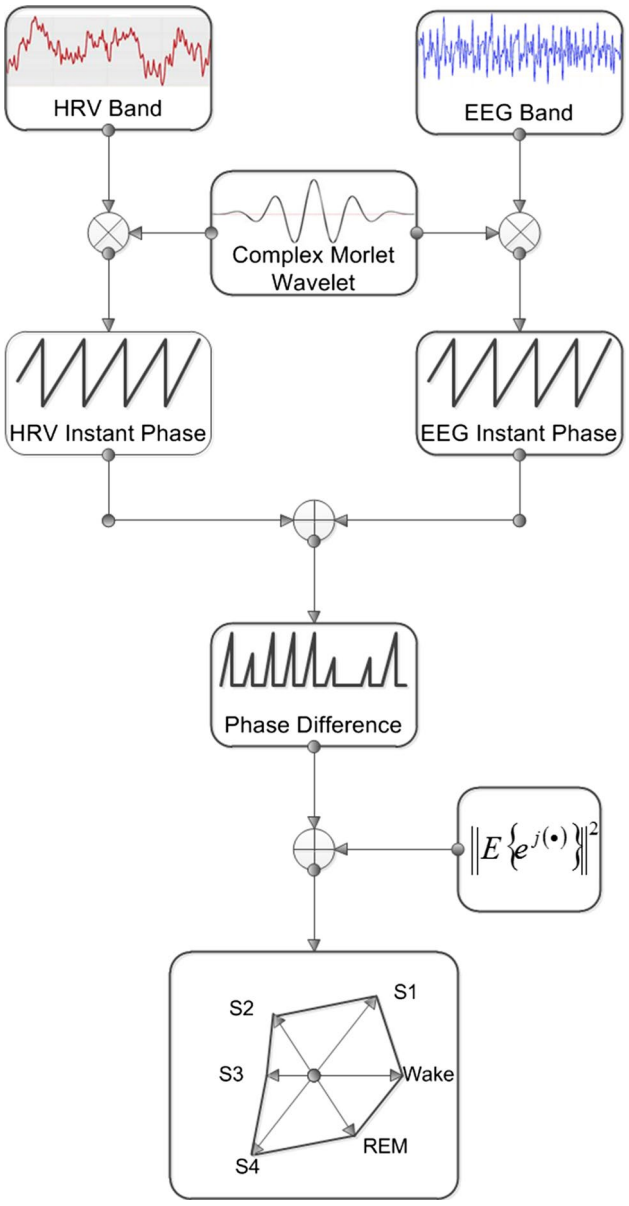

Fig. 1 Flow diagram of phase locking value (PLV) method. EEG and HRV decomposed bands are independently convolved with the complex-valued Morlet wavelet. The operation generates a time series of instant phases for EEG and HRV side, which are time instant-wise subtracted to find a vector of phase values, located within $[0, 2\pi)$ interval. Then, the magnitude and average of phase difference vector are computed to produce the PLV value at each sleep stage

bands separation and rational quotient. On this way, not only computational constraints are assertively enacted, but also analytical tractability can be addressed. The result derived from (13) reflects a magnitude between 0-to-1 range, which points out the strength of the interdependence between the scoped frequencies.

$$\begin{aligned}\zeta_{n,m} &= \left| E\{\mathbf{e}^{\iota\hat{\varphi}_{n,m}[k]}\} \right| \\ &= \sqrt{\left(E\{\cos\hat{\varphi}_{n,m}[k]\}\right)^2 + \left(E\{\sin\hat{\varphi}_{n,m}[k]\}\right)^2}\end{aligned} \tag{13}$$

Lastly, a normalisation routine is applied to locate the yielded features inside of a 0–1 interval, which facilitates the interpretation of the results and further insights.

2.4 Statistical analysis

An inspection of Gaussianity conditions upon the yielded time series is required, in order to convey an adequate statistical analysis seeking significant differences underlying the clinical cohorts [11, 20]. Henceforth, our computational approach practices multiple preparatory statistical tests, aiming to decide whether Gaussian distribution is the fit-test reference for the modelled data [19], as well as, (non-) parametric suitability and sample size determination [2]. The Bartlett test, Q–Q plot and Mardia kurtosis assessed the graphical or analytical divergence of expectation and covariance of the modelled data against the Gaussian distribution. As it was expected, the results of such tests suggested a pronounced deviation of the data points from the Gaussian tendency, endorsing the usage of Kruskal–Wallis as omnibus test [5]. Consequently, post hoc evaluations with heuristic correction of paired samples from healthy to insomnia, healthy to schizophrenia and insomnia to schizophrenia cohorts are tested using Mann–Whitney U rank test.

3 Results

Before introducing some remarks about interdependency mechanisms, it is noteworthy to contextualise some enthraling facts inferred from the clinical information,

Table 2 n:m integers, central frequency and variance relation for phase synchronisation between EEG and HRV power bands

Bands	δ	θ	α	ς	β	γ
f_c (Hz)	2	6	10	14	24	48
LF 0.055	1:40	1:120	1:200	1:280	1:480	1:960
$n^2 + m^2$	1601	14,401	40,001	78,401	230,401	921,601
HF 0.125	1:16	1:48	1:80	1:96	1:192	1:384
$n^2 + m^2$	257	2305	6401	9217	36,865	147,457

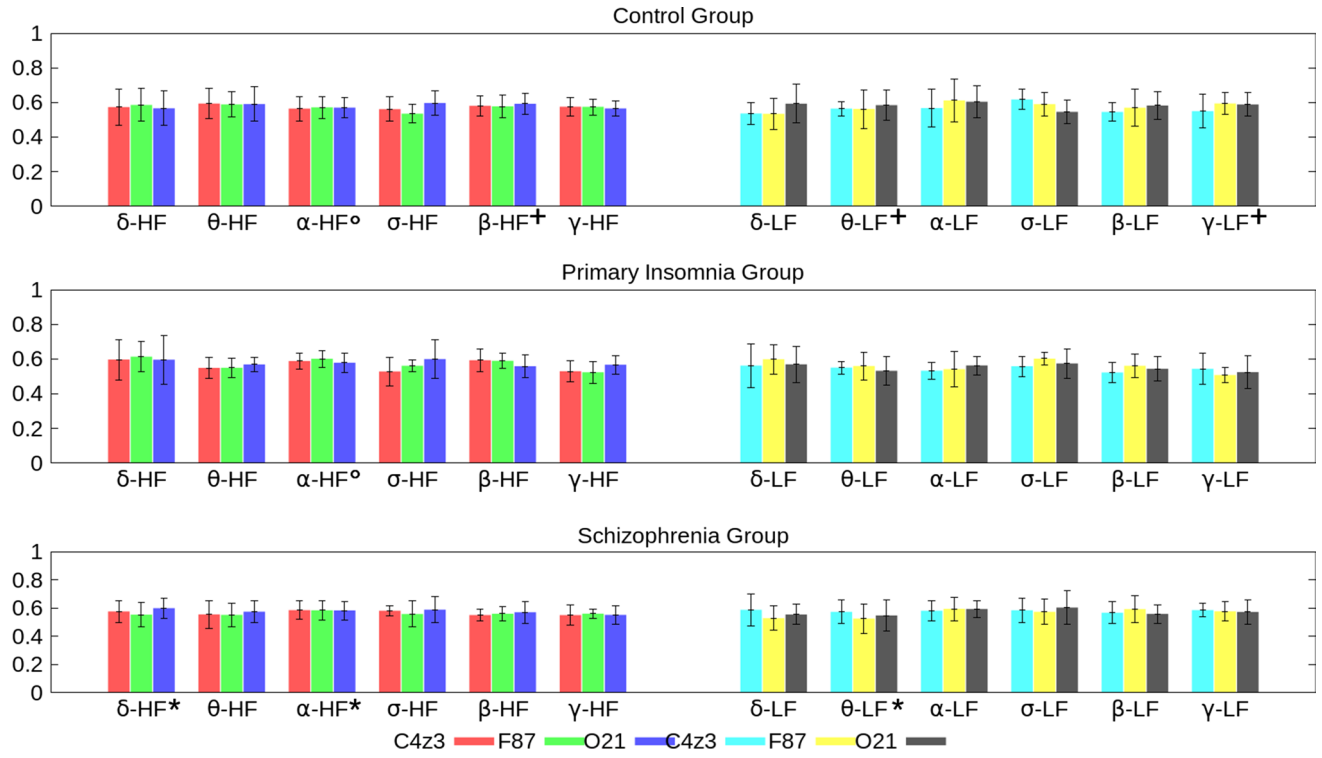

Fig. 2 Histogram of Pearson's coefficient or CCF at zero-th time lag including EEG $\delta, \theta, \alpha, \varsigma, \beta$ and γ versus HRV LF and HF bands for control, primary insomnia and schizophrenia cohorts. Each set of *coloured bars* represent the mean value of interhemispheric neural parcels: C_{4z3}, F_{87} and O_{21} with their corresponding cohorts' standard deviation as *error bars*. Statistically significant ($p < 0.05$) to distinguish schizophrenia patients from healthy and insomnia subjects, †statistically significant ($p < 0.05$) to distinguish healthy subjects from insomnia and schizophrenia patients, ◦statistically significant ($p < 0.05$) to distinguish healthy subjects from insomnia patients (colour figure online)

summarised in Table 1. The overall statistics of sleep parameters set out similar sleep onset latency, i.e. elapsed time from lights off to the appearance of the first S2 or REM stage, in control and insomnia groups although schizophrenia patients required in average 10 additional minutes to reach S2 sleep stage. In regard to REM latency, i.e. elapsed time from lights off to the occurrence of the first REM period, it was observed a progressive 17-min prolongation from control, passing to insomnia till schizophrenia patients. Evenly interesting, it should be the large standard deviation of this parameter, which suggested wide differences in the patterns for the completion of the first sleep cycle amongst the participants. An inverse relation is exhibited by the Wake percentage, since this stage population shortened, inasmuch as the subject's cohorts moved from control to schizophrenia subjects, no more than 5 % points. The remaining sleep onset-related stages (S1 and S2) reported almost the same global percentages for the considered clinical groups. A slight increment in S1 percentage was cast by insomnia patients, though. Referring to deep sleep stages, control subjects spent the shortest overall period inside of this state, whilst disordered patients dedicated no more than 20 min. At the end, the percentage of scored REM epochs placed insomnia group (10.3 %) at the bottom of the scale, surpassed by control (14.3 %) and schizophrenia patients (18.7 %) as the cohort with the largest REM duration. Hereafter, an interpretation of those initial sleep descriptors might be sorted out by means of biosignal processing and computational resources.

The results obtained across pre-processing, processing and statistical analyses only employed the subjects with the same arrangement of monopolar sensors (i.e. CTL1–CTL9, INS1–INS6 and SCZ1–SCZ10) to generate the interhemispheric neural parcels, whereas bipolar electrodes are excluded from further computations for compatibility reasons amongst the clinical subjects. Thus, the interneuronal areas are distinguished as: C_{4z3}, F_{87} and O_{21}, that means, the electrical activity generated in the central, occipital and frontal cortical regions was contrasted with the cardiac counterparts. Thereafter, the linear and non-linear values were individually extracted from each clinical recording. Depending on their original cohorts, the expectation and standard deviation were computed amongst the nine control, six primary insomnia and ten schizophrenia group members.

To begin, the linear analysis was set in motion by calculating the Pearson's coefficient, i.e. CCF value at zero-th time lag. Taking into account the six decomposed EEG

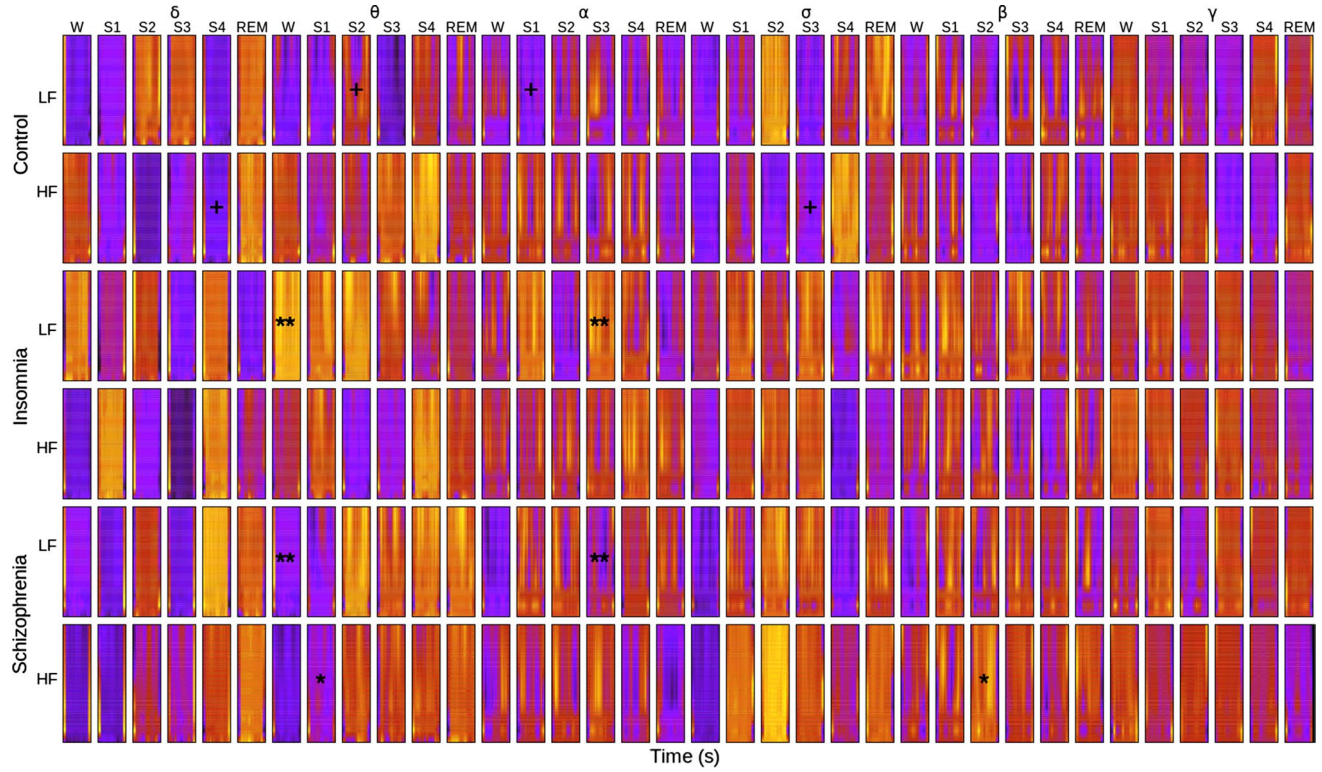

Fig. 3 Macro-periodogram of wavelet coherence considering EEG $\delta, \theta, \alpha, \varsigma, \beta$ and γ at C_{4z3} parcel against HRV LF and HF bands for control, insomnia and schizophrenia cohorts across sleeps stages wake, S1, S2, S3, S4 and REM. On the *x*-axis, each periodogram's cell portrays averaged out 30-s epochs corresponding to a particular sleep stage, and 12 pseudo-frequencies are ordered on the *y*-axis starting on *ca.* 89.8 Hz till (*top scale*) 0.04 Hz (*bottom scale*). The *colour scale* assigns the black–violet spectrum for low coherence values, whilst *red–yellow* intensities represent the surrounding unity values, i.e. high coherence. Statistically significant ($p < 0.05$) to distinguish schizophrenia patients from healthy and insomnia subjects, †statistically significant ($p < 0.05$) to distinguish healthy subjects from insomnia and schizophrenia patients, statistically significant ($p < 0.05$) to distinguish insomnia from schizophrenia patients (colour figure online)

power bands, two HRV frequencies and three clinical cohorts, the Fig. 2 displays the histogram with the attained mean values and whiskers to denote standard deviation. The first observation established a marked difference amongst control and patient groups related to the overall correlation coefficients, since healthy patients keep a threshold less or equal than 0.6 for each power band and neural parcel. In turn, primary insomnia and schizophrenia groups were consistently located in [0.6–0.8] interval, correspondingly. For control, EEG $\leftrightarrow$ HF activity maintained steady values at every scalp region moving from δ to γ power bands. A slightly different situation occurred with EEG $\leftrightarrow$ LF, where central and frontal neural areas weakened their correlations in 0.1 point against the occipital region. Insomnia cohort had a more regular pattern between EEG $\leftrightarrow$ HF and EEG $\leftrightarrow$ LF interactions, given that no substantial variations are manifested by bands or neural areas. Meanwhile, schizophrenia patients across central, occipital and frontal areas exhibited almost indistinct values for EEG $\leftrightarrow$ HF activity, but EEG $\leftrightarrow$ LF strengthened its correlation around 0.1 in the central region for $\delta, \theta \leftrightarrow$ LF interdependencies. Seemingly, non-significant dissimilarity underlay amongst EEG $\leftrightarrow$ HF and EEG $\leftrightarrow$ LF power bands inside of each clinical group, although further statistical analyses conducted a closer evaluation of every possible doublet of frequencies.

The second linear representative, wavelet-based coherence arranged one cycle of sleep stages (Wake to REM) into the TFA, accompanied by the described EEG/HRV power bands and clinical groups. From the macro-periodogram in Fig. 3, some annotations could be inferred, regarding the interdependency between EEG and HRV power bands in the designated neural parcel C_{4z3}. In a 0-to-1 scale, the coherence between low-regime EEG power bands, such as $\delta, \theta \leftrightarrow$ LF was particularly stronger (0.5–0.7) during wake and REM stages, reaching medium values (*ca.* 0.5) for insomnia patients and extreme levels (*ca.* 0.7) with schizophrenia subjects. Similarly, $\delta \leftrightarrow$ LF, HF bands intensified their coherence along S4 and REM stages for insomnia and schizophrenia groups. Moving to θ power band, light sleep stages (S1, S2) show top-scale values (0.75) over insomnia and schizophrenia cohorts. But one of the

most relevant facts was the constant spectral correlation or coherence between $\theta \leftrightarrow$ HF bands along the six sleep stages, when control volunteers were referred. The ς power band had also a recurrent impact over each sleep stage, casting a medium (0.5), high-medium (0.75) and maximum (0.95) coherence upon control, insomnia and schizophrenia groups, respectively. Focusing on high-regime EEG power bands (i.e. ς, β and γ), the absence of noticeable sensitivity was explicit, independent of sleep stages, HRV bands or cohort type although subtle spots (*ca.* 0.15) stood out for patients over control subjects. Taking into consideration macro-periodograms yielded by the remaining neural parcels (not shown here), it is ratified the brightening activity (0.6–0.7) of EEG low-regime $\delta, \theta \leftrightarrow$ LF/HF power bands, moving towards weaker levels at α-γ frequencies. Except for schizophrenia patients, whose coherence re-activated between $\alpha, \varsigma \leftrightarrow$ HF and $\beta, \gamma \leftrightarrow$ HF in frontal and occipital regions during wake and light sleep stages.

Within nonlinear analysis, the *n*:*m* phase synchronisation set out through the polar diagrams in Figs. 4 and 5, the 0-to-1 phase-locked coupling values between EEG $\leftrightarrow$ HRV power bands at C_{4z3} neural parcel, including six sleep stages and three clinical groups. The selected n and m integers, central frequencies f_c and $n^2 + m^2$ variance relation for the cross-frequency analysis are depicted in Table 2 as an attempt to illustrate the large deviation that cross-frequencies suffered, as far as, the central frequencies spread out from each other. Thereafter, relative large values might lead to unstable or spurious synchronisations. From here, schizophrenia patients exhibited a strong interdependency $(0.6 - 0.8)$ between EEG high-regime frequencies $\beta, \gamma \leftrightarrow$ HF along the entire sleep cycle, except for S4 stage. A similar situation was appreciated with $\varsigma, \gamma \leftrightarrow$ LF bands during light to deep sleep transition. Regarding insomnia group, $\delta, \theta, \varsigma \leftrightarrow$ HF power oscillations reached significant values around 0.8 in light and REM sleep, predominantly. On top of that, couplings over 0.8 were observed in $\alpha, \gamma \leftrightarrow$ LF in the initiation of light (S1, S2) and deep (S3) sleep stages with medium rank (less than 0.6) values for the rest of power bands and stages. Besides, control subjects sustained a half-way interdependency, i.e. 0.5, concerning all scoped power bands and sleep stages, which coincided with the outcomes of Pearson's correlation coefficients. The observations from the remaining neural parcels, which are not shown here, introduced additional remarks. For instance, the neural parcel F_{87} yields locking values in the interval $(0.8 - -1.0)$ when $\alpha, \varsigma \leftrightarrow$ LF oscillations were co-processed for insomnia case; and comparable phenomenon was attained by the schizophrenia group at $\gamma \leftrightarrow$ LF bands during S1, S2 and REM sleep stages. In turn, O_{21} parcel related the most intensive synchronisation during deep sleep stages (S3, S4) between $\delta, \theta \leftrightarrow$ LF in schizophrenia and $\alpha, \varsigma \leftrightarrow$ LF for insomnia.

Lastly, a Kruskal–Wallis test was conducted in order to cast significant differences ($p < 0.05$) amongst healthy, insomnia and schizophrenia groups, attending to all possible interactions of EEG $\leftrightarrow$ HRV power bands, electrode parcels and sleep stages. In general, CCF linear feature supported significant zero-lagged correlations when functional interdependence between $\alpha, \beta, \gamma \leftrightarrow$ HF, LF ($\chi^2 = 6.48, p = 0.039$ and $\chi^2 = 7.20, p = 0.027$) at deep sleep stages was tested. Its tempo-spectral counterpart, wavelet coherence nominated a wider number of significant differences involving light sleep stages with $\theta, \alpha \leftrightarrow$ LF ($\chi^2 = 6.48, p = 0.039$) and $\theta, \beta \leftrightarrow$ HF ($\chi^2 = 7.20, p = 0.027$) frequency pairs, as well as, $\delta, \varsigma \leftrightarrow$ HF ($\chi^2 = 6.48, p = 0.039$) during S4 sleep stage. In addition, statistical relevance was observed in $\theta \leftrightarrow$ LF ($\chi^2 = 7.20, p = 0.027$) across wake stage. Correspondingly, the nonlinear view represented by PLV features pointed out meaningful values on S2 sleep stage, precisely in $\gamma \leftrightarrow$ LF ($\chi^2 = 6.48, p = 0.039$). Overall, it was noticeable the concentration of significant values around S1–S4 stages when $\varsigma \leftrightarrow$ LF comes under examination, excluding wake and REM categories. Thus, Table 3 frames the significant results (p values) amongst clinical groups, discriminating pair of frequencies and sleep stages. Also, Figs 2, 3, 4 and 5 point out the statistically significant values according to these criteria.

Identifying how the clinical groups differed between each other, we undertook three simultaneous Mann–Whitney U tests with heuristic correction. The post hoc evaluations compared the possible combinations of cohorts, such as healthy to insomnia, healthy to schizophrenia and insomnia to schizophrenia. In order to determine which pairwise comparison assumed the largest contribution to the rank differences. Particularly, CCF feature with high EEG frequencies $\beta \leftrightarrow$ HF and $\alpha, \gamma \leftrightarrow$ LF ($z = 1.30, ranksum = 15, p = 0.08$) are statistically relevant to differentiate control subjects during deep sleep. Also, $\alpha \leftrightarrow$ HF cross-frequencies with a similar significant level ($z = -0.87, ranksum = 6, p = 0.08$) elicited a distinction of control-to-all and schizophrenia from insomnia patients. Despite of the significant values for S4, we advise some discretion on this result, due to the limited number of S4 epochs that healthy and schizophrenia groups reported (see Table 1). Followed by WCOH feature, post hoc tests stand out the applicability of $\delta, \varsigma \leftrightarrow$ HF ($z = -1.74, ranksum = 6, p = 0.08$) at deep sleep to discern healthy from disordered patients. And, $\theta, \beta \leftrightarrow$ HF ($z = 1.74, ranksum = 15, p = 0.08$) at light sleep to distinguish schizophrenia from the other cohorts. Concurrent to this, light sleep stages Wake and S3 at $\theta, \alpha \leftrightarrow$ LF evidenced appreciable differences ($z = 1.74, ranksum = 15, p = 0.08$) to separate insomnia and schizophrenia patients. By means of PLV feature, healthy subjects might be statistically

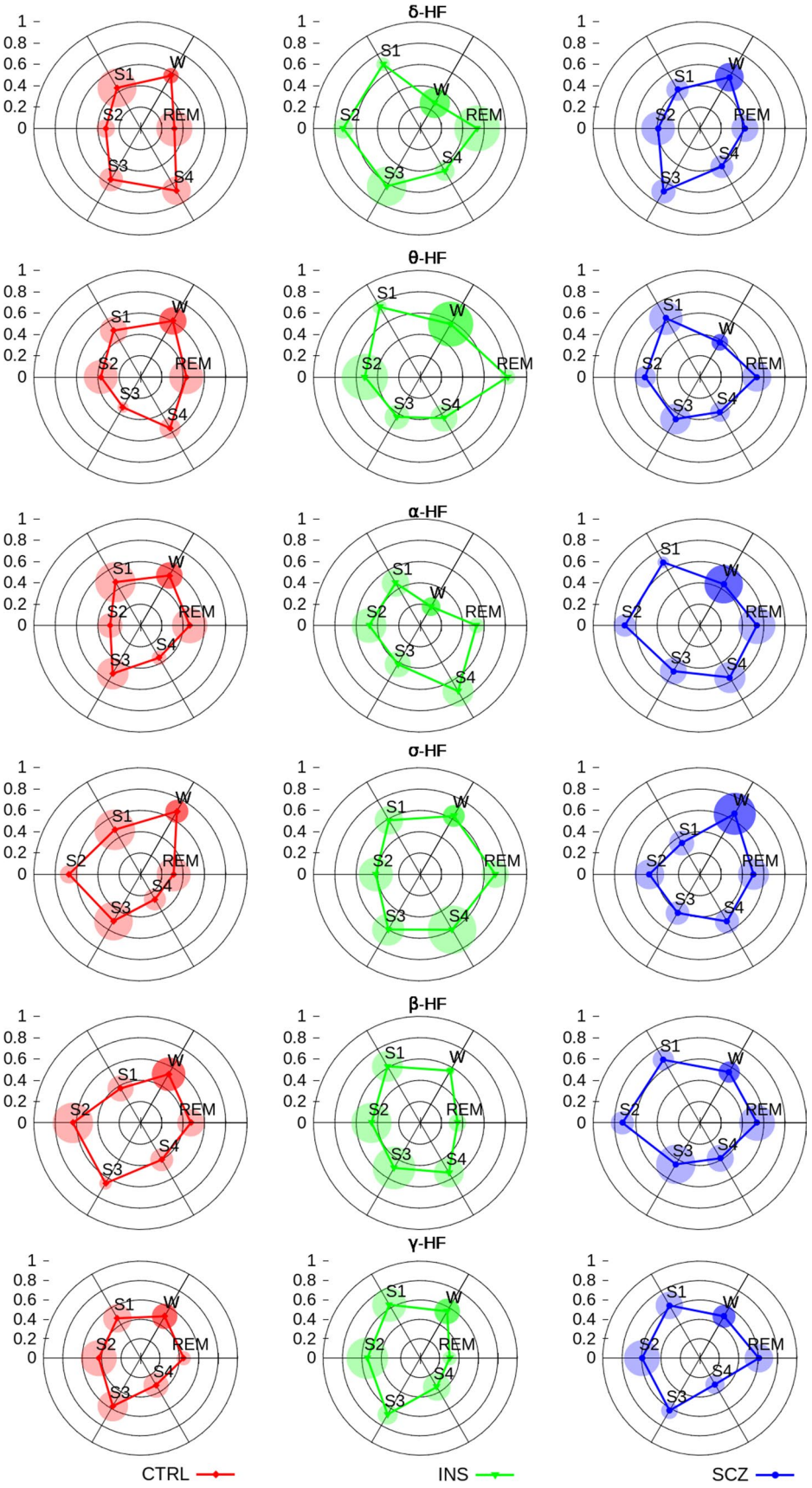

Fig. 4 Polar diagram of *n:m* phase synchronisation for control (CTL), insomnia (INS) and schizophrenia (SCZ) cohorts, identified by *red*, *green* and *blue line*, respectively. Phase locking value between C_{4_Z3}-$\delta, \theta, \alpha, \varsigma, \beta$ and $\gamma \leftrightarrow$ HRV HF band. The *coloured points* represent the mean PLV at each sleep stage, accompanied by a centred circle expressing the standard deviation amongst the group subjects and patients (colour figure online)

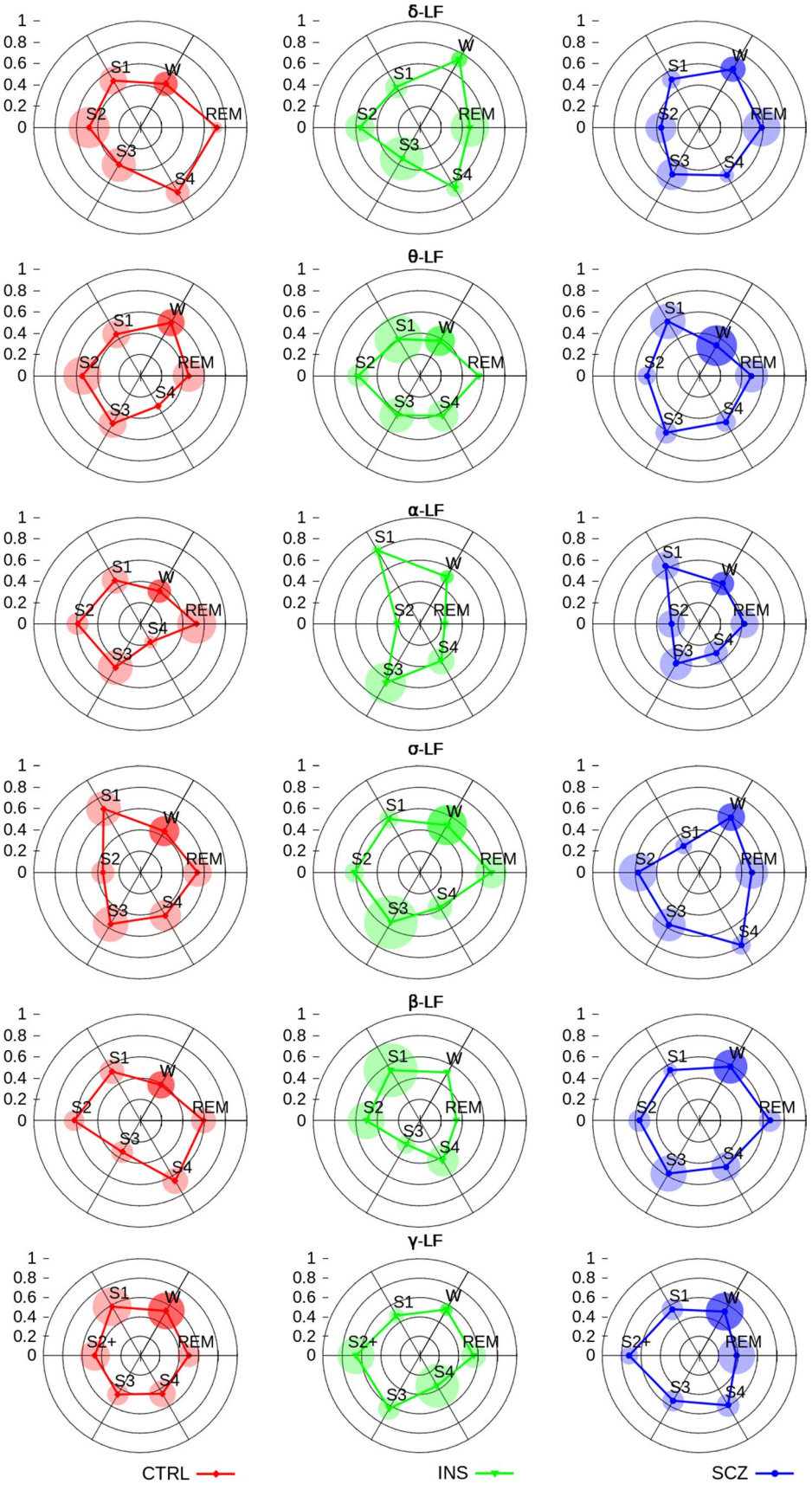

Fig. 5 Polar diagram of *n:m* phase synchronisation for control (CTL), insomnia (INS) and schizophrenia (SCZ) cohorts, identified by *red*, *green* and *blue line*, respectively. Phase locking value between $C_{4_{Z3}}$-$\delta, \theta, \alpha, \varsigma, \beta$ and $\gamma \leftrightarrow$ against HRV LF band. The *coloured points* represent the mean PLV at each sleep stage, accompanied by a centred circle expressing the standard deviation amongst the group subjects and patients. † statistically significant ($p < 0.05$) to distinguish healthy subjects from insomnia and schizophrenia patients (colour figure online)

Table 3 Kruskal–Wallis and Mann–Whitney tests p-values applied to clinical groups based on power bands and sleep stages

Method	$\delta \leftrightarrow$ HF	$\theta \leftrightarrow$ HF	$\alpha \leftrightarrow$ HF	$\varsigma \leftrightarrow$ HF	$\beta \leftrightarrow$ HF	$\gamma \leftrightarrow$ HF
CCF	Wake(6.48, 0.039)[a]	-	S3(7.20, 0.027)[c]	-	S3(7.20, 0.027)[b]	-
	-	-	S4(6.48, 0.039)[a]	-	-	-
WCOH	S4(6.48, 0.039)[b]	S1(7.20, 0.027)[a]	-	S3(6.48, 0.039)[b]	S2(6.48, 0.039)[a]	-
PLV	-	-	-	-	-	-
Method	$\delta \leftrightarrow$ LF	$\theta \leftrightarrow$ LF	$\alpha \leftrightarrow$ LF	$\varsigma \leftrightarrow$ LF	$\beta \leftrightarrow$ LF	$\gamma \leftrightarrow$ LF
CCF	-	S1(6.48, 0.039)[a]	-	-	-	S4(7.20, 0.027)[b]
	-	S3(7.20, 0.027)[b]	-	-	-	-
WCOH	-	Wake(7.20, 0.027)[d]	S1(6.48, 0.039)[b]	-	-	-
	-	S2(6.48, 0.039)[b]	S3(7.20, 0.027)[d]	-	-	-
PLV	-	-	-	-	-	S2(6.48, 0.039)[b]

$p < 0.05$ for Kruskal–Wallis test (χ^2, p)

[a] Post hoc statistically significant to distinguish schizophrenia patients

[b] Post hoc statistically significant to distinguish control subjects

[c] Post hoc statistically significant to distinguish control subjects from insomnia subjects

[d] Post hoc statistically significant to distinguish insomnia from schizophrenia patients

distinguished from insomnia and schizophrenia patients focusing on $\gamma \leftrightarrow$ LF ($z = -1.74, ranksum = 6, p = 0.08$) activity along S2 stages. One more time, the warning about the limited number of S4 epochs, applies for the interpretation of these results. Ultimately, it is worthwhile to note the important role of neither Wake nor REM stages in the differentiation of clinical groups, where the most significant statistical differences were cast using CCF and WCOH techniques (see Table 3).

4 Discussion

In our research, we proposed a comparative computational approach to differentiate healthy, insomnia and schizophrenia patients based on the functional interdependency between EEG and HRV power oscillations. Intrinsically, the synchronisation matter came up to characterise from a linear and nonlinear point of view the co-related or coherent interaction of ANS counterparts. However, synchronisation/de-synchronisation dichotomy cannot be unambivalently resolved. The occurrence of simultaneous high/low convergence of frequency components in terms of coherence or in/out-phase oscillations for PLV at separated cortical regions might lead to conflicting observations. Therefore, a statistical reasoning needed to be imparted to determine likelihoods rather than certain (de)coupling dynamics [33]. According to this, we initially indicated the limitations of CCF method to distinct, at least in an analytical sense, the inference of EEG oscillations with either HF or LF power bands. The homogeneous performance of Pearson's coefficient by confronting EEG $\leftrightarrow$ HF/LF in each clinical group, cast ambiguity about sympathetic and parasympathetic differentiators along the progression of sleep stages. Albeit it is worthy to indicate that the steady middle-rank correlation in (0.4–0.5) interval for control subjects coincided with previous findings only focused on healthy individuals [15, 21].

Opposite to this, wavelet coherence demonstrated a more adequate tracking of interdependencies, incorporating sleep stages, power bands and clinical groups. Such an advantage obeyed to its capability to spectrally quantify phase differences [21], whereas no forward/backward relationships were sought, this prowess beholds; otherwise, estimation methods for directionality driving should have been invoked. Previous investigations had claimed the growing activity of LF during Wake/REM stages and HF along non-REM episodes in healthy population [16, 17]. The results in macro-periodograms not only attested this argument, but also exposed the increasing coherence values for insomnia and schizophrenia groups, specially allocated into δ and θ frequency bands. Not surprisingly, Wake and REM stages were inherently associated with sympathetic coherence, given that, hassling conscious moments could be vividly emulated by dreaming sequences during REM sleep. Likewise, gradual relaxation was expected during non-REM stages, reflected by HF surpassing, as long as, vagal cardiac system withheld a commanding position. Notwithstanding, the novel fact consisted of adding up the prominent presence of δ and θ power bands to every clinical scenario, deferring in the strength of coherence amongst them. Therein, schizophrenia group intensified β and γ

activity in consonance with HRV bands, as a distinctive feature of this cluster. By ascribing that $\theta \leftrightarrow$ LF coherence reveals coupling dynamics between long-range brain regions, as well as, $\gamma \leftrightarrow$ HF defines more proximate interactions [32]. We suggest that functional interdependencies between EEG-to-HRV power bands, i.e. sympathetic and parasympathetic systems across sleep stages applied to all clinical subjects resemblant-wise. However, the underlying existence of slow and fast time-varying neuronal events (e.g. K-complexes, sawtooth waves, sleep spindles, etc.), in conjunction with cardiac activity, impacted time-frequency relations to produce discerning coherence estimations.

Despite of the argued robustness of linear methods against noise, spurious synchronisations or phase slips amongst nearby signals [28, 29]; the *n*:*m* phase synchronisation method allowed us to vindicate some emergent and aforementioned interactions from a nonlinear context. For instance, wavelet coherence and PLV agreed on the functional interdependencies of the sympathetic system during Wake and REM stages, moving to a more coherent and phase-coupled activity of HF band along non-REM sleep windows with similar intensity for insomnia and schizophrenia patients. However, the evidence gathered from the polar diagrams in Figs. 4 and 5 suggested that α /ς/γ bands seemed to contest this tendency by exhibiting an opposite behaviour; i.e. vagal regulation compromised its coupling strength during light and deep sleep stages, inasmuch as patients concerns. Such a dynamic might reveal a pronounced nonlinear differentiator of insomnia subjects referred to α/ς and extended to γ oscillation for schizophrenia group, which was confirmed by related studies [25]. Furthermore, this locking alternation could be the effect of loss of control between brainstem structures typified by psychiatric disorders [16]. It is noteworthy, the spread distance between central frequencies of high-regime EEG and HRV bands should lead to interpret these findings with some caution, given the probability of spurious synchronisations due to the large *n*:*m* quotient in those cases.

From the results of Kruskal–Wallis omnibus test and Mann–Whitney *U* post hoc tests, we could statistically attest some of the conclusions previously deducted. Firstly, CCF approach was considerably limited to EEG high frequencies at deep sleep stages to discern amongst the clinical groups, since neither necessary nor sufficient conditions could be stated from the progression of the remaining sleep stages and the interaction of EEG $\leftrightarrow$ HRV power bands. Counting on heavily localised significant values, no further propositions could be inferred from this feature in a statistical sense. By the nonparametric testing of wavelet coherence, this feature demonstrated an outstanding performance to track the distinctive trends between neuronal signals and vagal cardiac system during non-REM sleep stages, as it was indicated before [9, 16]. Even though, the underlying details for rejecting the null hypothesis always remain undisclosed in the design of an omnibus statistical test, the post hoc analyses offered substantial conclusions in terms of group's distinction.

We can posit that TFA-based methods have the authority to discriminate healthy and disordered subjects based on the functional interaction of $\delta, \theta, \varsigma$ and β bands and the parasympathetic activities. Foremost, the introduction of wavelet coherence revealed better than another the strong relationship of $\alpha \leftrightarrow$ LF to differentiate the healthy and psychiatric disordered cohorts. Such a finding was set forth not only at early stages, but also by the end of the sleep cycle. In turn, *n*:*m* phase synchronisation traced ostensible divergences into S2 stage, concerning high-regime EEG γ band and the sympathetic system to distinguish healthy population from psychiatric disordered one.

5 Conclusions

Our findings suggest the existence of relevant differences between control subjects and affected patients, in terms of cross-correlation, time–frequency coherence and phase-locked synchronisation values. Moreover, wavelet coherence demonstrated to be the most performant to estimate the influence of low-regime EEG bands over vagal cardiac activity during arousal and dreaming sleep stages, which was spanned by the appearance of unambiguous functional interactions into ς, β and γ power bands, when insomnia and schizophrenia patients respect. The nonlinear and statistical analysis led to elicit underlying interdependencies related to the δ with vagal cardiac circuit and ς with sympathetic system, which can be distinctively characterised insomnia patients from control and psychiatric disordered individuals. According to this, the mutual interaction of ANS sections represented by the cerebral lower brainstem, parasympathetic and sympathetic systems maintain unimpaired their interconnectivity structures. However, specific pathologies might lead to less efficient coupling, i.e. sub- and overestimated synchronisations in related processes of sleep regulation.

Further studies should be proposed to analyse in more detail the accuracy of nonlinear approaches, in order to disregard spurious synchronies, as a consequence of narrow/broad spectrum of the oscillations or noise distortion conditions. The augmentation of the subjects' sample size, as well as, the usage of surrogate data analysis and direction-driving techniques might rendezvous some answers to properly understand the actual interdependency between neuronal and cardiac components, not only from a biosignal processing perspective, but also founded on a physiological interest.

Acknowledgments The authors would like to thank the Sleep Laboratory of the Central Institute of Mental Health for undertaking the recruitment and collection of polysomnographic recordings, which served as the main experimental source for the present research work. R. Chaparro-Vargas acknowledges the financial support of COLCIENCIAS-COLFUTURO of the Colombian Government, as main sponsor for his doctorate studies.

References

1. Acharya UR, Joseph KP, Kannathal N, Lim CM, Suri JS (2006) Heart rate variability: a review. Med Biol Eng Comput 44(12):1031–1051
2. Bartlett JE, Kotrlik JW, Higgins CC (2001) Organizational research: determining appropiate sample size in survey research. Inf Technol Learn Perform J 19(1):43–50
3. Bartsch R, Kantelhardt JW, Penzel T, Havlin S (2007) Experimental evidence for phase synchronization transitions in the human cardiorespiratory system. Phys Rev Lett 98:054,102
4. Bob P (2012) Consciousness, schizophrenia and complexity. Cogn Syst Res 13(1):87–94
5. Chicharro D, Andrzejak RG (2009) Reliable detection of directional couplings using rank statistics. Phys Rev E 80:026,217
6. Chouinard S, Poulin J, Stip E, Godbout R (2004) Sleep in untreated patients with schizophrenia: a meta-analysis. Schizophr Bull 30(4):957–967
7. Dimitriadis S, Laskaris N, Del Rio-Portilla Y, Koudounis G (2009) Characterizing dynamic functional connectivity across sleep stages from EEG. Brain Topogr 22(2):119–133 Cited By (since 1996) 13
8. Dumont M, Jurysta F, Lanquart JP, Migeotte PF, van de Borne P, Linkowski P (2004) Interdependency between heart rate variability and sleep EEG: linear/non-linear? Clin Neurophysiol 115(9):2031–2040
9. Dumont M, Jurysta F, Lanquart JP, Noseda A, van de Borne P, Linkowski P (2007) Scale-free dynamics of the synchronization between sleep EEG power bands and the high frequency component of heart rate variability in normal men and patients with sleep apnea hypopnea syndrome. Clin Neurophysiol 118(12):2752–2764
10. Freeman D, Pugh K, Vorontsova N, Southgate L (2009) Insomnia and paranoia. Schizophr Res 108(1–3):280–284
11. Haidekker MA (2011) Advanced biomedical image analysis. Wiley, New York
12. Hegger R, Kantz H (1999) Practical implementation of nonlinear time series methods: the TISEAN package. Chaos 9:413–435
13. Iber C, Ancoli-Israel S, Chesson AL Jr, Quan SF (2007) The AASM manual for the scoring of sleep and associated events. Tech. rep., American Academy of Sleep Medicine
14. Jansson-Frjmark M, Lindblom K (2008) A bidirectional relationship between anxiety and depression, and insomnia? A prospective study in the general population. J Psychosom Res 64(4):443–449
15. Jurysta F, van de Borne P, Migeotte PF, Dumont M, Lanquart JP, Degaute JP, Linkowski P (2003) A study of the dynamic interactions between sleep EEG and heart rate variability in healthy young men. Clin Neurophysiol 114(11):2146–2155
16. Jurysta F, Lanquart JP, Sputaels V, Dumont M, Migeotte PF, Leistedt S, Linkowski P, van de Borne P (2009) The impact of chronic primary insomnia on the heart rate EEG variability link. Clin Neurophysiol 120(6):1054–1060
17. Jurysta F, Kempenaers C, Lancini J, Lanquart JP, Van De Borne P, Linkowski P (2010) Altered interaction between cardiac vagal influence and delta sleep eeg suggests an altered neuroplasticity in patients suffering from major depressive disorder. Acta Psychiatr Scand 121(3):236–239
18. Mallat S (1999) A wavelet tour of signal processing. Elsevier Academic Press, Amsterdam
19. Marusteri M, Bacarea V (2010) Comparing groups for statistical differences: How to choose the right statistical test? Biochem Med 20(1):15–32
20. Mesin L, Holobar A, Merletti R (2011) Advanced methods of biomedical signal processing. IEEE Press, New York
21. Mezeiova K, Palus M (2012) Comparison of coherence and phase synchronization of the human sleep electroencephalogram. Clin Neurophysiol 123(9):1821–1830
22. Morin C, LeBlanc M, Daley M, Gregoire J, Mrette C (2006) Epidemiology of insomnia: prevalence, self-help treatments, consultations, and determinants of help-seeking behaviors. Sleep Med 7(2):123–130
23. Moroni F, Nobili L, Carli FD, Massimini M, Francione S, Marzano C, Proserpio P, Cipolli C, Gennaro LD, Ferrara M (2012) Slow EEG rhythms and inter-hemispheric synchronization across sleep and wakefulness in the human hippocampus. NeuroImage 60(1):497–504
24. Nikulin VV, Jnsson EG, Brismar T (2012) Attenuation of long-range temporal correlations in the amplitude dynamics of alpha and beta neuronal oscillations in patients with schizophrenia. NeuroImage 61(1):162–169
25. Noh K, Shin KS, Shin D, Hwang JY, Kim JS, Jang JH, Chung CK, Kwon JS, Cho KH (2013) Impaired coupling of local and global functional feedbacks underlies abnormal synchronization and negative symptoms of schizophrenia. BMC Syst Biol 7(30):1–13
26. Palva J, Palva S, Kaila K (2005) Phase synchrony among neuronal oscillations in the human cortex. J Neurosci 25(15):3962–3972
27. Palva S, Monto S, Palva JM (2010) Graph properties of synchronized cortical networks during visual working memory maintenance. NeuroImage 49(4):3257–3268
28. Palva S, Palva JM (2012) Discovering oscillatory interaction networks with M/EEG: challenges and breakthroughs. Trends Cogn Sci 16(4):219–230
29. Pereda E, Quiroga RQ, Bhattacharya J (2005) Nonlinear multivariate analysis of neurophysiological signals. Prog Neurobiol 77(12):1–37
30. Petrovsky N, Ettinger U, Hill A, Frenzel L, Meyhoefer I, Wagner M, Backhaus J, Kumari V (2014) Sleep deprivation disrupts prepulse inhibition and induces psychosis-like symptoms in healthy humans. J Neurosci 34(27):9134–9140
31. Pikovsky A, Rosenblum M, Kurths J (2003) Synchronization a universal concept in nonlinear sciences. Cambridge University Press, Cambridge
32. Sakkalis V, Giurcaneanu C, Xanthopoulos P, Zervakis M, Tsiaras V, Yang Y, Karakonstantaki E, Micheloyannis S (2009) Assessment of linear and nonlinear synchronization measures for analyzing EEG in a mild epileptic paradigm. IEEE Trans Inf Technol Biomed 13(4):433–441
33. Schaefer C, Rosenblum MG, Abel HH, Kurths J (1999) Synchronization in the human cardiorespiratory system. Phys Rev E 60:857–870
34. Staner L (2010) Comorbidity of insomnia and depression. Sleep Med Rev 14(1):35–46
35. Task Force of The European Society of Cardiology, The North American Society of Pacing and Electrophysiology (1996) Heart rate variability. Eur Heart J 17:354–381
36. Timashev SF, Panischev OY, Polyakov YS, Demin SA, Kaplan AY (2012) Analysis of cross-correlations in electroencephalogram signals as an approach to proactive diagnosis of schizophrenia. Phys A Stat Mech Appl 391(4):1179–1194

37. von Klitzing L (1991) Heart rate of man is phase-coupled to an encephaloelectric signal. In: Annual international conference of the IEEE engineering in medicine and biology society
38. Wacker M, Witte H (2011) On the stability of the n:m phase synchronization index. IEEE Trans Biomed Eng 58(2):332–338
39. Zalesky A, Fornito A, Seal ML, Cocchi L, Westin CF, Bullmore ET, Egan GF, Pantelis C (2011) Disrupted axonal fiber connectivity in schizophrenia. Biol Psychiatry 69:80–89

Appendix G

Peer-reviewed conference paper

Title: Sleep Onset Detection based on Time-Varying Autoregressive Models with Particle Filter Estimation

Authors: Ramiro Chaparro-Vargas, P. Chamila Dissanayaka, Thomas Penzel, Beena Ahmed and Dean Cvetkovic

Publication: Proceedings of the 3rd IEEE Conference on Biomedical Engineering and Sciences

Year of Publication: 2014

Sleep Onset Detection based on Time-Varying Autoregressive Models with Particle Filter Estimation

Ramiro Chaparro-Vargas[†1] *Member*, P. Chamila Dissayanaka[†2], Thomas Penzel[3], Beena Ahmed[4] *Member*, Dean Cvetkovic[†5] *Member*

***Abstract*— In this paper, we introduce a computer-assisted approach for the characterisation of sleep onset periods. The processing of polysomnographic (PSG) recordings involves the modelling of Time-Varying Autoregressive Moving Average (TVARMA) processes with recursive particle filtering. The feature set engages the computation of electroencephalogram (EEG) frequency bands δ, θ, α, ς, β, mean amplitude of electrooculogram (EOG) and electromyogram (EMG) signals. This is subsequently transferred to an ensemble classifier to detect Wake (W), non-REM1 (N1) and non-REM2 (N2) sleep stages. As a result, novel contributions in terms of non-Gaussian modelling of biosignal processes, approximation to PSG distributions with particle filtering and time-frequency analysis by complex Morlet wavelets within sleep staging, are discussed. The findings revealed performance metrics achieving in the best cases 93.18% accuracy, 6.82% error and 100% sensitivity/specificity rates.**

I. INTRODUCTION

The transition state between wakefulness and sleep is commonly referred to as the sleep onset period or hypnagogic state, which is characterised by an initial drowsiness that fades to complete loss of sensory awareness of the surroundings [1]. Over the past decades, clinical diagnosis supported on computational aids has claimed an increasing interest, due to the variety of subtle and alike cues in the process of falling asleep [2]. Electroencepahlogram (EEG), electrooculogram (EOG) and electromyogram (EMG) signals play a significant role to characterise the hallmarks in the transition from wake to sleep stages. The problem related to the staging and time resolution, accompanied by the non-Gaussian and non-linear nature of those signals hinders the estimation of accurate sleep onset models.

In the recent years, significant work has been done in automatic sleep staging, compromising processing and classification for the whole sleep cycle. Autoregressive processes have been recurrently used to model EEG signals, as the derived coefficients can be utilised for discriminative comparisons. For instance, Zhovna and Shallom in [3] proposed a multichannel autoregressive model to perform automatic detection and classification, incorporating information theory algorithms for the definition of sleep stages. Their results, at least in terms of accuracy, were quite appealing with over 90% rates. Although, the estimation of parameters through the minimisation of Yule-Walker equations and disregarding of additional monitoring channels apart from EEG, opens enough room for improvement. Later, Krakovská and Mezeiová [4] presented a collection of time-based, stochastic, spectral and chaotic features, concurrent with discriminant analysis-based classification to strive automatic sleep scoring. Their performance ratios achieved mean error rates from 50%, detecting non-REM1 (N1) stages, until 10% for slow wave sleep (SWS). The integration of EOG and EMG channels produced a stronger resilience to ambiguous responses by the classifier, however, the overcrowded set of features drew forth some concerns about their complexity and time efficiency. Koley and Dey introduced an ensemble system fed by a large collection of time domain, frequency domain and non-linear features with support vector machine (SVM) sub-classifiers upon a single EEG channel [5]. They reported average accuracy, sensitivity and specificity rates of 95.88%, 88.32% and 97.42%, respectively. Nonetheless, those rates were reduced by N1 recognition. Recently, Álvarez-Estévez et al. reported a novel method for automatic analysis of sleep macrostructure using the full set of PSG signals in a fuzzy reasoning classifier [6]. Here, the results attained 71% of sensitivity, 95.4% specificity and 93.4% accuracy. Once more, N1 detection affected overall performance, owing to Wake (W) and SWS misclassification.

In this paper, we introduce a computer-assisted sleep staging approach, customised to detect and characterise sleep onset periods. By following the recommendations of recognised scoring manuals, the system strives to estimate specific events for Wake (W), non-REM1 (N1) and non-REM2 (N2) sleep stages; in order to differentiate with high time-frequency resolution, the transition from awake to consolidated sleep. To overcome the non-Gaussian and non-linear constraints, we propose characterising the PSG signals by means of TVARMA processes [7], expressed in terms of state-space realisations and estimated by particle filtering [8]. The major innovations are focused on the estimation strategy addressed by recursive particle filtering, this impresses time-variant orientation, simultaneous handling of abrupt and slow-paced events and predictive signal construction. In addition, complex Morlet wavelet transformation as the central piece of spectral densities computation, inherits the benefits of Time-Frequency Analysis (TFA) with sharpening

[†] Authors affiliated to the School of Electrical and Computing Engineering RMIT Univesity, Melbourne VIC 3000, Australia

[1] E-mail: ramiro.chaparro-vargas@rmit.edu.au

[2] E-mail: s3315014@student.rmit.edu.au

[3] T. Penzel is with the Interdisciplinary Centre for Sleep Medicine, Charité Universitätsmedizin Berlin, Berlin D-10117, Germany thomas.penzel@charite.de

[4] B. Ahmed is with the Electrical and Computer Engineering Department, Texas A&M University, Doha, Qatar beena.ahmed@qatar.tamu.edu

[5] E-mail: dean.cvetkovic@rmit.edu.au

resolutions. Our findings foresee important applications to conduct sleep onset detection, assuming non-Gaussian, non-linear and non-stationary conditions; which suppose a current challenge in biomedical signal processing.

II. METHODS

Clinical data recorded from 10 healthy (HEA) subjects was used in this study. Each subject undertook an overnight PSG recording including EEG, EOG and EMG chin at the Interdisciplinary Centre for Sleep Medicine at the Charité Universitätsmedizin Berlin. The study was approved by the local ethic committee of the Charité Universitätsmedizin Berlin. Table I depicts related statistics of subjects' sleeping patterns.

Following the AASM manual for the scoring of sleep and associated events [9], each 30-second epoch was scored as Wake (W), Stage1 (N1), Stage2 (N2), Stage3 (N3) and Rapid Eye Movement (REM) by sleep specialists. An arrangement of monopolar EEG/EOG channels compliant with 10-20 international system was employed, including ECG, EMG Chin, LEMG, REMG, LEOG, REOG, C3A2, C4A1, O1A2, O2A1, F3A2, F4A1. The sleep onset period is defined as the progressive transition from W stage till the appearance of the first N1 epoch. However, such a definition is extended to the occurrence of epochs with consolidated sleep spindles—N2 stage event—as a clear indication of sleep onset completion to move towards a consistent sleep [1] [2].

A. Biosignal estimation

We defined the non-linear and non-Gaussian EEG, EOG and EMG signals in terms of a Time-Varying Autoregressive Moving Average process with model order p and q, corresponding to the autoregressive (AR) and moving average (MA) parts. The system dynamics are modelled by means of non-Gaussian state-space realisations to stress the adaptative computation of the state vector $\mathbf{x}[k]$, which contains the TVARMA coefficients. A recursive estimation of the state vector improves adaptation to abrupt changes in the EEG signals [10], thanks to a non-Gaussian distributed state noise process $\eta[k]$. The resulting PSG signal $\mathbf{y}[k]$ is estimated upon the arrival of past observations $\mathbf{A}$, a time-changing state vector $\mathbf{x}[k]$ and an independent identically distributed (i.i.d) Gaussian noise process $\nu[k]$. Thus, let define the state and observation model equations as Eq. 1-2 denote.

$$\mathbf{x}[k] = \mathbf{x}[k-1] + \eta[k] \tag{1}$$

$$\mathbf{y}[k] = \mathbf{A}\mathbf{x}[k] + \mathbf{x}^{\mathrm{H}}[k]\mathbf{B}\nu[k] \tag{2}$$

where $\mathbf{x}[k]$ is the estimated vector of TVARMA coefficients. The system noise vector $\eta[k]$ is divided in two terms $[\eta_{\mathbf{p}}[k]\ \eta_{\mathbf{q}}[k]]$ to distinguish AR and MA noise processes, where $\eta_{\mathbf{p}}$ is Cauchy distributed with zero translation and $\varsigma^2_{\eta_{\mathbf{p}}}$ dispersion, $\eta_{\mathbf{p}} \sim \mathscr{C}(0, \varsigma^2_{\eta_{\mathbf{p}}}\mathbf{I})$. Similarly, $\eta_{\mathbf{q}}$ is Gaussian distributed with zero mean and $\sigma^2_{\eta_{\mathbf{q}}}$ variance, $\eta_{\mathbf{q}} \sim \mathscr{N}(0, \sigma^2_{\eta_{\mathbf{q}}}\mathbf{I})$. Respectively, $\mathbf{y}[k]$ represents the estimated signal, accompanied by $\mathbf{A}$ and $\mathbf{B}$ matrices in Eq. 3-4 to perform the weighted linear combinations. Lastly, $\nu[k]$ is the Gaussian distributed observation noise with zero mean and σ^2_{ν} variance, $\nu \sim \mathscr{N}(0, \sigma^2_{\nu}\mathbf{I})$. The Cauchy distribution introduced for the state noise is characterised by heavy-tailed deviations at both extremes to predict sudden fluctuations and fastened spreading at the middle region to handle smooth variations [11].

$$\mathbf{A} = [\mathbf{y}[k-1], \cdots, \mathbf{y}[k-p] | 0, \cdots, 0] \tag{3}$$

$$\mathbf{B} = \begin{bmatrix} \mathbf{0}_{p\times p} & \mathbf{0} \\ \mathbf{0} & \mathbf{I}_{(q+1)\times(q+1)} \end{bmatrix} \tag{4}$$

The estimation of the TVARMA coefficients set in $\mathbf{x}[k]$ is attained by recursive filtering of two stages: prediction and update. The former approximates the state probability density function (pdf) from one current observation to the next one moving forward; the latter makes use of the latest measurement to overwrite the prediction pdf. Such an estimation problem only requires to sequentially determine expectation vectors and covariance matrices of conditional distributions, applying the well-known Bayes theorem [12]. This type of filter is commonly known as particle filter, which employs a large set of samples or particles to approximate non-linear and non-Gaussian time series, e.g. EEG signals [10]. On this way, the estimated new measurements $\mathbf{y}[k]$ are generated attending to non-Gaussian state vectors $\mathbf{x}[k]$ with model orders $p = 8$ and $q = 2$, following the Akaike (AIC) and Bayesian Information Criterion (BIC). As well as, incoming past observations contained in $\mathbf{A}$ vector and $\mathbf{B}$ as selection matrix.

B. Features estimation

From the estimated signal $\mathbf{y}[k]$, a total of 9 features are extracted, in order to characterise the three initial sleep stages associated to sleep onset: W, N1 and N2 [13]. Those features quantify 6 EEG power spectral densities (PSD), 1 EEG amplitude envelope, 1 EOG average amplitude and 1 EMG chin mean amplitude. The abbreviation, source channel and related events are summarised in Table II.

The six EEG PSD are computed using a wavelet-based decomposition, which performs the transformation upon the original EEG signal with a complex Morlet kernel, as shown in Eq. 5 [14] [15]. This approach intends to surmount the disadvantages usually attributed to Fourier-based transformations [16]. By setting central frequencies ω_0 and bandwidths $\sigma^2_{t_k}$ for each EEG band, the presence of δ to β oscillations are observed within a high resolution time-frequency window [17]. The feature related to EEG amplitude envelope calculates the cumulative sum of local maximas, aiming to detect the dense occurrence of fast time-varying events, such as vertex shape waves (VSW) and K complexes. In regard to the remaining EOG and EMG chin channels, mean amplitudes are derived, whereas slow eye movements (SEM) and chin relaxation are common indications of W and N1 appearance, respectively.

$$\psi(t_k) = (\mathbf{e}^{\imath\omega_0 t_k} - \mathbf{e}^{\frac{-\omega_0^2\sigma^2_{t_k}}{2}})\mathbf{e}^{-\frac{\imath^2}{2\sigma^2_{t_k}}} \tag{5}$$

TABLE I

SUMMARY OF SUBJECT AND TECHNICAL DETAILS OF PSG RECORDINGS

Variable	Healthy (HEA)										Mean ± SD*
Subject ID	HEA1	HEA2	HEA3	HEA4	HEA5	HEA6	HEA7	HEA8	HEA9	HEA10	
Gender	m†	m	m	m	m	m	m	m	m	m	
N1 Latency (min)	10.5	11.5	6.9	6.4	18.6	164.8	6.1	137	16.8	138.7	51.73±66.17
N2 Latency (min)	14.5	12.5	14.4	9.4	9.1	167.3	12.1	149	20.3	140.7	54.93±67.59
SWS Latency (min)	21	58.5	109.9	23.4	16.1	168.8	23.6	142.5	31.3	154.7	74.98±62.18
REM Latency (min)	246.5	302.5	147.5	66	70	148.5	107	57	90.5	56	129.15±84.7
Wake (%)	8.4	34	7.9	10.2	4.5	14.1	3.5	4.6	8.7	5.6	10.15±8.96
N1 (%)	26.4	10.3	24.3	17.4	10.9	9.2	6	10.3	7.5	9	13.13±7.11
N2 (%)	43.8	28.1	31.6	14.6	47.5	34.2	44.7	34.8	33.8	33.7	34.68±9.46
SWS (%)	20.2	16.1	14.2	39.7	16.9	30.4	28.1	33.1	27.2	34.1	26±8.71
REM (%)	1.2	11.5	22	18.1	20.2	12.1	17.7	17.2	22.8	17.6	16.04±6.37
Sleep efficiency (%)	91.6	66	90.8	89.8	94	85.9	94.6	95.4	91.3	94.4	89±9

∗ SD = Standard deviation

† m = male

C. Classification

Our approach exploits the capabilities of an ensemble classifier to differentiate the three sleep stages related to sleep onset periods; i.e. W, N1 and N2 [18]. Then, the training as same as the testing data are selected out of the pool of manually scored epochs, resembling those stages. The ensemble classifier takes hundreds to thousands of weak sub-classifiers to generate a more comprehensive classifier to deal with non-stationary conditions over time—i.e. concept drift—and overestimated predictions [19]. Our ensemble classifier employs 300 tree-type sub-classifiers to allocate incoming feature into three possible categories: W, N1 and N2, as depicted in Figure 1. Lastly, the classifier was evaluated using leave-one-out (LOO) scheme, where only one subject's data at a time are used for testing, whilst the remainder subjects' datasets are used to train the classifier.

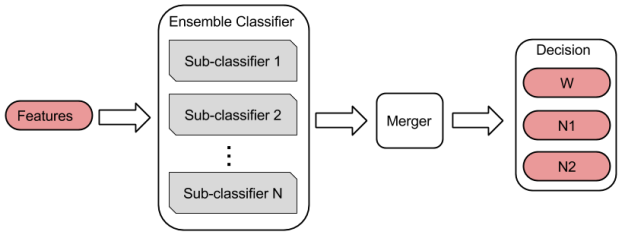

Fig. 1. Diagram of ensemble classifier. The epoch's features act as inputs to 300 tree-type sub-classifiers, followed by a merger to produce an unambiguous decision either as W, N1 or N2 stage.

D. Procedure

The experimental procedure consisted of the random selection of 75 training 30-second epochs per clinical subject. The definition of the sample size for the training data was in consequence with the sensitivity response of the classifier; the specifications of this technique are described in [20]. The epochs related to N2 latency in Table I for each subject were chosen to represent the testing data for the ensemble classifier. Once, training and testing epochs sets were conformed, one pilot epoch of each stage was used to determine the TVARMA$(8,2)$ coefficients by recursive filtering. Ultimately, the extraction of the aforementioned features was conducted, considering the PSG channels: EEG C3/A2, left EOG and EMG chin.

III. RESULTS

It is noteworthy to stress the key role of the particle filter in estimating the TVARMA$(8,2)$ coefficients by setting 300 particles and 2000 runs. Likewise, the EEG features designated to characterise W/N1/N2 stages, based on their δ, θ, α and ς spectral content, contributed to the staging differentiation.

Figure 2 depicts an example of one W epoch with its original waveform, estimated observation by the particle filter approximation, and the derived periodogram as output of the wavelet decomposition. The stacked densities of spectral power are an irrefutable proof of the convenience of EEG frequency-based features to characterise the sleep onset-related epochs. For instance, the dominant presence of α band with scattered sparkles of δ and θ oscillations, understood as combined low frequency activity, are recognised as W stage by the AASM manual [9].

TABLE II

FEATURES FOR SLEEP ONSET ESTIMATION

Feature	Channel	Event/Freq. Band (Hz)
PSD_δ	EEG C3	$0.5-2$ Hz
PSD_θ	EEG C3	$4-7$ Hz
PSD_α	EEG C3	$8-12$ Hz
PSD_ς	EEG C3	$11-15$ Hz
PSD_β	EEG C3	$16-32$ Hz
Amp_{EEG}	EEG C3	Vertex Shape Waves, K Complex
Amp_{EOG}	LEOG	Slow Eye Movement
Amp_{EMG}	EMG Chin	Movement

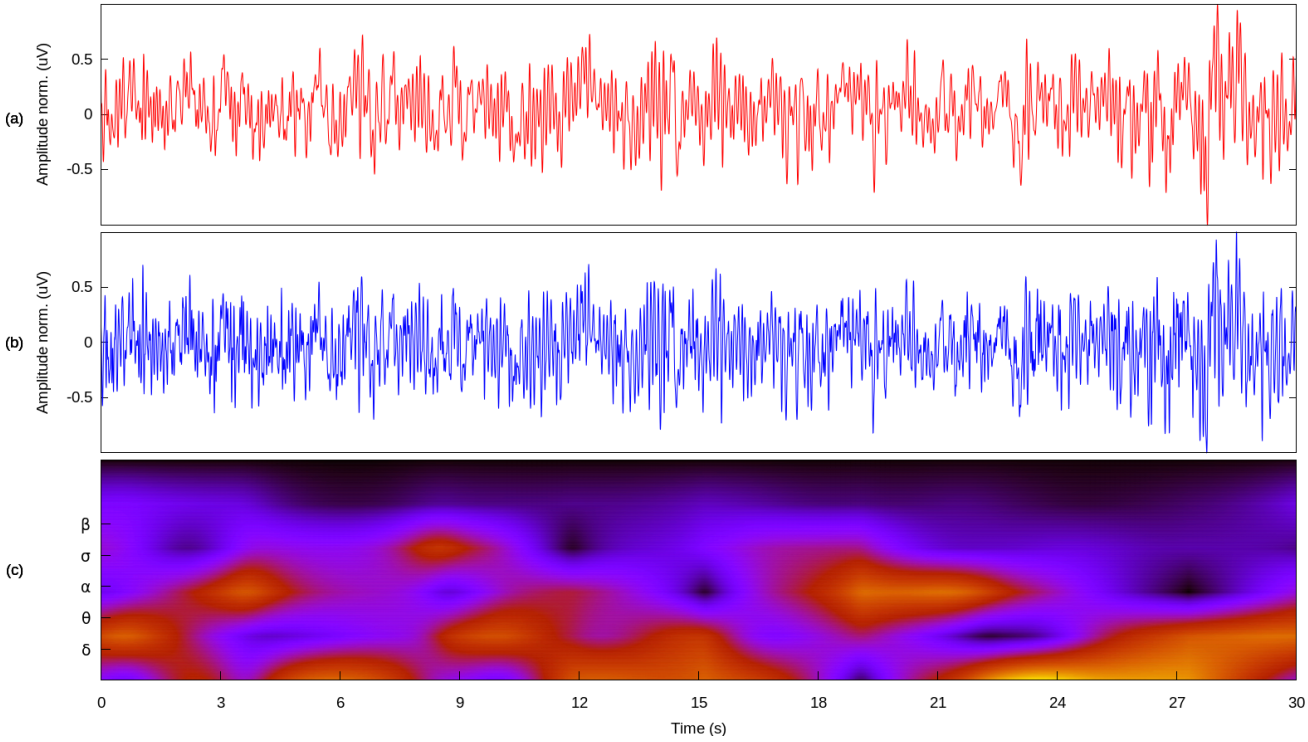

Fig. 2. Example of a 30-second EEG Wake epoch. (a) Original EEG signal recorded by C3 electrode (normalised amplitude). (b) Estimated TVARMA(8,2) EEG C3 signal by particle filter approximation (normalised amplitude). (c) Periodogram of power spectral densities with 30-second time length on x-axis versus δ, θ, α, ς and β frequency bands on y-axis. The colour-scale sets black-blue range as low power moving to red-yellow to represent high power densities.

In comparison to single EEG channel classification, adding the TVARMA coefficients and estimated features from the EOG and EMG signals to the classifier, led to an improvement in the accuracy between $6-18\%$, depending on the subject. Precisely, Figure 3 and 4 illustrate the approximated distributions processed from the EOG and EMG electrodes. The estimated distributions reinforced the pertinence of particle filtering to track either slow changes as high frequency activity. Once more, the approximation to the original time series distribution bore an outstanding likelihood to represent either slow time-varying events; e.g. slow eye movements (SEM), or pulse-type phenomena like spontaneous muscular movements with high frequency background. Table III depicts the example epochs' Root Mean Square Error (RMSE), which is a traditional measure of performance in filtering. In previous works [10] [21], some typical RMSE values reported for simulated chaotic systems were located between 10^{-3} to 6 units, depending on the number of particles and runs. Our approach held similar or even better values to confirm its application upon EEG, EOG and EMG signals.

Table IV presents the accuracy, error, sensitivity and specificity rates for each clinical subject, following a LOO scheme. Overall, the inverse proportional between accuracy and error rates exhibited mostly good results, reaching 93.18% as the best accuracy value and 50% as the less appealing for subject HEA4. Even more comforting are the sensitivity rates, since most of the subjects demonstrated

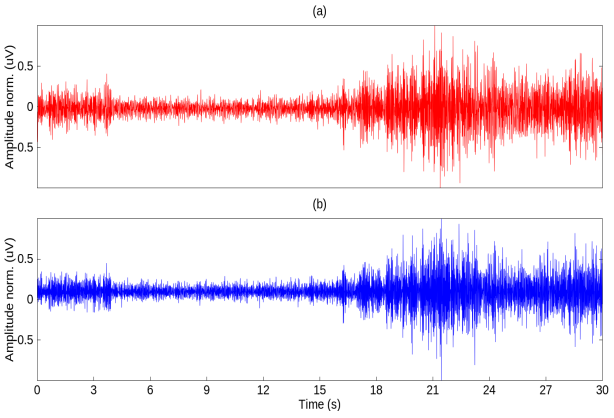

Fig. 3. Example of a 30-second EMG N1 epoch. (a) Original EMG signal recorded by chin electrode (normalised amplitude). (b) Estimated TVARMA(8,2) EMG chin signal by particle filter approximation (normalised amplitude).

TABLE III
RMSE FOR CHANNELS AND STAGES

Channel	W	N1	N2
EEG C3	0.0837	0.0204	0.0294
Left EOG	0.0580	0.0163	0.0169
EMG chin	0.1277	0.0914	0.5346

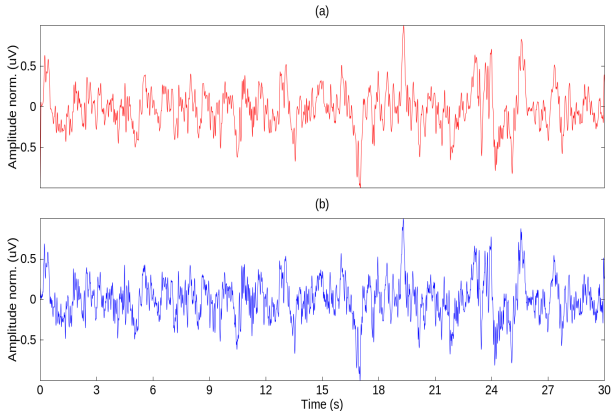

Fig. 4. Example of a 30-second EOG N2 epoch. (a) Original EOG signal recorded by left outer canthus electrode (normalised amplitude). (b) Estimated TVARMA(8,2) left EOG signal by particle filter approximation (normalised amplitude).

values from 85% till 100%, except for subjects HEA4 and HEA5 with 75% and 66.67%, respectively. This confirmed the adopted strategy in the selection of the training/testing sample size; as well as, the classifier efficiency to distinguish W epochs from the remaining stages, given that the amount of those epochs was considerably higher than N1/N2 during the first sleep cycle. However, the specificity was much lower, subjects HEA9 and HEA10 reached 22.24% and 0%, respectively. The reason for this underlies in the classifier's inter-subject misinterpretation of W and N1 stages, which traditionally had borne the degradation in computer-aided systems for sleep staging [3] [4] [22].

IV. DISCUSSION AND CONCLUSIONS

The characterisation of the sleep onset period was the primal aim of the research work that we have described. Usually, its dynamic starts at wakefulness, goes through N1, and finishes with N2 stage establishment [23] [24]. Those stages gather diverse physiological events, for instance, mixing frequency bands, instantaneous time-changing and slow-paced driving transitions, amongst others [2]. Here, we presented a novel approach supported on biomedical signal processing to accurately parameterise such events, expressed by EEG bands, VSW, sleep spindles, K-complexes, eye movements, etc. The first major contribution was the adoption of the state-space realisation for TVARMA processes, which coped with the typical constraints of PSG signals representation, like time-varying analysis and mathematical tractability [16]. Furthermore, the incorporation of recursive particle filtering as estimation method embodied the cornerstone to deal with non-Gaussian and non-linear limitations. Since, the oversight of those conditions in further processing and classification stages might lead to a weak characterisation, and then staging misinterpretation [8].

The TVARMA(8,2) model with particle filter estimation confirmed its efficiency to represent time and frequency-dependent events upon EEG, EOG and EMG signals. The advantage resided in the adaptability of the model to dynamically estimate the time-varying coefficients, engaging 8 AR and 2 MA coefficients. This fact suggested a competitive technique to estimate with statistical accuracy posterior distributions with non-Gaussian and non-linear properties; whilst parallel, scalable and computational burden aspects can be managed [11]. Foremost, we postulated the usage of complex Morlet-based wavelet transform for the computation of spectral contents within EEG signals. By that, we improved time-frequency resolution, whereas slow and time-varying events became equivalently traceable. As far we know, none previous works have implemented a biomedical signal processing aid of this kind to be applied within sleep studies. Albeit, some reports about advances in event-related synchronisation/desynchronisation (ERS/ERD) studies [11] [25] described some foundations to new scenarios in neurophysiology, and sleep staging concretely.

In regard to classification, accuracy and error rates indicated a comprehensive performance to detect sleep onset periods amongst the 10 clinical subjects. The capability of the ensemble classifier to differentiate W stage was better than another, because hypnagogic episodes commonly had a larger number of these kind of epochs. Foremost, the correct classification of N2 stages was enhanced by the detection of sleep spindles (i.e. ς band events), smoother EEG amplitudes and EOG/EMG potentials. However, the sensitivity and specificity metrics did set alarms on N1 stage classification; since, the low and medium rates were observed in subjects with higher N1 density. Conventionally, N1 scoring is one of the most difficult tasks in classification, due to the sort of events simultaneously happening, e.g. δ, θ, α activity, VSW, ripples, flattening and truncated spindles [2]. Then, some generated features tended to be misinterpreted by the ensemble classifier that is not following an empirical or rule-based classification model, which might be more suitable for sleep staging. Undoubtedly, this point will be a crucial flank of improvement in the future research.

Even though, most sleep staging systems promoted as computer-assisted platforms were oriented to the detection of the whole sleep cycle, instead of sleep onset periods; our findings are subject of comparison using the same performance metrics. For example, similar behaviour was obtained with respect to the average 90% accuracy rate in [6]. Also, our sensitivity and specificity were slightly behind Zhovna [3] and Koley [5] performance rates, when W/N1/N2 sleep stages concerned.

In conclusion, our approach dedicated to assist the detection of sleep onset periods, posited a robust mechanism for PSG signals estimation, attending to non-Gaussian and non-linear constraints from neuronal, ocular and muscular sources. The encountered findings allow us to endorse this approach as an efficient model to conduct sleep staging procedures based on time-variance awareness and online-oriented analysis. For that reason, the future efforts envisage the refinement of classification methods, including rule-based discrimination, as well as, differentiation of associated disorders.

TABLE IV

PERFORMANCE METRICS OF ENSEMBLE CLASSIFIER

Metric	HEA1	HEA2	HEA3	HEA4	HEA5	HEA6	HEA7	HEA8	HEA9	HEA10	Mean±SD
Accuracy (%)	80.77	86.61	63.64	50	64.71	**93.18**	63.41	84	79.55	**92.34**	75.82±14.49
Error (%)	19.23	13.33	36.36	50	35.29	**6.82**	36.59	16	20.45	**7.66**	24.17±14.49
Sensitivity (%)	85.71	95.65	92.31	75	66.67	95.14	**100**	87.5	**100**	93.20	89.12±10.85
Specificity (%)	60	100	44.44	58.52	100	100	51.72	50	22.27	0	58.7±33.7

ACKNOWLEDGEMENT

The work was supported by NPRP grant #[5-1327-2-568] from the Qatar National Research Fund, which is a member of Qatar Foundation. The statements made herein are solely the responsibility of the authors.

The authors would like to thank the Interdisciplinary Centre for Sleep Medicine at the Charité Universitätsmedizin Berlin (Germany) for undertaking the recruitment and collection of polysomnographic recordings, as well as, the sleep scorers dedicated to the assessment labours. Both parties served as the main experimental source for the present research work.

R. Chaparro-Vargas acknowledges the financial support of the alliance COLCIENCIAS and COLFUTURO foundation of the Colombian Government, as main sponsor of his doctorate studies.

REFERENCES

[1] C. Marzano, F. Moroni, M. Gorgoni, L. Nobili, M. Ferrara, and L. D. Gennaro, "How we fall asleep: regional and temporal differences in electroencephalographic synchronization at sleep onset," *Sleep Medicine*, vol. 14, no. 11, pp. 1112 – 1122, 2013.

[2] R. D. Ogilvie, "The process of falling asleep," *Sleep Medicine Reviews*, vol. 5, no. 3, pp. 247–270, 2001.

[3] I. Zhovna and I. D. Shallom, "Automatic detection and classification of sleep stages by multichannel EEG signal modeling," in *Engineering in Medicine and Biology Society, 2008. EMBS 2008. 30th Annual International Conference of the IEEE*, aug. 2008, pp. 2665 –2668.

[4] A. Krakovská and K. Mezeiová, "Automatic sleep scoring: A search for an optimal combination of measures," *Artificial Intelligence in Medicine*, vol. 53, no. 1, pp. 25 – 33, 2011.

[5] B. Koley and D. Dey, "An ensemble system for automatic sleep stage classification using single channel EEG signal," *Computers in Biology and Medicine*, vol. X, no. 0, pp. 1 – 10, 2012.

[6] D. Álvarez-Estévez, J. M. Fernández-Pastoriza, E. Hernández-Pereira, and V. Moret-Bonillo, "A method for the automatic analysis of the sleep macrostructure in continuum," *Expert Systems with Applications*, vol. 40, no. 5, pp. 1796 – 1803, 2013.

[7] R. Prado, "Sequential estimation of mixtures of structured autoregressive models," *Computational Statistics & Data Analysis*, vol. 58, no. 0, pp. 58 – 70, 2013.

[8] G. Kitagawa, *Introduction to Time Series Modeling*. CRC Press, 2009, ch. Analysis of Time Series with a State-Space Model, pp. 1–16.

[9] C. Iber, S. Ancoli-Israel, A. L. C. Jr., and S. F. Quan, "The AASM manual for the scoring of sleep and associated events," American Academy of Sleep Medicine, Tech. Rep., 2007.

[10] M. Arulampalam, S. Maskell, N. Gordon, and T. Clapp, "A tutorial on particle filters for online nonlinear/non-gaussian bayesian tracking," *Signal Processing, IEEE Transactions on*, vol. 50, no. 2, pp. 174–188, Feb 2002.

[11] C.-M. Ting, S.-H. Salleh, Z. Zainuddin, and A. Bahar, "Spectral estimation of nonstationary EEG using particle filtering with application to event-related desynchronization (ERD)," *IEEE Transactions on Biomedical Engineering*, vol. 58, no. 2, pp. 321–331, 2011.

[12] D. Gencaga, E. E. Kuruoglu, and A. Ertüzün, "Modeling non-Gaussian time-varying vector autoregressive processes by particle filtering," *Multidimensional Systems and Signal Processing*, vol. 21, no. 1, pp. 73–85, 2010.

[13] E. Pereda, R. Q. Quiroga, and J. Bhattacharya, "Nonlinear multivariate analysis of neurophysiological signals," *Progress in Neurobiology*, vol. 77, no. 12, pp. 1 – 37, 2005.

[14] S. Mallat, *A Wavelet Tour of Signal Processing*. Elsevier Academic Press, 1999.

[15] L. Mesin, A. Holobar, and R. Merletti, *Advanced Methods of Biomedical Signal Processing*, S. Cerutti and C. Marchesi, Eds. IEEE Press, 2011.

[16] N. V. Thakor and S. Tong, "Advances in quantitative electroencephalogram analysis method," *Annual Review of Biomedical Engineering*, vol. 6, no. 1, pp. 453–495, 2004.

[17] P. Stoica and R. Moses, *Spectral analysis of signals*, T. Robbins, Ed. Pearson Prentice Hall, 2005.

[18] C. Alippi, G. Boracchi, and M. Roveri, "Just-in-time classifiers for recurrent concepts," *Neural Networks and Learning Systems, IEEE Transactions on*, vol. 24, no. 4, pp. 620–634, April 2013.

[19] D. Brzezinski and J. Stefanowski, "Reacting to different types of concept drift: The accuracy updated ensemble algorithm," *Neural Networks and Learning Systems, IEEE Transactions on*, vol. 25, no. 1, pp. 81–94, Jan 2014.

[20] C. Beleites, U. Neugebauer, T. Bocklitz, C. Krafft, and J. Popp, "Sample size planning for classification models," *Analytica Chimica Acta*, vol. 760, no. 0, pp. 25 – 33, 2013.

[21] P. M. Djuric, J. H. Kotecha, F. Esteve, and E. Perret, "Sequential parameter estimation of time-varying non-gaussian autoregressive processes," *EURASIP Journal on Advances in Signal Processing*, vol. 2002, no. 8, p. 262156, 2002.

[22] E. Estrada, H. Nazeran, F. Ebrahimi, and M. Mikaeili, "EEG signal features for computer-aided sleep stage detection," in *Neural Engineering, 2009. NER '09. 4th International IEEE/EMBS Conference on*, 29 2009-may 2 2009, pp. 669 –672.

[23] A. Rodenbeck, R. Binder, P. Geisler, H. Danker-Hopfe, R. Lund, F. Raschke, H.-G. Wee, and H. Schulz, "A review of sleep EEG patterns. Part I: A compilation of amended rules for their visual recognition according to Rechtschaffen and Kales," *Somnologie*, vol. 10, no. 4, pp. 159–175, 2006.

[24] H. Danker-Hopfe, P. Anderer, J. Zeitlhofer, M. Boeck, H. Dorn, G. Gruber, E. Heller, E. Loretz, D. Moser, S. Parapatics, B. Saletu, A. Schmidt, and G. Dorffner, "Interrater reliability for sleep scoring according to the Rechtschaffen & Kales and the new AASM standard," *Journal of Sleep Research*, vol. 18, no. 1, pp. 74–84, 2009.

[25] J. Lee and K. Chon, "Time-varying autoregressive model-based multiple modes particle filtering algorithm for respiratory rate extraction from pulse oximeter," *Biomedical Engineering, IEEE Transactions on*, vol. 58, no. 3, pp. 790–794, March 2011.

Appendix H

Peer-reviewed conference paper

Title: Automated Sleep Onset Detection: An Approach based on Time-Frequency Estimation and Fuzzy Inference

Authors: Ramiro Chaparro-Vargas, Thomas Penzel, Beena Ahmed and Dean Cvetkovic

Publication: Proceedings of the 11th Annual Scientific Meeting of Australian Chronobiology Society

Year of Publication: 2014

Chapter 5

Automated Sleep Onset Detection: An Approach based on Time-Frequency Estimation and Fuzzy Inference

Chaparro-Vargas R[a], Penzel T[b], Ahmed B[c], Cvetkovic D[a]

[a] *School of Electrical and Computing Engineering RMIT University, Melbourne VIC 3000, Australia*

[b] *Interdisciplinary Centre for Sleep Medicine, Charite Universitaetsmedizin Berlin, Berlin D-10117, Germany*

[c] *Electrical and Computer Engineering Department, Texas A&M University, Doha, Qatar*

We introduce an automated approach for the characterisation of sleep onset periods. The processing of polysomnogram (PSG) recordings involves the modelling of Time-Varying Autoregressive Moving Average (TVARMA) processes with recursive particle filtering. The selected features involve electroencephalogram (EEG) frequency bands d, q, a, V, b, mean amplitude of electrooculogram (EOG) and electromyogram (EMG) signals, which are further transferred to a fuzzy inference system to detect Wake (W), non-REM1 (N1) and non-REM2 (N2) sleep stages. Thus, novel contributions in terms of non-Gaussian/non-linear modelling of biosignal processes and rule-based intuitive sleep staging, are discussed. The findings revealed performance metrics achieving in the best cases 77% accuracy, 94% sensitivity and 96% specificity rates

Citation: Chaparro-Vargas R, Penzel T, Ahmed B, Cvetkovic D (2015). Automated Sleep Onset Detection: An Approach based on Time-Frequency Estimation and Fuzzy Inference. In: Kennedy G, Sargent C (Eds). The Time of Your Life. Australasian Chronobiology Society, Melbourne, Australia, pp. 25-31.

The progression from awake to asleep the state is commonly known as the sleep onset period (SOP) or hypnagogic state, which is triggered by drowsiness moving towards a complete loss of sensory awareness of the surroundings [1]. The reduction of diagnosis time windows and inter-raters' reliability are common points of interest when automated systems are integrated as part of the medical treatment repertoire. Due to the variety of subtle and alike cues across the process of falling sleep [2], the engagement of advanced computational resources in the simultaneous of polysomnogram (PSG) recordings, i.e. electroencephalogram (EEG), electrooculogram (EOG) and electromyogram (EMG) signals turn crucial to characterise the hallmarks in the transition from wake to sleep stages. The aspects linked to the staging and time resolution, accompanied by the non-Gaussian and non-linear constraints of those signals hinder the estimation of accurate SOP.

*Address correspondence to: Ramiro Chaparro-Vargas School of Electrical and Computing Engineering RMIT University, Melbourne VIC 3000, Australia. E-mail: ramiro.chaparro-vargas@rmit.edu.au

In the last decades, a variety of important advances have been devoted to automatic sleep staging without paying specific attention to SOP detection, though. For example, Koley and Dey [3] introduced an ensemble system fed by time, frequency domain and non-linear features with support vector machine (SVM) sub-classifiers upon a single EEG channel. They reported average accuracy, sensitivity and specificity rates of 95.88%, 88.32% and 97.42%, respectively. However, the performance rates were negatively impacted by poor non-REM1 stage recognition. Recently, Alvarez-Estevez et al. [4] presented an automatic method for the analysis of sleep macrostructure using the full set of PSG signals in a fuzzy reasoning classifier. Here, the achieved results were 71% of sensitivity, 95.4% specificity and 93.4% accuracy. Once more, non-REM1 detection affected general performance, due to wake and slow wave misinterpretation. Despite of the myriad of research works on this direction, we consider that suggesting a sort of competition between human-made and computer-aided scoring does not entitle a major relevance whilst inter-raters' agreements set around 70-75%. Several studies [5-7] revealed rates of common agreement below 76% amongst sleep scorers' of diverse backgrounds. Therefore, the performance comparisons to be presented should be taken as mere quantitative performance indicators. The actual impact underlies the overall characterisation of SOP with their associated stage-by-stage events.

In this paper, our aim is to introduce a computer assisted approach to perform sleep staging in the characterisation of SOP. Following the guidelines of standardised scoring manuals [8], our approach estimates specific events belonging to Wake (W), non-REM1 (N1) and non-REM2 (N2) sleep stages. We propose characterising the PSG signals by means of Time Varying Autoregressive Moving Average (TVARMA) processes [9], estimated by recursive particle filtering to surmount non-Gaussian and non-linear conditions [10]. The particle filtering impresses time-variant orientation, hence simultaneous detection of abrupt and slow-paced events, is possible. In addition, the classification scheme supported by fuzzy logic addresses the decision making process to a logical relationship amongst user-defined rule set. Our findings allow us to posit the automated sleep onset detection approach as a novel model that leverages biomedical signal processing and sleep studies.

Methods

In this study, clinical PSG data recorded from 10 healthy (HEA) subjects were utilised in the analysis. Each subject undertook an overnight PSG recording at the Interdisciplinary Centre for Sleep Medicine at the Charite Universitaetsmedizin Berlin. The study was approved by the local Ethics Committee of the Charite Hospital. Table I depicts related statistics of subjects' sleeping patterns. Following the AASM manual for the scoring of sleep stages and associated events [8], each 30-second epoch was scored as Wake, non-REM1, non-REM2, non-REM3 and Rapid Eye Movement (REM) by sleep specialists. An arrangement of monopolar EEG/EOG/EMG channels compliant with 10-20 international system was employed, including ECG, EMG chin, left EMG, right EMG, left EOG, right EOG, C3A2, C4A1, O1A2, O2A1, F3A2, F4A1. The SOP is conventionally defined as the progressive transition from W stage till the appearance of the first N1 epoch. However, we extended such a definition to the occurrence of epochs with consolidated sleep spindles—N2 stage event—as a clear indication of sleep onset completion to move towards a consistent sleep [1-2].

A. Biosignal and features estimation The processing of PSG signals compromises two major tracks: biosignal estimation and feature extraction. The former builds an approximation model for each PSG signal, in order to facilitate mathematical tractability

TABLE I
SUMMARY OF SUBJECT AND TECHNICAL DETAILS OF PSG RECORDINGS

Variable	Healthy (HEA)										Mean ± SD*
Subject ID	HEA1	HEA2	HEA3	HEA4	HEA5	HEA6	HEA7	HEA8	HEA9	HEA10	
Gender	m†	m	m	m	m	m	m	m	m	m	
N1 Latency (min)	10.5	11.5	6.9	6.4	18.6	164.8	6.1	137	16.8	138.7	51.73±66.17
N2 Latency (min)	14.5	12.5	14.4	9.4	9.1	167.3	12.1	149	20.3	140.7	54.93±67.59
SWS Latency (min)	21	58.5	109.9	23.4	16.1	168.8	23.6	142.5	31.3	154.7	74.98±62.18
REM Latency (min)	246.5	302.5	147.5	66	70	148.5	107	57	90.5	56	129.15±84.7
Wake (%)	8.4	34	7.9	10.2	4.5	14.1	3.5	4.6	8.7	5.6	10.15±8.96
N1 (%)	26.4	10.3	24.3	17.4	10.9	9.2	6	10.3	7.5	9	13.13±7.11
N2 (%)	43.8	28.1	31.6	14.6	47.5	34.2	44.7	34.8	33.8	33.7	34.68±9.46
SWS (%)	20.2	16.1	14.2	39.7	16.9	30.4	28.1	33.1	27.2	34.1	26±8.71
REM (%)	1.2	11.5	22	18.1	20.2	12.1	17.7	17.2	22.8	17.6	16.04±6.37
Sleep efficiency (%)	91.6	66	90.8	89.8	94	85.9	94.6	95.4	91.3	94.4	89±9

∗ SD = Standard deviation
† m = male

and simultaneous representation of fast and slow time-varying events; such as vertex shapes waves (VSW), K complex (KC), sleep spindles (SS), slow eye movements (SEM), etc. By the adoption of TVARMA processes with model order p and q, the biosignals dynamics are modeled subject to non-Gaussian and non-linearity constraints. Those conditions represent an important challenge in biomedical signal processing, since underlying information is likely to be omitted when statistical Gaussianity and linearity are assumed. For clarity purposes, we define TVARMA processes by means of non-Gaussian state-space realizations [11], which allow us to describe the dynamics of a PSG signal with two model equations, i.e. state and observation, denoted by Eq. 1-2.

$$x[k] = x[k-1]+\eta[k] \quad (1)$$
$$y[k] = Ax[k]+x^{H}[k]B\nu[k] \quad (2)$$

Where x[k] is the estimated vector of TVARMA coefficients. The system noise vector η[k] is divided in two terms [η_p[k] η_q[k]] to distinguish AR and MA noise processes, where η_p is Cauchy distributed with zero translation and $\varsigma^2_{\eta p}$ dispersion, $\eta_p \sim \mathbf{C}(0,\varsigma^2_{\eta p}\mathbf{I})$. Similarly, η_q is Gaussian distributed with zero mean and $\sigma^2_{\eta q}$ variance, $\eta_q \sim \mathbf{N}(0,\sigma^2_{\eta q}\mathbf{I})$. In turn, y[k] represents the estimated biosignal, accompanied by A and B matrices to perform weighted linear combinations. Lastly, ν[k] is the Gaussian distributed observation noise with zero mean and σ^2_{ν} variance, $\nu \sim \mathbf{N}(0; \sigma^2_{\nu}\mathbf{I})$. It is noteworthy the introduction of the Cauchy distribution for the state noise, which is characterised by heavy-tailed deviations at both extremes to predict sudden fluctuations and fastened spreading at the middle region to handle smooth variations [12]. The estimation of the TVARMA coefficients contained in x[k] is attained by a recursive particle filter using a large set of samples or particles to approximate the non-Gaussian and non-linear biosignal, denoted as y[k].

The feature extraction track makes use of the estimated y[k] signal to compute a set of 16 features; including EEG relative power spectral densities (rPSD) and EOG/EMG mean amplitudes. In detail, the extracted features are: δ rPSD, θ rPSD, α_1 rPSD, α_2 rPSD, ς_1 rPSD, ς_2 rPSD, β_1 rPSD, β_2 rPSD, β_3 rPSD, count of VSW, count of KC, EOG count of peaks, EOG mean amplitude, EMG tibialis count of peaks, EMG chin mean amplitude and previous scored stage (explained in classification section). The PSD are computed using a complex Morlet wavelet transformation, which performs decomposition upon the original EEG signal to produce the aforementioned EEG bands [13]. Each absolute PSD value is normalised by the total EEG power density to generate the relative

power features. This approach ameliorates the disadvantages commonly encountered with Fourier-based transformations. The feature related to count sleep events (i.e. VSW and KC) computes the cumulative sum of local maximas or peaks. In regard to the remaining EOG and EMG channels, mean amplitudes are derived applying a conventional average operation.

B. Classification The final classification track exploits the capabilities of a Mamdani fuzzy inference system (FIS) to unambiguously differentiate the sleep stages related to SOP: W, N1 and N2. Our FIS employs the 16 extracted features to produce a logical ruleset, assigning a unique sleep stage to each epoch. The implemented ruleset follows the guidelines outlined in AASM manual for sleep scoring [8] and additional smoothing-type amendments based on the experience of trained scorers. The sixteenth feature, known as previous scored stage, is used for the FIS as a feedback input to make the present decision attending to the previous outcome, shielding the system against odd transitions in sleep progression, e.g. W-N2-W outcomes. The output consists of one automated hypnogram characterising the transition from wakefulness to sleep consolidation, i.e. SOP.

Results

The conducted experimental protocol is explained as follows. From the 10 subjects' hypnograms yielded by manual scoring, the SOP contained in the first sleep cycle was taken for further automated processing and classification. Each 30-second epoch associated to the SOP passed through biosignal and features estimation upon C4/A1, Right EOG, EMG tibialis and EMG chin channels. The 16 generated features were inserted into the FIS to obtain an automated hypnogram as product of the computer-assisted approach. The manually scored and automated hypnograms are compared epoch-by-epoch to determine a collection of performance metrics; such as accuracy, error, sensitivity and specificity rates.

The initial processing track supported on the TVARMA processes and recursive particle filter played a crucial role detecting the EEG power distributions, as well as, sleep transients in each SOP related epoch. The computed relative power bands and transient counters formed the backbone of the implemented fuzzy logic, considering a single EEG channel. Although, our approach integrated EOG and EMG features to assist the decision making in function of eyes and body movements, such as AASM scoring manual outlined. The remaining features relied on averaged amplitudes to narrow down W stage detection by identifying pronounced eyes, chin and limb movements, whereas N1 and N2 stages are characterised by a progressive reduction in the activity of the motor capabilities.

The fuzzy inference system allocated each feature value into one of three possible ranges or input fuzzy sets: low, medium and high. Depending on the assigned feature's range and defined set of rules, logical operations were performed to infer one of five possible output ranges for every SOP related stage: very low, low, medium, high or ultrahigh. At the end, only one stage was located within ultrahigh fuzzy set, with the classifier mapping this stage to the processed epoch. The completion of the mechanisms upon SOP epochs led to an automated hypnogram.

For instance, Figure 1 illustrates the joint application of processing and classification tracks upon HEA09 PSG recording. The hypnogram in the upper part was yielded by the manual scoring of the sleep specialists. It corresponds to the SOP of the first sleep cycle, albeit only the epochs in between the dotted lines were subject of processing and classification by our approach. Those epochs

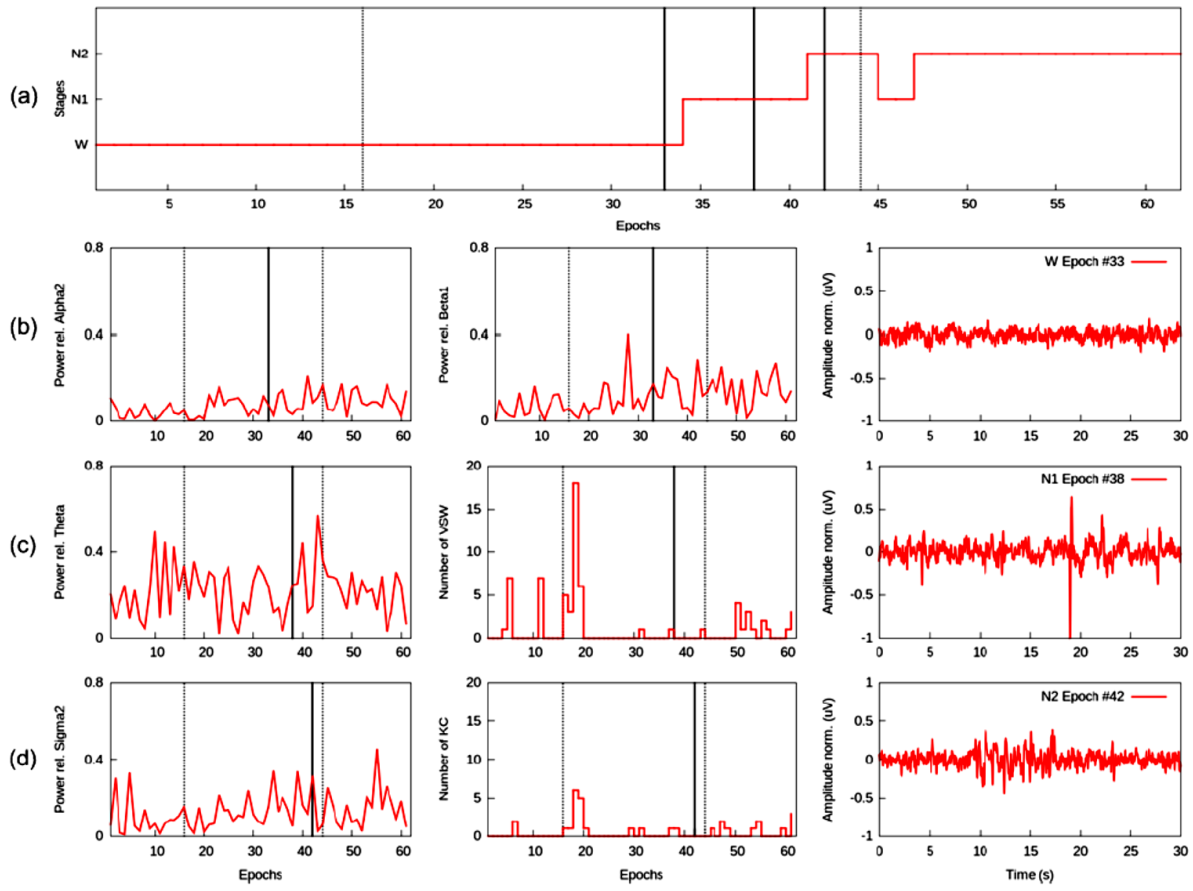

Figure 1. Example of extracted features of HEA09's first SOP and further applied fuzzy logic for classification. (a) Hypnogram of HEA09's first SOP. The dotted lines mark the initial and final epochs subject of processing and classification. (b) Relative power of EEG α_2 and β_1 bands versus sleep onset related epochs. The solid line marks the epoch detected by the FIS as W stage based on the values of selected features. (c) Relative power of EEG θ band and counter of VSW events versus sleep onset related epochs. The solid line marks the epoch detected by the FIS as N1 stage based on the values of selected features. (d) Relative power of EEG ς_2 band and counter of KC events versus sleep onset related epochs. The solid line marks the epoch detected by the FIS as N2 stage based on the values of selected features.

describe a classical sleep onset transition, starting at the awake state, following N1 transition to enter into a final N2 settlement. Figure 1b portrays α_2 and β_1 rPSD features interaction, as part of the fuzzy ruleset to classify PSG epoch #33 as W-type epoch, due to the mid-range power in those two EEG bands. In the next example, Figure 1c applies the same logic to the features θ rPSD and count of VSW, in order to attain the classification of PSG epoch #38 as an N1 epoch. Taking into account that N1 sleep stages are characterised by an attenuation of α and β activity followed by increased q power and VSW appearance. At the bottom, features ς_2 rPSD and count of KC were employed to map PSG epoch #42 as an N2 epoch, since a notorious increment in ς activity with scattered KC could be an indication of sleep spindles presence. The rightmost plots in Figure 1b-d depict the processed/classified EEG signals, which demonstrate the resemblance between visual scoring criteria and proposed fuzzy inference.

Based on the manual and fuzzy scoring, the performance metrics were generated to evaluate the degree of agreement in terms of accuracy, error, sensitivity and specificity rates. Table II summarises the obtained

performance results. On the right, it is showed the global metrics including the 10 healthy subjects. In turn, left-sided numbers represent the resulting metrics considering HEA01, HEA02, HEA08 and HEA09. Evidently, those four subjects attain higher rates than the overall cohort; such a situation obeyed to scoring criteria that unambiguously matched specialists' guidelines and fuzzy rules. Once, the other subjects became part of the evaluation, contradictory decision makings were observed between EEG-related features and EOG/EMG counterparts. This scenario promoted a series of disagreements in both scoring sources, producing a decline in the best case performance rates.

TABLE II
PERFORMANCE METRICS OF FUZZY INFERENCE SYSTEM

Metric	W	N1	N2	Metric	W	N1	N2
Acc.	64.1	64.4	61.5	Acc.	75.8	77.8	72.1
Err.	35.8	35.5	38.4	Err.	24.2	22.1	27.8
Sens.	83	34.1	21.3	Sens.	94.1	55.7	26.2
Spec.	41.1	71.2	91.4	Spec.	48.5	80.7	96.1

Discussion

The characterisation of the SOP describes time changing dynamics departing from wakefulness, going through N1, and finishing with N2 stage establishment [5-6]. The associated stages combine different physiological events, e.g. mixing frequency bands, fast and slow time-varying transients, amongst others [2]. Here, we introduced an automated approach supported on biomedical signal processing to estimate such events. One important contribution consisted on the adoption of TVARMA processes to cope with inherent constraints of PSG signals representation, whilst robustness and low complexity were achieved. Furthermore, the role of the recursive particle filtering as estimation method aided to handle non-Gaussian and non-linear limitations. Hence, disregarding those conditions in next processing and classification tracks could provoke a weak staging characterisation and misinterpretation [10]. Secondly, the incorporation of a fuzzy inference system spotted the flexibility of rule-based schemes of classification. The definition of input/output fuzzy sets and customisable ruleset facilitated the adaptation of manual scoring guidelines into the automated classification approach.

The dispute of human-based against computer assisted scoring could be recalled, supported on the obtained performance metrics. Similarly, inter-raters' reliability is an agitated topic of discussion within sleep studies, yet. Our findings contributed to vindicate most of the disagreements previously identified by the scientific community for the sleep stages delimitation [7, 14]. For example, the majority of inter-raters' disagreements takes place during the scoring of adjacent sleep stages, as well as, low coincidence rates on the first N2 epoch owing to poor recognition of the first KC and SS. The aforementioned issues reflected a lack of consensus amongst scorers, due to mutually exclusive or ambivalent guidelines, particularly referred to transitions from attenuated bands to mixed frequencies dominance or the absence of amplitude criteria over VSW, KC or SS waveforms. Therefore, Rosenberg et al. [7] posit 75% of accuracy rate as a fair score of agreement. If we apply such a criterion to our approach, then a sufficient performance has been reached. From our perspective, there is no merit trying to overcome visual scoring rates by means of computer-assisted systems, when inter-raters' reliability hardly surpasses 78% [5]. Alternatively, computer-assisted approaches should be focused on the optimisation of time-to-diagnosis windows and event-specific discernment between ambiguous guidelines. The approach, here presented, thrived on those objectives as an automated tool for assistance in sleep onset periods characterisation.

Acknowledgements

The work was supported by NPRP grant #[5-1327-2-568] from the Qatar National Research Fund, which is a member of Qatar Foundation. The statements made herein are solely the responsibility of the authors. The authors would like to thank the Interdisciplinary Centre for Sleep Medicine at the Charite Universitaetsmedizin Berlin (Germany) for undertaking the recruitment and collection of polysomnographic recordings, as well as, the sleep scorers dedicated to the assessment labours. Both parties served as the main experimental source for the present research work. R. Chaparro-Vargas acknowledges the financial support of the alliance COLCIENCIAS of the Colombian Government and COLFUTURO foundation, as main sponsor of his doctorate studies.

References

1. C. Marzano, F. Moroni, M. Gorgoni, L. Nobili, M. Ferrara, and L. D. Gennaro, "How we fall asleep: regional and temporal differences in electroencephalographic synchronization at sleep onset," Sleep Medicine, vol. 14, no. 11, pp. 1112 – 1122, 2013.
2. R. D. Ogilvie, "The process of falling asleep," Sleep Medicine Reviews, vol. 5, no. 3, pp. 247–270, 2001.
3. B. Koley and D. Dey, "An ensemble system for automatic sleep stage classification using single channel EEG signal," Computers in Biology and Medicine, vol. X, no. 0, pp. 1 – 10, 2012.
4. D. Alvarez-Estevez, J. M. Fernandez-Pastoriza, E. Hernandez-Pereira, and V. Moret-Bonillo, "A method for the automatic analysis of the sleep macrostructure in continuum," Expert Systems with Applications, vol. 40, no. 5, pp. 1796 – 1803, 2013.
5. A. Rodenbeck, R. Binder, P. Geisler, H. Danker-Hopfe, R. Lund, F. Raschke, H.-G. Wee, and H. Schulz, "A review of sleep EEG patterns. Part I: A compilation of amended rules for their visual recognition according to Rechtschaffen and Kales," Somnologie, vol. 10, no. 4, pp. 159–175, 2006.
6. H. Danker-Hopfe, P. Anderer, J. Zeitlhofer, M. Boeck, H. Dorn, G. Gruber, E. Heller, E. Loretz, D. Moser, S. Parapatics, B. Saletu, A. Schmidt, and G. Dorffner, "Interrater reliability for sleep scoring according to the Rechtschaffen & Kales and the new AASM Standard," Journal of Sleep Research, vol. 18, no. 1, pp. 74–84, 2009.
7. R. Rosenberg and S. Van Hout, "The american academy of sleep medicine inter-scorer reliability program: sleep stage scoring," J Clin Sleep Med, vol. 9, no. 1, pp. 81–87, 2013.
8. C. Iber, S. Ancoli-Israel, A. L. C. Jr., and S. F. Quan, "The AASM manual for the scoring of sleep and associated events," American Academy of Sleep Medicine, Tech. Rep., 2007.
9. R. Prado, "Sequential estimation of mixtures of structured autoregressive models," Computational Statistics & Data Analysis, vol. 58, no. 0, pp. 58 – 70, 2013.
10. G. Kitagawa, Introduction to Time Series Modeling. CRC Press, 2009, ch. Analysis of Time Series with a State-Space Model, pp. 1–16.
11. A. Galka, K. F. K. Wong, T. Ozaki, H. Muhle, U. Stephani, and M. Siniatchkin, "Decomposition of neurological multivariate time series by state space modelling," Bulletin of Mathematical Biology, vol. 73, pp. 285–324, 2011.
12. C.-M. Ting, S.-H. Salleh, Z. Zainuddin, and A. Bahar, "Spectral estimation of nonstationary EEG using particle filtering with application to event-related desynchronization (ERD)," IEEE Transactions on Biomedical Engineering, vol. 58, no. 2, pp. 321–331, 2011.
13. S. Mallat, A Wavelet Tour of Signal Processing. Elsevier Academic Press, 1999.
14. C. Berthomier, X. Drouot, M. Herman-Stoca, P. Berthomier, J. Prado, D. Bokar-Thire, O. Benoit, J. Mattout, , and M.-P. d'Ortho, "Automatic analysis of single-channel sleep EEG: Validation in healthy individuals," Sleep, vol. 30, no. 11, pp. 1587–1595, May 2007.

Appendix I

Peer-reviewed conference paper

Title: Characterising Insomnia: A Graph Spectral Theory Approach

Authors: Ramiro Chaparro-Vargas Beena Ahmed, Thomas Penzel and Dean Cvetkovic

Publication: Proceedings of the 37th Annual International Conference of the IEEE Engineering in Medicine and Biology Society

Year of Publication: 2015

Characterising Insomnia: A Graph Spectral Theory Approach

Ramiro Chaparro-Vargas* Beena Ahmed‡ Thomas Penzel† Dean Cvetkovic⋆

***Abstract*— This paper introduces a computational approach to characterise healthy controls and insomniacs based on graph spectral theory. Based upon expert-generated hypnograms of sleep onset periods, a network of sleep stages transitions is derived to compute four similarity distances amongst subjects' sleeping patterns. A subsequent statistical analysis is performed to differentiate the 16-subject healthy group from a 16-patient disordered cohort. Our findings demonstrated that the similarity distances based on eigenvalues determination, i.e. d_1 and d_4 were the most reliable and robust measures to characterise insomniacs, discriminating 93% and 87% of the affected population, respectively.**

I. INTRODUCTION

Sleep research is bringing significant attention to the diagnosis and treatment of pathologies with psychiatric and physical symptoms [1], [2]. Disorders associated with sleep deprivation, such as insomnia, are an example [3], [4]. Insomnia can result in mild to severe disruptions in the well-being of the patient, including daytime sleepiness, anxiety, depression, paranoia or even schizophrenia [5]. The opportune identification of insomnia requires the analysis of patient's physiological and behavioural traits, a tedious and time-consuming task for the patients and physicians. The deployment of computational approaches can significantly increase the accuracy of diagnosis and assessment time.

In this paper, we introduce a computational approach to measure the degree of similarity upon sleep onset periods of healthy controls and insomniacs. The similarity distance is based on graph spectral theory, which characterises a network of stages' transitions, derived from the sleep onset patterns of a hypnogram.

The hypnogram is a primary sleep monitoring tool; it graphically represents sleep stages transitions determined from the polysomnogram (PSG) recordings, specifically electroencephalogram (EEG), electrooculogram (EOG) and electromyogram (EMG) signals [6]. The detection of key waveforms: Vertex Shape Waves (VSW), K-complexes (KC), Sleep Spindles (SS) and major movements assist the association of body activity fluctuations with standardised sleep stages [7]. Likewise, underlying oscillations distinguished as: δ (0.5-4 Hz), θ (4-7 Hz), α (7-12 Hz), ς (12-16 Hz) and β (16-40 Hz) frequency bands play a complementary role in the sleep characterisation.

The graph spectral theory uses graph networks with vertices (nodes) and edges (links) to model complex patterns in terms of low complexity metrics [8], [9], [10]. We use this concept to transform hypnogogic patterns, i.e. sleep onset periods, into a network of transitions amongst sleep stages: Wake, non-REM1 and non-REM2. Thereafter, the set of sleep stages transitions are translated into a distance measure to determine the degree of similarity between the sleep onset periods of healthy controls and insomniacs, capable of characterising the two groups. To the best of our knowledge, no previous work has attempted to formally address the characterisation of insomnia following this approach.

II. METHODS

A. Hypnogram Characterisation

We used expert scored hypnograms to derive of a network of sleep stages transitions based upon graph spectral theory, as depicted in Figure 1. The network consisted of three vertices (one for each sleep onset stage) connected by two weighted directed edges with the inverse of the number of transitions coming in and out at one stage. The difference of the hypnograms and sleep transition networks was assessed in terms of their eigenvalues and eigenvectors (i.e. graph spectrum), although their structures were homogeneous (a.k.a isomorphic networks). From the networks, the degree and adjacency matrices were derived with the properties of being spectrum-invariant and vertex tagging independent [11].

Let us denote a pair of subjects' networks as G and H, a distance measurement between the two determined the spectral similarity of the subjects' hypnograms. The first distance $d_1(G,H)$ subtracted the diagonal matrix of non-inverted weights (degree matrices $\mathbf{D}_{G,H}$) and the full-rank matrix of inverted directed weights (adjacency matrices $\mathbf{A}_{G,H}$) to yield Laplacian matrices $\mathbf{L}_{G,H}$. Then, an Eigenvalue Decomposition (EVD) computed the eigenvalues λ,μ of the networks G and H [11], respectively, such that a scalar non-negative value was found, as referred in (1). Distances $d_2(G,H)$ and $d_3(G,H)$ used adjacency $\mathbf{A}_{G,H}$ and incidence matrices $\mathbf{C}_{G,H}$ to realise an EVD and a Singular Value Decomposition (SVD), correspondingly. The resulting factorised matrices containing eigenvalues $\Lambda_{G,H}$, singular values $\Sigma_{G,H}$ and eigenvectors $\mathbf{Q}_{G,H}$, $\mathbf{U}_{G,H}$, $\mathbf{V}_{G,H}$ were utilised in the transformation $\Delta = \mathbf{C}_G - \mathbf{U}_G^{\mathrm{T}}\mathbf{U}_H\mathbf{C}_H\mathbf{V}_H^{\mathrm{T}}\mathbf{V}_G$ [8] to obtain the distance of the two networks, following the formulas in (2) and (3). Lastly, distance $d_4(G,H)$ evaluated a Cauchy-Lorentz probability density function (pdf) $\rho_{G,H}(\omega)$ as a

*Affiliated to the School of Electrical and Computing Engineering, RMIT University, Melbourne VIC 3001, Australia ramiro.chaparro-vargas@rmit.edu.au

†Affiliated to the Interdisciplinary Centre for Sleep Medicine, Charité Universitätsmedizin Berlin, Berlin, Germany thomas.penzel@charite.de

‡Affiliated to the Electrical and Computer Engineering Program, Texas A&M University at Qatar beena.ahmed@qatar.tamu.edu

⋆Affiliated to the School of Electrical and Computing Engineering, RMIT University, Melbourne VIC 3001, Australia dean.cvetkovic@rmit.edu.au

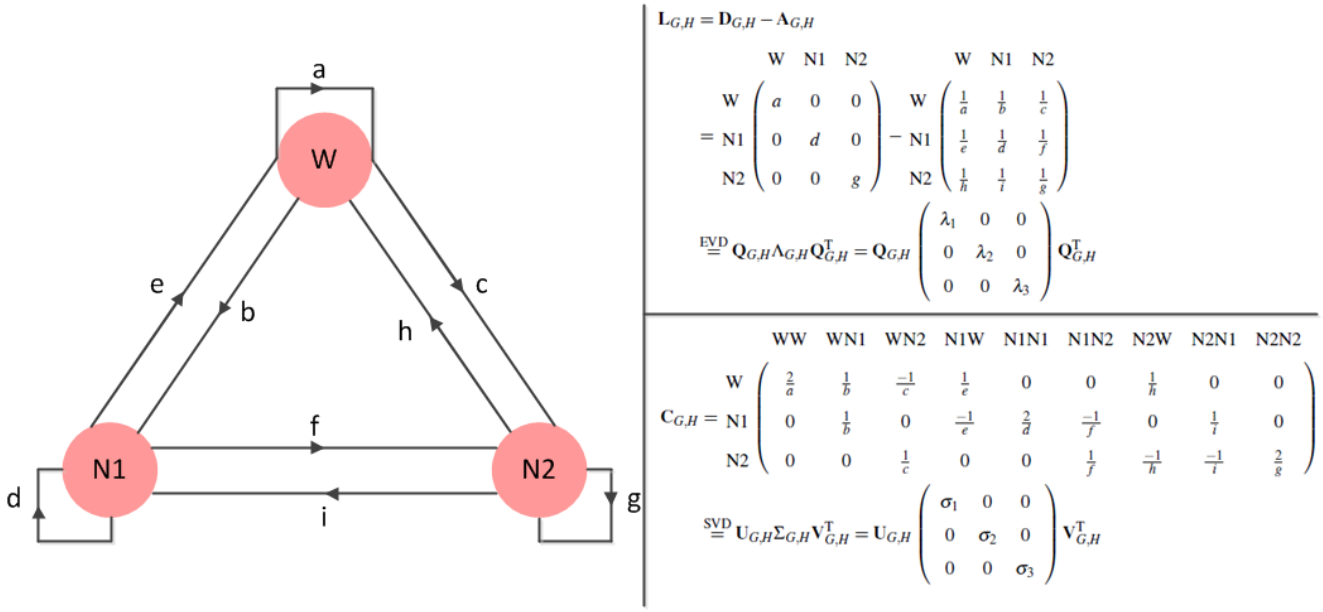

$$\mathbf{L}_{G,H} = \mathbf{D}_{G,H} - \mathbf{A}_{G,H}$$

$$= \begin{array}{c} \\ \mathrm{W} \\ \mathrm{N1} \\ \mathrm{N2} \end{array} \begin{array}{c} \begin{array}{ccc} \mathrm{W} & \mathrm{N1} & \mathrm{N2} \end{array} \\ \begin{pmatrix} a & 0 & 0 \\ 0 & d & 0 \\ 0 & 0 & g \end{pmatrix} \end{array} - \begin{array}{c} \\ \mathrm{W} \\ \mathrm{N1} \\ \mathrm{N2} \end{array} \begin{array}{c} \begin{array}{ccc} \mathrm{W} & \mathrm{N1} & \mathrm{N2} \end{array} \\ \begin{pmatrix} \frac{1}{a} & \frac{1}{b} & \frac{1}{c} \\ \frac{1}{e} & \frac{1}{d} & \frac{1}{f} \\ \frac{1}{h} & \frac{1}{i} & \frac{1}{g} \end{pmatrix} \end{array}$$

$$\overset{\mathrm{EVD}}{=} \mathbf{Q}_{G,H}\Lambda_{G,H}\mathbf{Q}_{G,H}^{\mathrm{T}} = \mathbf{Q}_{G,H} \begin{pmatrix} \lambda_1 & 0 & 0 \\ 0 & \lambda_2 & 0 \\ 0 & 0 & \lambda_3 \end{pmatrix} \mathbf{Q}_{G,H}^{\mathrm{T}}$$

$$\mathbf{C}_{G,H} = \begin{array}{c} \\ \mathrm{W} \\ \mathrm{N1} \\ \mathrm{N2} \end{array} \begin{array}{c} \begin{array}{ccccccccc} \mathrm{WW} & \mathrm{WN1} & \mathrm{WN2} & \mathrm{N1W} & \mathrm{N1N1} & \mathrm{N1N2} & \mathrm{N2W} & \mathrm{N2N1} & \mathrm{N2N2} \end{array} \\ \begin{pmatrix} \frac{2}{a} & \frac{1}{b} & \frac{-1}{c} & \frac{1}{e} & 0 & 0 & \frac{1}{h} & 0 & 0 \\ 0 & \frac{1}{b} & 0 & \frac{-1}{e} & \frac{2}{d} & \frac{-1}{f} & 0 & \frac{1}{i} & 0 \\ 0 & 0 & \frac{1}{c} & 0 & 0 & \frac{1}{f} & \frac{-1}{h} & \frac{-1}{i} & \frac{2}{g} \end{pmatrix} \end{array}$$

$$\overset{\mathrm{SVD}}{=} \mathbf{U}_{G,H}\Sigma_{G,H}\mathbf{V}_{G,H}^{\mathrm{T}} = \mathbf{U}_{G,H} \begin{pmatrix} \sigma_1 & 0 & 0 \\ 0 & \sigma_2 & 0 \\ 0 & 0 & \sigma_3 \end{pmatrix} \mathbf{V}_{G,H}^{\mathrm{T}}$$

Fig. 1. Graphical network representation of a subject's hypnogram and related matrices. Left: Network of sleep stages transitions including 3 vertices and 9 directed weighted edges according to the total number of transitions. Upper-right: Representation of Laplacian $\mathbf{L}_{G,H}$, degree $\mathbf{D}_{G,H}$ and adjacency $\mathbf{A}_{G,H}$ matrices from the derived network. Lower-right: Representation of incidence matrices $\mathbf{C}_{G,H}$ as an alternative to adjacency notation in $d_3(G,H)$ computation.

function of the eigenvalues ω computed from the Laplacian matrices $\mathbf{L}_{G,H}$. The integrated difference of the two networks distributions drew forth a scalar similarity distance, explained in (4).

$$d_1(G,H) = \begin{cases} \sqrt{\dfrac{\sum_{i=0}^{N-1}(\lambda_i-\mu_i)^2}{\sum_{i=0}^{N-1}\lambda_i^2}} & \text{if} \quad \sum_{i=0}^{N-1}\lambda_i^2 \leq \sum_{i=0}^{N-1}\mu_i^2 \\ \sqrt{\dfrac{\sum_{i=0}^{N-1}(\lambda_i-\mu_i)^2}{\sum_{i=0}^{N-1}\mu_i^2}} & \text{if} \quad \sum_{i=0}^{N-1}\mu_i^2 \leq \sum_{i=0}^{N-1}\lambda_i^2 \end{cases} \tag{1}$$

$$d_2(G,H) = \frac{1}{N}\sqrt{\sum_{i,j=1}^{N}\lambda_{i,j}^2} \tag{2}$$

$$d_3(G,H) = \frac{1}{N}\sqrt{\sum_{i,j=1}^{N}\sigma_{i,j}^2} \tag{3}$$

$$d_4(G,H) = \sqrt{\int_0^{\infty}[\rho_G(\omega)-\rho_H(\omega)]^2 \mathrm{d}\omega} \tag{4}$$

B. Clinical Data

For this study 20 healthy (H) subjects and 20 insomnia (I) patients undertook an overnight polysomnogram recording at the Interdisciplinary Centre for Sleep Medicine at the Charité Universitästmedizin Berlin. A set of monopolar EEG, EOG and EMG channels were used, compliant with the 10-20 international system for scalp montage, as follows: one EEG (C4A1), two EOG (left and right) and two EMG (chin and left tibialis). A designated group of sleep specialists performed the sleep stages scoring, according to the guidelines of the American Association of Sleep Medicine (AASM) manual [7]. Each 30-second epoch was scored as wake (W), non-REM1 (N1), non-REM2 (N2), non-REM3 (N3) or Rapid Eye Movement (REM). We considered the sleep stages linked to sleep onset periods: W, N1 and N2, adopting an extended definition for sleep onset based on the concepts in [12], [13], [14]. Sleep onset period includes the transition from W to N2 stage, which marks the appearance of consolidated sleep spindles indicating onset completion. The local Ethics Committee of the Charité Universitästmedizin Berlin approved the study and the subjects granted consent for the procedures.

We examined the 40 PSG recordings to identify datasets with artefacts or severe disruptions. A total of 4 healthy and 4 insomnia datasets were excluded, due to major ECG/EMG artefacts or interrupted activity. The similarity distances were computed using the software MathWorks® MATLAB 8.5 with its Signal Processing and Statistical Analysis toolboxes.

III. RESULTS

Figure 2 presents the standard deviation (SD) of the similarity distances for each healthy subject. The red squared markers represent the SD of the set of distances from each subject to the other 15 in the healthy group, whilst blue triangular markers denote the SD of the distance from each subject to the 16 subjects in the insomnia group. Due to the high inter-subject variability, the SD better summarised

the similarity trends between the control and insomniacs. Despite having the same network structure for each subject, i.e. 3 vertices with 9 weighted directed edges, the distances d_1, d_2, d_3 and d_4 changed due to the type of matrices or distributions used in their computation (see Figure 1). For example, d_1 had a small SD $(0.05-0.1)$, i.e. high similarity of sleeping patterns for subjects H03-H08 compared to the distances of the control subjects. The control subjects had SD $(0.1-0.15)$ higher than that of insomniacs $(0.05-0.1)$, which meant, a decreasing similarity amongst the sleep onset patterns. The d_2 and d_3 SD captured closer values for subjects H01-H11 $(0.01-0.02)$ than most of the insomniacs $(0.01-0.05)$. They succeeded in establishing the similarity of control sleep onset patterns with respect to their healthy peers, as could be preassumed. The d_4 SD confirmed for most subjects lower deviations amongst controls $(0.1-0.2)$ and higher values $(0.15-0.2)$ compared to insomniacs, denoting higher similarity amongst the entire control group. Here, the distances were computed by the construction of a Cauchy-Lorentz distribution as a function of eigenvalues. This suggested the prowess of graph spectral theory in the characterisation of paired sleeping patterns with homogeneous network structure.

We performed an unpaired two-tailed t-test to evaluate the null hypothesis of no difference in the similarity distances between healthy controls and insomniacs. The statistical test consisted of a round of 32 sets of comparisons, i.e. 16 controls and 16 insomniacs. Each comparison took the distance measures of one particular subject to the 16 healthy controls versus the distance measure of that subject to the 16 insomniacs. Overall, the t-tests compared similarity distances of control vs. control, control vs. insomniac and insomniac vs. insomniac. The significance values appeared between the distance measures of control vs. insomniac subjects.

Table I presents the resulting p-values with Bonferroni correction set at $p < 0.0031$. The statistical results show that d_1 and d_4 measures had the highest amount of significance values, which is consistent with the observations made from the SD diagrams in Figure 1. There were significant differences in the results of both distance measures for subjects $I03$ ($p_{d_1,d_4} < 0.0001$) to $I16$ ($p_{d_1} < 0.000044, p_{d_4} < 0.000028$). Respectively, $d_{1,4}$ distinguished 93% and 87% of healthy controls from insomnia sleeping onset patterns. On the other hand, $d_{2,3}$ had significance differences for only two insomniac subjects I10 ($p_{d_3} < 0.00027$) and I11 ($p_{d_3} < 0.00023$).

TABLE I

UNPAIRED TWO-TAILED T-TEST p-VALUES.

	I01	I02	I03	I04	I05	I06	I07	I08
d_1	0.016	**0.003**	**0.001**	**0.001**	**0.0009**	**0.0009**	**0.0009**	**0.0003**
d_2	0.009	0.005	0.005	0.005	0.004	0.004	0.004	0.004
d_3	0.068	0.070	0.070	0.070	0.071	0.072	0.070	0.068
d_4	0.223	0.023	**0.001**	**0.001**	**0.001**	**0.001**	**0.0001**	**0.0001**
	I09	I10	I11	I12	I13	I14	I15	I16
d_1	**0.0001**	**2e−5**	**1e−5**	**5e−5**	**5e−5**	**5e−5**	**4e−5**	**4e−5**
d_2	0.004	0.023	0.019	0.035	0.034	0.033	0.028	0.028
d_3	0.064	**0.0002**	**0.0002**	0.122	0.124	0.120	0.118	0.119
d_4	**1e−5**	**1e−5**	**1e−5**	**3e−5**	**3e−5**	**3e−5**	**2e−5**	**2e−5**

$p <$ **0.0031**

IV. DISCUSSION AND CONCLUSIONS

The similarity distances d_1 and d_4 were the most performant measures for insomnia characterisation. The analysis of stages transitions along sleep onset periods based on graph spectral theory differentiated most of the diagnosed insomnia patients from the healthy controls.

In this paper, we used a scalar measure to simplify the complexity of the sleep onset pattern, taking into account the availability of expert generated hypnograms. Our results showed that the eigenvalue-based measures, d_1 and d_4, exhibited better stability, robustness and less susceptibility to odd dynamics, such as collapsing distances to null values. It should be noted that the eigenvalues estimate the degree of similarity between two sleep onset patterns [11], thus providing an unique set of hypnogogic fingerprints for a subject, collected from the processing of a single to multiple nights' recordings. The eigenvalues interpret the pattern of transitions amongst stages with a negligible chance of duplicity, thus simplifying the analysis of tens to hundreds of transitions into a scalar measure. That can be used to differentiate healthy from insomnia subjects.

Analytical and statistical findings attested the competence of our approach in the computer-assisted diagnosis of insomnia. The standard deviations of similarity distances in Figure 2 progressively evidenced the resemblance of healthy against insomnia sleep onset periods. The measure d_4 established the most clear separation thanked to the non-Gaussian Cauchy-Lorentz distribution in function of eigenvalues. This method granted more probabilistic significance to outlying sleep onset patterns, i.e. inter-subject variability. The p-values in Table I statistically confirmed the prowess of eigenvalues-based characterisation with over 85% of accuracy rates for insomniacs identification. Moreover, the application of graph spectral theory with eigenvalues analysis on sleep and its related disorders is a novel approach to what is a difficult problem.

For future work, we will investigate the similarity distances to assess the impact of inter-rater's variability, as well as identify discrepancies amongst criteria that would have an impact on the characterisation of insomnia. We also aim to enhance the computational capabilities of the system to perform automated sleep staging. Finally, we will present our approach to larger cohort of subjects to validate our results.

ACKNOWLEDGMENT

The work was supported by NPRP grant #[5-1327-2-568] from the Qatar National Research Fund, which is a member of Qatar Foundation. The statements made herein are solely the responsibility of the authors.

The authors would like to thank the Interdisciplinary Centre for Sleep Medicine at the Charité Universitätsmedizin Berlin (Germany) for undertaking the recruitment and collection of polysomnographic recordings, as well as, the sleep scorers dedicated to the assessment labours. Both parties

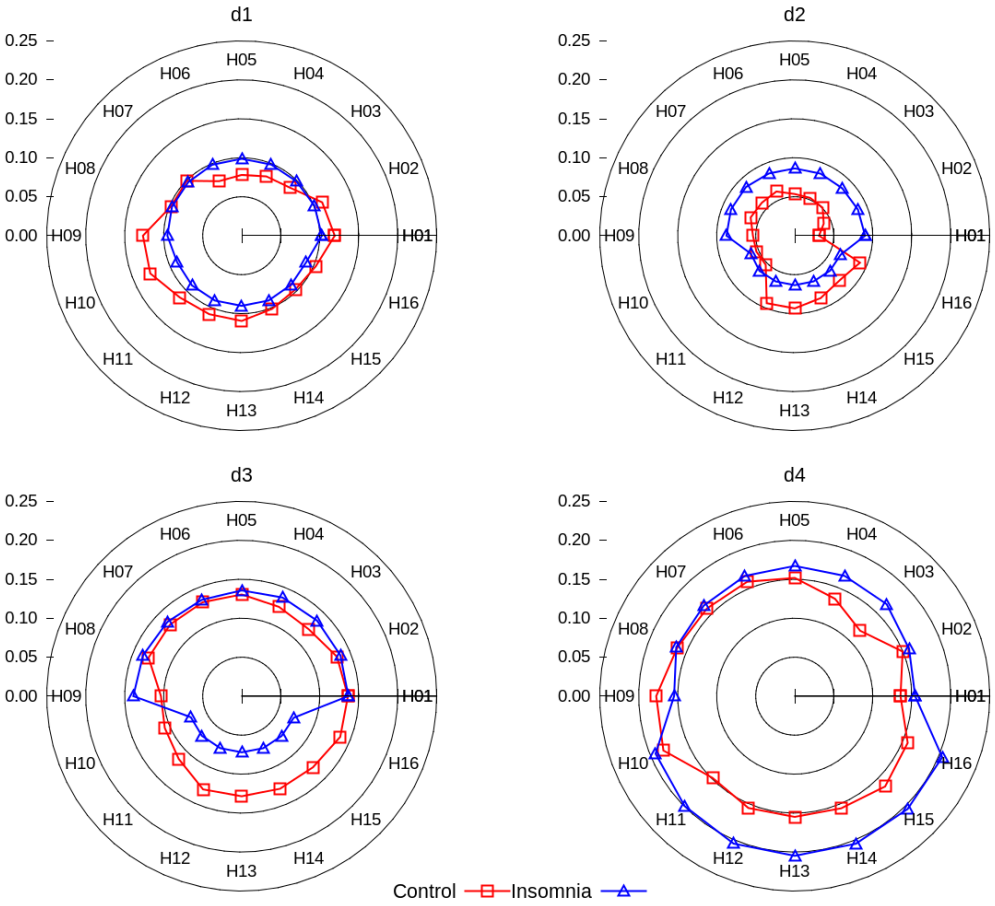

Fig. 2. Standard deviations of similarity distances for each control versus healthy and insomniac cohorts based on expert scored hypnograms.

served as the main experimental source for the present research work.

R. Chaparro-Vargas acknowledges the financial support of the alliance COLCIENCIAS and COLFUTURO foundation of the Colombian Government, as main sponsor of his doctorate studies.

REFERENCES

[1] E. Pereda, R. Q. Quiroga, and J. Bhattacharya, "Nonlinear multivariate analysis of neurophysiological signals," *Progress in Neurobiology*, vol. 77, no. 12, pp. 1 – 37, 2005.

[2] L. Mesin, A. Holobar, and R. Merletti, *Advanced Methods of Biomedical Signal Processing*, S. Cerutti and C. Marchesi, Eds. IEEE Press, 2011.

[3] P. Bob, "Consciousness, schizophrenia and complexity," *Cognitive Systems Research*, vol. 13, no. 1, pp. 87 – 94, 2012.

[4] J. Maes, J. Verbraecken, M. Willemen, I. D. Volder, A. van Gastel, N. Michiels, I. Verbeek, M. Vandekerckhove, J. Wuyts, B. Haex, T. Willemen, V. Exadaktylos, A. Bulckaert, and R. Cluydts, "Sleep misperception, EEG characteristics and autonomic nervous system activity in primary insomnia: A retrospective study on polysomnographic data," *International Journal of Psychophysiology*, no. 0, pp. –, 2013.

[5] D. Freeman, K. Pugh, N. Vorontsova, and L. Southgate, "Insomnia and paranoia," *Schizophrenia research*, vol. 108, no. 1-3, pp. 280–284, March 2009.

[6] D. Gencaga, E. Kuruoglu, and A. Ertüzün, "Modeling non-gaussian time-varying vector autoregressive processes by particle filtering," *Multidimensional Systems and Signal Processing*, vol. 21, no. 1, pp. 73–85, 2010.

[7] C. Iber, S. Ancoli-Israel, A. L. C. Jr., and S. F. Quan, "The AASM manual for the scoring of sleep and associated events," American Academy of Sleep Medicine, Tech. Rep., 2007.

[8] M. Ipsen and A. S. Mikhailov, "Evolutionary reconstruction of networks," *Phys. Rev. E*, vol. 66, p. 046109, Oct 2002.

[9] D. Jakobson and I. Rivin, "Extremal metrics on graph I," *Forum Mathematics*, vol. 14, no. 1, pp. 147–163, 2002.

[10] P. Stoica and R. Moses, *Spectral analysis of signals*, T. Robbins, Ed. Pearson Prentice Hall, 2005.

[11] G. Jurman, R. Visintainer, and C. Furlanello, "An introduction to spectral distances in networks," *Frontiers in Artificial Intelligence and Applications*, vol. 226, pp. 227–234, 2011, cited By (since 1996)1.

[12] R. D. Ogilvie, "The process of falling asleep," *Sleep Medicine Reviews*, vol. 5, no. 3, pp. 247–270, 2001.

[13] H. Merica and R. D. Fortune, "State transitions between wake and sleep, and within the ultradian cycle, with focus on the link to neuronal activity," *Sleep Medicine Reviews*, vol. 8, no. 6, pp. 473 – 485, 2004.

[14] C. Marzano, F. Moroni, M. Gorgoni, L. Nobili, M. Ferrara, and L. D. Gennaro, "How we fall asleep: regional and temporal differences in electroencephalographic synchronization at sleep onset," *Sleep Medicine*, vol. 14, no. 11, pp. 1112 – 1122, 2013.

Appendix J

Peer-reviewed Journal Paper

Title: Insomnia Characterisation: From Hypnograms to Graph Spectral Theory

Authors: Ramiro Chaparro-Vargas, Beena Ahmed, Niels Wessel, Thomas Penzel and Dean Cvetkovic

Publication: IEEE Transactions on Biomedical Engineering

Year of Publication: 2016

Insomnia Characterisation: From Hypnogram to Graph Spectral Theory

Ramiro Chaparro-Vargas, *Member, IEEE,* Beena Ahmed, *Member, IEEE,* Niels Wessel, Thomas Penzel *Senior Member, IEEE,*, and Dean Cvetkovic, *Member, IEEE*

***Abstract*—*Objective:* To quantify and differentiate control and insomnia sleep onset patterns through biomedical signal processing of overnight polysomnograms. *Methods:* The approach consisted of three tandem modules: 1) biosignal processing module, which used state-space time-varying autoregressive moving average (TVARMA) processes with recursive particle filter; 2) hypnogram generation module that implemented a fuzzy inference system (FIS); and 3) insomnia characterisation module that discriminated between control and subjects with insomnia using a logistic regression model trained with a set of similarity measures (d_1, d_2, d_3, d_4). The study employed sleep onset periods from 16 control and 16 subjects with insomnia. *Results:* State-spaced TVARMA processes with recursive particle filtering provided resilience to nonlinear, nonstationary and non-Gaussian conditions of biosignals. FIS managed automated sleep scoring robust to inter-subjects' and inter-raters' variability. The similarity distances quantified in a scalar measure the transitions amongst sleep onset stages, computed from expert and automated hypnograms. A statistical set of unpaired two-tailed t-tests suggested that distances d_1, d_2 and d_3 had larger statistical significance ($p_{d_1} < 6.5 \times 10^{-5}, p_{d_2} < 2.1 \times 10^{-4}, p_{d_3} < 4.5 \times 10^{-7}$) to characterise sleeping patterns. The logistic regression model classified control and subjects with insomnia with sensitivity 87%, specificity 75% and accuracy 81%. *Conclusion:* Our approach can perform a supportive role in either biosignal processing, sleep staging, insomnia characterisation or all the previous, coping with time-consuming procedures and massive data volumes of standard protocols. *Significance:* The introduction of graph spectral theory and logistic regression for the diagnosis of insomnia represents a novel concept, attempting to describe complex sleep dynamics throughout transitions networks and scalar measures.**

***Index Terms*—Fuzzy logic, graph spectral theory, insomnia, PSG, sleep onset period.**

I. Introduction

Sleep research is receiving increasing attention due to the strong relationship between psychiatric and physiological pathologies related to sleep deprivation and insomnia disorder [1], [2], [3]. Insomnia can trigger chronic sleepiness during wake hours, anxiety, and more severely, depression, paranoia or even schizophrenia [4]. However, the diagnosis of insomnia is not a straightforward issue, requiring the patient's detailed medical and sleep history as well as information collected via specialised questionnaires and face-to-face consultations. This can be followed up by an overnight polysomnogram (PSG) recording that monitors brain, eyes, muscles and cardiorespiratory activity to rule out any underlying sleep disorders [5]. The biosignals collected in these PSG recordings are then analysed to score the sleep stages and identify disordered patterns. These tasks are burdensome and time-consuming not only for the sleep experts, but also for the patients. Therefore, the deployment of accurate computer-assisted systems offers a feasible solution to reduce the time required to analyse the PSG recordings.

Computer-aided systems commonly disregard the nonlinear, nonstationary, non-Gaussian constraints on the PSG signals, namely the electroencephalogram (EEG), electrooculogram (EOG) and electromyogram (EMG) thus impacting their accuracies [6]. These constraints hinder the proper identification of key waveforms, such as Vertex Shape Waves (VSW), K-complexes (KC), Sleep Spindles (SS), major movements, etc. The same occurs with the underlying dynamics linked to the EEG δ (0.5-4 Hz), θ (4-7 Hz), α (7-12 Hz), ς (12-16 Hz) and β (16-40 Hz) frequency bands. Also, slow (SEM) eye movements and rapid eye movements (REM) are susceptible to mischaracterisation, due to the lack of proper assumptions based on the mentioned constraints. Various works [7], [8], [9], [10], [11] have dealt with EEG analysis by means of autoregressive models, Kalman filtering and polynomial estimation methods. The scope of these works is restricted as they use linear and Gaussian assumptions to model EEG signals, which can be insufficient to analyse the varied transient events present in sleep. Our processing module adopts time-varying models accompanied by Bayesian methods to overcome the nonlinear, non-Gaussian and time-varying conditions, leading to the extraction of higher quality features [12].

Here, we are proposing a modular system that differentiates control and insomnia cohorts by quantifying their sleep onset transitions. First, the processing module implements a time-varying generalisation model to compute the features characterising sleep onset. Second, the hypnogram generation module uses the computed features to infer sleep stages and sleep macrostructure. And lastly, the characterisation module computes similarity distances comparing the generated hypnograms of control and subjects with insomnia, which are inputted to a logistic regression model to differentiate between the two sleeping patterns. Each computational module can be utilised independently or holistically depending on the analysis goal. Each

R. Chaparro-Vargas is with the School of Electrical and Computing Engineering, RMIT University, Melbourne VIC, Australia.

B. Ahmed is with the Electrical and Computer Engineering Program, Texas A&M University at Qatar.

N. Wessel is with the Department of Physics, Humboldt-Universität zu Berlin, Berlin, Germany.

T. Penzel is with the Interdisciplinary Centre for Sleep Medicine, Charité Universitätsmedizin Berlin, Berlin, Germany.

D. Cvetkovic is with the Health Innovation Research Institute (HIRi) and School of Electrical and Computing Engineering, RMIT University, Melbourne VIC, Australia.

Manuscript received ; revised .

module attempts to overcome inaccuracies in the computer-aided 1) processing of PSG signals, 2) hypnogram generation caused by inter-subject variability, and 3) identification of disordered populations.

The hypnogram generation module classifies the sleep stages based upon spectrum and amplitude-dependent features and case-specific considerations to cope with the inter-subject and inter-rater variability [13]. The manual AASM sleep scoring guidelines [14] do not fully address differences due to inter-subject variability leaving the scoring open to raters' subjective interpretation. Such a situation compromises the right association of sleep transients and frequency bands to particular sleep stages in a hypnogram. Several studies on this topic [15], [16], [17], [18] have suggested potential pathways of improvement towards unified scoring. Our proposed hypnogram generation module takes into account those recommendations by applying fuzzy inference system with human-like reasoning.

The characterisation of subjects with insomnia into simpler indexes or metrics is challenging. Graph spectral theory offers a practical solution as it can be used to model sleep stages fluctuations in terms of low-complex instances, like transition networks consisting of vertices (nodes) and edges (links) [19], [20], [21]. We apply this concept to initially translate hypnogogic patterns, i.e. sleep onset periods, to a network of transitions amongst sleep onset stages: Wake, nonREM1 and nonREM2. Thereupon, a distance measure is computed from these sleep transitions to quantify the degree of similarity between two subjects' sleep onset periods. Logistic regression is lastly applied on these stages transitions to differentiate control from subjects with insomnia. To the best of our knowledge, no previous work has attempted to formally address the characterisation of sleep disorders by the assessment of similarity metrics extracted from sleep onset patterns.

The remainder of the manuscript is organised as follows: Section III describes the biomedical signal processing techniques used in the proposed three modules. Section II describes the clinical data collected to test our approach. Section IV presents the results obtained with our system, which are discussed in Section V accompanied by conclusions and directions for future work.

II. Materials

In this study, we used data from 20 control (H) subjects and 20 insomnia (I) patients recruited to undertake an overnight PSG recording at the Interdisciplinary Centre for Sleep Medicine at the Charité Universitästmedizin Berlin and RMIT University. The study was approved by the local Ethics Committee of the Charité Universitästmedizin Berlin and the subjects granted consent for their procedures. The summary of sleep parameters per subject are found in the online supplementary material of the present manuscript.

The selected channels were: one EEG (C4-A1), two EOG (left and right EOG) and two EMG (chin and left tibialis), compliant with the 10-20 international system. The sampling rate was 200 Hz, 30 seconds of epoch segmentation and no preprocessing filtering was conducted. A group of sleep specialists performed the sleep stages scoring, according to the guidelines of the AASM manual [14]. Each 30-second epoch was evaluated and mapped to a particular stage: wake (W), nonREM1 (N1), nonREM2 (N2), nonREM3 (N3) and Rapid Eye Movement (REM). We focused on the sleep stages associated with sleep onset periods, i.e. W, N1 and N2 to characterise insomnia as they are more related to the sleep initiation and maintenance. Amongst the different definitions given to sleep onset [22], [23], [24], we adopted a more comprehensive description consisting of the transition from W to N2 stage, where the appearance of consolidated sleep spindles appear giving a clear indication of onset completion.

A total of 8 PSG recordings, distributed in 4 control and 4 insomnia, were excluded from the study group due to ECG/EMG artefacts and discontinuous records. From each subject, the first sleep cycle was further analysed, i.e. biosignal processing, automatic hypnogram generation and insomnia characterisation modules. All epochs between the first W epoch until the last N2 epoch (prior to first N3 epoch) were considered as the common reference for sleep onset period.

III. Methods

Figure 1 presents our modular approach to insomnia characterisation.

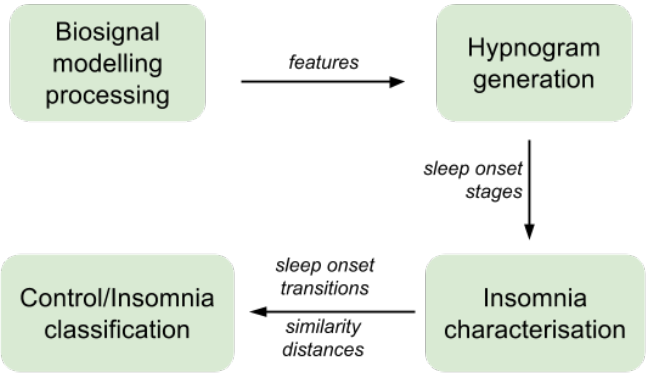

Fig. 1. Block diagram of our modular computational approach for insomnia characterisation. The system uses biosignal processing based on TVARMA$(8,2)$ models and particle filtering to extract the biosignal features, which are fed into a fuzzy inference system to automatically generate a hypnogram of the subject's sleep onset period. From the hypnogram, a sleep stages transition network is derived to compute unidimensional metrics or similarity distances using graph spectral theory. Finally, a logistic regression classifies the subjects into control or insomnia groups.

A. Biosignal Modelling and Processing

As PSG signals are constrained by nonlinear, nonstationary and non-Gaussian conditions, in our approach we used Time Varying Autoregressive Moving Average TVARMA processes with orders p,q to model the abrupt and slow shifts of PSG signals [25], [26]. Our approach computes instantaneous estimates of the PSG signal in the time and frequency domains to produce non-Gaussian state-space of the signal. The state-space realisations can be described using two model equations,

i.e. system (1) and observation (2), which generalise fluctuations occurring within 30-second PSG epochs to estimate the information and noise content in the biosignals.

$$\mathbf{x}[k] = \mathbf{x}[k-1] + \eta[k] \tag{1}$$

$$\mathbf{y}[k] = \mathbf{A}\mathbf{x}[k] + \mathbf{x}^{\mathrm{H}}[k]\mathbf{B}\nu[k] \tag{2}$$

where $\mathbf{x}[k]$ is the estimated vector of TVARMA(p,q) coefficients for the PSG epoch. The system model (1) noise vector $\eta[k]$ is divided in two terms $[\eta_{\mathbf{p}}[k]\ \eta_{\mathbf{q}}[k]]$ to distinguish AR(p) and MA(q) noise processes, where $\eta_{\mathbf{p}}$ is Cauchy distributed with zero translation and $\varsigma^2_{\eta_{\mathbf{p}}}$ dispersion, $\eta_{\mathbf{p}} \sim \mathscr{C}(0, \varsigma^2_{\eta_{\mathbf{p}}}\mathbf{I})$. $\eta_{\mathbf{q}}$ is Gaussian distributed with zero mean and $\sigma^2_{\eta_{\mathbf{q}}}$ variance, $\eta_{\mathbf{q}} \sim \mathscr{N}(0, \sigma^2_{\eta_{\mathbf{q}}}\mathbf{I})$. $\mathbf{y}[k]$ represents the estimated epoch, accompanied by $\mathbf{A}$ and $\mathbf{B}$ matrices as in (3)-(4) to perform weighted linear combinations. $\nu[k]$ is the Gaussian distributed observation model noise (2) with zero mean and σ^2_{ν} variance, $\nu \sim \mathscr{N}(0, \sigma^2_{\nu}\mathbf{I})$.

$$\mathbf{A} = [\mathbf{y}[k-1], \cdots, \mathbf{y}[k-p] | 0, \cdots, 0] \tag{3}$$

$$\mathbf{B} = \begin{bmatrix} \mathbf{0}_{p\times p} & \mathbf{0} \\ \mathbf{0} & \mathbf{I}_{(q+1)\times(q+1)} \end{bmatrix} \tag{4}$$

Akaike (AIC) and Bayesian Information Criterion (BIC) determined the optimal orders (p,q) of the TVARMA processes. First, a sample size equivalent to one third of the recorded epochs was randomly selected to be modelled by the pair of orders $(2,1)$, $(4,1)$, $(6,1)$, $(8,1)$, $(10,1)$, $(2,2)$, $(4,2)$, $(6,2)$, $(8,2)$, $(10,2)$. Secondly, their corresponding AIC and BIC values were computed. And finally, the definitive model orders applicable to the total number of PSG epochs was chosen when the following stopping criterion was fulfilled: the difference between the latest AIC/BIC value compared to the previous one is less than the time-series' standard deviation [27]. Thus, the final pair of model orders was $(8,2)$.

Modelling the system noise with the non-Gaussian Cauchy-Lorentz distribution enables the TVARMA(8,2) state-space processes to deal simultaneously with sudden and subtle shifts of the input epoch. The Cauchy-Lorentz distribution is heavy-tailed granting a larger probabilistic significance to sudden fluctuations; its tighter dispersion in the central region allows it to follow smooth variations [27]. The state-space realisations concentrate all the meaningful information of the epoch in the system vector $\mathbf{x}[k]$.

We implemented a recursive Monte Carlo filter, best known as particle filter [28] to overcome the non-Gaussian constraint in the system vector $\mathbf{x}[k]$ estimation. The filter estimates a posterior probability density function (pdf) for the system vector $\mathbf{x}[k]$ supported on the current system's state, as well as, past and incoming samples of the epoch [12]. Initially, the particle filter uses the system model (1) to build up the system's pdf $\mathbf{x}[k]$, subject to the previous system's state $\mathbf{x}[k-1]$ and the noise process $\eta[k]$. Subsequently, the most recent estimation of $\mathbf{x}[k]$ adjusts the predicted state pdf to an updated distribution upon the arrival of one or few incoming epoch samples or observations $\mathbf{y}[k]$, instead of a complete dataset batch [12]. In this manner, the recursive particle filter performs a series of sample-oriented (particles) approximations to build a pdf, considering the time-changing fluctuations of the epoch. The recursive manipulation of the particles improves the accuracy of the pdf by a resampling procedure to reduce the overutilisation of a specific subset of particles [28]. This process is commonly adopted in the construction of recursive particle filters, which is known as the Sequential Importance Sampling (SIS) algorithm [12].

Once the system vector $\mathbf{x}[k]$ or coefficients of the PSG epoch are obtained by combining TVARMA(8,2) state-space processes [29] with a recursive particle filter, we computed a set of features that better characterise the properties of the EEG/EOG/EMG biosignals. For the EEG channel, we computed the δ (0.5-4 Hz), θ (4-7 Hz), α_1 (7-9.5 Hz), α_2 (9.5-12 Hz), ς_1 (12-14 Hz), ς_2 (14-16 Hz), β_1 (16-18 Hz), β_2 (18-30 Hz) and β_3 (30-40 Hz) instantaneous power bands, accompanied by transients counters per epoch, i.e. VSW, KC and SS detection based on rapid time-frequency changes [30]. To achieve this, we computed a series of wavelet-based decompositions by the convolution of the coefficients obtained from the system's state $\mathbf{x}[k]$ and a bank of wavelet filters, which use complex Morlet mother wavelets $\psi(t_k)$ with central frequencies ω_0 and bandwidths $\sigma^2_{t_k}$ referred to the EEG bands. Thereafter, the relative instantaneous power is computed for each EEG band by taking the instant value of the band normalised by the δ-β_3 total power in the processed epoch.

Similarly, rapid and slow eye movement features are derived from the differential amplitude of left and right EOG channels following a threshold criterion to detect the events; viz. sustained ocular activity above 30% of the zero-level baseline with 100μV as maximum amplitude for more than 500 ms, is tagged as slow movement, whereas pulse-type activity above 70% the zero-level baseline for less than 500 ms implies rapid eye movement. The features associated to chin tension and limb movements come from the detection of brief ($<$ 500 ms) and peaked (70% from zero-level) activity in the amplitude levels of EMG channels [14]. The cluster of EEG, EOG and EMG features permits the full characterisation of the sleep stages associated with sleep onset periods and thereby the construction of an associated hypnogram. Table I summarises the group of extracted features during PSG epoch processing.

TABLE I
FEATURES FOR THE GENERATION OF SUBJECT'S SLEEP ONSET HYPNOGRAM

#	Feature	Channel	Event/Freq. Band (Hz)
1	$\mathrm{P}_{\delta}[k]$	EEG C4A1	$0.5-4$
2	$\mathrm{P}_{\theta}[k]$	EEG C4A1	$4-7$
3	$\mathrm{P}_{\alpha_1}[k]$	EEG C4A1	$7-9.5$
4	$\mathrm{P}_{\alpha_2}[k]$	EEG C4A1	$9.5-12$
5	$\mathrm{P}_{\varsigma_1}[k]$	EEG C4A1	$12-14$, SS
6	$\mathrm{P}_{\varsigma_2}[k]$	EEG C4A1	$14-16$, SS
7	$\mathrm{P}_{\beta_1}[k]$	EEG C4A1	$16-18$
8	$\mathrm{P}_{\beta_2}[k]$	EEG C4A1	$18-30$
9	$\mathrm{P}_{\beta_3}[k]$	EEG C4A1	$30-40$
10-11	A_{EEG}	EEG C4A1	VSW, KC
12-13	A_{EOG}	EOG left/right	Slow/Rapid eye movement
14	A_{EMG}	EMG chin	Chin tension
15	A_{EMG}	EMG tibialis	Limb movement

B. Hypnogram Generation

Sleep onset compromises overlapping stages whose boundaries cannot be precisely delimited. As the fuzzy logic-based classifier addresses decision making in the form of human-like decision rules it is well-suited to generate the hypnograms [30]. It is thus able to tolerate the imprecision, uncertainty and overlapping states characterising sleep states [31]. We implemented a Mamdani Fuzzy Inference System (FIS) to map an input space represented by the set of extracted features to an output space of sleep onset stages with a list of 'if-then' statements or fuzzy rules in between. In other words, a trapezoidal membership function quantifies the degree of affiliation of each feature into a 0 to 1 range, achieving partial and shared membership for one or more than one of the designed input fuzzy sets: low, medium and high. [32]. Our system builds the input space with the 15 extracted features plus one feedback variable, designated as previous scored stage. This feedback variable is the output of a first round of classification. Thus, we shield the decisions against odd transitions, e.g. W-N2-W, by introducing some smoothing rules. The fuzzy sets are overlapped, fitting the features' minimum and maximum values across the 32 subjects [32]. For instance, power band-dependent fuzzy sets are lower and upper bounded as follows: low (0-0.25), medium (0.2-0.7) and high (0.7-1); and amplitude-dependent sets are: low (0-0.2), medium (0.15-0.4) and high (0.35-0.65). Output fuzzy sets for sleep staging decision extend the degree of affiliation to infralow (0-20), low (20-40), medium (40-60), high (60-80) and ultrahigh (80-100) to seamlessly match the tight transition of sleep onset stages. Lastly, more than 60 fuzzy rules enact the guidelines of the AASM manual [14] for sleep scoring with amendments based on the suggestions of experienced scorers.

C. Insomnia Characterisation

1) Transition Networks and Graph Spectral Theory: The expert scored or automated hypnogram produced by the two previous modules can be represented alternatively as a network of sleep stages transitions. Figure 2 depicts the transition network with 3 vertices, one per sleep onset stage, connected by a pair of weighted directed edges denoting the inverse of the total number of transitions from one stage to the other and vice versa. Each expert or automated hypnogram can be similarly translated to a sleep transition network.

In this paper, we attached transition networks to graph spectral theory to describe sleep onset patterns in terms of graph-related matrices and spectra. This concept enables the simplification of elaborated multistage and time-varying systems, e.g. sleep stage transitions, into low-complex or even unidimensional metrics. For example, the comparison of two networks with homogeneous structures (isomorphic networks) is defined as a function of their eigenvalues and eigenvectors, i.e. graph spectrum, rather than their graphical representation. To attain this, let G and H be the transition networks of two subjects, which have the same structure as in Figure 2 but different edges' weights according to their individual transitions amongst sleep stages. Initially, degree $\mathbf{D}_{G|H}$, adjacency $\mathbf{A}_{G|H}$ and incidence $\mathbf{C}_{G|H}$ matrices are derived, being spectrum-invariant and vertex naming independent [33]. Figure 2 shows the matrices definition based on the transition network. Then, four different metrics are computed to determine the graph spectral similarity between subjects' networks by a series of operations and decompositions upon the related matrices, these metrics are denoted as similarity distances.

The first similarity distance $d_1(G,H)$ between G and H networks performs a subtraction between the diagonal matrix of noninverted weights (degree matrix $\mathbf{D}_{G|H}$) and the full-rank matrix of inverted directed weights (adjacency matrix $\mathbf{A}_{G|H}$) to produce a Laplacian matrix $\mathbf{L}_{G|H}$. Upon the Laplacian matrix, an Eigenvalue Decomposition (EVD) finds the eigenvalues λ_i from G network and μ_i from H [33], such that a scalar nonnegative value is calculated applying the relation in (5).

$$\mathbf{L}_{G|H} = \mathbf{D}_{G|H} - \mathbf{A}_{G|H} \overset{\text{EVD}}{=} \mathbf{Q}_{G|H} \begin{pmatrix} \lambda_1 & 0 & 0 \\ 0 & \lambda_2 & 0 \\ 0 & 0 & \lambda_3 \end{pmatrix} \mathbf{Q}_{G|H}^{\mathrm{T}}$$

$$d_1(G,H) = \begin{cases} \sqrt{\dfrac{\sum_{i=0}^{N-1} (\lambda_i - \mu_i)^2}{\sum_{i=0}^{N-1} \lambda_i^2}} & \text{if} \quad \sum_{i=0}^{N-1} \lambda_i^2 \leq \sum_{i=0}^{N-1} \mu_i^2 \\ \sqrt{\dfrac{\sum_{i=0}^{N-1} (\lambda_i - \mu_i)^2}{\sum_{i=0}^{N-1} \mu_i^2}} & \text{if} \quad \sum_{i=0}^{N-1} \mu_i^2 \leq \sum_{i=0}^{N-1} \lambda_i^2 \end{cases} \tag{5}$$

The similarity distance $d_2(G,H)$ use the adjacency matrices $\mathbf{A}_{G|H}$ to perform an EVD. The factorization produces two eigenvector matrices $\mathbf{Q}_{G|H}$, $\mathbf{Q}_{G|H}^{\mathrm{T}}$ and one eigenvalues diagonal matrix $\Lambda_{G|H}$, which pass to a final transformation Δ as in (6) [19]. The Frobenius norm $\|\Delta\|_F$ measures the distance between the two transitions networks using the equation in (7).

$$\mathbf{A}_{G|H} \overset{\text{EVD}}{=} \mathbf{Q}_{G|H} \Lambda_{G|H} \mathbf{Q}_{G|H}^{\mathrm{T}}$$

$$\Delta = \mathbf{A}_G - \mathbf{Q}_G^{\mathrm{T}} \mathbf{Q}_H \mathbf{A}_H \mathbf{Q}_H^{\mathrm{T}} \mathbf{Q}_G = \begin{pmatrix} \delta_1 & 0 & 0 \\ 0 & \delta_2 & 0 \\ 0 & 0 & \delta_3 \end{pmatrix} \tag{6}$$

$$d_2(G,H) = \frac{1}{N} \sqrt{\sum_{i,j=1}^{N} \delta_{i,j}^2} \tag{7}$$

The similarity distance $d_3(G,H)$ follows the same steps as $d_2(G,H)$, however, an incidence matrix $\mathbf{C}_{G|H}$ triggers the calculation rather than the adjacency matrix $\mathbf{A}_{G|H}$. Hence, a Singular Value Decomposition (SVD) factorises the ill-ranked incidence matrix in two eigenvector matrices $\mathbf{U}_{G|H}$, $\mathbf{V}_{G|H}$ and one singular values diagonal matrix $\Sigma_{G|H}$. The transformation $\hat{\Delta}$ in (8) uses those matrix by-products to calculate the Frobenius norm $\left\|\hat{\Delta}\right\|_F$ as the formula in (9).

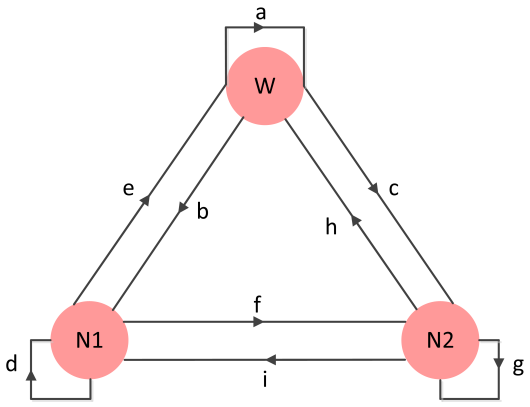

$$\mathbf{L} = \mathbf{D} - \mathbf{A}$$

$$= \begin{array}{c} \\ \text{W} \\ \text{N1} \\ \text{N2} \end{array} \begin{array}{c} \begin{array}{ccc} \text{W} & \text{N1} & \text{N2} \end{array} \\ \begin{pmatrix} a & 0 & 0 \\ 0 & d & 0 \\ 0 & 0 & g \end{pmatrix} \end{array} - \begin{array}{c} \\ \text{W} \\ \text{N1} \\ \text{N2} \end{array} \begin{array}{c} \begin{array}{ccc} \text{W} & \text{N1} & \text{N2} \end{array} \\ \begin{pmatrix} \frac{1}{a} & \frac{1}{b} & \frac{1}{c} \\ \frac{1}{e} & \frac{1}{d} & \frac{1}{f} \\ \frac{1}{h} & \frac{1}{i} & \frac{1}{g} \end{pmatrix} \end{array}$$

$$\mathbf{C} = \begin{array}{c} \\ \text{W} \\ \text{N1} \\ \text{N2} \end{array} \begin{array}{c} \begin{array}{ccccccccc} \text{WW} & \text{WN1} & \text{WN2} & \text{N1W} & \text{N1N1} & \text{N1N2} & \text{N2W} & \text{N2N1} & \text{N2N2} \end{array} \\ \begin{pmatrix} \frac{2}{a} & \frac{1}{b} & \frac{-1}{c} & \frac{1}{d} & 0 & 0 & \frac{1}{g} & 0 & 0 \\ 0 & \frac{1}{b} & 0 & \frac{-1}{d} & \frac{2}{e} & \frac{-1}{f} & 0 & \frac{1}{h} & 0 \\ 0 & 0 & \frac{1}{c} & 0 & 0 & \frac{1}{f} & \frac{-1}{g} & \frac{-1}{h} & \frac{2}{i} \end{pmatrix} \end{array}$$

Fig. 2. Sleep stages transition network and related matrices based upon a subject's hypnogram. A transition network consists of 3 vertices (i.e. one per sleep onset stages W/N1/N2) and 9 directed edges with a weight equal to the inverse of the total number of transitions between the corresponding vertices. Three matrices are derived from the transition network: degree **D**, adjacency **A** and incidence **C**. The adjacency **A** and incidence **C** matrices values correspond to the inverse of the total number of transitions from one stage to another. And the degree matrix **D** only includes the noninverse of the total transitions from each node to itself, therefore it is diagonal. The Laplacian matrix **L** comes from the subtraction of the diagonal degree matrix **D** and the adjacency **A** matrix.

$$\mathbf{C}_{G|H} \overset{\text{SVD}}{=} \mathbf{U}_{G|H}\Sigma_{G|H}\mathbf{V}^{\text{T}}_{G|H}$$

$$\hat{\Delta} = \mathbf{C}_G - \mathbf{U}^{\text{T}}_G\mathbf{U}_H\mathbf{C}_H\mathbf{V}^{\text{T}}_H\mathbf{V}_G = \begin{pmatrix} \hat{\delta}_1 & 0 & 0 \\ 0 & \hat{\delta}_2 & 0 \\ 0 & 0 & \hat{\delta}_3 \end{pmatrix} \tag{8}$$

$$d_3(G,H) = \frac{1}{N}\sqrt{\sum_{i,j=1}^{N}\hat{\delta}^2_{i,j}} \tag{9}$$

The distance $d_4(G,H)$ evaluates a probabilistic approximation, computing a Cauchy-Lorentz pdf $\rho_{G|H}(\omega)$ in function of heuristic-defined constants $K = 0.10771$ and $\gamma = 0.08$, and the eigenvalues ω_i extracted from the Laplacian matrices $\mathbf{L}_{G|H}$. The integration of the difference of both networks distributions, explained in (10), draws forth a similarity distance.

$$\mathbf{L}_{G|H} = \mathbf{D}_{G|H} - \mathbf{A}_{G|H} \overset{\text{EVD}}{=} \mathbf{Q}_{G|H}\begin{pmatrix} \omega_1 & 0 & 0 \\ 0 & \omega_2 & 0 \\ 0 & 0 & \omega_3 \end{pmatrix}\mathbf{Q}^{\text{T}}_{G|H}$$

$$d_4(G,H) = \sqrt{\int_0^\infty [\rho_G(\omega) - \rho_H(\omega)]^2 \text{d}\omega} \tag{10}$$

We conducted an unpaired two-tailed t-test to evaluate the null hypothesis that there is no difference in the distances amongst peer subjects (i.e. control-control and insomnia-insomnia) within the same group compared to the distances amongst control and insomnia patients. The t-test assumes that the similarity distances consisted of independent random samples coming from normal distributions with equal means but unknown variances. Prior a two-sample F-test evaluates whether the data come from distributions with equal or unequal variances. The t-test compared the similarity distances computed between hypnograms of subjects in these two groups 1) each control subject and all other control subjects (HXX→HXY) plus each insomnia patient and all other insomnia patients (IXX→IXY) versus 2) each control subject and all the insomnia subjects (HXX→IXX) plus each insomnia subject and all control subjects (IXX→HXX).

2) Subject Classification: We then trained a logistic regression classifier to differentiate between control and insomnia sleep onset patterns using the number of transitions made amongst W, N1 and N2 stages in the hypnogram. The logistic regression model is given by (11).

$$\begin{aligned} logit(\text{E}\{\mathbf{y}^i|\mathbf{x}^i\}) = logit(p^i) &= ln\left(\frac{p^i}{1-p^i}\right) = \hat{\beta}\mathbf{x}^i \\ &= \hat{\beta}^i_0 + \hat{\beta}^i_1\text{WW}^i + \cdots + \hat{\beta}^i_9\text{N2N2}^i \end{aligned} \tag{11}$$

where the Bernoulli distributed variable $\mathbf{y}^i$ is predicted by the product of the regression coefficients $\hat{\beta}$ and i^{th} subject's sleep onset stages transitions $\mathbf{x}^i = \{\text{WW}^i, \text{WN1}^i, \ldots, \text{N2N2}^i\}$. The logistic model was then tested using a leave-one-out crossvalidation (LOOCV), i.e. the regression coefficients $\hat{\beta}$ are estimated using 31 subjects during the training phase, and the 32^{th} subject is used to the test the model. Finally, we compute the sensitivity, specificity and accuracy performance rates between the foreknown and predicted distributions of the cohorts, where 0 denotes control and 1 insomnia.

IV. Results

A. Biosignal Modelling and Processing

We reported in [34] the performance of the modelling and processing module. The cited work demonstrated the efficacy of the approach to estimate frequency bands and transients within PSG signals. The difference between the original and approximated signals was measured in terms of root mean square error (RMSE); obtaining in average 4.4×10^{-2} for EEG signal, 4.2×10^{-2} for EOG and 2.5×10^{-1} for EMG. Based upon the reliability of the proposed model, frequency and amplitude-dependent features in Table I were selected based on an analysis of their periodograms.

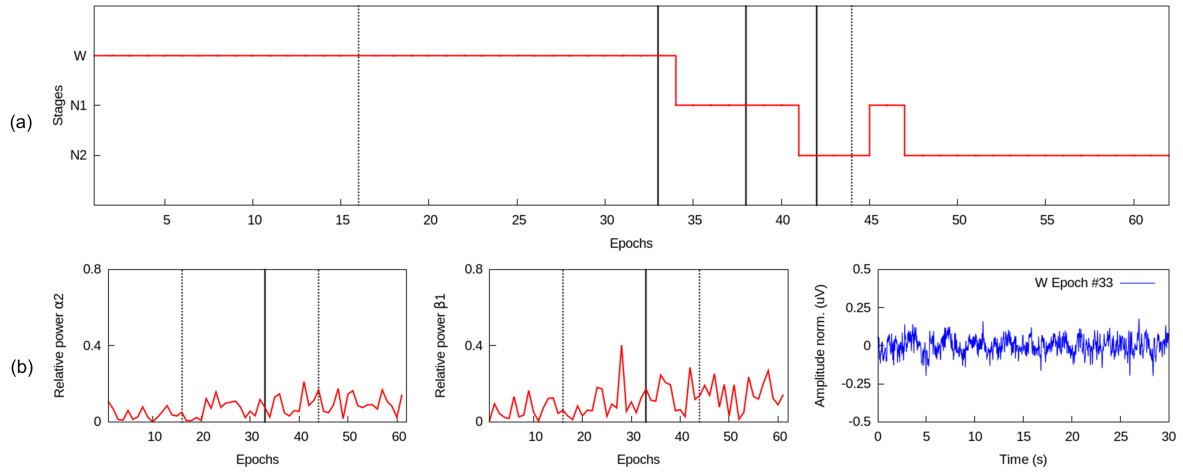

Fig. 3. Fuzzy logic classification for the automatic generation of sleep onset hypnograms. A subset of features are displayed to explain the mechanics of the fuzzy inference system in the mapping of powers, amplitudes and events to sleep stages. (a) The hypnogram corresponds to the first sleep onset cycle of subject H09. The dotted lines delimit the initial and final epochs that went through the classification process. The solid lines locate the specific epochs that are classified as part of the sleep onset period in the example, i.e. epoch #33. (b) Relative power of EEG α_2 band and β_1 bands versus sleep onset epochs to detect epoch #33 as W.

B. Hypnogram Generation

The FIS classified the sleep epochs into the defined input fuzzy sets to yield sleep stage decisions based on the features values, following more than 60 fuzzy rules. Figure 3 illustrates the applied fuzzy method behind the automated generation of hypnograms for sleep onset periods. Figure 3a depicts the entire first sleep onset cycle of subject H09, the dotted lines mark initial and final epochs, where the classification took place. The solid lines point out the specific epochs subject of fuzzy inference in the example. To classify epoch #33 as a W epoch in Figure 3b, the relative power in α_2 and β_1 bands reached values around 0.2, which fit into the middle input fuzzy set. According to the 'if-then' statements that governed the FIS, those conditions granted the highest degree of membership to W stage. The same logic concerned the classification of epochs #38 and #42 as N1 and N2, shown in the supplementary material. The former employed the relative power of θ band and number of VSW events, whilst the latter the relative power in ς_2 band and number of KC features. The decision was supported by the dominant θ activity and VSW transients during N1 episodes, as well as, convergent occurrence of KC and SS—associated with the ς_2 band—at N2 stages. The generation of subjects' hypnograms followed the aforementioned process.

C. Insomnia Characterisation

1) Transition Networks and Graph Spectral Theory: Figure 4 displays the standard deviation of the d_1 and d_4 similarity distances between each of the control subjects and all the other control and subjects with insomnia, computed using expert scored and automated hypnograms. The red squared pointers denote the standard deviation of the set of distances for each of the 16-subject control cohort, whilst the blue triangular pointers indicate the standard deviations referred to the 16-subject insomnia group. Figure 4 depicts how strongly inter-subjects' variability affected the similarity distances between sleep onset patterns of control and insomnia groups. A greater variation in the standard deviation of similarity distances between control and insomnia patients compared to the distances amongst control subjects, suggested that the sleep onset patterns of insomnia cohort differentiate from those of the control group. The comparison of standard deviations computed from expert and automated-scored hypnograms demonstrated how inter-raters' variability influenced the similarity distances of both groups. Nuances in some sleep stages transitions led to slightly different hypnograms, and thereby transition networks with different similarity distances were produced. For instance, d_1 assessed using expert scored hypnograms, has larger deviations (0.2) for half of the control subjects in respect to the control group. This means, d_1 shows an alternated variability in the sleep onset patterns of control vs. insomnia and control vs. control. The same alternated deviations is observed in the automated version, but the individual controls with larger deviations with respect to the control and insomnia groups differ. For subjects H01, H05-H09, H14, H16 the similarity deviation for d_1 remains smaller $(0.1-0.2)$ for control and more dispersed $(0.2-0.25)$ for insomnia. The deviations for distance d_4 obtained from expert and automated scoring not only show larger origin-out deviations for all the subjects, but also the control group is consistently spread out over a shorter range (0.3) as opposed to the insomnia group (0.4). Polar diagrams of d_2 and d_3 are included in the supplementary material.

The inter-subjects' and inter-raters' variability inhibited the distinctive characterisation of control and insomnia patterns in the polar diagrams. Then, a statistical analysis allowed us to unmask significant differences, whilst the influence of the spreading factor introduced by each subject and scoring mode can be smoothened through large distances-compared distributions. We conducted an unpaired two-tailed t-test to

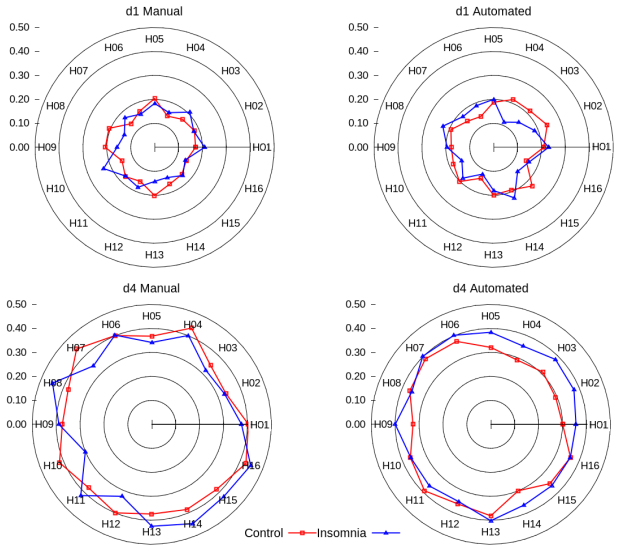

Fig. 4. Standard deviations of similarity distances for each control vs. control and insomnia cohorts. Each similarity distance is compared based on whether it is derived from expert-scored or automatic hypnogram. The red squared pointers denote the standard deviation of the set of distances for the 16-subject control cohort with respect to each control subject. The blue triangular pointers indicate the standard deviations referred to the 16-patient insomnia group with respect to each control subject.

test the hypothesis that the similarity distances between control and insomnia cohorts are significantly different. The t-test compared each possible similarity distance between control and patients, assumed as independent random samples of normal distributions with equal means but unknown variances. The statistical test consisted of two parts: the first one used the expert scored hypnograms to obtain the significance values; the second part re-ran the same protocol counting on automated hypnograms. The obtained p-values with Bonferroni correction revealed significant differences between the similarity distances of control-to-control vs. control-to-insomnia and insomnia-to-insomnia vs. insomnia-to-control groups. Table II summarises the t-values and p-values for each similarity distance and group comparison.

TABLE II
UNPAIRED TWO-TAILED T-TEST STATISTICS OF SIMILARITY DISTANCES

Distance	t-value,p-value (Expert)	t-value,p-value (Automatic)
d_1	$t=-2.28, p=0.02$	$t=-4.01, p=\mathbf{0.0019}$
d_2	$t=0.50, p=0.61$	$t=-3.71, p=\mathbf{0.0019}$
d_3	$t=-5.07, p=\mathbf{0.0019}$	$t=-0.47, p=0.63$
d_4	$t=-1.39, p=0.16$	$t=-2.22, p=0.02$

$p < 0.0031$

For distances computed from expert scored hypnograms, d_3 was found to be significantly different between the peer and disordered cohorts. d_1 and d_2 for the control and insomnia groups were also significantly different using automated hypnograms. The statistical results supported the usage of a classifier based on the sleep stages transitions to differentiate insomnia patients from control subjects, whereas $d_1 - d_4$ were all derived from the graph spectrum of stages transition networks.

2) Subjects Classification: Table III depicts the performance of the logistic classifier in terms of the confusion matrix, sensitivity, specificity and accuracy rates, comparing expert and automated hypnograms. The performance of the logistic regression was higher when tested with automated hypnograms as compared to expert scored hypnograms. One control and two subjects with insomnia less were misclassified using the automated hypnograms.

TABLE III
CONFUSION MATRICES AND PERFORMANCE RATES OF LOGISTIC REGRESSION USING EXPERT VS. AUTOMATIC HYPNOGRAMS

	EXPERT			AUTOMATIC	
	Control	Insomnia		Control	Insomnia
Control	13	3	Control	14	2
Insomnia	6	10	Insomnia	4	12
Sens= 0.81	Spec= 0.62	Acc= 0.71	Sens= **0.87**	Spec= **0.75**	Acc= **0.81**

V. DISCUSSION AND CONCLUSIONS

In this paper we have presented a three module approach for the computer-assisted diagnosis of insomnia. The first biosignal processing module in our approach used state-spaced TVARMA(8,2) processes with recursive particle filter to generate features that overcome the nonlinear, nonstationary and non-Gaussian constraints of biosignals, thus accurately approximating PSG signals. For accurate sleep staging, the second hypnogram generation module implemented a fuzzy-logic decision structure that incorporated rule-based scoring guidelines used by sleep experts and additional conditions that accounted for inter-subject variability and overlooked scoring criteria. The final insomnia characterization module translated the complexity of the sleep onset pattern in hypnograms, either expert or automatically generated, into a set of simple, similarity distances using graph spectral theory. A logistic regression classifier trained to discriminate between control and insomnia sleep onset patterns using the stages transitions provided highly-rated performance metrics: sensitivity (87%), specificity (75%) and accuracy (81%).

The promising results reported here are due to a number of novel contributions in our modules. The first novel contribution was the use of state-spaced TVARMA(8,2) processes with recursive particle filter to generate biosignal features. Although, autoregressive models have been extensively utilised for quantitative EEG analysis [35], [25], particle filtering to estimate non-Gaussian distributions has still not been used with sleep studies [34]. The Cauchy-Lorentz-distributed particle filter used in the module enabled tracking of sudden events (e.g. VSW, KC, SS) and gradual shifts, like δ or θ frequencies [34].

Our second novel contribution was the use a fuzzy rule-set that included rules that addressed discrepancies in sleep staging. Currently most of these discrepancies occur due to the inconclusive marking of VSW, KC or SS transients in transitionary stages. N1 sleep stage disagreement has led to a lack of agreement between human vs. human and human vs. machine scorers [17], [15], [36]. Some studies [18], [13], [37] have proposed recommendations such as using a more objective

amplitude criteria or the identification of band attenuation or low amplitude mixed frequencies in epochs to detect N1 stage. Our automated hypnogram generation module included these suggestions in its fuzzy ruleset.

Finally our last novel contribution is the application of graph spectral theory to map the dynamics of sleep onset patterns to stage-oriented networks, transitions matrices and eigenvalues, thus quantifying the transitions in a hypnogram into similarity distances. The eigenvalues used to compute the scalar similarity distances form a set of hypnogogic fingerprints for each subject, which map the transition patterns amongst sleep stages with a minimal chance of duplicity. To the best of our knowledge, there are no previous works attempting an approach of this sort to characterize insomnia.

Our approach provides not only a computer-aided detection of sleep transients and frequency bands; but also enables the assessment of sleep statistics throughout automated hypnograms. Conventional classification approaches do not allow such a level of customisation. Though the three modules in our approach are inter-related, they can also be used independently, depending on the desired goal. For instance, the insomnia characterisation module can be performed with expert scored instead of computer generated hypnograms.

For future work, a further investigation needs to be conducted on the usage of similarity distances to characterise additional pathologies related to sleep and psychiatric disorders. The usage of graph spectral theory in sleep studies can also be explored further to delimit the leverage on eigenvalue computation when several sleep nights are considered. The size of the used clinical cohort used to validate our methods will be increased to fully test the suitability of the proposed methods.

ACKNOWLEDGEMENT

The work was supported by NPRP grant #[5-1327-2-568] from the Qatar National Research Fund, which is a member of Qatar Foundation. The statements made herein are solely the responsibility of the authors.

The authors would like to thank the Interdisciplinary Centre for Sleep Medicine at the Charité Universitätsmedizin Berlin (Germany) for undertaking the recruitment and collection of polysomnographic recordings, as well as, the sleep scorers dedicated to the assessment labours.

R. Chaparro-Vargas acknowledges the financial support of the alliance Colciencias and Colfuturo foundation of the Colombian Government, as main sponsor of his doctorate studies.

REFERENCES

[1] P. Bob, "Consciousness, schizophrenia and complexity," *Cognitive Systems Research*, vol. 13, no. 1, pp. 87–94, 2012.

[2] J. Maes, J. Verbraecken, M. Willemen *et al.*, "Sleep misperception, EEG characteristics and autonomic nervous system activity in primary insomnia: A retrospective study on polysomnographic data," *International Journal of Psychophysiology*, vol. 91, no. 3, pp. 163–71, Mar 2013.

[3] A. Schlemmer, U. Parlitz, S. Luther *et al.*, "Changes of sleep-stage transitions due to ageing and sleep disorder," *Philos Trans A Math Phys Eng Sci.*, vol. 13, no. 373, pp. 20–34, 2015.

[4] D. Freeman, K. Pugh, N. Vorontsova *et al.*, "Insomnia and paranoia," *Schizophrenia research*, vol. 108, no. 1-3, pp. 280–284, March 2009.

[5] World Health Organization, *The ICD-10 Classification of Mental and Behavioural Disorders: Diagnostic Criteria for Research*, ser. ICD-10 classification of mental and behavioural disorders. World Health Organization, 1993.

[6] D. Gencaga, E. Kuruoglu, and A. Ertüzün, "Modeling non-gaussian time-varying vector autoregressive processes by particle filtering," *Multidimensional Systems and Signal Processing*, vol. 21, no. 1, pp. 73–85, 2010.

[7] P. M. Djuric, J. H. Kotecha, F. Esteve *et al.*, "Sequential parameter estimation of time-varying non-gaussian autoregressive processes," *EURASIP Journal on Advances in Signal Processing*, vol. 2002, no. 8, pp. 865–875, 2002.

[8] J. Lee and K. Chon, "Time-varying autoregressive model-based multiple modes particle filtering algorithm for respiratory rate extraction from pulse oximeter," *Biomedical Engineering, IEEE Transactions on*, vol. 58, no. 3, pp. 790–794, March 2011.

[9] J. Liu and M. West, "Combined parameter and state estimation in simulation-based filtering," in *Sequential Monte Carlo Methods in Practice*, ser. Statistics for Engineering and Information Science, A. Doucet, N. Freitas, and N. Gordon, Eds. Springer New York, 2001, pp. 197–223.

[10] R. Prado, "Sequential estimation of mixtures of structured autoregressive models," *Computational Statistics & Data Analysis*, vol. 58, no. 0, pp. 58–70, 2013.

[11] S. Tong, Z. Li, Y. Zhu *et al.*, "Describing the nonstationarity level of neurological signals based on quantifications of time and frequency representation," *Biomedical Engineering, IEEE Transactions on*, vol. 54, no. 10, pp. 1780–1785, oct. 2007.

[12] M. Arulampalam, S. Maskell, N. Gordon *et al.*, "A tutorial on particle filters for online nonlinear/non-gaussian bayesian tracking," *Signal Processing, IEEE Transactions on*, vol. 50, no. 2, pp. 174–188, Feb 2002.

[13] H. Danker-Hopfe, P. Anderer, J. Zeitlhofer *et al.*, "Interrater reliability for sleep scoring according to the Rechtschaffen & Kales and the new AASM standard," *Journal of Sleep Research*, vol. 18, no. 1, pp. 74–84, 2009.

[14] C. Iber, S. Ancoli-Israel, A. L. C. Jr. *et al.*, "The AASM manual for the scoring of sleep and associated events," American Academy of Sleep Medicine, Tech. Rep., 2012.

[15] J. Caffarel, G. J. Gibson, J. P. Harrison *et al.*, "Comparison of manual sleep staging with automated neural network-based analysis in clinical practice," *Medical & Biological Engineering & Computing*, vol. 44, no. 1-2, pp. 105–110, 2006.

[16] C. Berthomier and X. D. et al., "Automatic analysis of single-channel sleep EEG: Validation in healthy individuals," *Sleep*, vol. 30, no. 11, pp. 1587–1595, May 2007.

[17] P. Anderer, A. Moreau, M. Woertz *et al.*, "Computer-assisted sleep classification according to the standard of the american academy of sleep medicine: Validation study of the AASM version of the somnolyzer 24x7," *Neuropsychobiology*, vol. 62, no. 4, pp. 250–264, 2010.

[18] R. Rosenberg and S. Van Hout, "The american academy of sleep medicine inter-scorer reliability program: sleep stage scoring," *J Clin Sleep Med*, vol. 9, no. 1, pp. 81–87, 2013.

[19] M. Ipsen and A. S. Mikhailov, "Evolutionary reconstruction of networks," *Phys. Rev. E*, vol. 66, p. 046109, Oct 2002.

[20] D. Jakobson and I. Rivin, "Extremal metrics on graph I," *Forum Mathematics*, vol. 14, no. 1, pp. 147–163, 2002.

[21] P. Stoica and R. Moses, *Spectral analysis of signals*, T. Robbins, Ed. Pearson Prentice Hall, 2005.

[22] R. D. Ogilvie, "The process of falling asleep," *Sleep Medicine Reviews*, vol. 5, no. 3, pp. 247–270, 2001.

[23] H. Merica and R. D. Fortune, "State transitions between wake and sleep, and within the ultradian cycle, with focus on the link to neuronal activity," *Sleep Medicine Reviews*, vol. 8, no. 6, pp. 473–485, 2004.

[24] C. Marzano, F. Moroni, M. Gorgoni *et al.*, "How we fall asleep: regional and temporal differences in electroencephalographic synchronization at sleep onset," *Sleep Medicine*, vol. 14, no. 11, pp. 1112–1122, 2013.

[25] E. Pereda, R. Q. Quiroga, and J. Bhattacharya, "Nonlinear multivariate analysis of neurophysiological signals," *Progress in Neurobiology*, vol. 77, no. 12, pp. 1–37, 2005.

[26] G. Kitagawa, *Introduction to Time Series Modeling*. CRC Press, 2009, ch. Non-Gaussian State-Space Model, pp. 1–17.

[27] C.-M. Ting, S.-H. Salleh, Z. Zainuddin *et al.*, "Spectral estimation of nonstationary EEG using particle filtering with application to event-related desynchronization (ERD)," *IEEE Transactions on Biomedical Engineering*, vol. 58, no. 2, pp. 321–331, 2011.

[28] G. Kitagawa, *Introduction to Time Series Modeling*. CRC Press, 2009, ch. The Sequential Monte Carlo Filter, pp. 1–15.

[29] A. Galka, K. F. K. Wong, T. Ozaki *et al.*, "Decomposition of neurological multivariate time series by state space modelling," *Bulletin of Mathematical Biology*, vol. 73, pp. 285–324, 2011.
[30] D. Álvarez-Estévez, J. M. Fernández-Pastoriza, E. Hernández-Pereira *et al.*, "A method for the automatic analysis of the sleep macrostructure in continuum," *Expert Systems with Applications*, vol. 40, no. 5, pp. 1796 – 1803, 2013.
[31] D. Dubois and H. Prade, *Fuzzy Sets and Systems: Theory and Applications*, N. York, Ed. Academic Press, 1980.
[32] A. Kaufmann and M. Gupta, *Introduction to Fuzzy Arithmetic*, B. Esposito, Ed. V.N. Reinhold, 1985.
[33] G. Jurman, R. Visintainer, and C. Furlanello, "An introduction to spectral distances in networks," *Frontiers in Artificial Intelligence and Applications*, vol. 226, pp. 227–234, 2011.
[34] R. Chaparro-Vargas, P. Dissayanaka, T. Penzel *et al.*, "Sleep onset detection based on time-varying autoregressive models with particle filter estimation," in *Biomedical Engineering and Sciences (IECBES), 2014 IEEE Conference on*, Dec 2014, pp. 436–441.
[35] N. V. Thakor and S. Tong, "Advances in quantitative electroencephalogram analysis method," *Annual Review of Biomedical Engineering*, vol. 6, no. 1, pp. 453–495, 2004.
[36] A. Rodenbeck, R. Binder, P. Geisler *et al.*, "A review of sleep EEG patterns. Part I: A compilation of amended rules for their visual recognition according to rechtschaffen and kales," *Somnologie*, vol. 10, no. 4, pp. 159–175, 2006.
[37] H. Danker-Hopfe, D. Kunz, G. Gruber *et al.*, "Interrater reliability between scorers from eight european sleep laboratories in subjects with different sleep disorders," *Journal of Sleep Research*, vol. 13, no. 1, pp. 63–69, 2004.

Ramiro Chaparro-Vargas received the M.Sc. degree in Communications Engineering in 2010 from the Technical University of Munich, Munich, Germany. Currently, he is working towards the Ph.D. degree in the School of Electrical and Computing Engineering at RMIT University, Melbourne, Australia. His research interest resides in signal processing and computational modelling applied to biomedical applications, particularly in neurophysiology. IEEE member since 2004.

Beena Ahmed received the electrical engineering B.Sc. (Hons.) degree in 1993 from the University of Engineering and Technology, Lahore. In 2004, she obtained her Ph.D. degree from the University of New South Wales, Sydney, Australia. Currently, she works as Senior Lecturer at the Electrical and Computer Engineering, Texas A&M University at Qatar. Member of IEEE EMB Chapter since 2009.

Niels Wessel received the mathematics B.Sc. degree in 1995 from the Humboldt-Universität zu Berlin, Germany. In 1998, he obtained his Ph.D. degree from the University of Postdam. Since 2009, he is the head of the Cardiovascular Physics group at the Humboldt-Universität zu Berlin.

Thomas Penzel received the Physics diploma in 1986 from the University Marburg, Germany. In 1991, he obtained his doctorate in Human biology from the University Marburg, Germany. was appointed as professor of physiology at the medical school in Marburg. Since 1982 he worked in the sleep laboratory in Marburg being responsible for development of biomedical methodologies for diagnosis and therapy of sleep disorders. He has been a member of the board of the German Sleep Society from 1993. Member of IEEE EMB German Chapter since 2006.

Dean Cvetkovic received the M.Eng. and Ph.D. degree respectively in 2002 and 2005 from the RMIT University, Melbourne, Australia. At the present, he is a Senior Lecturer in Biomedical and Electronics Engineering at School of Electrical and Computer Engineering (RMIT University) and a member of Health Innovations Research Institute (HIRi). His research at RMIT University spans over the last 15 years in the engineering areas of biomedicine, electronics, mechatronics and design engineering education. Member of IEEE EMB Chapter since 2008.

Appendix K

Peer-reviewed conference paper

Title: Searching Arousals: A Fuzzy Logic Approach

Authors: Ramiro Chaparro-Vargas, Beena Ahmed, Thomas Penzel and Dean Cvetkovic

Publication: Proceedings of the 37th Annual International Conference of the IEEE Engineering in Medicine and Biology Society

Year of Publication: 2015

Searching arousals: A fuzzy logic approach

Ramiro Chaparro-Vargas* Beena Ahmed‡ Thomas Penzel† Dean Cvetkovic⋆

Abstract— **This paper presents a computational approach to detect spontaneous, chin tension and limb movement-related arousals by estimating neuronal and muscular activity. Features extraction is carried out by Time Varying Autoregressive Moving Average (TVARMA) models and recursive particle filtering. Classification is performed by a fuzzy inference system with rule-based decision scheme based upon the AASM scoring rules. Our approach yielded two metrics: arousal density and arousal index to comply with standardised clinical benchmarking. The obtained statistics achieved error deviation around ± 1.5 to ± 30. These results showed that our system can differentiate amongst 3 different types of arousals, subject to inter-subject variability and up-to-date scoring references.**

I. INTRODUCTION

Sleep macrostructure is build upon the occurrence of oscillations and transients within cyclic stages [1]. Microarousals, or simply arousals are transients, typically found during light, deep or rapid eye movement sleep (REM). The implications of arousals upon regular sleeping patterns and their relationship to sleep pathophysiologies has yet to be defined [2]. The polysomnogram (PSG) signals: electroencephalogram (EEG) and electromyogram (EMG) are typically used to detect the different types of arousals.

Autoregressive processes have been used in the modelling of different biological signals [3], [4], [5], disregarding their application for the analysis of sleep micro and macrostructure. Furthermore, most of the approaches have analysed neurological or muscular features under linear and Gaussian conditions; such assumptions have hindered their interpretation and the extraction of significant information. For example, arousals are short-term events in time domain, but also display interweaving fluctuations of power bands over frequency spectrum. Time-varying autoregressive models accompanied by particle filter estimation [6] offer a promising solution to track these rapid power fluctuations. Thereupon, the extracted features have a high resolution in time and frequency domains.

The computer-assisted detection of arousals deals with a classification problem that requires fine features, inter-subject and scorer-specific considerations, given the existent variability [7]. The available scoring manuals, e.g. R&K, ASDA or AASM [8], have different criteria to mark the onset and offset of arousals using multiple channels. However, there is still a lack of understanding and consensus about these guidelines amongst specialists. A few studies have pointed out potential areas of improvement to achieve a more homogeneous decision making [9], [10]. Computer-assisted solutions have the potential of accurate arousal detection that can be tolerant to inter-rater and inter-subject variability.

We propose a computational approach to perform fuzzy logic-based arousal detection to 20 healthy subjects. The methods acknowledge subjects and scorers-dependent disagreements that commonly compromise the proper characterisation of sleep components, sleep microfragmentation, hyperarousals or even insomnia disorder [2].

*Affiliated to the School of Electrical and Computing Engineering, RMIT University, Melbourne VIC 3001, Australia ramiro.chaparro-vargas@rmit.edu.au

†Affiliated to the Interdisciplinary Centre for Sleep Medicine, Charité Universitätsmedizin Berlin, Berlin, Germany thomas.penzel@charite.de

‡Affiliated to the Electrical and Computer Engineering Program, Texas A&M University at Qatar beena.ahmed@qatar.tamu.edu

⋆Affiliated to the School of Electrical and Computing Engineering, RMIT University, Melbourne VIC 3001, Australia dean.cvetkovic@rmit.edu.au

II. METHODS

A. Biosignal Processing

TVARMA(8,2) state-space processes cope with abrupt and subtle shifts in the input biosignal by modelling the state noise with the Cauchy-Lorentz distribution, a non-Gaussian approach. The distribution exhibit heavy-tailed regions to grant a more significant probabilistic weight to abrupt transitions, and a tighter dispersion in the central zone to track smooth variations [11]. To determine the model coefficients, we developed a recursive particle filter that estimates the posterior probability density functions (pdf), supported on the present system state, past and arriving observations [6]. Akaike and Bayesian information criterion were used to find optimal orders p and q, being set to 8 and 2 thereof.

Each 30-second epochs were divided in 3-second windows, i.e. 10 windows per epoch. The computation of window's spectral features was done by the convolution of the epoch's TVARMA(8,2) coefficients and a bank of filters based on complex Morlet mother wavelets with specific central frequencies and bandwidths [12]. From the EEG channels, we calculated θ (4-7 Hz), α (7-12 Hz), ς (12-16 Hz) and β (14-18 Hz) instantaneous power bands. The instantaneous θ, α, ς and β relative powers $\mathrm{P}[k]$ were averaged to yield only 4 representative θ, α, ς and β band powers for each 3-second window. These features accompanied by averaged amplitude levels upon EMG chin and tibialis channels composed the whole features set in Table I.

B. Arousal Detection

As per the AASM, a spontaneous arousal was defined as an abrupt shift of EEG frequency including θ, α and/or frequencies greater than 16 Hz (but no spindles) that lasts

TABLE I
FEATURES FOR SLEEP AROUSAL DETECTION

#	Feature	Channel	Event/Freq. Band (Hz)
1	$P_\theta[k]$	EEG C4A1, O1A2	$4-7$
2	$P_\alpha[k]$	EEG C4A1, O1A2	$7-12$
3	$P_\varsigma[k]$	EEG C4A1, O1A2	$12-16$
4	$P_\beta[k]$	EEG C4A1, O1A2	$16-30$
5	A_{EMGc}	EMG chin	Chin tension
6	A_{EMGt}	EMG tibialis	Limb movement

at least 3 s, with at least 10 s of stable sleep preceding the change. Concomitant increases in submental EMG lasting at least one second during REM sleep was marked as spontaneous arousal with chin tension. Limb movement arousal were identified through activity in the tibialis EMG. The marking of arousal is not straightforward. They can be accompanied by an increase in α or β and an attenuation of θ or ς power bands, as well as possible activity in the submental and limb muscles. Fuzzy logic is an appropriate tool to detect spontaneous and limb arousals as it can tolerate a higher degree of uncertainty in PSG signals [13]. The developed Mamdani Fuzzy Inference System (FIS) maps a collection of input variables, i.e. power and amplitude-related features, to four possible arousal decisions: none, spontaneous, spontaneous with chin tension and limb. The FIS consisted of three input fuzzy sets to allocate the features values using trapezoidal membership functions. The fuzzy sets intervals and overlapping thresholds are evenly distributed: low $(0-0.3)$, medium $(0.25-0.6)$ and high $(0.55-1)$ to cover the 0-1 range of normalised instantaneous power bands and amplitudes [13]. The overlapping design of fuzzy sets enabled feature values to belong to more than one set at a time, the degree of membership quantified on a 0-1 scale. A mid-high value $(0.3-1)$ in the averaged relative power of α or β band within a 3-second window suggests an arousal existence. Hereafter, the averaged relative power of θ or ς band along the 3 previous 3-second windows, i.e. the former 9 seconds, needed to hold sustained mid-high values. The FIS employed 60 human-like decision rules or if-then statements to map fuzzy inputs to a particular output state. The decision rules are based upon interpretations of the arousal scoring guidelines. The final output consisted on a reconstructed hypnogram with labelled arousal locations, which reproduced the accustomed outputs of sleep clinical assessments.

C. Clinical Data

For the present study, 20 male healthy (H) subjects undertook an overnight polysomnogram recording at the facilities of the Interdisciplinary Centre for Sleep Medicine at the Charité Universitästmedizin Berlin. The study was approved by the local Ethics Committee of the Charité Universitästmedizin Berlin.

Arousal detection was performed using two EEG (C4-A1, O1-A2) and two EMG (chin and left tibialis) channels. Sleep staging was performed as per the guidelines of the AASM manual [8] with each 30-second epoch mapped to a standardised stage: wake (W), non-REM1 (N1), non-REM2 (N2), non-REM3 (N3) and Rapid Eye Movement (REM). Additionally, related parameters marked apnoea/hyponoea, oxygen saturation, snoring and arousals. We examined the 20 PSG recordings to identify datasets with artefacts or severe disruptions. A total of 6 datasets were excluded, due to major heartbeat-type artefacts or discontinuous records. We only consider for analysis the first sleep cycle, i.e. the sleep progression running from the first W stage going through N1-N2-N3 stages until REM sleep consolidation.

The biosignal processing and arousal detection were implemented using MathWorks® MATLAB 8.5 with its Signal Processing and Fuzzy Logic toolboxes.

III. RESULTS

The detection of spontaneous, chin tension and limb movement arousals depended on the logical association of input variables, rules and output categories within the fuzzy framework. Figure 1 deconstructs the classification process using epochs #22 and #42 as an example to describe the interaction of the FIS' components. In Figure 1a, the hypnogram of the first sleep cycle recorded from subject H01 is displayed. The dotted lines mark the epochs where arousals were automatically detected in the W-N1-N2-N3 and REM stages. The solid lines highlight two particular epochs (#22, #42) with spontaneous arousals to demonstrate their fuzzy process of detection. Figure 1b shows the windowing of EEG epochs #22 and #42, that means, ten 3-second windows to be characterised by the four EEG-dependent features. Figure 1c depicts the trends of β and ς band powers in epoch #22. In the fourth 3-second window an increase above 0.4 in β band is accompanied by a medium 0.2 ς relative power in the previous windows. Under those conditions, the FIS had enough merit to declare the occurrence of an spontaneous arousal for that epoch. Similarly in epoch #42, a peak of power (0.58) in α band with pre-existing 9 seconds of constant 0.2 relative power for θ band indicated the presence of an arousal. Extending this decision principle to all the epochs and channels, our system was capable of detecting arousals for the entire cohort of subjects.

To complement the graphical representation of sleep stages, epochs and arousals over a hypnogram; we computed two standardised parameters related to arousal events: the number of arousals and arousal index (ArI) [8]. These two parameters allowed us to compare the expert scoring conducted by the expert raters versus our computer-assisted approach as given in Table II. Due to the high level of inter-subject variability, the error rate of our arousal detector varied considerably across the subjects. For instance, subjects H01, H11 and H15 had low error deviations in the arousal index (ArI): ± 7.05, ± 3.69 and ± 1.15, correspondingly. Conversely, subjects H07 and H12 had deviations around ± 30 directed either by over or underrating of arousals density during NREM sleep stages. Foremost, the larger disagreements were related to above average number of scored arousals (e.g. 60 marks for H07) or complete lack of events (e.g. 0 marks for H12) on the expert scoring

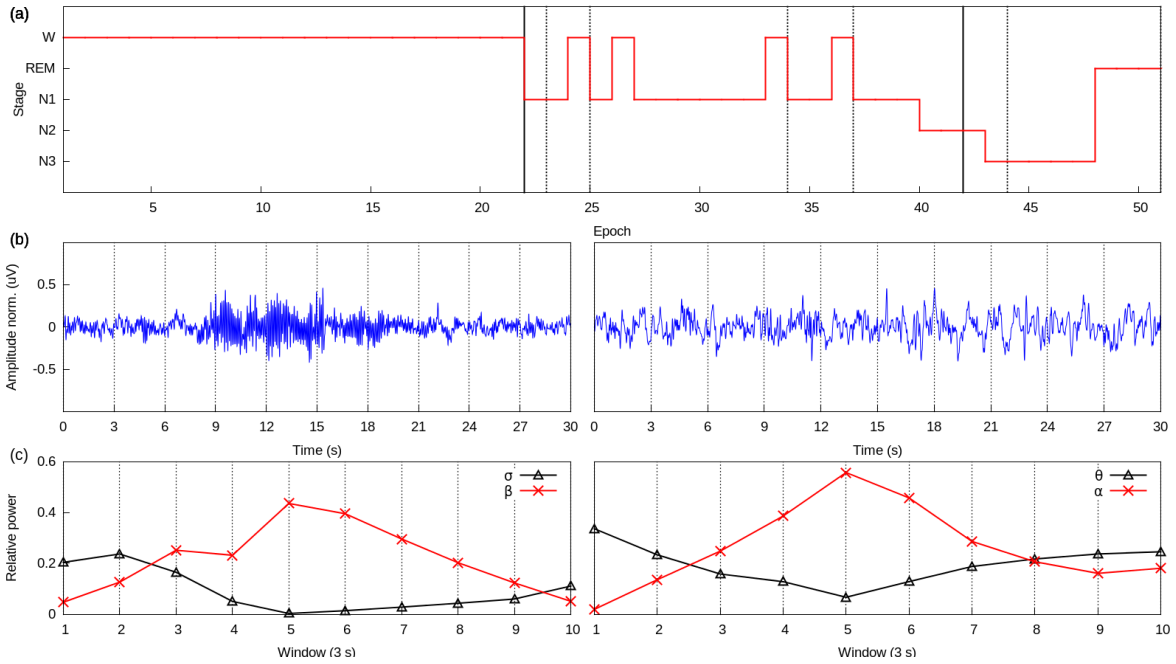

Fig. 1. Arousal detection based on fuzzy inference system. (a) Hypnogram of the first sleep cycle recorded from subject H01. The dotted lines localise the epochs with detected arousals. The solid lines mark the epochs #22, #42 of the two spontaneous arousals detected by the fuzzy inference system. (b) 3-second windowing of epoch #22 with detected α frequency shift and epoch #42 driving β band fluctuations. The dotted lines delimit the 3-second windows used to evaluate the average relative power corresponding to θ, α, ς and β bands. (c) Relative power bands of EEG epochs #22 and #42 against 3-second windows.

side. Based on the AASM recommendations, our proposed system was strictly aligned to the frequency regimes, arousal duration, preceding sleep duration, cortical derivations and aside events; therein.

TABLE II
AROUSALS METRICS FOR NREM AND REM SLEEP

		H01	H02	H04	H05	H07	H08	H09
Expert	Ar NREM	18	1	0	1	60	0	1
	Ar REM	0	0	0	0	0	0	1
	Ar Index †	**42.35**	0.96	0	1.76	**48.15**	0	0.41
Auto	Ar NREM	14	17	9	8	15	34	20
	Ar REM	1	2	2	6	7	9	5
	Ar Index	**35.29**	18.38	20.95	24.71	**17.36**	16.48	10.38
	ArI error	**7.05**	-14.41	-20.95	-22.94	**30.78**	-16.48	-9.96
		H11	H12	H13	H15	H16	H17	H20
Expert	Ar NREM	12	0	1	11	1	42	1
	Ar REM	0	0	0	1	0	0	0
	Ar Index	**22.15**	**0**	1.22	**13.84**	0.91	35.24	0.65
Auto	Ar NREM	10	35	7	9	21	13	17
	Ar REM	0	7	0	2	4	2	5
	Ar Index	**18.46**	**30.92**	8.57	**12.69**	22.55	12.58	14.34
	ArI error	**3.69**	**−30.92**	-7.34	**1.15**	-21.65	22.65	-13.69

† $\frac{\#\ Arousals}{First\ Cycle\ Sleep\ Time} * 60$

IV. DISCUSSION AND CONCLUSIONS

In this paper, we have proposed a computational system to detect spontaneous and body movement-related arousals, based on objective criteria from the latest AASM standard. Our system offers to sleep clinicians, a reliable tool for primary diagnosis attending to provide more conclusive assessments.

The computer-assisted detection of arousals pursued with the TVARMA(8,2) models and Mamdani FIS tracked abrupt frequency shifts to identify spontaneous, chin tension and limb movement types. The rule-based classification with human-oriented reasoning evaluated features' tendencies rather than certain states, whereas most band powers and amplitudes shifts suddenly occur. The fuzzy membership functions reflected the features variations in a smoother way due to the subtle transition from one fuzzy set to another, i.e. low, medium and high. Being part of more than one set at a time improved the detection rates, since frequency shifts happening in less than a 3-second window still had margins of detection due to the sensitivity of the fuzzy rules from low-to-medium or low-to-high power values. This suggests that our approach can manage issues like inter-subjects variability [7]. Our findings supported the promotion of uncertain thresholds of detection to counterbalance the trade-off between accuracy and subjects' nuances [14]. One major improvement introduced by the AASM manual [8] over former standards (e.g. R&K or ASDA) in regard to arousal detection, was the definition of minimum time windows for wake-related frequency shifts (3 s), foregoing sleep-related bands (10 s), suggested scalp derivations (central and occipital) and supporting channels (EMG or ECG). Our approach complied with these conditions to ameliorate biased assessments responding to differing criteria [10].

The disagreements between expert and automated detections were predominantly due to the overrating or null marking of arousal events during NREM stages. The expert

scoring reported no arousals for subjects H04, H08 and H12; whilst the automated scoring marked 17, 34 and 35 events, correspondingly. The total absence of arousals is not consistent with the expected recurrent occurrence of spontaneous arousals in normal sleep [15]. The high number of expert detected arousals in contiguous epochs for subjects H07 and H17, could due to the limited application of AASM marking rules prescribing 1) the minimum window length and 2) the presence of stable sleep between independent events. The proposed FIS avoided similar marking deviations by strictly applying these AASM rules. Moreover, the system was able to mark arousals during REM sleep, due to the presence of band power shift and increased chin tension as per AASM recommendations, even though they are commonly disregarded due to the unavailability of EMG chin channel, hidden low amplitude α activity inside of the dominant high amplitude δ waves, or both.

To our knowledge, there is only one other system that performed arousal detection by means of linear discrimination and artificial neural networks [15]. Its performance was measured in terms of classification metrics, such as error (10.5%), sensitivity (50.9%), specificity (97.1%), area under the curve (74%) rates and arousal index. These results can be partially compared to the performance of our system as we only employed the statistical metrics defined by the AASM (i.e. number of arousal and the arousal index) and adopted amongst sleep specialists. On this regard, both studies agreed on 20 as average arousal index amongst corresponding subjects, supporting the occurrence of arousals as recurring microevents within the normal sleep macrostructure.

In future works, we would like to enhance the detection capabilities of the system to better manage inter-subjects variability using refined human-like ruleset. Also, we are interested in recruiting additional scorers to analyse the inter-rater variability, between sleep specialists and computer-aided systems. We would like to extend the detection system to additional arousal classes, such as cardiovascular or respiratory-dependent and limb movement arousals.

ACKNOWLEDGMENT

The work was supported by NPRP grant #[5-1327-2-568] from the Qatar National Research Fund, which is a member of Qatar Foundation. The statements made herein are solely the responsibility of the authors.

The authors would like to thank the Interdisciplinary Centre for Sleep Medicine at the Charité Universitätsmedizin Berlin (Germany) for undertaking the recruitment and collection of polysomnographic recordings, as well as, the sleep scorers dedicated to the assessment labours. Both parties served as the main experimental source for the present research work.

R. Chaparro-Vargas acknowledges the financial support of the alliance COLCIENCIAS and COLFUTURO foundation of the Colombian Government, as main sponsor of his doctorate studies.

REFERENCES

[1] C. Marzano, F. Moroni, M. Gorgoni, L. Nobili, M. Ferrara, and L. D. Gennaro, "How we fall asleep: regional and temporal differences in electroencephalographic synchronization at sleep onset," *Sleep Medicine*, vol. 14, no. 11, pp. 1112 – 1122, 2013.

[2] F. Jurysta, J.-P. Lanquart, V. Sputaels, M. Dumont, P.-F. Migeotte, S. Leistedt, P. Linkowski, and P. van de Borne, "The impact of chronic primary insomnia on the heart rate EEG variability link," *Clinical Neurophysiology*, vol. 120, no. 6, pp. 1054–1060, 2009.

[3] I. Zhovna and I. D. Shallom, "Automatic detection and classification of sleep stages by multichannel eeg signal modeling," in *Engineering in Medicine and Biology Society, 2008. EMBS 2008. 30th Annual International Conference of the IEEE*, aug. 2008, pp. 2665 –2668.

[4] J. Lee and K. Chon, "Time-varying autoregressive model-based multiple modes particle filtering algorithm for respiratory rate extraction from pulse oximeter," *Biomedical Engineering, IEEE Transactions on*, vol. 58, no. 3, pp. 790–794, March 2011.

[5] R. Prado, "Sequential estimation of mixtures of structured autoregressive models," *Computational Statistics & Data Analysis*, vol. 58, no. 0, pp. 58–70, 2013.

[6] M. Arulampalam, S. Maskell, N. Gordon, and T. Clapp, "A tutorial on particle filters for online nonlinear/non-gaussian bayesian tracking," *Signal Processing, IEEE Transactions on*, vol. 50, no. 2, pp. 174–188, Feb 2002.

[7] H. Danker-Hopfe, P. Anderer, J. Zeitlhofer, M. Boeck, H. Dorn, G. Gruber, E. Heller, E. Loretz, D. Moser, S. Parapatics, B. Saletu, A. Schmidt, and G. Dorffner, "Interrater reliability for sleep scoring according to the Rechtschaffen & Kales and the new AASM standard," *Journal of Sleep Research*, vol. 18, no. 1, pp. 74–84, 2009.

[8] C. Iber, S. Ancoli-Israel, A. L. C. Jr., and S. F. Quan, "The AASM manual for the scoring of sleep and associated events," American Academy of Sleep Medicine, Tech. Rep., 2007.

[9] P. Anderer, A. Moreau, M. Woertz, M. Ross, G. Gruber, S. Parapatics, and G. Dorffner, "Computer-assisted sleep classification according to the standard of the american academy of sleep medicine: Validation study of the AASM version of the somnolyzer 24x7," *Neuropsychobiology*, vol. 62, no. 4, pp. 250–264, 2010.

[10] R. Rosenberg and S. Van Hout, "The american academy of sleep medicine inter-scorer reliability program: sleep stage scoring," *J Clin Sleep Med*, vol. 9, no. 1, pp. 81–87, 2013.

[11] C.-M. Ting, S.-H. Salleh, Z. Zainuddin, and A. Bahar, "Spectral estimation of nonstationary EEG using particle filtering with application to event-related desynchronization (ERD)," *IEEE Transactions on Biomedical Engineering*, vol. 58, no. 2, pp. 321–331, 2011.

[12] S. p. Mallat, *A Wavelet Tour of Signal Processing*. Elsevier Academic Press, 1999.

[13] A. Kaufmann and M. Gupta, *Introduction to Fuzzy Arithmetic*, B. Esposito, Ed. V.N. Reinhold, 1985.

[14] R. Agarwal, "Automatic detection of micro-arousals," in *Engineering in Medicine and Biology Society, 2005. IEEE-EMBS 2005. 27th Annual International Conference of the*, Jan 2005, pp. 1158–1161.

[15] D. Alvarez-Estevez and V. Moret-Bonillo, "Identification of electroencephalographic arousals in multichannel sleep recordings," *Biomedical Engineering, IEEE Transactions on*, vol. 58, no. 1, pp. 54–63, Jan 2011.

References

U. R. Acharya, K. P. Joseph, N. Kannathal, C. M. Lim, and J. S. Suri. Heart rate variability: A review. *Medical & Biological Engineering & Computing*, 44(12):1031 – 1051, 2006.

R. Agarwal. Automatic detection of micro-arousals. In *Engineering in Medicine and Biology Society, 2005. IEEE-EMBS 2005. 27th Annual International Conference of the*, pages 1158–1161, Jan 2005.

D. Álvarez-Estévez and V. Moret-Bonillo. Identification of electroencephalographic arousals in multichannel sleep recordings. *Biomedical Engineering, IEEE Transactions on*, 58(1):54–63, Jan 2011.

D. Álvarez-Estévez, J. Fernández-Pastoriza, E. Hernández-Pereira, and V. Moret-Bonillo. A method for the automatic analysis of the sleep macrostructure in continuum. *Expert Systems with Applications*, 40(5):1796 – 1803, 2013.

P. Anderer, A. Moreau, M. Woertz, M. Ross, G. Gruber, S. Parapatics, and G. Dorffner. Computer-assisted sleep classification according to the standard of the american academy of sleep medicine: Validation study of the AASM version of the somnolyzer 24x7. *Neuropsychobiology*, 62(4):250–264, 2010.

APA. *Diagnostic and Statistical Manual of Mental Disorders: DSM-IV-TR*. Diagnostic and Statistical Manual of Mental Disorders: DSM-IV-TR. American Psychiatric Association, 2000. ISBN 9780890420256.

M.S. Arulampalam, S. Maskell, N. Gordon, and T. Clapp. A tutorial on particle filters for online nonlinear/non-gaussian bayesian tracking. *Signal Processing, IEEE Transactions on*, 50(2):174–188, Feb 2002.

K.J. Bar, M.K. Boettger, M. Koschke, S. Schulz, P. Chokka, and V.K. Yeragani. Nonlinear complexity measures of heart rate variability in acute schizophrenia. *Clinical Neurophysiology*, 118:2009–2015, 2007.

J. E. Bartlett, J. W. Kotrlik, and C. C. Higgins. Organizational research: Determining appropiate sample size in survey research. *Information Technology, Learning, and Performance Journal*, 19(1):43–50, 2001.

R. Bartsch, J. W. Kantelhardt, T. Penzel, and S. Havlin. Experimental evidence for phase synchronization transitions in the human cardiorespiratory system. *Physics Review Letters*, 98:054102, Feb 2007.

C.H. Bastien, T. Ceklic, P. St-Hilaire, F. Desmarais, A.D. Perusse, J. Lefranois, and M. Pedneault-Drolet. Insomnia and sleep misperception. *Pathologie Biologie*, 62(5): 241–251, 2014.

C. Berthomier, X. Drouot, M. Herman-Stoca, P. Berthomier, J. Prado, D. Bokar-Thire, O. Benoit, J. Mattout, and M. P. d'Ortho. Automatic analysis of single-channel sleep EEG: Validation in healthy individuals. *Sleep*, 30(11):1587–1595, May 2007.

P. Bob. Consciousness, schizophrenia and complexity. *Cognitive Systems Research*, 13 (1):87 – 94, 2012.

R. Boostani, K. Sadatnezhad, and M. Sabeti. An efficient classifier to diagnose of schizophrenia based on the eeg signals. *Expert Systems with Applications*, 36(3): 6492–6499, 2009.

D. Buysse. Diagnostic classification of sleep and arousal disorders. Technical report, American Sleep Disorders Association, 1979.

D. Buysse. The international classification of sleep disorders. Technical report, American Sleep Disorder Association, 1990.

J. Caffarel, G. J. Gibson, J. P. Harrison, C. J. Griffiths, and M. J. Drinnan. Comparison of manual sleep staging with automated neural network-based analysis in clinical practice. *Medical & Biological Engineering & Computing*, 44(1-2):105–110, 2006.

K. Cervena, F. Espa, L. Perogamvros, S. Perrig, H. Merica, and V. Ibanez. Spectral analysis of the sleep onset period in primary insomnia. *Clinical Neurophysiology*, 125(5):979–987, May 2013.

C. Chang, Z. Ding, S. F. Yau, and F.H.Y. Chan. A matrix-pencil approach to blind separation of colored nonstationary signals. *Signal Processing, IEEE Transactions on*, 48(3):900 –907, 2000.

R.Y. Cho, R.O. Konecky, and C.S. Carter. Impairments in frontal cortical gamma synchrony and cognitive control in schizophrenia. *Proceedings of the National Academy of Sciences*, 103(X):19878–19883, 2006.

S. Chouinard, J. Poulin, E. Stip, and R. Godbout. Sleep in untreated patients with schizophrenia: A meta-analysis. *Schizophrenia Bulletin*, 30(4):957–967, 2004.

A. Cichocki and S. Amari. *Adaptive Blind Signal and Image Processing*. Wiley, 2005.

Chiara Cirelli and Giulio Tononi. Is sleep essential? *PLoS Biol*, 6(8):1–7, 08 2008.

H. Danker-Hopfe, D. Kunz, G. Gruber, G. Klsch, J. L. Lorenzo, S. L. Himanen, B. Kemp, T. Penzel, J. Rschke, H. Dorn, A. Schlgl, E. Trenker, and G. Dorffner. Interrater reliability between scorers from eight european sleep laboratories in subjects with different sleep disorders. *Journal of Sleep Research*, 13(1):63–69, 2004.

H. Danker-Hopfe, P. Anderer, J. Zeitlhofer, M. Boeck, H. Dorn, G. Gruber, E. Heller, E. Loretz, D. Moser, S. Parapatics, B. Saletu, A. Schmidt, and G. Dorffner. Interrater reliability for sleep scoring according to the Rechtschaffen & Kales and the new AASM standard. *Journal of Sleep Research*, 18(1):74–84, 2009.

A. Delorme and S. Makeig. EEGLAB: An open source toolbox for analysis of single-trial EEG dynamics including independent component analysis. *Journal of Neuroscience Methods*, 134(1):9 – 21, 2004.

S. Devuyst, T. Dutoit, P. Stenuit, M. Kerkhofs, and E. Stanus. Cancelling ECG artifacts in EEG using a modified independent component analysis approach. *EURASIP Journal on Advances in Signal Processing*, 2008:1–13, 2008.

S.I. Dimitriadis, N.A. Laskaris, Y. Del Rio-Portilla, and G.C. Koudounis. Characterizing dynamic functional connectivity across sleep stages from EEG. *Brain Topography*, 22(2):119–133, 2009. cited By (since 1996) 13.

P. M. Djuric, J. H. Kotecha, F. Esteve, and E. Perret. Sequential parameter estimation of time-varying non-gaussian autoregressive processes. *EURASIP Journal on Advances in Signal Processing*, 2002(8):262156, 2002.

D. Dubois and H. Prade. *Fuzzy Sets and Systems: Theory and Applications*. Academic Press, 1980.

M. Dumont, F. Jurysta, J.-P. Lanquart, P.-F. Migeotte, P. van de Borne, and P. Linkowski. Interdependency between heart rate variability and sleep EEG: linear/non-linear? *Clinical Neurophysiology*, 115(9):2031 – 2040, 2004.

M. Dumont, F. Jurysta, J.-P. Lanquart, A. Noseda, P. van de Borne, and P. Linkowski. Scale-free dynamics of the synchronization between sleep EEG power bands and the high frequency component of heart rate variability in normal men and patients with sleep apneahypopnea syndrome. *Clinical Neurophysiology*, 118(12):2752 – 2764, 2007.

E. Estrada, H. Nazeran, G. Sierra, F. Ebrahimi, and S.K. Setarehdan. Wavelet-based EEG denoising for automatic sleep stage classification. In *Electrical Communications and Computers (CONIELECOMP), 2011 21st International Conference on*, pages 295 –298, 28 2011-march 2 2011.

Y. Fei-Long and L. Zhi-Zeng. The EEG de-noising research based on wavelet and Hilbert transform method. In *Computer Science and Electronics Engineering (ICCSEE), 2012 International Conference on*, volume 3, pages 361 –365, march 2012.

B. Feige, C. Baglioni, K. Spiegelhalder, V. H., C. Nissen, and D. Riemann. The microstructure of sleep in primary insomnia: An overview and extension. *International Journal of Psychophysiology*, 89(2):171 – 180, 2013.

F. Ferrarelli, M.J. Peterson, S. Sarasso, B.A. Riedner, M.J. Murphy, R.M. Benca, P. Bria, N.H. Kalin, and G. Tononi. Reduced sleep spindle activity in schizophrenia patients. *American Journal of Psychiatry*, 164(1):483–492, 2007.

F. Ferrarelli, R. Huber, M.J. Peterson, M. Massimini, M. Murphy, B.A. Riedner, A. Watson, P. Bria, and G. Tononi. Thalamic dysfunction in schizophrenia suggested by whole-night deficits in slow and fast spindles. *American Journal of Psychiatry*, 167 (1):1339–1348, 2010.

L. Fraiwan, K. Lweesy, N. Khasawneh, H. Wenz, and H. Dickhaus. Automated sleep stage identification system based on timefrequency analysis of a single eeg channel and random forest classifier. *Computer Methods and Programs in Biomedicine*, 108 (1):10 – 19, 2012.

D. Freeman, K. Pugh, N. Vorontsova, and L. Southgate. Insomnia and paranoia. *Schizophrenia Research*, 108(1-3):280–284, March 2009.

A. Galka, K. F. K. Wong, T. Ozaki, H. Muhle, U. Stephani, and M. Siniatchkin. Decomposition of neurological multivariate time series by state space modelling. *Bulletin of Mathematical Biology*, 73:285–324, 2011.

D. Gencaga, E. Kuruoglu, and A. Ertuzun. Modeling non-gaussian time-varying vector autoregressive processes by particle filtering. *Multidimensional Systems and Signal Processing*, 21(1):73–85, 2010.

J.C. Gillin, W. Duncan, K.D. Pettigrew, B.L. Frankel, and F. Snyder. Sucessful separation of depressed, normal and insomniac subjects by eeg sleep data. *Archives of General Psychiatry*, 36(1):85–90, 1979.

Mark A. Haidekker. *Advanced Biomedical Image Analysis*. Wiley, 2011.

J. Hedner, D.P. White, A. Malhotra, S. Herscovici, S.D. Pittman, D. Zou, L. Grote, and Pillar G. Sleep staging based on autonomic signals: A multi-center validation study. *Clinical Sleep Medicine*, 7(3):301–306, 2011.

B.L. Henry, A. Minassian, M.P. Paulus, M.A. Geyer, and W. Perry. Heart rate variability in bipolar mania and schizophrenia. *Journal of Psychiatric Research*, 44(3):168–176, 2010.

C. Iber, S. Ancoli-Israel, A. L. Chesson Jr., and S. F. Quan. The AASM manual for the scoring of sleep and associated events. Technical report, American Academy of Sleep Medicine, 2007.

G. Inuso, F. La Foresta, N. Mammone, and F.C. Morabito. Brain activity investigation by EEG processing: Wavelet analysis, Kurtosis and Renyi's entropy for artifact detection. In *Information Acquisition, 2007. ICIA '07. International Conference on*, pages 195 –200, july 2007.

M. Ipsen and A. S. Mikhailov. Evolutionary reconstruction of networks. *Physics Review E*, 66:046109, Oct 2002.

G.L. Iverson, M.B. Gaetz, E.J. Rzempoluck, P. McLean, W. Linden, and R. Remick. A new potential marker for abnormal cardiac physiology in depression. *Journal of Behavioral Medicine*, 28(6):507–511, 2005.

D. Jakobson and I. Rivin. Extremal metrics on graph I. *Forum Mathematics*, 14(1): 147–163, 2002.

G. Jurman, R. Visintainer, and C. Furlanello. An introduction to spectral distances in networks. *Frontiers in Artificial Intelligence and Applications*, 226:227–234, 2011. cited By (since 1996)1.

F. Jurysta, P. van de Borne, P.-F. Migeotte, M. Dumont, J.-P. Lanquart, J.-P. Degaute, and P. Linkowski. A study of the dynamic interactions between sleep EEG and heart rate variability in healthy young men. *Clinical Neurophysiology*, 114(11):2146 – 2155, 2003.

F. Jurysta, J.-P. Lanquart, V. Sputaels, M. Dumont, P.-F. Migeotte, S. Leistedt, P. Linkowski, and P. van de Borne. The impact of chronic primary insomnia on the heart rate EEG variability link. *Clinical Neurophysiology*, 120(6):1054 – 1060, 2009.

F. Jurysta, C. Kempenaers, J. Lancini, J.-P. Lanquart, P. Van De Borne, and P. Linkowski. Altered interaction between cardiac vagal influence and delta sleep EEG suggests an altered neuroplasticity in patients suffering from major depressive disorder. *Acta Psychiatrica Scandinavica*, 121(3):236–239, 2010.

A. Kaufmann and M.M. Gupta. *Introduction to Fuzzy Arithmetic*. V.N. Reinhold, 1985.

G. Kitagawa. *Introduction to Time Series Modeling*, chapter Analysis of Time Series with a State-Space Model, pages 1–16. CRC Press, 2009.

G. Klosh, B. Kemp, T. Penzel, A. Schlogl, P. Rappelsberger, E. Trenker, G. Gruber, J. Zeithofer, B. Saletu, W.M. Herrmann, S.L. Himanen, D. Kunz, M.J. Barbanoj, J. Roschke, A. Varri, and G. Dorffner. The SIESTA project polygraphic and clinical database. *Engineering in Medicine and Biology Magazine, IEEE*, 20(3):51–57, May 2001.

B. Koley and D. Dey. An ensemble system for automatic sleep stage classification using single channel EEG signal. *Computers in Biology and Medicine*, X(0):1 – 10, 2012.

S. Leistedt, M. Dumont, J.P. Lanquart, F. Jurysta, and P. Linkowski. Characterization of the sleep eeg in acutely depressed men using detrended fluctuation analysis. *Clinical Neurophysiology*, 118(4):940–950, 2007.

S.-F. Liang, C.-E. Kuo, Y.-H. Hu, Y.-H. Pan, and Y.-H. Wang. Automatic stage scoring of single-channel sleep eeg by using multiscale entropy and autoregressive models. *Instrumentation and Measurement, IEEE Transactions on*, 61(6):1649 –1657, june 2012.

J. Liu and M. West. Combined parameter and state estimation in simulation-based filtering. In Arnaud Doucet, Nando Freitas, and Neil Gordon, editors, *Sequential Monte Carlo Methods in Practice*, Statistics for Engineering and Information Science, pages 197–223. Springer New York, 2001.

J. Maes, J. Verbraecken, M. Willemen, I. De Volder, A. van Gastel, N. Michiels, I. Verbeek, M. Vandekerckhove, J. Wuyts, B. Haex, T. Willemen, V. Exadaktylos, A. Bulckaert, and R. Cluydts. Sleep misperception, EEG characteristics and autonomic nervous system activity in primary insomnia: A retrospective study on polysomnographic data. *International Journal of Psychophysiology*, 91(3):163–71, Mar 2013.

S. Mallat. *A Wavelet Tour of Signal Processing*. Elsevier Academic Press, 1999.

C. Marzano, F. Moroni, M. Gorgoni, L. Nobili, M. Ferrara, and L. De Gennaro. How we fall asleep: Regional and temporal differences in electroencephalographic synchronization at sleep onset. *Sleep Medicine*, 14(11):1112 – 1122, 2013.

A.G. Mayers and D.S. Baldwin. The relationship between sleep disturbance and depression. *International Journal of Psychiatry in Clinical Practice*, 10(1):2–16, 2006.

H. Merica and R. D. Fortune. State transitions between wake and sleep, and within the ultradian cycle, with focus on the link to neuronal activity. *Sleep Medicine Reviews*, 8(6):473 – 485, 2004.

L. Mesin, A. Holobar, and R. Merletti. *Advanced Methods of Biomedical Signal Processing*. IEEE Press, 2011.

K. Mezeiova and M. Palus. Comparison of coherence and phase synchronization of the human sleep electroencephalogram. *Clinical Neurophysiology*, 123(9):1821 – 1830, 2012.

C.M. Morin, M. LeBlanc, M. Daley, J.P. Gregoire, and C. Mrette. Epidemiology of insomnia: Prevalence, self-help treatments, consultations, and determinants of help-seeking behaviors. *Sleep Medicine*, 7(2):123 – 130, 2006.

V. V. Nikulin, E. G. Jnsson, and T. Brismar. Attenuation of long-range temporal correlations in the amplitude dynamics of alpha and beta neuronal oscillations in patients with schizophrenia. *NeuroImage*, 61(1):162 – 169, 2012.

C. Nissen, Feige B., Knig A., Voderholzer U., Berger M., and Riemann D. Delta sleep ratio as a predictor of sleep deprivation in response in major depression. *Journal of Psychiatric Research*, 35(3):155–163, 2001.

E.A. Nofzinger, D.J. Buysse, A. Germain, J.C. Price, J.M. Miewald, and D.J. Kupfer. Functional neuroimaging evidence for hyperarousal in insomnia. *American Journal of Psychiatry*, 161(11):940–950, 2004.

K. Noh, K. S. Shin, D. Shin, J. Y. Hwang, J. S. Kim, J. H. Jang, C. K. Chung, J. S. Kwon, and K.-H. Cho. Impaired coupling of local and global functional feedbacks underlies abnormal synchronization and negative symptoms of schizophrenia. *BMC Systems Biology*, 7(30):1–13, 2013.

L. Novelli, R. Ferri, and O. Bruni. Sleep classification according to AASM and Rechtschaffen and Kales: Effects on sleep scoring parameters of children and adolescents. *Journal of Sleep Research*, 19:238–247, 2009.

R. D. Ogilvie. The process of falling asleep. *Sleep Medicine Reviews*, 5(3):247–270, 2001.

World Health Organization. *The ICD-10 Classification of Mental and Behavioural Disorders: Diagnostic Criteria for Research*. ICD-10 classification of mental and behavioural disorders / World Health Organization. World Health Organization, 1993. ISBN 9789241544559.

J.M. Palva, S. Palva, and K. Kaila. Phase synchrony among neuronal oscillations in the human cortex. *Journal of Neuroscience*, 25(15):3962–3972, April 2005.

T. Penzel, M. Hirshkowitz, J. Harsh, and R. D. Chervin. Digital analysis and technical specifications. *Journal of Clinical Sleep Medicine*, 3:109–120, 2007.

E. Pereda, R. Q. Quiroga, and J. Bhattacharya. Nonlinear multivariate analysis of neurophysiological signals. *Progress in Neurobiology*, 77(12):1 – 37, 2005.

N. Petrovsky, U. Ettinger, A. Hill, L. Frenzel, I. Meyhoefer, M. Wagner, J. Backhaus, and V. Kumari. Sleep deprivation disrupts prepulse inhibition and induces psychosis-like symptoms in healthy humans. *The Journal of Neuroscience*, 34(27):9134–9140, 2014.

R. Prado. Sequential estimation of mixtures of structured autoregressive models. *Computational Statistics & Data Analysis*, 58(0):58 – 70, 2013.

A. Rechtschaffen and A. Kales. A manual of standardized terminology, techniques and scoring system for sleep stages of human subjects. Technical report, Brain Information Service - Brain Research Institute University of California, 1968.

A. Rodenbeck, R. Binder, P. Geisler, H. Danker-Hopfe, R. Lund, F. Raschke, H.-G. Wee, and H. Schulz. A review of sleep EEG patterns. Part I: A compilation of amended rules for their visual recognition according to Rechtschaffen and Kales. *Somnologie*, 10(4):159–175, 2006.

R. Romo-Vázquez, H. Vélez-Pérez, R. Ranta, V. Louis Dorr, D. Maquin, and L. Maillard. Blind source separation, wavelet denoising and discriminant analysis for EEG artefacts and noise cancelling. *Biomedical Signal Processing and Control*, 7(4):389 – 400, 2012.

R.S. Rosenberg and S. Van Hout. The american academy of sleep medicine inter-scorer reliability program: Sleep stage scoring. *Clinical Sleep Medicine*, 9(1):81–87, 2013.

V. Sakkalis, C.D. Giurcaneanu, P. Xanthopoulos, M.E. Zervakis, V. Tsiaras, Y. Yang, E. Karakonstantaki, and S. Micheloyannis. Assessment of linear and nonlinear synchronization measures for analyzing EEG in a mild epileptic paradigm. *Information Technology in Biomedicine, IEEE Transactions on*, 13(4):433 –441, july 2009.

S. Schulz, K.J. Bar, and A. Voss. Respiratory variability and cardiorespiratory coupling analyses in patients suffering from schizophrenia and their healthy first-degree relatives. *Biomedical Technology*, 104(57):12, 2012.

K. Spiegelhalder, W. Regen, B. Feige, J. Holz, H. Piosczyk, C. Baglioni, D. Riemann, and C. Nissen. Increased EEG sigma and beta power during NREM sleep in primary insomnia. *Biological Psychology*, 91(3):329 – 333, 2012.

L. Staner. Comorbidity of insomnia and depression. *Sleep Medicine Reviews*, 14(1):35 – 46, 2010.

Luc Staner, Francoise Cornette, Damien Maurice, Geoffrey Viardot, Oliver Le Bon, Jose Haba, Corinne Staner, Remy Luthringer, Alain Muzet, and Jean-Paul Macher. Sleep microstructure around sleep onset differentiates major depressive insomnia from primary insomnia. *Journal of Sleep Research*, pages 319–330, 2003.

P. Stoica and R. Moses. *Spectral analysis of signals*. Pearson Prentice Hall, 2005.

N. V. Thakor and S. Tong. Advances in quantitative electroencephalogram analysis method. *Annual Review of Biomedical Engineering*, 6(1):453–495, 2004.

S. F. Timashev, O. Y. Panischev, Y. S. Polyakov, S. A. Demin, and A. Y. Kaplan. Analysis of cross-correlations in electroencephalogram signals as an approach to proactive diagnosis of schizophrenia. *Physica A: Statistical Mechanics and its Applications*, 391(4):1179 – 1194, 2012.

K.H. Ting, P.C.W. Fung, C.Q. Chang, and F.H.Y. Chan. Automatic correction of artifact from single-trial event-related potentials by blind source separation using second order statistics only. *Medical Engineering & Physics*, 28(8):780 – 794, 2006.

W. Treynor, R. Gonzalez, and S. Nolen-Hoeksema. Rumination reconsidered: A psychometric analysis. *Cognitive Therapy and Research*, 27(3):247–259, 2003.

K. Udupa, T.N. Sathyaprabha, J. Thirthalli, K.R. Kishore, G.S. Lavekar, T.R. Raju, and B.N. Gangadhar. Alteration of cardiac autonomic functions in patients with major depression: a study using heart rate variability measures. *Journal of Affective Disorders*, 100(1-3):137–141, 2007.

P.A. Uhlhaas. Dysfunctional long-range coordination of neural activity during gestalt perception in schizophrenia. *Journal of Neuroscience*, 26(X):8168–8175, 2006.

P.J. Uhlhaas and W. Singer. Abnormal neural oscillations and synchrony in schizophrenia. *Nature Reviews, Neuroscience*, 11(X):100–113, 2010.

A. Zalesky, A. Fornito, M. L. Seal, L. Cocchi, C.-F. Westin, E. T. Bullmore, G. F. Egan, and C. Pantelis. Disrupted axonal fiber connectivity in schizophrenia. *Biology Psychiatry*, 69:80–89, 2011a.

A. Zalesky, A. Fornito, M. L. Seal, L. Cocchi, C.-F. Westin, E. T. Bullmore, G. F. Egan, and Christos Pantelis. Disrupted axonal fiber connectivity in schizophrenia. *Biology Psychiatry*, 69:80–89, 2011b.

I. Zhovna and I. D. Shallom. Automatic detection and classification of sleep stages by multichannel EEG signal modeling. In *Engineering in Medicine and Biology Society, 2008. EMBS 2008. 30th Annual International Conference of the IEEE*, pages 2665 –2668, aug. 2008.